Distribution Statement

Distribution A: Public Release.

The views presented here are those of the author and are not to be construed as official or reflecting the views of the Uniformed Services University of the Health Sciences, the Department of Defense or the U.S. Government.

Characterization of persistence and a novel cytoskeletal protein in *Chlamydia trachomatis*

by

Mary Rose Brockett

Dissertation submitted to the Faculty of the
Emerging Infectious Diseases Graduate Program
Uniformed Services University of the Health Sciences
In partial fulfillment of the requirements for the degree of
Doctor of Philosophy 2021

UNIFORMED SERVICES UNIVERSITY OF THE HEALTH SCIENCES
SCHOOL OF MEDICINE GRADUATE PROGRAMS
Graduate Education Office (A 1045), 4301 Jones Bridge Road, Bethesda, MD 20814

APPROVAL OF THE DOCTORAL DISSERTATION IN THE EMERGING INFECTIOUS DISEASES GRADUATE PROGRAM

Title of Dissertation: "Characterization of persistence and a novel cytoskeletal protein in *Chlamydia trachomatis*"

Name of Candidate: Mary Brockett
Doctor of Philosophy Degree
September 30, 2021

DISSERTATION AND ABSTRACT APPROVED:

DATE:

[redacted] 9/30/21
Dr. D. Scott Merrell
DEPARTMENT OF MICROBIOLOGY & IMMUNOLOGY
Committee Chairperson

[redacted] 10/28/21
Dr. George Liechti
DEPARTMENT OF MICROBIOLOGY & IMMUNOLOGY
Dissertation Advisor

[redacted] 9/30/21
Dr. Kristi Frank
DEPARTMENT OF MICROBIOLOGY & IMMUNOLOGY
Committee Member

[redacted] 9/30/21
Dr. Kumaran Ramamurthi
NATIONAL CANCER INSTITUTE, NATIONAL INSTITUTES OF HEALTH
Committee Member

Acknowledgements

First, I would like to thank my mentor, Dr. George Liechti, for providing me with guidance, mentorship, and support throughout my doctoral studies. The 'struggs' were real in grad school, but thank you for believing in me even when I didn't believe in myself. And thank you for always pushing me to do my best work. I am honored to be your first graduate student.

Next, I would like to thank my thesis committee, Drs. D. Scott Merrell (chair), Kristi Frank, and Kumaran Ramamurthi for guidance and support throughout my dissertation work.

I would like to thank my collaborators (especially Drs. Junghoon Lee and Scot Ouellette); without you all the bactofilin story would not have been as robust. Thank you to all of the 'chlamydiologists' who shared reagents, strains, and/ or *Chlamydia* specific tips/ tricks.

I would like to thank the Utica College Biology Department faculty for helping me find my passion for scientific research (especially Dr. Jessica Thomas).

I would also like to thank the past and present members of the Liechti Lab for their never-ending support and encouragement. You all made the long hours and weird time points seem less daunting.

Thank you to my Maryland family: Dr. S. Stephanie Garcia-Buntley, Dr. Candace Rouchon, Nontokozo Mdluli-Berndt, Aissata Diallo, and Dr. Mahmuda Afrin Badhan. I will forever be grateful to you all for making Maryland feel a little bit more like home.

Thank you to my girls (Letisha Da Silva, Rosemarie Etienne, Nazifa Alam, Farwa Dalawar, and Mindy Pfeffer) for your friendship and for being my greatest cheerleaders.

Last but not least, I would like to thank my fiancé (Patrick) and my family (especially my parents, my siblings [Mike and Kim], and my Grandma Brockett) for your constant support,

love, and motivation. Without you all (especially my parents), I would not be where I am today. Thank you for all the sacrifices you made for me.

Dedication

I dedicate this thesis to my late grandfather Louis William “Bill” Brockett who always told everyone his granddaughter would be a doctor someday. I did it, Grandpa! ❤️

I would also like to dedicate this thesis to my niece and nephew (Sophia and Gabriel). Stay curious and never stop asking questions.

Copyright Statement

The author hereby certifies that the use of any copyrighted material in the dissertation manuscript entitled: "Characterization of persistence and a novel cytoskeletal protein in *Chlamydia trachomatis*" is appropriately acknowledged and, beyond brief excerpts, is with the permission of the copyright owner.



Mary R. Brockett
Emerging Infectious Diseases
Uniformed Services University
October 28, 2021

Abstract

Title of Thesis:
Characterization of persistence and a novel cytoskeletal protein in *Chlamydia trachomatis*

Mary Rose Brockett, Doctor of Philosophy in Emerging Infectious Diseases, 2021

Thesis directed by:
Dr. George W. Liechti, Assistant Professor, Department of Microbiology and Immunology

The regulation of cell division is critically important for intracellular pathogens. *Chlamydia trachomatis*, an obligate intracellular bacterium, must replicate rapidly in order to sustain an active infection. Paradoxically, the pathogen must release its infectious forms only when conditions are suitable for their extracellular survival. It has been previously demonstrated that *C. trachomatis* must first decrease in size in order to transition to their infectious forms. However, *C. trachomatis* does not utilize a peptidoglycan-containing cell wall and lacks many of the canonical genes associated with regulating bacterial cell size and division. Our overall goal was to investigate how *C. trachomatis* initiates cell division and how halting cell division affects the interactions between the pathogen and its host.

Cell division in *Chlamydia spp.* begins via an initial polar expansion of the bacterial cell membrane, and the mechanism by which this initial polarity is established is unknown. To investigate the potential role of the chlamydial cytoskeletal protein $BacA_{CT}$ in this process, we utilized fluorescent fusion constructs, CRISPRi, and high-resolution imaging to examine the protein's localization within chlamydial cells, identify its interaction partners, and measure its effects on the bacterium's size and shape. Although we did not find a role for $BacA_{CT}$ in cell polarity, we did observe a significant defect in cell size regulation when $BacA_{CT}$ was depleted

from chlamydial cells. Our observations suggest that $BacA_{CT}$ may play a role in enhancing the stability of the microbe's inner membrane during cell division.

Under stress conditions, *Chlamydia spp*. halt cell division, pausing the microbe's development and preventing the production of infectious progeny. While it is known that this 'aberrant' state is triggered by several mechanisms, little is known about how induction of persistence affects interactions between *C. trachomatis* and the host cell. We examined how interrupting cell division affects the physiology of *C. trachomatis* by exposing the pathogen to six aberrance-inducing conditions; we found differences in the microbe's ability to produce infectious progeny, synthesize peptidoglycan, produce/ secrete Type III Secretion System effectors, and maintain cell size. We hypothesize that persistence may allow *C. trachomatis* to remain intracellular during an active immune response.

TABLE OF CONTENTS

Acknowledgements iii

Dedication v

Copyright Statement vi

Abstract vii

Chapter 1: Introduction 2

Chlamydia trachomatis 2
Early history and classification 2
Epidemiology and disease presentation 2
Diagnosis, treatment, and prevention 4
Other important members of the order *Chlamydiales* 6
Developmental cycle 8
Role of PG in bacteria 8
Discovery of chlamydial PG 9
Genetic advances toward solving the 'chlamydial anomaly' 10
Chlamydia spp. divide independent of FtsZ 10
Unique features of PG biosynthesis/ assembly in *Chlamydia spp* 11
Visualization of chlamydial PG 13
Cell division: binary fission vs. 'polarized division' 14
Bactofilins 15
Bacterial cytoskeleton 15
Characteristics of bactofilins 16
Role of bactofilins in bacteria 17
Cell shape/ differentiation 17
Cell polarity/ chromosomal segregation 18
Motility 19
Persistence in *Chlamydia spp*. 20
Characteristics of chlamydial 'persistence' 20
Known inducers of persistence 20
Mechanisms of AB induction 21
IFNγ/ tryptophan starvation 21
Iron starvation 22
in vivo relevance of chlamydial aberrant forms 22
Clinical infections 22
Animal infections 23
Goals and specific aims 24

Chapter 2: A dynamic, ring-forming bactofilin critical for maintaining cell size in the obligate intracellular bacterium *Chlamydia trachomatis* 30

Abstract 31

Introduction 32
Materials and methods 33
Organisms and cell culture 33
Bioinformatics analysis 34
Cloning 35
Transformation of *Chlamydia trachomatis* 36
Viable EB/ IFU assay 37
Labeling of chlamydial peptidoglycan and MreB 37
Indirect immunofluorescence (IFA) microscopy 38
BACTH assay 39
Transcriptional analyses in *Chlamydia trachomatis* 39
Results 40
The chlamydial gene, *ct276/ ctl_0528*, encodes a bactofilin ortholog 40
$BacA_{CT}$ polymers are dynamic, alternating between puncta and ring-like structures 41
$BacA_{CT}$ does not associate with cell division components 43
Inducible knockdown of $BacA_{CT}$ alters chlamydial morphology 45
Knockdown of $BacA_{CT}$ has minimal impact on peptidoglycan ring formation and progression through the developmental cycle 47
$BacA_{CT}$ knockdown can be complemented to restore normal morphology 48
Discussion 73
Acknowledgments 75

Chapter 3: Persistence alters the interaction between *Chlamydia trachomatis* and its host cell 77

Abstract 78
Importance 78
Introduction 79
Materials and methods 82
Bacterial strains and cell lines 82
Chlamydial infections 83
Analysis of the total bacterial volume within individual inclusion 83
Quantification of inclusion forming units (IFU) 84
Fluorescent labeling of PG, cell nuclei, actin filaments, and inclusion membrane proteins 85
Homotypic Fusion Assay 86
Infection of HEK-Blue-hNOD1 and -Null1 cells with *C. trachomatis* and NF-κB reporter assay 86
Azithromycin study 87
Investigation of compound C1 effects under high iron conditions 88
Results 89
C. trachomatis aberrant body formation results in cell division arrest and temporarily pauses the developmental cycle 89
Persistent forms of *Chlamydia* differ in their capacity to assemble septal peptidoglycan ... 91
Aberrant *Chlamydia* forms differ in their ability to release PG-derived, immunostimulatory muropeptides 92
The timing of persistence induction directly affects *Chlamydia* morphology and PG-derived muropeptide release 94

Persistent forms of *Chlamydia* differ in the presentation of mid- and late-stage effector proteins 96
Persistent forms of *Chlamydia* exhibit differences in their ability to undergo homotypic fusion and induce actin cage formation 97
Iron depletion-induced persistence enhances the susceptibility of *C. trachomatis* to azithromycin treatment 99
Discussion 119
Acknowledgments 126
Declarations of interest 127

Chapter 4: Discussion 128

Overall summary 128
Result summary from chapter two 128
Ring-forming bactofilins: implications, limitations and future directions 131
Result summary from chapter three 134
Chlamdyial aberrance vs. persistence: implications, limitations and future directions 135
Overarching themes and conclusions 141

Appendix A: Additional unpublished data from chapter 2 145

Introduction 145
$BacA_{CT}$ expression has no effect on chlamydial viability 145
$BacA_{CT}$ filament characterization 147
Materials and methods 148
Results and discussion 148
Cell division inhibitors prevent $BacA_{CT}$ ring formation 148
..... 152

Appendix B: Additional unpublished data from chapter 3 153

Introduction 153
Results and discussion: essential amino acid starvation (induced by isoleucine supplementation) 153
Figures 155

References 160

LIST OF TABLES

Supplementary table 1. The list of strains, plasmids and primers used in this study..... 69

LIST OF FIGURES

Figure 1. Biphasic developmental cycle for *Chlamydia trachomatis*..... 26
Figure 2. Comparison of cell division proteins from *C. trachomatis* and *E. coli* 27
Figure 3. Model of polarized cell division in *Chlamydia*. 28
29
Figure 4. Bactofilin Domain Architecture 29
Figure 5. The chlamydial gene *ct276*/*ctl_0528* (*bacA$_{CT}$*) encodes a bactofilin protein. 50
Figure 6. BacA$_{CT}$ contains a β-helical core domain that is universally conserved in all bactofilins. 53
54
Figure 7. BacA$_{CT}$_mCherry localization is dynamic and alters between puncta, filaments, and ring-like structures. 54
56
Figure 8. BacA$_{CT}$ ring morphology observed in fixed and living cells via super resolution microscopy. 56
Figure 9. BacA$_{CT}$ forms filaments that do not colocalize or interact with peptidoglycan or proteins associated with cell division in *Chlamydia* species. 58
Figure 10. Conditional knockdown of *bacA$_{CT}$* expression alters the morphology of *C. trachomatis*. 60
Figure 11. The effect of dCas9 over-expression without gRNA in *C. trachomatis*. 62
Figure 12. Conditional knockdown of *bacA$_{CT}$* expression has minimal impact on chlamydial peptidoglycan (PG) synthesis or developmental cycle progression. 64
Figure 13. Knockdown of BacA$_{CT}$ does not alter peptidoglycan ring formation..... 65
Figure 14. Ectopic expression of BacA$_{CT}$ complements the morphological defects during knockdown of *bacA$_{CT}$* expression in *C. trachomatis*. 66
68
Figure 15. 3D super-resolution images of BacA$_{CT}$_6xH-complemented *bacA$_{CT}$* knockdown strain. 68
Figure 16. *C. trachomatis* aberrant body formation results in cell division arrest and pausing of the developmental cycle..... 102
Figure 17. The effects of T3SS inhibitor on the development of *C. trachomatis* are significantly reduced in cells supplemented with exogenous iron..... 103
104
Figure 18. Aberrant Chlamydia forms differ in their ability to synthesize peptidoglycan. 104
Figure 19. Aberrant *Chlamydia* forms differ in their ability to synthesize immunostimulatory peptidoglycan. 105
Figure 20. The presence of PG and differences in cell / inclusion size are dependent on the timing of persistence induction. 107
Figure 21. The presence of immunostimulatory peptidoglycan is dependent on the timing of persistence induction..... 108
Figure 22. *Chlamydia* ABs differ in their presentation of early-stage inclusion membrane proteins..... 109
Figure 23. *Chlamydia* ABs differ in presentation of mid- and late- stage inclusion membrane proteins..... 110

111
Figure 24. *Chlamydia* ABs differ in their presentation of the mid-stage inclusion membrane protein IncA. 112
Figure 25. Assessment of inclusion trafficking to the nucleus and actin cage formation. 113
Figure 26. *Chlamydia* ABs differ in their presentation of the late-stage inclusion membrane protein CT813. 115
116
Figure 27. Iron-depletion-induced persistence enhances the susceptibility of *C. trachomatis* to azithromycin treatment. 116
Figure 28. Persistence halts the *Chlamydia* developmental cycle while simultaneously altering bacteria-host cell interactions. 117
Figure 29. Modeling chlamydial persistence in the context of infection. 118
Figure 30. Membrane stabilization mechanisms are spatially restricted and differ between *Chlamydia*'s developmental forms. 144
Figure 31. Induction of $BacA_{CT}$ fusion constructs does not affect chlamydial development 146
Figure 32. Treatment with cell division inhibitors prevents $BacA_{CT}$ filament formation. 150
Figure 33. $BacA_{CT}$-mCherry rings exhibit reversible dissociation following inhibition of MreB. 151
Figure 34. $BacA_{CT}$ polymerization resumes upon the removal of ampicillin. 152
Figure 35. Aberrant body formation inhibited by amino acid limitation (via the addition of exogenous isoleucine) partially results in cell division arrest and pausing of the *Chlamydia* developmental cycle 156
Figure 36. Cell division is only partially inhibited by amino acid limitation (via the addition of exogenous isoleucine). 157
Figure 37. Inclusion maturation was partially inhibited by amino acid limitation (via the addition of exogenous isoleucine) 158
Figure 38. Assessment of inclusion trafficking to the nucleus upon exposure to amino acid limitation (via the addition of exogenous isoleucine). 159

Chapter 1: Introduction

CHLAMYDIA TRACHOMATIS

Early history and classification

Chlamydia trachomatis is a Gram negative, obligate intracellular bacterium associated with infections of the human eye and genital track. The microbe was first described in 1907 by Halberstaedter and von Prowazek after they observed membrane bound vessels (inclusions) containing small particles (*C. trachomatis*) in scrapings from an inflamed conjunctiva (204; 246). *Chlamydia spp*. were initially thought to be protozoan, and as chlamydial inclusions appeared to wrap around host cell nuclei like a 'cloak', the microbe was named *Chlamydozoa* after the Greek word chlamys, which means cloak (246). It was later renamed 'trachoma inclusion conjunctivitis agent' (246), and classified as a virus, as it could not be grown via typical culture methods, and no examples of bacteria capable of only intracellular growth existed at that time. *C. trachomatis* was first successfully propagated in the laboratory utilizing techniques similar to those used for propagating viruses: infection of chicken embryos, and later by infection of tissue culture cell lines (246). These organisms were again reclassified as obligate intracellular bacteria after imaging studies appeared to demonstrate that *Chlamydia spp*. divide by binary fission (78; 98; 152; 153) and that their growth could be inhibited by the antibiotic penicillin (96; 190; 273).

Epidemiology and disease presentation

There are currently 19 different serovars of *C. trachomatis* recognized (139), and each is associated with a specific disease presentation. *C. trachomatis* is the causative agent of non-congenital blindness (trachoma biovar: serovars A-C), sexually transmitted genital tract infections (genital tract biovar: serovars D-K), and invasive urogenital or anorectal infection

(lymphogranuloma venereum, LVG, biovar: serovars L1–L3) (68). Trachoma, the inflammation of the conjunctiva caused by ocular *C. trachomatis* infections, is the leading cause of non-congenital blindness (60; 276). Repeated ocular chlamydial infections can result in the scarring of the conjunctiva, causing the eyelashes to turn inwards (trichiasis). This can lead to the scarring of the eye and eventually result in blindness (276). The World Health Organization (WHO) estimates that approximately 1.9 million people have been blinded or visually impaired due to trachoma (234). Trachoma is contracted by close contact with exudates from infected eyes and noses (276). Flies can also serve as vectors and mediate transmission between persons (161). The burden of trachoma falls primarily on females, as they assume the caretaker role in many societies around the world, and thus, are often repeatedly exposed and reinfected (53).

Genital chlamydial infections are the most commonly reported bacterial sexually transmitted infection in the United States and worldwide (43; 174). In 2019, 1,808,703 cases of *C. trachomatis* were reported to the CDC (43); however, due to over half of infections resulting in no recognizable symptomology, this number is likely an under estimate (68). Nearly two-thirds of reported cases of *C. trachomatis* in 2019 were in teens and young adults (43). The prevalence of *C. trachomatis* is also disproportionally higher in adolescent girls and young women compared to other subgroups within the human population (43). Co-infections are also highly prevalent. Depending on the population examined, between 20 and 70% of persons with a genital chlamydial infection are also co-infected with another Gram negative bacterial pathogen, *Neisseria gonorrhoeae* (44; 162; 175; 214; 247). This coinfection status can affect treatment recommendations as *N. gonorrhoeae* is highly resistant to most antibiotics.

Female chlamydial infections typically begin in the lower genital tract (at the urethra or the cervix) and can ascend to the upper genital tract (uterus or the fallopian tubes) (24).

Chlamydial infections in males most often start as urethritis, but can also present as epididymitis (257). Males often present with painful urination and discharge, while many females exhibit no or limited symptomology. Up to 80% of female genital tract infections are asymptomatic, and as many as 40% of cases can result in infections of the upper genital tract. These upper genital tract infections can have devastating consequences on reproductive health (68). Untreated female upper genital tract infections can lead to pelvic inflammatory disease, infertility, and ectopic pregnancies (68; 207). It is also important to note that *C. trachomatis* can also have a negative impact on male fertility, as genital infections have been associated with low sperm quality (47).

Lymphogranuloma venereum (LGV) is a more invasive urogenital or anorectal infection, which typically involves the unilateral swelling of the inguinal lymph nodes. Occasionally there is a cutaneous genital ulcer, but this tends to resolve prior to the swelling of the inguinal lymph nodes. An additional manifestation of LGV is proctitis or proctocolitis, which can result in anorectal pain, discharge, bleeding, and other gastrointestinal symptoms (90).

C. trachomatis serovars normally associated with genital tract infections are also associated with non-genital infections. Vertical transmission of *C. trachomatis* from gestational parent to neonate can occur during childbirth. *C. trachomatis* is the causative agent in 2-40% of neonatal conjunctiva or ophthalmia neonatorum (164), and this range is thought to largely be a product of a patient's location and socioeconomic status. Symptoms can include purulent discharge from the eyes, inflammation of the eyelids, and periorbital edema (13). If left untreated, these infections can result in vision loss and/ or pneumonia in the neonate (148).

Diagnosis, treatment, and prevention

In 2019, 142 million persons worldwide were reported to be at an enhanced risk for ocular trachoma infections (234). Although trachoma can be cleared by the immune system,

individuals generally do not acquire long term protection after an initial case. Due to the high prevalence of trachoma in endemic regions, reinfection is common. Mass antibiotic campaigns in the past have tried to reduce the burden of ocular chlamydial infections; however, antibiotic usage alone is unlikely to eradicate trachoma, given the high rate of asymptomatic infections. "SAFE", a campaign developed by the WHO to eradicate trachoma, utilizes a number of techniques to try to treat symptomology while also decreasing the population burden in under-developed countries. Recommendations include surgery for those facing trichiasis (which leads to blindness), the administration of antibiotics for symptomatic cases, and improved facial cleanliness practices for all members of hard-hit communities. Environmental improvements are also recommended, such as improved access to clean water, safe sanitation facilities, and control of flies. Despite these well-coordinated efforts, the WHO goal to globally eradicate trachoma by 2020 was not met (60). There are currently no vaccines against *C. trachomatis*.

Comprehensive sexual education is important for the prevention of genital chlamydial infections, as the highest risk group is adolescents and young adults (274). The use of barrier contraceptives, such as latex condoms, has been demonstrated to reduce transmission of the pathogen (274). Genital chlamydial infections are treatable with a single dose of azithromycin or a seven-day course of doxycycline administered twice daily. Currently, treatment with doxycycline is recommended, as azithromycin treatment failures have been linked to an inability of the drug to reach high concentrations at various body sites (129; 208). There is also increasing concern that, due to high rates of *C. trachomatis* co-infection with *N. gonorrhoeae*, treatment with azithromycin is actually leading to enhanced antibiotic resistance in *N. gonorrhoeae* (253; 280). Given concern about patients' compliance with week-long antibiotic treatment regimens, a single dose of azithromycin is often still prescribed. It is recommended that patients get retested

after the conclusion of antibiotic treatment and that their sexual partners also get tested and treated (274). It is projected that between 5 and 23% of cases result in treatment failure, and reinfection from sexual partners is likely a contributing factor (14; 82; 101; 223). The current course of treatment for the more invasive LGV serovars of *C. trachomatis* is a three-week course of doxycycline taken twice daily (274). This clinical recommendation is based off of the assumption that infections with LGV serovars are more difficult to treat; however, to date no clinical study has provided any direct or indirect evidence of this (91).

The most sensitive screening method for chlamydial infections is Nucleic Acid Amplification Testing (NAAT) (51). Screening for *C. trachomatis* is recommended for all sexually active females under the age of 25 and for females with high risk factors: those having a new partner, multiple partners, or a *C. trachomatis* positive partner (43). The goal of this screening is to prevent pelvic inflammatory disease and other sequelae. Although screening is not currently recommended for sexually active males, certain risk factors do enhance the need for testing (274). Furthermore, it is recommended that pregnant persons get screened several times during their pregnancy and be treated with azithromycin if they test positive for *C. trachomatis* (164). Azithromycin is the drug of choice for pregnant persons due to the need for only a single dose (compliance) and because it has fewer side effects compared to other antibiotics (281). Unfortunately, untreated chlamydial infection during pregnancy can have serious consequences, including preeclampsia, preterm delivery, and low birth weight (99; 151; 177). In addition, treatment will prevent infection of the neonate conjunctiva during birth (164). If a neonate does contract neonatal chlamydial conjunctiva, they are treated with oral erythromycin to prevent vision loss and/ or pneumonia (164).

Other important members of the order *Chlamydiales*

Chlamydia pneumoniae is a causative agent of respiratory illness in humans. Although it is commonly associated with atypical pneumonia, infections can be asymptomatic or cause mild respiratory disease (133). Seropositivity for *C. pneumoniae* has been observed to be higher than 80% in some adult populations (105). Pneumonia caused by *C. pneumoniae* cannot be treated with the antibiotics typically used to treat other bacterial pneumonias and instead requires treatment with azithromycin, doxycycline, or fluoroquinolones for more than two weeks (133). Additionally, *C. pneumoniae* is associated with chronic illnesses such as atherosclerosis, chronic obstructive pulmonary disease, and reactive arthritis (89). *C. pneumoniae* has been successfully isolated from various animal species, and it is hypothesized that this microbe was originally a zoonotic pathogen prior to adapting to the human niche (171).

Chlamydia psittaci is the causative agent of respiratory and/ or gastrointestinal disease in birds and can cause zoonotic infections in humans. *C. psittaci* infections arise from the inhalation of secretions during close contact with an infected bird and can cause an atypical pneumonia disease in humans called psittacosis. In addition to respiratory symptoms, an infection with *C. psittaci* can also result in fever, malaise, and headaches (47); however, *C. psittaci* infections can also be asymptomatic. Given its debilitating symptomology and the ease with which it can be contracted and spread via inhalation, *C. psittaci* has been classified as a category B select agent due to concerns over its possible weaponization and use in bioterrorism (216).

The other members of the *Chlamydiales* cause infections in animals (10). *Chlamydia spp.* that are capable of causing infections in vertebrate hosts include: *C. muridarum* (mice), *C. pecorum* (koalas and other mammals), *C. suis* (swine), *C. abortus* (sheep and cattle), *C. felis* (felines), and *C. caviae* (guinea pigs) (10; 47). *C. abortus* has been reported to cause spontaneous

abortions in humans (206), and both *C. muridarum* and *C. caviae* are commonly used to model chlamydial infections of the murine and guinea pig genital tract respectively (57; 176).

Developmental cycle

Chlamydia spp. have a unique biphasic developmental cycle (68) (Fig. 1). The pathogen's infectious, non-replicative form (Elementary body, EB) infects a cell by binding to receptors on the cell surface; the bacterium is subsequently internalized in a process that is still not entirely understood. The resulting *Chlamydia*-containing, membrane bound compartment is called an inclusion. To mediate intracellular survival, EBs secrete effector proteins into the cell cytoplasm via a type III secretion system (T3SS). Within the inclusion, EBs transition into the microbe's replicative form (Reticulate body, RB) at approximately 8 hours post infection (hpi). RB division is dependent on peptidoglycan (PG), which is not present in *Chlamydia's* infectious form (141; 143). As the asynchronous developmental cycle progresses, RBs asynchronously transition back into EBs, beginning around 24 hpi. They then exit the host cell through either lysis or extrusion (release in a membrane bound vesicle) between 40 and 72 hpi (depending on the serovar). Under stress-inducing conditions, *Chlamydia spp.* can transition into an intracellular, metabolically active, non-replicating form (Aberrant body, AB) (Fig. 1). Once the stressor is removed, ABs can transition back into RBs and the pathogen's developmental cycle can continue (68).

ROLE OF PG IN BACTERIA

The cell wall or sacculus surrounds the cell membrane in most bacterial species, and is essential for their survival. The main component of the cell wall is PG, which is a polymer composed of glycan strands that are crosslinked by stem peptides. The glycan chains are composed of repeating disaccharides (*N*-acetylglucosamine (GlcNac) and *N*-acetylmuramic acid

(MurNac) linked by β-1,4 bonds). The stem peptide consists of unique amino acids; Gram negative bacteria utilize L-Alanine-D-Glutamine- *meso*-diaminopimelic acid (*m*DAP)- D-Alanine-D-Alanine, while in Gram positive bacteria, L-Lysine replaces *m*DAP in the third position of the stem peptide (256). PG enables bacteria to maintain thier shape, provides resistance to changes in turgor pressure, and is essential for cell division (256).

Discovery of chlamydial PG

A number of early studies provided indirect evidence that *Chlamydia spp*. utilize PG. In the early 1940s, it was demonstrated that chlamydial infections in chick embryos and mouse infection models could be resolved by treatment with penicillin, an antibiotic that targets PG assembly (96; 159; 268). These early results conflicted with clinical data at the time, which indicated that penicillin was not an effective treatment for human chlamydial infections (19; 63; 160). It was not until the 1960s that transmission electron micrographs (TEM) clearly demonstrated that the bacterium's morphology was directly altered upon treatment with penicillin; antibiotic-treated bacteria appeared enlarged compared to untreated controls (81; 103; 261). Following the discovery that penicillin inhibits PG assembly, subsequent studies confirmed the presence of these enlarged chlamydial forms following exposure to PG biosynthesis-inhibiting antibiotics, such as penicillin (154; 239; 243; 261) and D-cycloserine (167). Cell enlargement was thought to be the result of the successful inhibition of cell division.

Despite this early evidence, the presence of PG in *Chlamydia* species was disputed for another 50 years. While division could be inhibited by penicillin and other PG-targeting antibiotics in a number of *Chlamydia spp*., researchers were unable to visually or biochemically detect a canonical PG-containing cell wall. Many researchers attempted to demonstrate the presence of sugars and amino acids unique to PG, such as muramic acid, but their results were

often inconclusive. Using biochemical techniques, several research groups reported the presence of muramic acid in cell preparations from *Chlamydia spp*. (12; 113; 195; 236); however, others disputed these findings (72; 77; 149; 242). This paradox, susceptibility to PG-targeting antibiotics despite the absence of PG, was coined the 'chlamydial anomaly' (166).

Genetic advances toward solving the 'chlamydial anomaly'

When the first genome of a *Chlamydia spp*. was successfully sequenced in the early 1990s, chlamydiologists discovered that *C. trachomatis* encodes almost all of the genes associated with the PG biosynthesis pathway (157; 235). Transcriptional analysis of genes that encode the PG biosynthetic enzymes revealed that they appeared to be upregulated after the EB-to-RB transition, which coincides with the initiation of cell division in *Chlamydia spp*. (6; 7; 21). Subsequent studies confirmed the enzymatic function of the encoded proteins, while genetic complementation of *E. coli* deletion mutants further confirmed their functionality (56; 97; 124; 142; 155; 156; 158; 191; 192). The first functional chlamydial PG biosynthesis enzyme to be characterized was UDP-N-acetylglucosamine 1-carboxyvinyltransferase (MurA), which catalyzes the first committed step in PG biosynthesis (158). *C. trachomatis* is predicted to contain three single function penicillin binding proteins (PBPs), homologs of PBP2, PBP3, and PBP5/ 6 (12; 125; 179; 235), and these proteins are the targets of penicillin. Both PBP2 and PBP3 are predicted to function as transpeptidases, while PBP5/ 6 is predicted to function as a carboxypeptidase (12; 125; 179; 235).

***Chlamydia spp.* divide independent of FtsZ**

As a result of more than 700 million years of reductionist evolution during its adaptation to intracellular life, *C. trachomatis* maintains a much smaller genome than most other extracellular microbes (100). *Chlamydia spp*. lack a number of genes that are widely conserved

in most other bacterial species, including genes involved in fundamental cellular processes such as division and amino acid biosynthesis (228). When bacteria divide, PG biosynthesis is directed to the division septum by FtsZ, a tubulin-like protein that acts as the central organizer of the division complex (23). FtsZ polymers form a ring at mid-cell, which researchers propose provides the mechanical force for constriction of the cell while also recruiting other key Fts family proteins to the site of division. However, members of the Chlamydiae lack FtsZ, as well as the associated regulatory proteins that are typically associated with the division complex (ZipA, ZapA-D, MinC, FtsA, FtsB, FtsE, FtsP, and FtsX) (111).

The Rod complex is traditionally associated with side wall PG biosynthesis and with the process of elongation in rod-shaped bacteria (61). Although Chlamydiae lack FtsZ, these microbes have co-opted the Rod complex to spatially regulate the site of cell division (121; 184; 186; 210). The actin-like, filament-forming protein MreB acts as the division plane organizer in *C. trachomatis* by promoting localized PG synthesis and by recruiting other Rod complex-associated proteins to the division site (73; 109; 121; 185). The N-terminus of the MreB protein has been shown to be essential for interactions with RodZ and other divisome proteins, such as FtsK (137). When MreB polymerization is inhibited, *C. trachomatis* is unable to complete cell division (109; 141; 143; 184). Bacterial two-hybrid assays performed in *E. coli* confirmed interactions between chlamydial MreB and RodZ homologs (75; 185; 186), and it has been demonstrated that chlamydial RodZ is capable of directing chlamydial MreB to the divisome in a heterologous *E. coli* system in which both *E. coli* FtsZ and MreB are inhibited and absent, respectively (210).

Unique features of PG biosynthesis/ assembly in *Chlamydia spp*.

Despite early progress in categorizing the chlamydial PG biosynthesis pathway, the sequencing of the *C. trachomatis* genome also cast some doubt as to whether the microbe could complete the synthesis pathway. A number of key genes involved in the synthesis of the amino acids present in the PG stem peptide and the assembly of glycan chains were not initially identified in the chlamydial genome (235). The stem peptide of bacterial PG is composed of unique amino acids, such as the D-isomers of alanine and glutamine, as well as *m*-DAP. D-amino acids are typically synthesized by enzymes called racemases. However, *Chlamydia spp*. do not encode alanine or glutamate racemases in their genomes (235). Instead, they utilize enzymes that have been co-opted to serve alternate functions, such as serine hydroxymethyltransferase (GlyA) or diaminopimelate epimerase (DapF), respectively (56; 142). *C. trachomatis* also possess a unique modification in the first amino acid of the stem peptide. Typically, the MurC enzyme ligates the L-alanine to MurNac, making it the amino acid present in the first position of the stem peptide. However, the *C. trachomatis* MurC ($MurC_{CT}$) is more promiscuous in its substrate recognition than the *E. coli* homolog, and it can incorporate L-alanine, L-serine, and glycine into the first position of the stem peptide (97). $MurC_{CT}$ is also fused to the microbe's D-alanyl-D-alanine ligase (Ddl), which ligates the penultimate and terminal D-alanine amino acids together, prior to their incorporation into the stem peptide (97; 156). *Chlamydia spp*. also lack N-succinyl-aminoketopimelate aminotransferase, tetrahydrodipicolinate succinylase, and succinyl-diaminopimelate desuccinylase (235), enzymes that are necessary for the production of *m*-DAP, the third amino acid in the stem peptide of Gram negative bacteria. *Chlamydia spp*. also lack MurI, the racemase enzyme responsible for converting L-glutamine to D-glutamine, the second amino acid in the stem peptide (235). The chlamydial DapF enzyme, an epimerase that

converts L, L-DAP to D, L-*m*-DAP, has recently been shown to be capable of converting L-glutamine to D-glutamine (142; 155), effectively replacing the role of MurI.

Typically, bacteria rely on lytic enzymes, such as hydrolases (amidases) and lytic transglycosylases, to degrade PG to remodel the cell wall. Unlike most bacteria, Chlamydia *spp*. encode a single amidase, AmiA (235), which is unique in that it possesses both amidase and DD-carboxypeptidase activity (124). The enzyme is also unique in that it lacks a critical regulatory domain present in the vast majority of most other bacterial amidases, and the enzyme is enzymatically active from the time that it is first transcribed in surrogate systems (124). Although *Chlamydia spp*. do not encode any traditional lytic transglycosylases, *Waddlia chondrophila*, a relative of *Chlamydia spp*., encodes a SpoIID homolog that has lytic transglycosylase activity and can degrade PG *in vitro* (112). This SpoIID homolog is also conserved in *C. trachomatis* and is predicted to function similarly (112). Hydrolytic enzymes that cleave either amide (amidases), peptide (endopeptidases or carboxypeptidases) or glycosidic (lytic transglycosylases) bonds in PG have also been identified and characterized in *Chlamydia spp*. (111; 112; 124).

Visualization of chlamydial PG

Studies that allowed PG to be visualized within chlamydial cells not only confirmed its presence, but also provided insights into the fundamental biology of these microbes. The first successful visualization of PG in *Chlamydia spp*. was achieved using anti-sera raised against purified mycobacteria cell walls (36). In both species of *Chlamydia* examined, a protein the researchers designated septum (SEP) appeared to form ‘ring-like’ structures at the mid-cell of dividing RBs. Exposure to penicillin caused the arrangement of SEP to become 'irregular' (36). Several years later, the localization of PG in *C. trachomatis* was confirmed via a novel labeling

technique that utilized modified D-amino acid dipeptide probes (143). These probes, when added to tissue culture media, can traverse the host cell and inclusion membranes and be taken up by intracellular bacteria. The probes are D-ala-D-ala analogs and are recognized by the MurF enzyme, which incorporates them into the stem peptide of PG (143). Several pathogenic *Chlamydia spp.,* including *C. trachomatis*, *C. caviae*, *C. muridarum*, and *C. psittaci* also form ring-like PG structures (division planes) at the mid-cell of their replicative forms and puncta at their cell poles that likely represent sites of division termination (141; 143).

CELL DIVISION: BINARY FISSION VS. 'POLARIZED DIVISION'

Bacteria typically divide by a process called binary fission. During binary fission, the mother cell must double in size while the bacterial genome is replicated. After replication, the two chromosomes must successfully separate for a successful division event to occur. Once the DNA chromosomes separate, they each must localize to the appropriate location within the cell to ensure equal distribution in the subsequent progeny. Localized PG synthesis and turnover then occurs at mid cell, resulting in septation and the formation of two equally sized daughter cells (255).

C. trachomatis has long been thought to divide by binary fission, and observations demonstrating this are in large part what led to the microbe's eventual classification as a bacterial species. However, more recent observations indicate that binary fission in these organisms is the result of a uniquely asymmetric process (2; 141). Utilizing TEM, researchers have previously demonstrated the presence of apparent unequal cell division events in clinical samples obtained from human cervical swabs taken from patients with chlamydial infections (140). At the time, these observations were dismissed as fixation artifacts or believed to result from a sample being sectioned in such a way as to skew the image towards one bacterial

hemisphere in the Z-plane. More recently, fluorescence microscopy studies have provided evidence that *C. trachomatis* divides by a unique three-step mechanism that begins with an initial asymmetry (2; 54; 141) (Fig. 3). The RB undergoes localized membrane expansion at a cell pole, in conjunction with the localized enrichment of the microbe's major outer membrane protein (MOMP) (2). Despite this initial asymmetry, the process eventually results in daughter cells of equal size. *C. muridarum* also appears to utilize a similar process during cell division (54; 141). This is a relatively recently described division model, and as such, many questions remain about the process. What causes the initial asymmetry? What proteins are involved in establishing polarity in *Chlamydia spp*.? Future live-cell imaging studies will likely be needed to further validate this asymmetrical model of chlamydial cell division.

The use of PG synthesis inhibitors has helped further clarify the role of PBPs in polarized chlamydial cell division. Inhibition of PBP2 or PBP3 via mecillinam or piperacillin/ penicillin G, respectively, results in unique PG configurations (54). No PG rings are observed in the mecillinam treated cells; rather, a polar patch of PG is visualized below polarly localized MOMP at a single pole in the bacterium. Furthermore, there is no asymmetric expansion of the membrane when *C. trachomatis* is treated with mecillinam. However, following the treatment of cells with penicillin G or piperacillin, both incomplete and complete PG rings are observed at the base of newly expanding daughter cells (54). Although all of these inhibitors disrupt cell division, the mecillinam results indicate that PBP2 plays an important role in the early stages of cell division, while PBP3 appears to be more important for the growth of the daughter cell (54).

BACTOFILINS

Bacterial cytoskeleton

The cytoskeleton is important for controlling the temporal and spatial organization of a bacterial cell (80). There are three main categories of cytoskeletal elements in bacteria: actin-like proteins, tubulin-like proteins, and intermediate filament-like proteins. Tubulin-like proteins were the first cytoskeletal proteins to be described and were named due to their structural similarity to eukaryotic tubulin (145; 146). The most well-known and well-conserved tubulin-like protein is FtsZ, a filament-forming protein that is essential for division in most bacteria (23; 260). The second class of cytoskeletal proteins is actin-like proteins. An example of an actin-like protein is MreB, which directs peripheral, side-wall PG synthesis and is important for maintaining 'rod-shape' in rod shaped bacteria (107). The third class of cytoskeletal proteins is intermediate-like filaments. One well known example of an intermediate-like filament is CreS in *Caulobacter crescentus*, which forms at the inner-curvature of the bacterium and aids in maintaining the bacterial cell's shape (9).

Recently, an additional class of cytoskeletal proteins was discovered and designated bactofilin proteins (131). This class of cytoskeletal proteins is known for their ability to spontaneously form polymers or filaments without the addition of co-factors or other interaction partners (126; 131; 254). Bactofilins differ from intermediate-filaments in that they do not contain coiled-coil regions (254). They have several functions in different bacteria species, including aiding in cell division, establishing cell polarity, enabling chromosomal segregation, modifying cell shape, assisting cellular differentiation, and facilitating motility (25; 40; 59; 108; 118; 126; 131; 144; 226; 245; 254; 282). It is important to note that individual bactofilin proteins may function in one or more of these roles, as evidenced by the first bactofilin proteins identified and described, BacA and BacB, which are encoded by *C. crescentus* (131).

Characteristics of bactofilins

Bactofilin proteins do not form crystals and are highly insoluble (226); thus these proteins cannot be studied by canonical structural methods, such as x-ray crystallography and liquid-state nuclear magnetic resonance (NMR) (226). However, several other methods have been instrumental in the characterization of bactofilin proteins: solid-state NMR, TEM, scanning TEM, and electron cryotomography (59; 118; 226; 245; 254; 282). Bactofilin proteins can be identified by a conserved domain (DUF583) (254), which is generally sandwiched between a N-terminal and C-terminal domain. DUF583 contains a series of repeated ß helices that are necessary for spontaneous filament formation (254) (Fig. 4). Alanine scanning mutagenesis has been utilized to identify specific amino acids that are necessary for polymerization; when these specific amino acids are mutated, polymerization is disrupted (254). Several other studies have identified particular amino acids within the ß helices in bactofilins of interest that are necessary for polymerization (118; 282). Specifically, hydrophobic interactions within this region are thought to provide bactofilins the innate ability to form polymers (118; 254; 282). The N-terminal domain is typically associated with the cytoplasmic membrane and contains an amphipathic region (59), whereas the C-terminal domain has differing functions in different organisms (94).

Role of bactofilins in bacteria

Cell shape/ differentiation

In the late 1990s, before the term bactofilin was coined, the gene *ccmA* (curved cell morphology) was identified in a transposon mutagenesis screen in *Proteus mirabilis*. The insertion of the transposon caused a morphological change and a swarming defect (94). The transposon insertion defects were observed primarily in the swarmer cells, possibly due to the higher expression of CcmA within swarmers. The morphology changes reduced the ability of the

bacteria to form migration rafts, and thus prevented swarming (94). While studies on *P. mirabilis* CcmA were never conducted to identify the canonical ß helical core of bactofilins, *P. mirabilis* CcmA is predicted to be a bactofilin protein.

Another bactofilin ($CcmA_{HP}$) was identified from *Helicobacter pylori* during a transposon mutagenesis screen looking for cell-shape mutants (238). Upon deletion of *ccmA, H. pylori* cells lost their typical helical morphology, appeared as slightly curved rods, and exhibited a unique PG fragment profile (238). An inner membrane scaffolding protein, Csd5, was shown to stabilize the interaction of $CcmA_{HP}$ with MurF, the enzyme that catalyzes the addition of the terminal D-alanines to the stem peptide chain during PG biosynthesis (25), thus linking $CcmA_{HP}$ to localized PG biosynthesis in *H. pylori*. $CcmA_{HP}$ localizes to regions of positive curvature, while MreB localizes to regions of negative curvature in (245). Researchers proposed that these two proteins guide PG synthesis in *H. pylori*, with MreB guiding new sidewall synthesis and $CcmA_{HP}$ maintaining the curvature of the helical shape (245).

BacM from *M. xanthus* has also been demonstrated to directly affect cell shape (126). Deletion of *bacM* resulted in the alteration of the bacterium's morphology with cells becoming 'crooked.' The addition of a C-terminal tag to BacM perturbed its ability to localize and caused the cells to become deformed, while the addition of a N-terminal tag to BacM did not. Thus, the C-terminus is likely important for BacM to properly function in *P. mirabilis* (126). This study illustrates that the contribution of each bactofilin domain should be considered during characterization studies.

Cell polarity/ chromosomal segregation

Bactofilins can also contribute to the establishment of cell polarity and mediate chromosomal segregation in a number of bacterial species. *C. crescentus* possesses two

bactofilin paralogs, BacA and BacB (131). BacA and BacB localize to the one pole of *C. crescentus* that will eventually form a stalk (131). These proteins localize prior to the transition into the stalked cell and remain polarly-localized throughout the rest of the bacterium's development. BacA and BacB interact with penicillin binding protein C (PBPC) both *in vitro* and *in vivo*, and it has been suggested that their localization acts as a spatial cue for the recruitment of PBPC (131).

Another bacterium, *Myxococcus xanthus,* encodes four bactofilins within its genome: *bacM, bacN*, *bacO*, and *bacP* (126; 144). Three of these genes, *bacN*, *bacO*, and *bacP*, are encoded within the same putative operon, while *bacM* is encoded directly downstream of the operon containing the chromosomal partitioning genes *parA* and *parB* (144). BacN, BacO, and BacP localize with the chromosomal partitioning system proteins and are necessary for chromosomal replication and segregation (144).

Motility

Several bactofilin proteins have been shown to be important for bacterial motility. *Bacillus subtilis* encodes two bactofilin paralogs, BacE and BacF. These bactofilins are important for the assembly of both the filament and hook components of the flagellum, specifically in the export of flagellar proteins (67), and the deletion of both bactofilin genes results in motility defects that can be complemented when both genes are expressed in the amylase locus (67).

M. xanthus also encodes three bactofilin homologs, BacN, BacO, and BacP, that are important for cell motility. Deletion of all three genes results in Type IV pili-dependent cell motility defects; however, this result was not consistent between laboratories (126; 144). The creation of single gene deletion mutants demonstrated that only the deletion of *bacP* results in a

Type IV pili-dependent cell motility defect (40). BacP was shown to provide spatial cues for the localization of small GTPases that control localization of proteins involved in cell motility (40).

PERSISTENCE IN *CHLAMYDIA SPP.*

Characteristics of chlamydial 'persistence'

As previously mentioned, penicillin is not effective in clearing chlamydial infections in human patients (19; 63; 160). TEM revealed that the morphology of *C. trachomatis* in cells treated with penicillin and other cell wall targeting antibiotics differed from untreated controls, with *Chlamydia* RBs appearing enlarged and swollen (81; 103; 261) (154; 239; 243; 261) (167). These enlarged forms, or 'aberrant bodies' (AB), were described as viable but incapable of completing cell division and producing infectious progeny (243). A fascinating study showed that after continuous exposure to penicillin for more than three months, *C. psittaci* could still be recovered from infected cells. Furthermore, once penicillin was removed from the cell culture medium, the microbe resumed the production of infectious EBs. This observation demonstrated the reversibility of aberrance in *Chlamydia spp*., which later became one of the defining features of the pathogen's 'persistent state' (76). There are currently four defining phenotypes associated with the chlamydial persistent state: i) enlarged cell size, ii) a halt in cell division, iii) an inability to produce infectious progeny (EBs), and iv) the reversibility of these phenotypes upon removal of a stressor.

Known inducers of persistence

Although ABs were initially discovered as a result of exposure to β-lactam-based antibiotics, several additional induction conditions have been described. These include: exposure to interferon gamma (IFNγ) (tryptophan starvation) (18) (17); iron (212) and amino acid (50; 194) starvation; heat shock (116); infection of immune cells, such as monocytes (127) and

macrophages (83; 172); and co-infection with viruses, such as Herpes Simplex Virus (27; 58). There is also additional evidence that aberrant chlamydial forms may occur during natural infections. ABs have been observed in *in vivo* animal infection models as well as in tissues collected from human patients (30; 205; 211). In addition to *Chlamydia spp*., similar morphological changes that are consistent with the aberrance phenotype have been observed in distantly related organisms, such as *W. chondrophila*, following exposure to several experimental conditions *in vitro* (221). A number of studies have compared different aberrance induction conditions at the structural (166), transcriptional (20; 169; 187) and translational (26; 34) levels; however, few studies have extensively investigated how aberrance affects the interaction of *Chlamydia spp*. with their host cells.

Mechanisms of AB induction

IFNγ/ tryptophan starvation

The immune system in primate responds to intracellular bacterial infections with the production of the cytokine IFNγ, which then results in the intracellular production of indoleamine 2, 3-dioxygenase (IDO). IDO breaks down tryptophan within eukaryotic cells into two byproducts, kynurenine and N-formylkynurenine. This in turn starves *C. trachomatis* of tryptophan, as the microbe lacks a complete tryptophan biosynthesis pathway and so must acquire all of its tryptophan from its host cell (106; 241). As a defense against this ancient form of innate immunity, *C. trachomatis* downregulates global protein synthesis when tryptophan levels in a cell are low (20). As a result, low levels of IFNγ expression do not result in the clearance of *Chlamydia* from infected host cells, but rather reduces protein synthesis and induces an aberrant/ persistent state (18). Several studies have demonstrated persistence induction resulting from IFNγ exposure (20; 106; 165; 172), and IFNγ-treated bacteria have alterations in

surface antigen presentation, such as Heat shock protein 60 (Hsp60) and MOMP (18). In addition to broad changes in translation, transcriptional analysis of IFNγ-induced ABs indicates the existence of significant alterations in gene expression (20; 249).

Iron starvation

Iron depletion has also been shown to induce AB formation in *C. trachomatis* (212). Classical AB phenotypes, such as an inability to produce infectious progeny and abnormal inclusion development, are observed in response to the addition of iron chelators to cell culture growth media (5; 74; 212). Iron is an important regulatory molecule for *Chlamydia spp*. (203), and a transcriptional analysis of *C. trachomatis* under iron-restricted conditions found significant alterations in gene expression during AB formation (249). A comparison of transcriptional profiles between iron restriction-induced and IFNγ-induced persistence also revealed comparable changes in the expression of key cell division and RB-EB conversion genes (249).

in vivo relevance of chlamydial aberrant forms

Clinical infections

The existence and importance of *Chlamydia* ABs in human and animal infections is a contentious subject (16; 29; 275; 278). Much of the evidence for the existence of ABs in human infections is considered inconclusive, as these studies are mostly observational in nature and do not address whether the forms observed were viable at the time of sample fixation. ABs have been detected in human samples via TEM and immunohistochemistry in samples obtained from human cervical swabs (140) and urethral and endocervical curettage (32). As mentioned previously, there are inherent limitations with use of TEM for detecting ABs; the fixation process for preparing samples can easily affect the morphology of bacterial membranes and result in chemical artifacts. Genetic material has been isolated from culture-negative patients

after treatment with antibiotics (193); however, the presence of *C. trachomatis*-specific nucleic acids does not necessarily indicate the presence of viable bacteria (251).

Despite the shortcomings of this earlier work, the persistence phenotype may likely be relevant in natural infections, and the reactivation of ABs may contribute to reinfections (237). After tracking women for up to five years after diagnosis and treatment of genital chlamydia, five out of seven of these women had reoccurring infections with *C. trachomatis* with highly conserved genomic sequences. Since these sequences contained the initial mutations with only a few additional mutations in the following years, researchers hypothesized that these women might be infected with the same strain despite several rounds of antibiotic treatment (237).

Animal infections

There have been several descriptions of naturally occurring chlamydial ABs during animal infections. ABs have been detected in both naturally occurring and model gastrointestinal infections of *C. abortus* and *C. suis* (205). Although it is not well understood what triggered the formation of ABs during these infections, the researchers conducting these studies proposed that they may have resulted from a co-infection of *Chlamydia spp.* and *Salmonella spp.* (205). This co-infection may have triggered the induction of aberrance, similar to what has been observed in other co-infections with *Chlamydia spp.* (such as Herpes Simplex Virus) (205). Additional evidence for the existence of ABs has been demonstrated in the female genital tract during murine infection (211). Researchers proposed that the formation of ABs may be due to the presence of polymorphonuclear leukocytes in the genital tracts, as the morphology of the reported ABs was similar to ABs induced by IFNγ in tissue culture experiments (211).

Animal models of chlamydial persistence have been developed in an attempt to explore how these forms might play a role during active infections. In one such model, chlamydial

persistence is induced during murine infection with the antibiotic amoxicillin (198). Cultivable levels of *C. muridarum* were recovered in the control group, while the amoxicillin treatment group exhibited a significant reduction in bacterial shedding, and enlarged ABs were detectable in infected tissues by TEM (198). There are not many studies that directly demonstrate frontline antibiotic treatment failure in ABs. However, as previously described, one study demonstrated a significantly higher rate of azithromycin treatment failure in the amoxicillin treated mice than in the control mice (199), indicating that some forms of persistence may enhance the resistance of *Chlamydia spp*. to frontline antibiotics (199).

Additionally, there is also a murine respiratory infection model of *C. psittaci* amoxicillin-induced persistence. The model was developed to compare differentially expressed genes during aberrance-inducing conditions *in vitro* and *in vivo* (45), and researchers found differences in the transcriptional response between these two conditions (46). These observations highlight that *in vitro* conditions do not always mimic what occurs *in vivo* and emphasize that future studies on persistence in *Chlamydia spp*. should focus on how these morphological forms affect the viability of the microbe *in vivo*.

GOALS AND SPECIFIC AIMS

The overall goal of this dissertation was to gain a further understanding of the cell division processes of the obligate intracellular bacterium, *C. trachomatis*. We wanted to understand factors that allow *C. trachomatis* to establish polarity (in order to initiate the first stage in polarized cell division), test conditions that lead to cell division arrest, and establish how the interaction between host and pathogen changes when chlamydial cell division is inhibited.

My first specific aim was to identify and characterize the putative chlamydial bactofilin, $BacA_{CT}$ (Chapter 2). Initially, we hypothesized that $BacA_{CT}$ was a key protein in the

establishment of polarity in *C. trachomatis*. We carried out an *in vitro* and *in vivo* characterization of $BacA_{CT}$, utilizing fluorescent fusion constructs to examine its localization, a targeted conditional knockdown strain to gauge how the absence of the protein affected cell morphology, and a BATCH analysis to examine potential interaction partners. We did not find a role for $BacA_{CT}$ in cell polarity, but we did observe that it formed ring-like filament structures comparable in size and shape to the chlamydial PG ring and that a significant defect in cell size regulation occurred during knock-down studies utilizing CRISPRi. By characterizing and elucidating the role of this bactofilin in *C. trachomatis,* we furthered our understanding of the pathogen's basic physiology.

My second specific aim was to determine the physiological differences between aberrant/ persistent *Chlamydia* forms and to delineate how their differences affect *C. trachomatis*'s interaction with its host cell (Chapter 3). This was achieved by exposing *C. trachomatis* to six aberrance-inducing conditions and then comparing its ability to: i) produce infectious progeny, ii) generate immunostimulatory PG, iii) actively secrete T3SS effector proteins, and iv) successfully expand the inclusion membrane during the span of the microbe's developmental cycle. By characterizing the molecular underpinnings of ABs and their interactions with the host cell, we have begun to build a model for how their unique physiology may play a biologically relevant role during chlamydial infections.

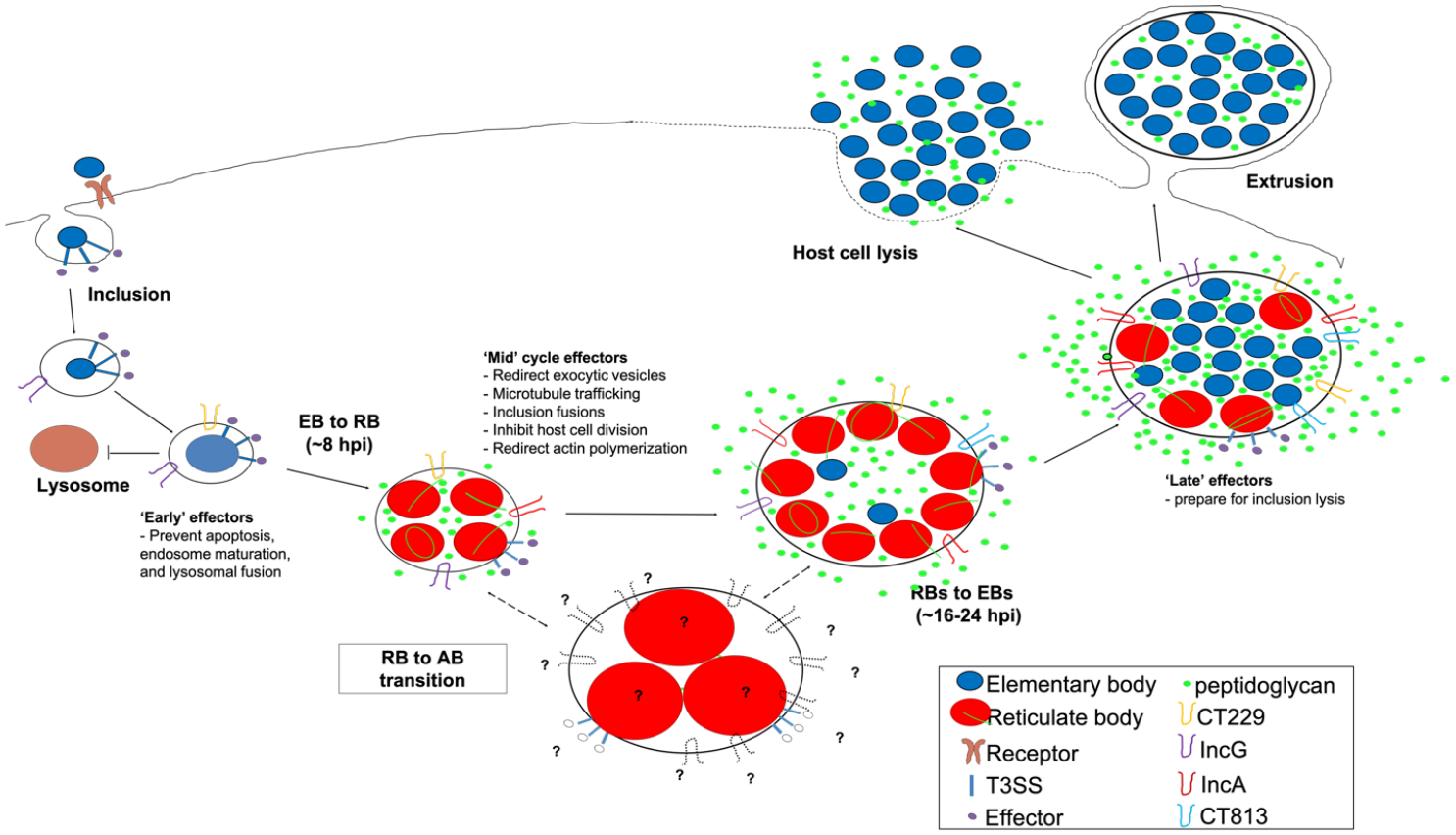


Figure 1. Biphasic developmental cycle for *Chlamydia trachomatis*.
The obligate intracellular bacterium *C. trachomatis* utilizes a biphasic developmental cycle. Infectious, non-replicative elementary bodies (EBs) infect host cells, enter a membrane bound compartment (inclusion) and secrete effector proteins via a T3SS. T3SS effectors prevent fusion of the inclusion with the lysosome, and enable *C. trachomatis* to manipulate the host cell's cytoskeletal and vesicular transport machinery. Within the inclusion, EBs transition into the microbe's replicative form (RBs) that utilize peptidoglycan to divide. As the asynchronous developmental cycle progresses, RBs transition back into EBs and exit the host cell through lysis or extrusion. Under certain stress conditions, the developmental cycle is halted and the bacteria become aberrant until the stress is removed. It is not clearly understood whether immunostimulatory PG is produced and/ or if the T3SS is functioning during this aberrance state. Furthermore, it is not understood what implications aberrance has on the interactions between *Chlamydia* and the host cell.

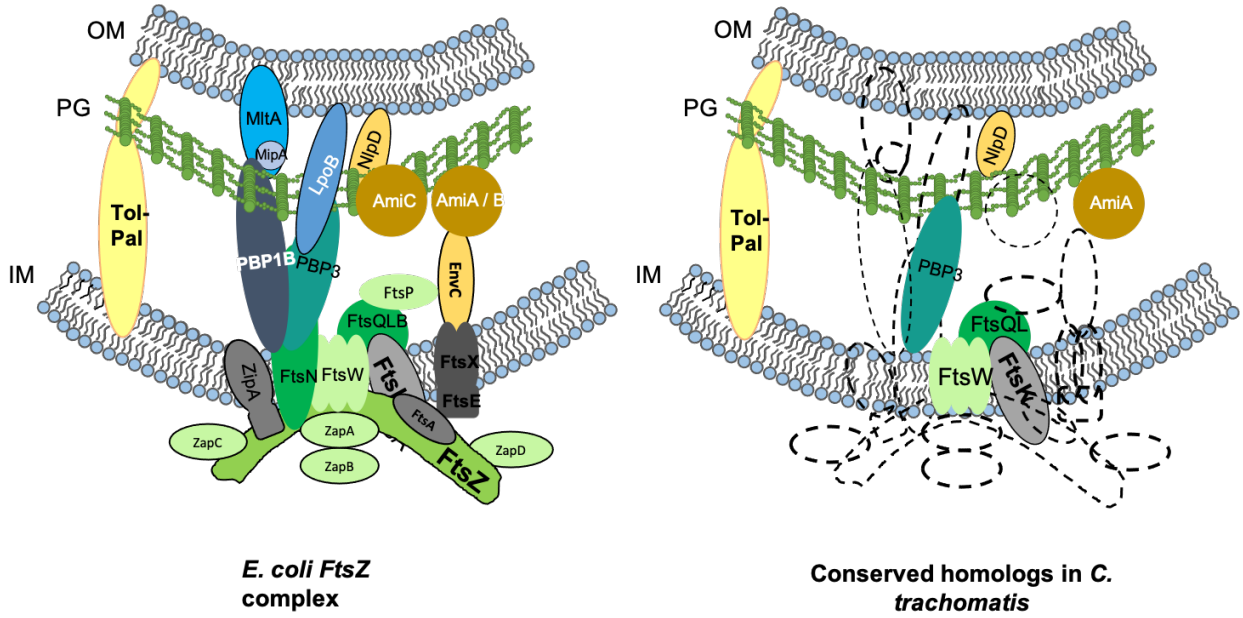


Figure 2. Comparison of cell division proteins from *C. trachomatis* (right) and *E. coli* (left). Tmembers of the Chlamydiae lack FtsZ, as well as the associated regulatory proteins that are typically associated with the division complex (ZipA, ZapA-D, MinC, FtsA, FtsB, FtsE, FtsP, and FtsX). This image from the cell division chapter in Chlamydia Biology from Genome to Disease used with permission from the author (1).

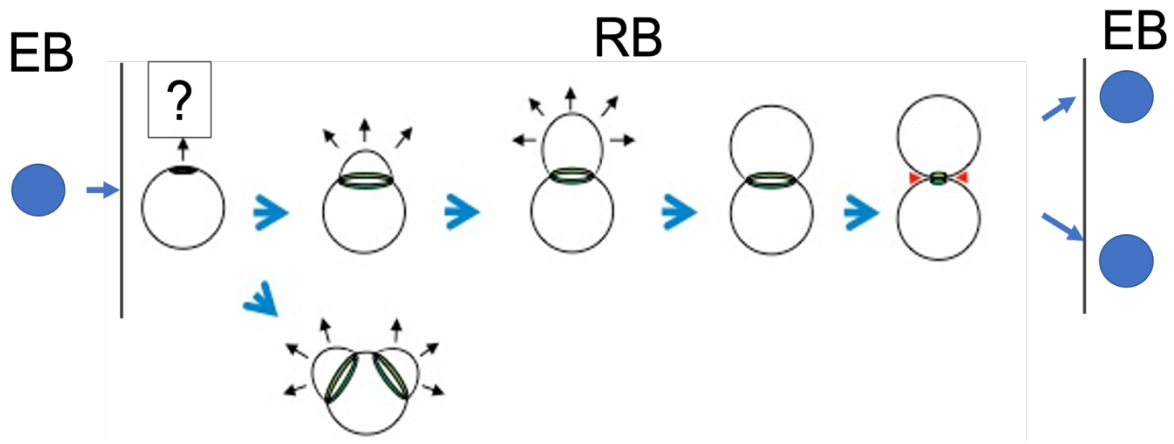
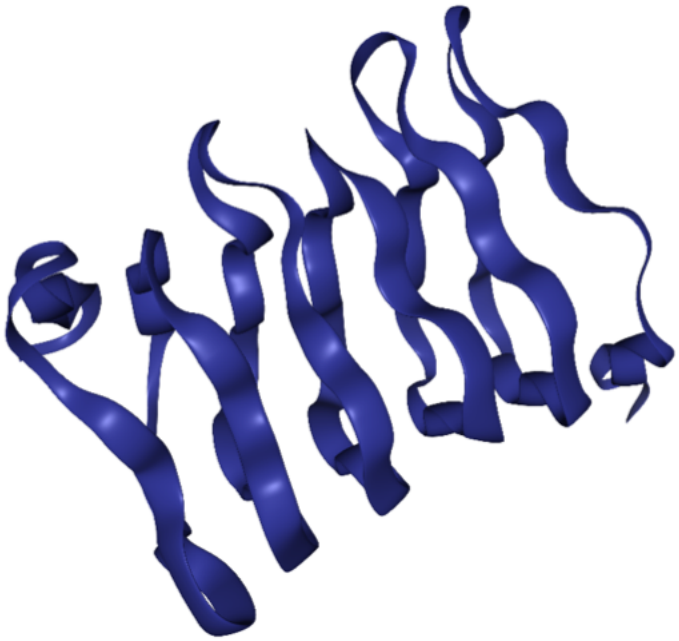


Figure 3. Model of polarized cell division in *Chlamydia*.
The chlamydial EBs (blue) convert to RBs (white) at approximately 8-10 hours post infection (hpi). RBs complete their first cell division events between 10-12 hpi. Recently, a model of polarized cell division was proposed, in which the cell division machinery initially localizes to one pole of the RB. There is an extension of membrane at this pole of the bacterium, which continues to extend until there are two equal hemispheres; however, bidirectional events have also been observed. The subsequent septation event results in two equally sized cells. Around 16-24 hpi, RBs begin transitioning back into infectious EBs. This image was modified from the cell division chapter in Chlamydia Biology from Genome to Disease (1).

A



B



Figure 4. Bactofilin Domain Architecture
(A) Structural prediction of the bactofilin domain of BacA encoded by *Caulobacter crescentus*. (B) Bactofilins are composed of three (N-terminal, Beta helical, C-terminal) domains.

Chapter 2: A dynamic, ring-forming bactofilin critical for maintaining cell size in the obligate intracellular bacterium *Chlamydia trachomatis*

PUBLISHED AS: Brockett MR*, Lee J*, Cox JV, Liechti GW, Ouellette SP. 2021. A dynamic, ring-forming bactofilin critical for maintaining cell size in the obligate intracellular bacterium *Chlamydia trachomatis*. Infect Immun 89: e0020321. https://doi.org/10.1128/IAI.00203-21.

*: authors contributed equally to this work

AUTHOR CONTRIBUTIONS: All experiments were conducted by MRB except: the transcriptional analysis of *bacA*$_{CT}$, the BACTH analyses, and the CRISPRi knockdown studies (conducted by the Ouellette Lab). The Ouellette Lab also in parallel conducted imaging studies with their independently constructed fusion proteins and also quantified the frequency of BacA$_{CT}$ localization. GWL constructed the bacA$_{CT}$-his plasmid and analyzed the spatial dimensions and fluorescence intensity of BacA$_{CT}$-mCherry. GWL and MRB conducted imaging studies together.

ABSTRACT

Bactofilins are polymer-forming cytoskeletal proteins that are widely conserved in bacteria. Members of this protein family have diverse functional roles such as orienting subcellular molecular processes, establishing cell polarity, and aiding in cell shape maintenance. Using sequence alignment to the conserved bactofilin domain, we identified a bactofilin ortholog, $BacA_{CT}$, in the obligate intracellular pathogen *Chlamydia trachomatis*. *Chlamydia* species are obligate intracellular bacteria that undergo a developmental cycle alternating between infectious, non-dividing EBs (elementary bodies) and non-infectious, dividing RBs (reticulate bodies). As *Chlamydia* divides by a polarized division process, we hypothesized that $BacA_{CT}$ may function to establish polarity in these unique bacteria. Utilizing a combination of fusion constructs and high-resolution fluorescence microscopy, we determined that $BacA_{CT}$ forms dynamic, membrane-associated filament- and ring-like structures in *Chlamydia's* replicative RB form. Contrary to our hypothesis, these structures are distinct from the microbe's cell division machinery and do not colocalize with septal peptidoglycan or MreB, the major organizer of the bacterium's division complex. Bacterial two-hybrid assays demonstrated $BacA_{CT}$ interacts homotypically but does not directly interact with proteins involved in cell division or peptidoglycan biosynthesis. To investigate the function of $BacA_{CT}$ in chlamydial development, we constructed a conditional knockdown strain using a newly developed CRISPR interference system. We observed that reducing *bacA*$_{CT}$ expression significantly increased chlamydial cell size. Normal RB morphology was restored when an additional copy of *bacA*$_{CT}$ was expressed *in trans* during knockdown. These data reveal a novel function for chlamydial bactofilin in maintaining cell size in this obligate intracellular bacterium.

INTRODUCTION

Chlamydia trachomatis is the causative agent of non-congenital infectious blindness (trachoma biovar: serovars A-C), the leading cause of bacterial sexually transmitted genital tract infections (genital tract biovar: serovars D-K), and the cause of invasive urogenital or anorectal infection (lymphogranuloma venereum biovar: serovars L1–L3) (68). Untreated genital infections can result in urethritis in men and cervicitis, pelvic inflammatory disease (PID), and ectopic pregnancy in women. The vast majority of this disease burden in the US is borne by young women between the ages of 15-24 (43). *C. trachomatis* is an obligate intracellular bacterium that has a unique biphasic developmental cycle (68). The infectious, non-replicative elementary body (EB) attaches to and is endocytosed by susceptible host cells. Within a host-derived, membrane-bound compartment (inclusion), the EB differentiates into its replicative form, the reticulate body (RB). The RB grows and divides within the inclusion before asynchronously differentiating into EBs to exit the host cell. Most bacterial species utilize the glycopolymer peptidoglycan to maintain cell shape and membrane integrity (65). The peptidoglycan layer is highly dynamic and is actively shaped and remodeled throughout bacterial growth and division. Localized peptidoglycan synthesis and hydrolysis is directed by filament-forming, cytoplasmic cytoskeletal proteins (66). The actin-like protein MreB directs peptidoglycan synthesis around the cell periphery, while the tubulin-like protein FtsZ organizes peptidoglycan synthesis at the site of division (69). FtsZ polymers form a ring that directs new peptidoglycan synthesis and recruits other key Fts family proteins to the site of division (65).

As a result of more than one billion years of adaptation to an intracellular environment (84) , *Chlamydia* species are physiologically unique in that they lack a number of genes that are

essential in other bacteria, such as *ftsZ* (100; 235). It was recently determined that *C. trachomatis* utilizes MreB to direct septal peptidoglycan biosynthesis and that MreB function is essential for *C. trachomatis* division (141; 184). Paradoxically, *C. trachomatis* does not generate side-wall peptidoglycan and maintains only a thin septal band of peptidoglycan at its division septum (141; 143). As peptidoglycan acts as a major structural support between the inner and outer membranes in Gram-negative bacteria, it is presently unclear how *Chlamydia* species maintain membrane integrity and provide structural support for transmembrane complexes in their replicative forms.

In addition to FtsZ and MreB, a new bacterial protein family of self-assembling, polymer-forming landmark proteins has been described: bactofilins. These novel cytoskeletal proteins have been identified in a large number of bacterial species (131; 226; 254; 282) and perform a variety of critical cellular functions, such as establishing cell polarity (131), maintaining cell shape by directing localized peptidoglycan biosynthesis and degradation enzymes, and aiding in chromosomal segregation during cell division (144). In this study, we identified and characterized a chlamydial bactofilin ortholog, $BacA_{CT}$. Using a combination of fixed and live-cell imaging in conjunction with a recently described CRISPRi technique, we demonstrate that $BacA_{CT}$ functions in maintaining membrane integrity outside of the chlamydial septum by forming dynamic, ring-like structures whose dimensions are similar to the previously characterized chlamydial peptidoglycan ring.

MATERIALS AND METHODS

Organisms and cell culture

McCoy (kind gift of Dr. Harlan Caldwell, NIH) and L2 mouse fibroblast cell lines and HeLa (ATCC, Manassas, VA) human epithelial cell line were cultured at 37ºC with 5% CO2 in

Dulbecco's Modified Eagle Medium (DMEM; Invitrogen, Waltham, MA) containing 10% fetal bovine serum (FBS; Hyclone, Logan, UT) and 10 μg/mL gentamicin (Gibco, Waltham, MA). *C. trachomatis* serovar L2 (strain 434/Bu) lacking the endogenous plasmid (-pL2; kind gift of Dr. Ian Clarke, Univ. Southampton) was infected and propagated in McCoy cells for use in transformations. HeLa cells were infected with chlamydial transformants in DMEM containing 10% FBS, 10 μg/mL gentamicin, 1 U/mL penicillin G, and 1 μg/mL cycloheximide. All cell cultures and chlamydial stocks were routinely tested for *Mycoplasma* contamination using the *Mycoplasma* PCR detection kit (Sigma, St. Louis, MO). *C. trachomatis* strain L2/434 Bu was obtained from the laboratory of Dr. Anthony Maurelli (University of Florida). *E. coli* TOP1 cells were used for subcloning and propagating of the shuttle vector, pREF100, whereas *E. coli* NEB10 β (New England Biolabs, Ipswich, MA) cells were used for pBOMB and pTLR2 vectors. BACTH vectors were cloned and propagated in *E. coli* NEB5αI^{q} cells (NEB). *E. coli* was grown at 30ºC or 37ºC in LB broth. Chlamydial transformations and EB recovery assays were performed in L2 or McCoy cells (mouse fibroblast-derived cell lines), while imaging infection studies were performed in HeLa cells. All chemicals and antibiotics were obtained from Sigma unless otherwise noted.

Bioinformatics analysis

Sequences for *C. trachomatis* serovar L2/434 and other chlamydial species, *Caulobacter crescentus*, *Myxococcus xanthus*, and *Thermus thermophilus* were obtained from the NCBI database (https://www.ncbi.nlm.nih.gov/) (122). Protein sequence alignment was performed using Clustal Omega website (https://www.ebi.ac.uk/Tools/msa/clustalo/) (147) and the ESPript3 program (http://espript.ibcp.fr) (213). The 3D-structure prediction was generated using SWISS-MODEL server (https://swissmodel.expasy.org/) (258) and RaptorX web-based applications.

Visualization of pathogenic chlamydial BacA structural predictions was performed with the UCSF Chimera imaging, analysis, and visualization suite (197).

Cloning

The plasmids and primers used in this study are described in Supplemental Table 1. The wild-type *C. trachomatis ct276* gene was amplified by PCR with Phusion DNA polymerase (NEB) using 100 ng *C. trachomatis* L2 genomic DNA as a template. Some gene segments were directly synthesized as a gBlock fragment (Integrated DNA Technologies, Coralville, IA). The PCR products were purified using a PCR purification kit (Qiagen, Hilden, Germany). The HiFi Assembly reaction master mix (NEB) was used according to the manufacturer's instructions in conjunction with plasmids pASK-GFP-mKate2-L2 (kind gift of Dr. P. Scott Hefty, Univ. of Kansas) cut with FastDigest AgeI and EagI (Thermofisher, Waltham, MA), pBOMB4-Tet (kind gift of Dr. Ted Hackstadt) cut with EagI and KpnI, or pKT25 or pUT18C cut with BamHI and EcoRI, depending on the construct being prepared. The CRISPRi plasmid targeting ct276 was constructed by amplifying the *S. aureus* dCas9 from pX603-AAv-CMV::NLS-dSaCas9(D10A,N580A)-NLS-3xHA-bGHpA (a kind gift of Dr. Feng Zhang; Addgene plasmid 61594 (209) and inserting it into a modified pBOMB4-Tet vector (180)). A gRNA specific to the non-template strand at the 5' end of *ct276* was then introduced or not into the BamHI site of the Sa_dCas9 encoding plasmid (see Table 1). All plasmids were also dephosphorylated with FastAP (ThermoFisher). The products of the HiFi reaction were transformed into either NEB10 β (for chlamydial transformation plasmids) or NEB5αI^{q} (for BACTH) competent cells (NEB) and plated on appropriate antibiotics, and plasmids were subsequently isolated from individual colonies grown overnight in LB broth by using a mini-prep kit (Qiagen). For chlamydial transformation, the constructs were transformed into dam^{-} dcm^{-} competent cells (NEB) and

purified as de-methylated constructs. To create the mCherry fusion construct, mCherry was amplified from pBOMB-tet-mCherry (15) and inserted into the expression vector pREF100 (210) (a kind gift from Dr. Anthony Maurelli). The *bacA*$_{CT}$ and *mCherry* amplicons were joined together by overlapping PCR. The insert PCR product and pREF100 were double digested with NotI and PstI (NEB). Digested PCR products were ligated into the pREF100 shuttle vector downstream of an anhydrous tetracycline (aTc) inducible promoter. pREF100: *bacA-His* or pREF100:*bacA-mCherry* plasmids were transformed into chemically competent TOP10 *E. coli*. Plasmids were extracted, sequenced, and transformed into either *C. trachomatis* strain L2/434 Bu or strain -pL2 via exposure to $CaCl_2$, described below.

Transformation of *Chlamydia trachomatis*

McCoy or HeLa cells were plated in a six-well plate the day before beginning the transformation procedure. *C. trachomatis* serovar L2 without plasmid (-pL2) (kind gift of Dr. Ian Clarke) was incubated with 2 µg demethylated plasmid in Tris-$CaCl_2$ buffer (10 mM Tris-Cl pH 7.5, 50 mM $CaCl_2$) for 30 min at room temperature. During this step, the McCoy/ HeLa cells were washed with 2 mL Hank's Balanced Salt Solution (HBSS) media containing $Ca2^+$ and $Mg2^+$ (Gibco). After that, cells were infected with the transformants in 2 mL HBSS per well. The plate was centrifuged at 400 x g for 15 min at room temperature and incubated at 37ºC for 15 min. The inoculum was aspirated, and DMEM containing 10% FBS and 10 µg/mL gentamicin was added per well. At 8 h post infection (hpi), the media was changed to media containing 1 µg/mL cycloheximide and either 1 or 2 U/mL penicillin G (for pBOMB4-Tet constructs) or 100 µM spectinomycin (for pREF100 constructs), and the plate was incubated at 37ºC until 48 hpi. At 48 hpi, the transformants were harvested and used to infect a new McCoy or HeLa cell monolayer. These harvest and infection steps were repeated every 44-48 hpi until mature

inclusions were observed. Chlamydial transformants were then plaque purified at least once (to ensure clonal populations) and propagated to high titer stocks for use in subsequent experiments.

Viable EB/ IFU assay

L2 mouse fibroblast cells were infected with *C. trachomatis* L2 434/Bu: pREF100-*bacA$_{CT}$-mCherry* or pREF100-*bacA$_{CT}$-his* at a MOI of ~1 in a 24-well plate with 0, 1, or 10 ng/mL of aTc for 44 hours. EBs were then mechanically harvested with glass beads and 200 μL of 1X sucrose-phosphate-glutamate (SPG) buffer (160 g of sucrose, 0.415 g of KH_2PO_4, 0.976 g of $NaHPO_4$, 0.576 g of glutamic acid diluted in 800 mL of water [pH 7.4 to 7.6]). BacA$_{CT}$-mCherry EBs were stored at -80°C, while BacA$_{CT}$-His EBs were used immediately to re-infect a new monolayer of cells. To re-infect cells, EBs were serially diluted and placed on L2 cell monolayers, seeded in a 96-well plate. At 24 hpi, 20 fields of view of GFP$^+$ inclusion forming units (IFU) were counted in duplicate for each treatment condition. Three biological replicates were performed. Similar experiments were performed for *C. trachomatis* L2 transformants carrying the pTLR2-bacA$_{CT}$_6xH::L2 plasmid with no significant differences noted between induced and uninduced conditions for either plasmid backbone (data not shown).

Labeling of chlamydial peptidoglycan and MreB

HeLa cells were infected with *C. trachomatis* L2 434/Bu: pREF100:bacA$_{CT}$-His or *C. trachomatis* L2 434/Bu: pREF100:bacA$_{CT}$- mCherry and induced with 10 ng/mL of anhydrotetracycline (aTc) at 2hpi. At 10.5, 21, and 44 hpi, cells were washed 3 times with 1X PBS, permeabilized with methanol and 0.5% Triton X (5 mins each) prior to blocking with 3% Bovine Serum Albumin (BSA) for 1 hour and antibody labeling. Peptidoglycan was metabolically labelled with D-amino acid dipeptide probes (1mM EDA-DA) and click chemistry as previously described (141; 143). His-tagged BacA$_{CT}$ was labeled with anti-His primary

antibody (mouse) and secondary antibody anti-mouse AlexFluor 594, at the dilutions 1:200 and 1:2000, respectively. Similarly, to label MreB and BacA, HeLa cells were infected with *C. trachomatis* L2 434/Bu: pREF100: $bacA_{CT}$-mCherry and induced with 10 ng/mL of aTc. At 21 hpi, cells were washed 3 times with 1X PBS, permeabilized with methanol and 0.5% Triton X (5 mins each) prior to blocking with 3% Bovine Serum Albumin (BSA) for 1 hour and antibody labeling. Major Outer Membrane Protein (MOMP) was labeled with anti-MOMP primary antibody (goat) and secondary antibody (donkey anti-goat AlexaFluor 405) at the dilutions 1:500 and 1:1000 respectively. MreB was labeled with rabbit, anti-MreB primary antibody (121) (generously provided to us by Dr. Scott Hefty of University of Kansas) and anti-rabbit secondary conjugated to AlexaFluor 488. For live cell confocal microscopy studies, HeLa cells seeded in chamber wells were infected with *C. trachomatis* L2 434/Bu: pREF100: $bacA_{CT}$-mCherry and induced with 10ng/mL of aTc at 2 hpi. Cells were imaged utilizing a Zeiss LSM 710 confocal microscope under tissue culture conditions (see above). Z-stacks were acquired at a variety of time points post infection and were used to illustrate changes occurring using single imaging planes or to generate maximum intensity projections. All video editing was done using Zen Black software (Zeiss).

Indirect immunofluorescence (IFA) microscopy

HeLa cells were seeded in 24-well plates on coverslips at a density of 105 cells per well the day before infection. Chlamydial strains expressing wild-type or truncated Ct276 with a six-histidine tag at the C-terminus were used to infect HeLa cells in DMEM media containing penicillin G and cycloheximide. At 6 hpi, 10 nM anhydrotetracycline (aTc) was added. At 10.5 hpi, the coverslips of infected cells were washed with DPBS and fixed with fixing solution (3.2% formaldehyde and 0.022% glutaraldehyde in DPBS) for 2 min. The samples were then washed

three times with DPBS and permeabilized with ice-cold 90% methanol for 1 min. Afterwards, the fixed cells were labeled with primary antibodies including goat anti-major outer-membrane protein (MOMP; Meridian, Memphis, TN) and mouse or rabbit anti-six histidine tag (Genscript, Nanjing, China and Abcam, Cambridge, UK, respectively). For experiments using CRISPR interference, a rabbit anti-Sa_Cas9 was used (Abcam). Secondary antibodies, donkey anti-goat antibody (594), donkey anti-rabbit antibody (647), and donkey anti-mouse (488) were used to visualize the primary antibodies. The secondary antibodies were obtained from Invitrogen. Coverslips were observed by using Zeiss LSM 800/980 confocal microscopes, a Zeiss AxioImager.Z2 with Apotome2, or a Zeiss ELYRA PS.1 super-resolution microscope as noted in the figure legends. Average RB size as displayed in Figures 7 and 9 and the inclusion sizes were measured using FIJI software. For induced samples, the dCas9-positive cells were measured. The data were represented by box plot. For the inclusion size, we measured the longest and shortest diameters and took the average of these measurements.

BACTH assay

The pKT25 and pUT18C vectors encoding the genes of interest or empty vectors were co-transformed into competent DHT1 *E. coli*, an adenylate cyclase-deficient strain, and spread onto M63 minimal media plates containing 50 μg/mL ampicillin, 25 μg/mL kanamycin, 0.5 mM IPTG, 0.2% maltose, 40 μg/mL X-gal, and 0.04% casamino acids. The plates were incubated at 30ºC for up to seven days. Blue colonies indicate positive interactions whereas no growth or small white colonies indicate no interactions. β-galactosidase assays were performed as described elsewhere on overnight cultures grown in M63 minimal medium broth containing the same supplements except for X-gal (137; 186).

Transcriptional analyses in *Chlamydia trachomatis*

HeLa cells were infected with the *C. trachomatis* L2 transformants carrying the Sa_dCas9 +/- gRNA plasmid. At 4hpi, Sa_dCas9 expression was induced. Total RNA and DNA were collected from replicate wells using Trizol (Invitrogen) and the DNeasy Tissue (Qiagen) kit as described elsewhere (2). After DNase treatment of total RNA, cDNA was synthesized using Superscript III reverse transcriptase (Invitrogen), and equal volumes of cDNA were used in qPCR reactions (2). Similarly, equal mass of DNA was used from each sample in qPCR reactions to quantify chlamydial genomes, which were used to normalize transcript data (182).

RESULTS

The chlamydial gene, *ct276/ ctl_0528*, encodes a bactofilin ortholog

Recently, a number of studies have revealed the importance of a novel class of cytoskeletal proteins in bacteria. These proteins have been designated bactofilins, and they have been associated with diverse functions such as determining cellular polarity and maintaining cell shape (131). Given that pathogenic *Chlamydia* species divide by a polarized division mechanism (2; 54; 137), we hypothesized that they possess a bactofilin homolog that could serve to establish polarity in this unique organism. Bactofilins retain a conserved domain, DUF583 (150), that forms a β-helical core region essential for the polymerization of protein monomers (131; 226; 254; 282). We used this domain to bioinformatically search for a chlamydial homolog, and our analysis revealed that the gene *ct276/ ctl_0528* encodes a 194 amino acid protein with this conserved feature. Homologs of this gene are present in all pathogenic species of *Chlamydia* examined and are located 3' to the *dnaA2* gene (Fig. 5A, Fig. 6). Interestingly, no homolog for $BacA_{CT}$ is encoded in the genomes of any of the '*Chlamydia*-related' bacteria that make up the other members of the order Chlamydiales, such as *Parachlamydia acanthamoebae, Simkaniae*

negevensis, and *Waddlia chondrophila*. Pathogenic *Chlamydia* species differ from these *Chlamydia*-related bacteria in one key way: they lack a peptidoglycan sacculus.

Sequence alignments and *in silico* protein prediction models indicate that the β-helical core is highly conserved at the amino acid (Fig. 5B, >57% identity/similarity) and structural (Fig. 6) levels. As the closest structural homolog with a solved crystal structure in the Protein Data Base (PDB) is the bactofilin encoded by *Caulobactor vibrioides* (*bacA*, PDB: 2N3B.1.A), we chose to rename the gene encoding the chlamydial bactofilin as *bacA$_{CT}$*. Since the capacity to form filaments is a characteristic of all bactofilin proteins, we tested the ability of BacA$_{CT}$ to interact homotypically using the bacterial adenylate cyclase-based two hybrid (BACTH) system. We found that BacA$_{CT}$ interacts with itself (Fig. 5C), as expected, similar to results previously reported in a much larger protein-protein interaction study that utilized a yeast two hybrid system (233). Based on these data, we conclude that BacA$_{CT}$ is a canonical bactofilin.

Given that *Chlamydia* is characterized by its unique developmental cycle, we monitored the transcription of *bacA$_{CT}$* to determine whether its expression pattern was associated with early cycle events (i.e. EB to RB differentiation), mid cycle events (i.e. growth and division of the RB), or late cycle events (i.e. RB to EB differentiation). We determined that *bacA$_{CT}$* transcription peaks at 16h post-infection (hpi) (Fig. 5D), consistent with previous studies (21) and indicating that protein may function in RB growth and division.

BacA$_{CT}$ polymers are dynamic, alternating between puncta and ring-like structures

Bactofilin proteins exhibit different functions in different bacterial species that can often be inferred based on their localization within a microbe. For example, BacA from *C. crescentus* localizes to a single pole and contributes to stalk synthesis by recruiting PbpC (131), whereas

CcmA in *Helicobacter pylori* localizes to positively curved regions of the helical cell envelope and directs peptidoglycan remodeling enzymes responsible for maintaining the microbe's unique helical shape (238). We wanted to determine where $BacA_{CT}$ localizes within *Chlamydia* RBs. To investigate the subcellular localization of $BacA_{CT}$, we constructed C-terminal hexahistidine (6xH) and mCherry $BacA_{CT}$ fusion constructs for expression in the *C. trachomatis* strain L2 434/Bu. Constructs were cloned into shuttle plasmids under the control of an anhydrotetracycline (aTc) inducible promoter and transformed into *C. trachomatis*, as described previously (137; 229). Cell division genes are precisely regulated in bacteria, and their overexpression often causes fitness defects, including in *Chlamydia* (64; 185). To eliminate this possibility, we first examined whether the induction of $BacA_{CT}$ fusion constructs affects the fitness of *C. trachomatis* transformants by quantifying the ability of the organism to complete its developmental cycle and generate infectious elementary bodies (or inclusion forming units, IFU). We found that the induction of our $BacA_{CT}$ constructs resulted in no measurable differences in the number of IFU recovered at 44 hpi, regardless of the concentration of aTc (data in Appendix A). Similar results were obtained when expressing $BacA_{CT}$-6xH from a different plasmid backbone (pTLR2; data not shown). Therefore, induction of $BacA_{CT}$, with either a 6xH or an mCherry tag, does not adversely affect progression through the developmental cycle.

We next utilized our $BacA_{CT}$-mCherry expressing strain to document the organization and localization of $BacA_{CT}$ in actively growing chlamydial RBs via live-cell imaging microscopy. We observed that the fusion protein predominantly accumulated in puncta, filaments, or partial 'ring-like' structures (Fig. 7A, B). A quantitative analysis of the spatial dimensions and fluorescence intensity associated with individual bactofilin structures in *Chlamydia* indicated that, when accounting for differences in volume, puncta forms displayed much higher mean

fluorescence intensity measurements than filaments or ring-like structures (Fig. 7C, Fig. 8). We hypothesized that this might indicate that puncta differ from filamentous/ ring-like forms either by the density of their monomeric bactofilin proteins or as a result of differences in filament tension. As these strains retain their parental $BacA_{CT}$, we could not exclude the possibility that our fusion constructs simply tend to associate better with puncta than with rings / filamentous forms. However, an alternative explanation is that rather than two completely different structures, these forms are actually transient and interchangeable. To test this possibility, we conducted a series of time course studies to determine the dynamics of these structures in living cells. We observed that larger $BacA_{CT}$_mCherry puncta are capable of transitioning into ring-like forms in the span of approximately 30 minutes (Fig. 7D), suggesting that, similar to the peptidoglycan ring-like structures inherent to pathogenic *Chlamydia* species (141) , these structures are dynamic. Based on these data, we hypothesize that $BacA_{CT}$ functions in stabilizing cell morphology during the division process.

$BacA_{CT}$ does not associate with cell division components

Chlamydia divides by a polarized division process (2). Given the dynamic nature of the $BacA_{CT}$ rings and their apparent similarity in characteristics to the PG ring, we hypothesized that $BacA_{CT}$ may function in the establishment of polarity and thus interact/intersect with the division machinery. We began by examining $BacA_{CT}$ localization during the initial stages of the developmental cycle. HeLa cells were infected with the transformant, and expression of the 6xH construct was induced at 6 hpi. Infected cells were fixed to preserve their polarity at 10.5 hpi, a time when *C. trachomatis* is in its initial division (2), and processed for immunofluorescence analysis to detect both the 6xH tag and the major outer membrane protein (MOMP) of the *Chlamydia* organism. Note the polar localization of the MOMP label in the budding daughter

cell. We observed that $BacA_{CT}$_6xH accumulated at or near the membrane of chlamydial RBs in short filamentous structures (Fig. 9A). Filaments were not restricted to a particular site within the RB, exhibiting a roughly equal distribution between the budding daughter cell (upper panel – 29%), the opposite pole of the dividing RB (middle panel – 31%), and in association with the division plane (lower panel - 40%). Thus, $BacA_{CT}$ forms membrane-associated filaments that do not appear to preferentially localize to any particular site in the dividing RB. However, we cannot exclude that there is a preference for an initial assembly site based on uncharacterized context-dependent cues.

To determine whether we could also visualize ring structures using the $BacA_{CT}$-6xH strain, we observed samples using 3D-SIM super-resolution. Infected cells were induced for expression of $BacA_{CT}$-6xH at 8 hpi and fixed and processed for imaging at 24 hpi as described above. The 3D maximum projection from composite images in Figure 7B demonstrate clear ring shapes, filaments, and puncta consistent with our live-cell imaging results. Importantly, we have made the same observations using different genetic constructs from different plasmid backbones thus reinforcing our conclusion that $BacA_{CT}$ is a filament- and ring-forming bactofilin.

We next evaluated $BacA_{CT}$ localization with respect to the forming division septum, as indicated by the chlamydial PG structure, during the middle stages of the developmental cycle. We utilized the PG-labeling, D-amino acid dipeptide probe EDA-DA (141; 143), which is incorporated into newly synthesized bacterial PG by UDP-N-acetylmuramoyl-tripeptide-D-alanyl-D-alanine ligase (MurF) (134; 141; 143). An examination of the localization of $BacA_{CT}$ filaments in RBs within fixed, *Chlamydia*-infected cells at 18 hpi revealed the presence of both filaments as well as punctate structures, similar to our observations at the early stage of the developmental cycle and to our live-cell imaging data (Fig. 7). However, neither filaments nor

puncta appeared to consistently co-localize with PG rings (Fig. 9C-D). As further evidence that $BacA_{CT}$ does not directly associate with the division apparatus, we also labeled MreB, a major organizer of the chlamydial division and PG biosynthesis machinery (137; 141; 184; 210). We have previously shown that the PG ring and MreB co-localize in *C. trachomatis* (141), and, in line with our PG results in Fig. 9, we similarly found no co-localization of $BacA_{CT}$ with $MreB_{CT}$ (Fig. 8C).

Finally, we utilized a bacterial adenylate cyclase-based two hybrid (BACTH) system to test $BacA_{CT}$ interaction with several key components of the *C. trachomatis* divisome (MreB (137; 143; 184; 210), RodZ (121; 186), FtsK (184), FtsQ (185), FtsL (185), and FtsW) as well as with DnaA2 (encoded in an apparent operon with $bacA_{CT}$), and DnaA1. We were unable to detect any interaction between $BacA_{CT}$ and any of these proteins (Fig. 9E), indicating that $BacA_{CT}$ does not appear to influence cell division through direct protein-protein interactions with this subset of cell division proteins. Overall, our data indicate that $BacA_{CT}$ does not function directly in cell division.

Inducible knockdown of $BacA_{CT}$ alters chlamydial morphology

To further investigate the function of $BacA_{CT}$, we down-regulated its expression using CRISPRi technology that we recently developed for *Chlamydia* (180; 181). A chlamydial expression plasmid was constructed encoding an aTc-inducible dCas9 ortholog from *S. aureus* (209) and a constitutively expressed gRNA targeting the non-template strand of the 5' region of the $bacA_{CT}$ coding region. This vector was transformed into *C. trachomatis* L2 and subsequently used for experimentation. As a control, we also created a transformant carrying a plasmid encoding only the aTc-inducible dCas9.

Cells were infected with the transformants, and nucleic acids were collected under uninduced and induced conditions at 11.5, 16.5, and 24 hpi. Transcript levels were measured for *bacA*$_{CT}$, the co-transcribed *dnaA2*, as well as an unrelated gene, *euo*, expressed early in the developmental cycle and associated with stress responses in *Chlamydia* (21; 183; 266). Transcripts for *bacA*$_{CT}$ were significantly reduced, roughly ten-fold, after dCas9 expression was induced in the transformant carrying the gRNA targeting *bacA*$_{CT}$, whereas no consistent biologically meaningful change (>2x) across time points was observed in transcript levels of the co-transcribed *dnaA2* or the unrelated *euo* (Fig. 10A-C). Conversely, the transcript level of *bacA*$_{CT}$ was decreased at each timepoint we assessed.

Of note, the dCas9 expression appears heterogeneous as the dCas9 ortholog encodes a degradation tag to reduce leakiness (180; 272). Thus, some bacteria are labeled very brightly with the antibody whereas others less so. This complicates imaging since adjusting the exposure time to detect dCas9 in all organisms results in over-exposure of the image. Theoretically, only one dCas9 protein is required to bind its gRNA target on the chromosome to block transcription, and detecting one protein copy by immunofluorescence is unlikely. Thus, the presence or absence of dCas9 expression within a bacterium should not be the only factor considered when determining whether knockdown was successful. More importantly, *bacA*$_{CT}$ transcripts were reduced by over 80% within the knocked down population at 24hpi, and we noted significant morphological changes in these populations compared to the uninduced control (Fig. 10A-C). Upon knocking down *bacA*$_{CT}$ expression, *Chlamydia* RBs were enlarged and displayed patchy and non-uniform localization of the chlamydial Major Outer Membrane Protein (MOMP). The enlargement of the RB forms was quantified from 216 bacteria each in the uninduced and induced cultures, from 9 and 18 inclusions, respectively, revealing that knockdown of *bacA*$_{CT}$

resulted in organisms that were more than twice the size of normal RB forms (Fig. 10D). The average diameter of the inclusions from induced conditions was ~17 μm whereas the diameter of inclusions from uninduced cultures was ~14μm ($p<0.05$). The biological relevance of the slightly larger inclusions in the induced cultures is not apparent, but it may be related to the larger organisms residing in them. In the dCas9 only control, no changes were observed in transcript levels for any of the measured genes, and we did not observe any morphological defects (Fig. 11A, C).

Knockdown of $BacA_{CT}$ has minimal impact on peptidoglycan ring formation and progression through the developmental cycle

We next assessed effects of *bacA*$_{CT}$ knockdown on peptidoglycan labeling to determine whether the larger RB reflected the fact that the cells were in some way disrupted in their ability to divide. For example, penicillin can block chlamydial cell division, which results in aberrantly enlarged organisms with disorganized peptidoglycan structures (143; 184). Peptidoglycan localization appeared to be largely unaffected, although larger ring structures were noticeably coincident with the presence of aberrantly enlarged reticulate bodies that exhibited a budding morphology (Fig. 12A-B; Fig. 13). Therefore, the generation of the septum does not appear to be impacted by the reduction in $BacA_{CT}$ levels.

To examine the degree to which knocking down *bacA*$_{CT}$ expression affected the chlamydial developmental cycle, we quantified the number of inclusion forming units (IFU), a proxy for EB generation, and the genomic DNA level during the developmental cycle. We quantified both the number of GFP-positive inclusions, indicative of bacteria carrying the CRISPRi plasmid encoding a constitutively expressed GFP, and those that labeled only with the antibody targeting MOMP, indicative of all bacteria. The ratio of GFP^+ inclusions to $MOMP^+$ inclusions gives a measure of plasmid stability, which can be negatively impacted by

overexpressing, or potentially knocking down, a target gene (217). Importantly, no effect on chlamydial growth was detected after expressing dCas9 alone (Fig. 12). Knocking down *bacA*$_{CT}$ transcripts resulted in roughly a two-fold decrease in MOMP$^+$ IFUs and a three-fold decrease in GFP$^+$ IFUs (Fig. 12C). Furthermore, the genomic DNA levels were not significantly changed (Fig. 12D), suggesting that *bacA*$_{CT}$ knockdown does not grossly affect developmental cycle progression within the parameters of our experimental conditions. Overall, these results indicate that disrupting BacA$_{CT}$ levels negatively impacts chlamydial morphology and support the hypothesis that BacA$_{CT}$ is a morphological determinant in *Chlamydia*.

BacA$_{CT}$ knockdown can be complemented to restore normal morphology

We next sought to complement the knockdown phenotype by expressing either *bacA*$_{CT}$*_6xH* or *bacA*$_{CT}$*_mCherry* as a transcriptional fusion with dCas9. After induction with aTc, dCas9 will repress the chromosomal expression of *bacA*$_{CT}$ while the plasmid copy of *bacA*$_{CT}$*_6xH* or *bacA*$_{CT}$*_mCherry* is expressed. To measure transcriptional changes in chromosomal *bacA*$_{CT}$, we introduced synonymous changes in the plasmid copy of *bacA*$_{CT}$*_6xH* or *bacA*$_{CT}$*_mCherry* that eliminated binding of the qPCR primers used as well as the gRNA binding site. When we performed this experiment, we measured a decrease in *bacA*$_{CT}$ transcripts as noted above (Fig. 14A, B). Importantly, when we imaged bacteria from uninduced and induced conditions, we observed both dCas9 and BacA$_{CT}$ labeling within RBs in the induced conditions only (Fig. 14C, E). Critically, the RBs exhibited normal morphology under these conditions with BacA$_{CT}$ ring forms clearly visible (Fig. 15), thus indicating successful complementation of the knockdown phenotype. RB diameters of the BacA$_{CT}$ _6xH complemented strain were quantified from 190 bacteria each from 6 and 7 inclusions in the uninduced and induced conditions, respectively. For the BacA$_{CT}$_mCherry complemented strain, RB diameters were measured from

211 bacteria each from 5 inclusions of both conditions. All inclusions were of equal average diameter between the uninduced and induced conditions. These data reveal that complementation with either fusion protein restored normal RB size (Fig. 14D, F). These data also suggest that both fusion proteins are functional, consistent with our data presented above.

When taken together, our data demonstrate that $BacA_{CT}$ 1) associates with the bacterial membrane, 2) fails to localize or interact with components of the bacterium's cell division machinery, and 3) directly influences the size of *Chlamydia*'s replicative form. Thus, we hypothesize that $BacA_{CT}$ functions as a dynamic, membrane stabilizing agent during the pathogen's growth and division process.

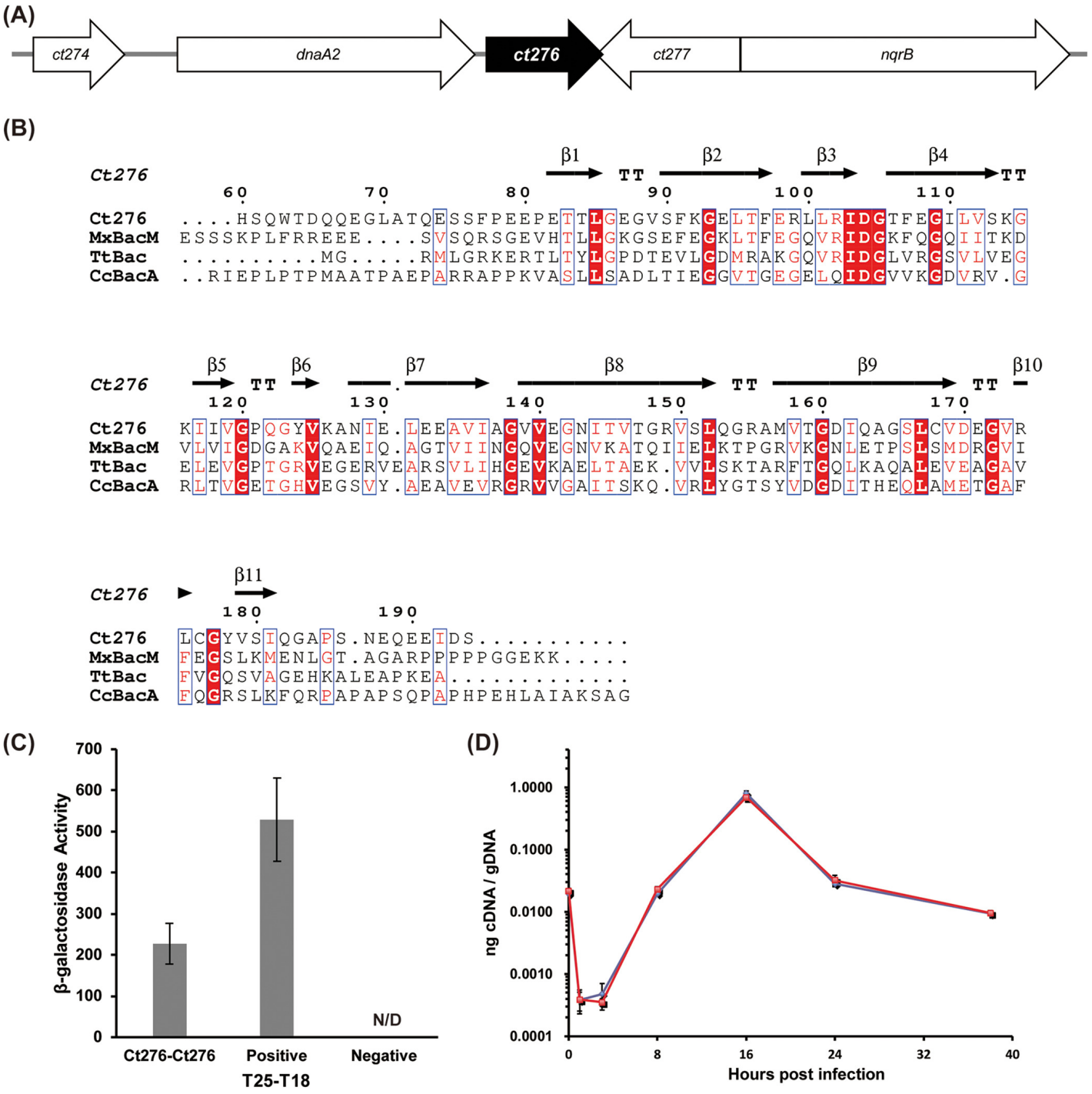
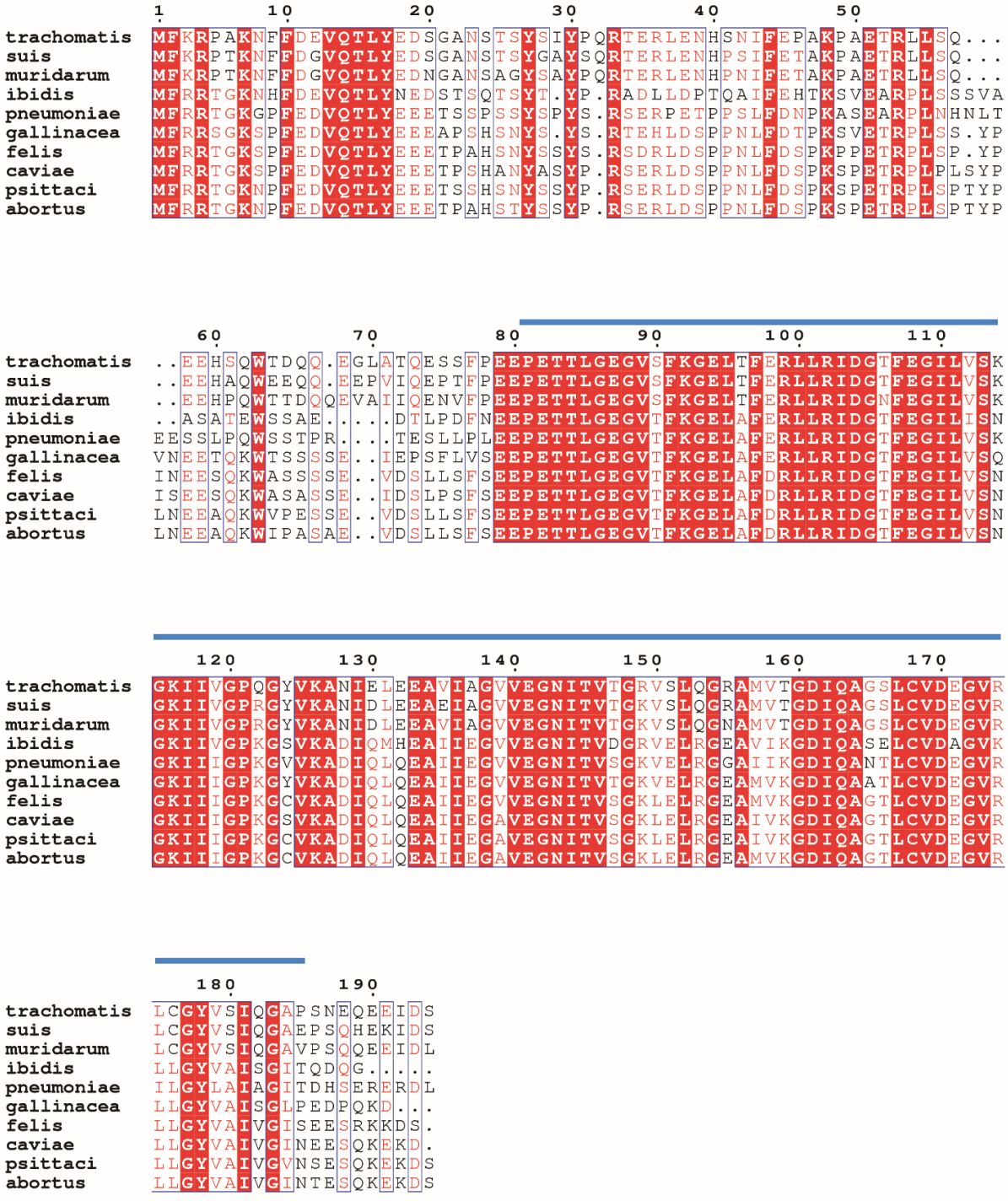


Figure 5. The chlamydial gene *ct276*/*ctl_0528* (*bacA*$_{CT}$) encodes a bactofilin protein. (A) Illustration of the *bacA*$_{CT}$ locus from *C. trachomatis* serovar D UW-3/Cx. Gene order and orientation are highly conserved in all pathogenic *Chlamydia* species examined. (B) Amino acid alignments of *bacA*$_{CT}$ with other DUF583 domain-containing bactofilins

(*Myxococcus xanthus* BacM, *Thermus thermophilus* Bac, and *Caulobacter crescentus* BacA). The DUF583 domain, a characteristic structural region of all bactofilin proteins, is composed of sequential beta sheets (black arrows). (C) The capacity for $BacA_{CT}$ monomers to directly interact with each other was quantified utilizing a bacterial adenylate cyclase-based two-hybrid (BACTH) system. Readouts were assessed by β-galactosidase assay. A positive control is an interaction between T25-Zip and T18-Zip, the GCN4 leucine zipper motif, and a negative control is the lack of interaction between T25 and T18-Ct276. The entire assay was conducted in biological triplicates, and error bars represent standard deviations of the means. N/D, not detected. (D) Expression profile of $bacA_{CT}$ during the developmental cycle of *C. trachomatis*. Each data point represents the mean from three technical replicates, and data are shown from two independent biological replicates (red versus black).

(A)


1 10 20 30 40 50
trachomatis MFKRPAKNFFDEVQTLYEDSGANSTSYSIYPQRTERLENHSNIFEPAKPAETRLLSQ...
suis MFKRPTKNFFDGVQTLYEDSGANSTSYGAYSQRTERLENHPSIFETAKPAETRLLSQ...
muridarum MFKRPTKNFFDGVQTLYEDNGANSAGYSAYPQRTERLENHPNIFETAKPAETRLLSQ...
ibidis MFRRTGKNHFDEVQTLYNEDSTSQTSYT.YP.RADLLDPTQAIFEHTKSVEARPLSSSVA
pneumoniae MFRRTGKGPFEDVQTLYEEETSSPSSYSPYS.RSERPETPPSLFDNPKASEARPLNHNLT
gallinacea MFRRSGKSPFEDVQTLYEEEAPSHSNYS.YS.RTEHLDSPPNLFDTPKSVETRPLSS.YP
felis MFRRTGKSPFEDVQTLYEEETPAHSNYSSYS.RSDRLDSPPNLFDSPKPPETRPLSP.YP
caviae MFRRTGKSPFEDVQTLYEEETPSHANYASYP.RSERLDSPPNLFDSPKSPETRPLPLSYP
psittaci MFRRTGKNPFEDVQTLYEEETSSHSNYSSYP.RSERLDSPPNLFDSPKSPETRPLSPTYP
abortus MFRRTGKNPFEDVQTLYEEETPAHSTYSSYP.RSERLDSPPNLFDSPKSPETRPLSPTYP
60 70 80 90 100 110
trachomatis ..EEHSQWTDQQ.EGLATQESSFPEEPETTLGEGVSFKGELTFERLLRIDGTFEGILVSK
suis ..EEHAQWEEQQ.EEPVIQEPTFPEEPETTLGEGVSFKGELTFERLLRIDGTFEGILVSK
muridarum ..EEHPQWTTDQQEVAIIQENVFPEEPETTLGEGVSFKGELTFERLLRIDGNFEGILVSK
ibidis ..ASATEWSSAE.....DTLPDFNEEPETTLGEGVTFKGELAFERLLRIDGTFEGILISN
pneumoniae EESSLPQWSSTPR.....TESLLPLEEPETTLGEGVTFKGELAFERLLRIDGTFEGILVSK
gallinacea VNEETQKWTSSSSE..IEPSFLVSEEPETTLGEGVTFKGELAFERLLRIDGTFEGILVSQ
felis INEESQKWASSSSE..VDSLLSFSEEPETTLGEGVTFKGELAFDRLLRIDGTFEGILVSN
caviae ISEESQKWASASSE..IDSLPSFSEEPETTLGEGVTFKGELAFDRLLRIDGTFEGILVSN
psittaci LNEEAQKWVPESSE..VDSLLSFSEEPETTLGEGVTFKGELAFDRLLRIDGTFEGILVSN
abortus LNEEAQKWIPASAE..VDSLLSFSEEPETTLGEGVTFKGELAFDRLLRIDGTFEGILVSN
120 130 140 150 160 170
trachomatis GKIIVGPQGYVKANIELEEAVIAGVVEGNITVTGRVSLQGRAMVTGDIQAGSLCVDEGVR
suis GKIIVGPRGYVKANIDLEEAEIAGVVEGNITVTGKVSLQGRAMVTGDIQAGSLCVDEGVR
muridarum GKIIVGPRGYVKANIDLEEAVIAGVVEGNITVTGKVSLQGNAMVTGDIQAGSLCVDEGVR
ibidis GKIIVGPKGSVKADIQMHEAIIEGVVEGNITVDGRVELRGEAVIKGDIQASELCVDAGVK
pneumoniae GKIIIGPKGVVKADIQLQEAIIEGVVEGNITVSGKVELRGGAIIKGDIQANTLCVDEGVR
gallinacea GKIIIGPKGYVKADIQLQEAIIEGVVEGNITVTGKVELRGEAMVKGDIQAATLCVDEGVR
felis GKIIIGPKGCVKADIQLQEAIIEGVVEGNITVSGKLELRGEAMVKGDIQAGTLCVDEGVR
caviae GKIIIGPKGSVKADIQLQEAIIEGAVEGNITVSGKLELRGEAIVKGDIQAGTLCVDEGVR
psittaci GKIIIGPKGCVKADIQLQEAIIEGAVEGNITVSGKLELRGEAIVKGDIQAGTLCVDEGVR
abortus GKIIIGPKGCVKADIQLQEAIIEGAVEGNITVSGKLELRGEAMVKGDIQAGTLCVDEGVR
180 190
trachomatis LCGYVSIQGAPSNEQEEIDS
suis LCGYVSIQGAEPSQHEKIDS
muridarum LCGYVSIQGAVPSQQEEIDL
ibidis LLGYVAISGITQDQG.....
pneumoniae ILGYLAIAGITDHSERERDL
gallinacea LLGYVAISGLPEDPQKD...
felis LLGYVAIVGISEESRKKDS.
caviae LLGYVAIVGINEESQKEKD.
psittaci LLGYVAIVGVNSESQKEKDS
abortus LLGYVAIVGINTESQKEKDS

(B)



Figure 6. $BacA_{CT}$ contains a β-helical core domain that is universally conserved in all bactofilins. (A) Amino acid sequence alignment of pathogenic *Chlamydia sp*. BacA. β-helical core domain is delineated by the blue bar. (B) Structural predictions of $BacA_{CT}$ encoded pathogenic *Chlamydia* species.

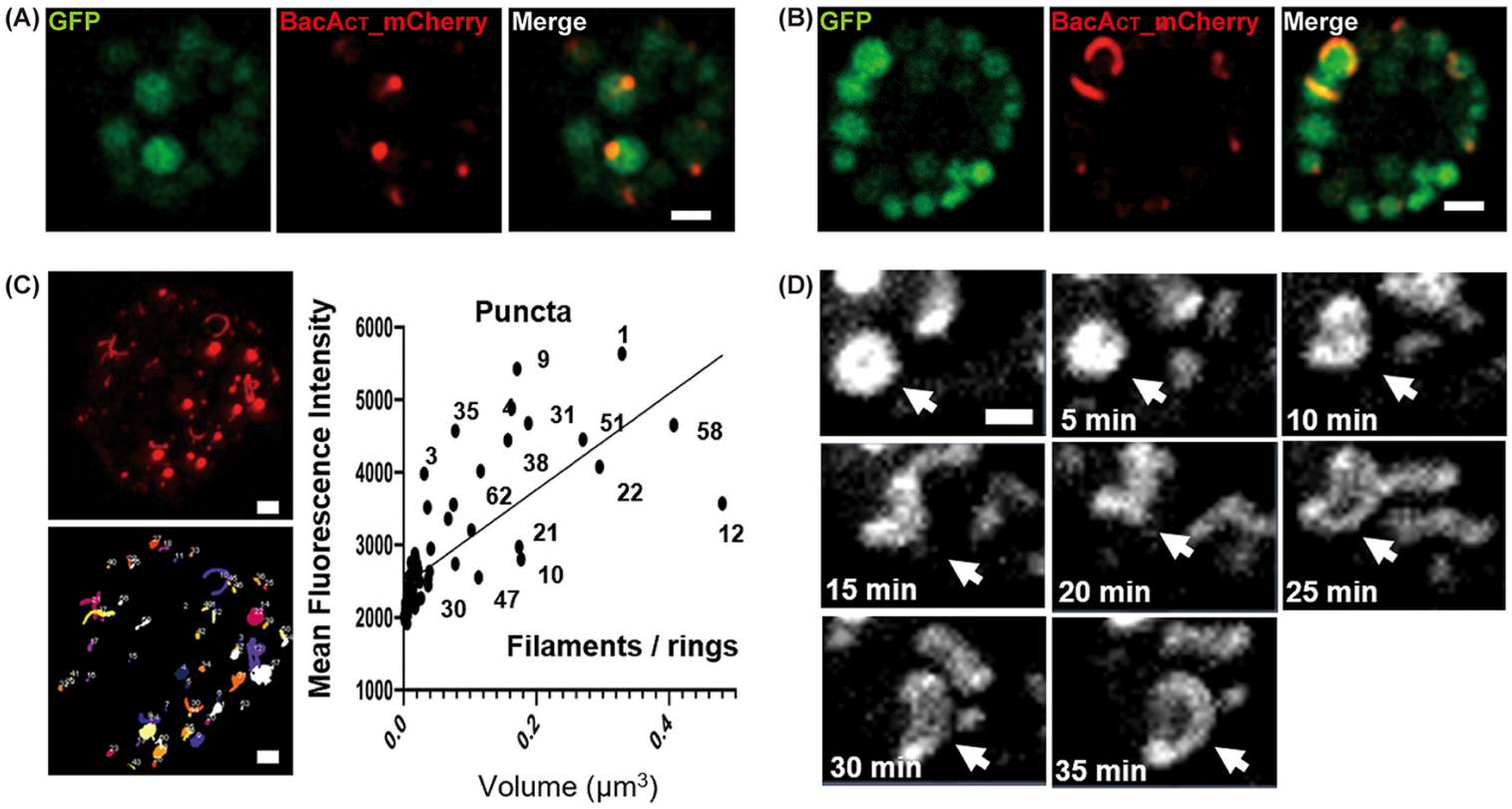
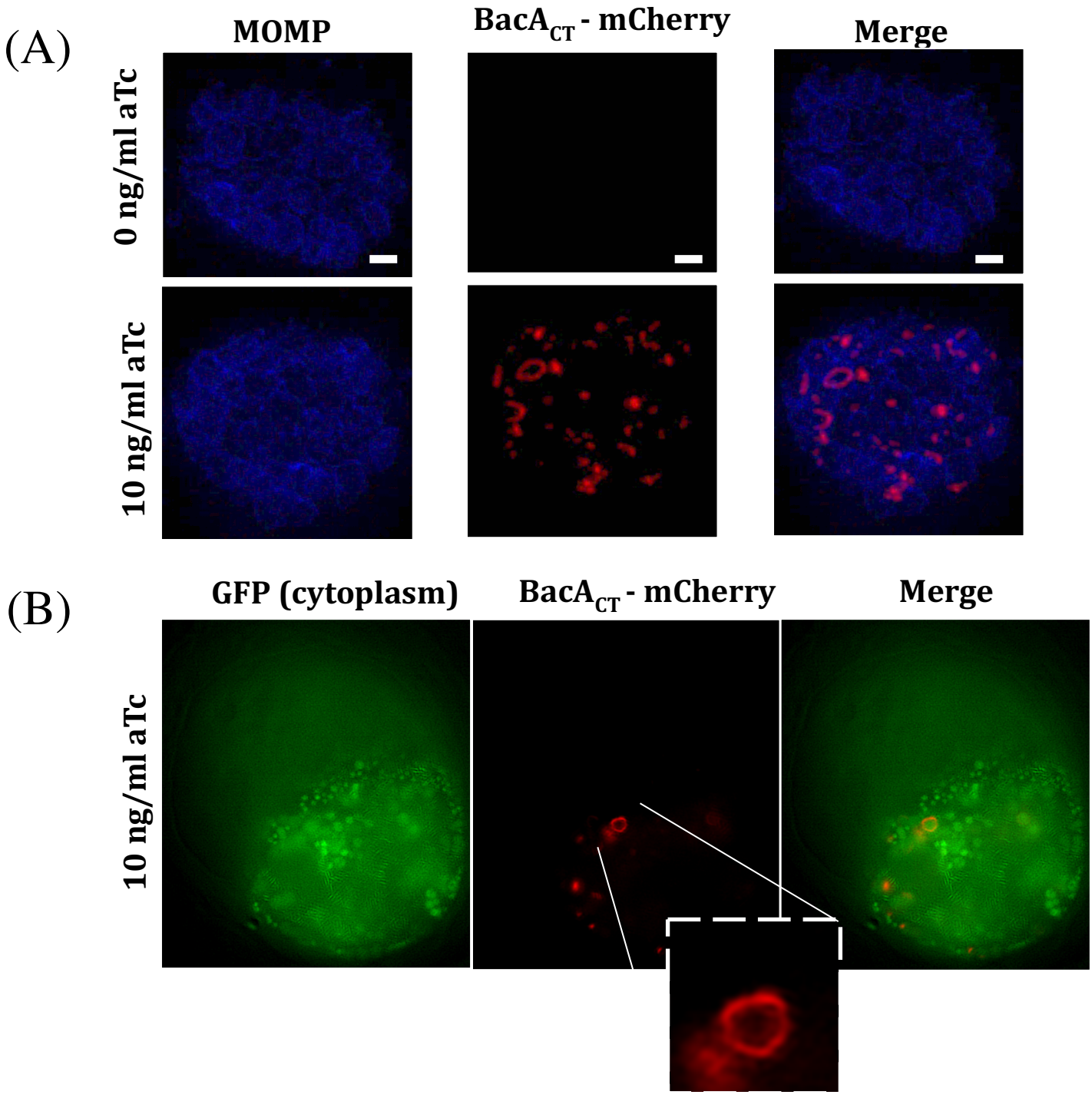


Figure 7. $BacA_{CT}$_mCherry localization is dynamic and alters between puncta, filaments, and ring-like structures.

Live-cell imaging of *C. trachomatis* L2 434/Bu expressing a $BacA_{CT}$ C-terminal mCherry fusion protein (from pREF100-bacA_{CT}-mCherry) induced at 2 h postinfection with 10 ng/ml aTc. Examples of polar puncta (A) and filaments and partial ring-like forms (B) are shown. Constitutively expressed cytoplasmic GFP is shown in green. Figures represent single imaging planes and are representative of ~30 fields of view observed. Images were acquired on a Zeiss LSM 980 confocal microscope. Bars, 1 µm. (C) Analysis of $BacA_{CT}$-mCherry filament dimensions and density. Image (top) is representative of 1 of 10 inclusions for which the mCherry positive objects were defined by 3D mapping software (bottom), and mean fluorescence pixel intensities are plotted against object volume (right). Images were acquired on a Zeiss ELYRA PS.1 superresolution microscope. Bars, 1 µm. (D) Time-lapse microscopy of an expanding $BacA_{CT}$ ring. Z-stacks were taken once every 5 min for 30 min, and images presented are maximum intensity projections. The mCherry-positive $BacA_{CT}$ structure being tracked throughout the time course is designated by the white arrows. Images were acquired on a Zeiss LSM 710 confocal microscope. Bar, 0.5 µm.


(A)
MOMP
BacA$_{CT}$ - mCherry
Merge
0 ng/ml aTc
10 ng/ml aTc
(B)
GFP (cytoplasm)
BacA$_{CT}$ - mCherry
Merge
10 ng/ml aTc

(C)

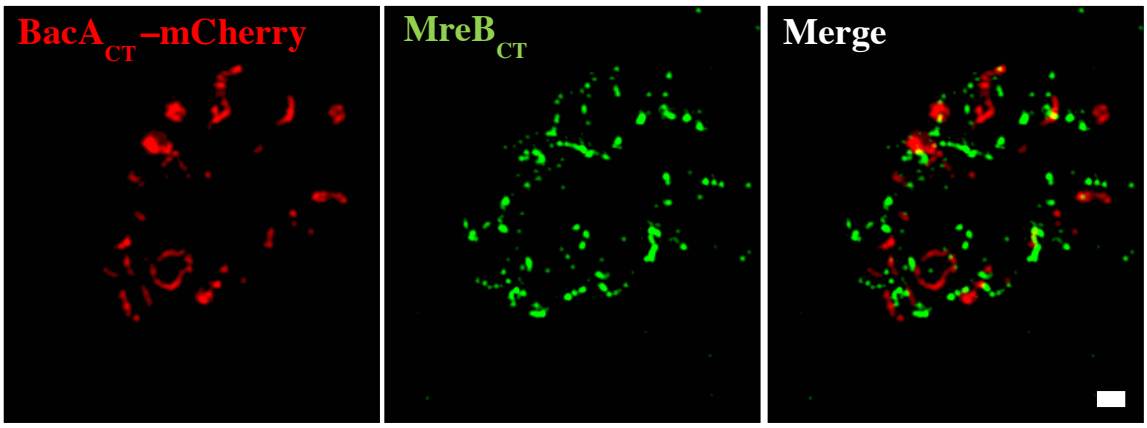


Figure 8. BacA$_{CT}$ ring morphology observed in fixed and living cells via super resolution microscopy.
(A) Cells were grown in the presence or absence of 10 ng/mL anhydrotetracycline. At 18 hours post infection, cells were fixed, permeabilized, and labeled with polyclonal antibodies against mCherry (red) and *Chlamydia*'s Major Outer Membrane Protein, MOMP (blue). Representative Z-stack images were taken via super-resolution microscopy. (B) HeLa cells were infected with *C. trachomatis* L2 434/Bu: pREF100:BacA$_{CT}$-mCherry with 10 ng/mL aTc induction. GFP^{+} *Chlamydia* (green) and BacA$_{CT}$-mCherry (red). Images were taken at 37 hpi. (C) MreB does not co-localize with BacA$_{CT}$. Super resolution microscopy of *C. trachomatis* expressing BacA$_{CT}$-mCherry (red) 18 hours post infection. Cells were fixed, permeabilized, and immunolabeled utilizing polyclonal antibodies to mCherry and the chlamydial cell division protein, MreB. Images are max intensity projections and representative of ~20 imaged fields. Scale bar, 1 μm.

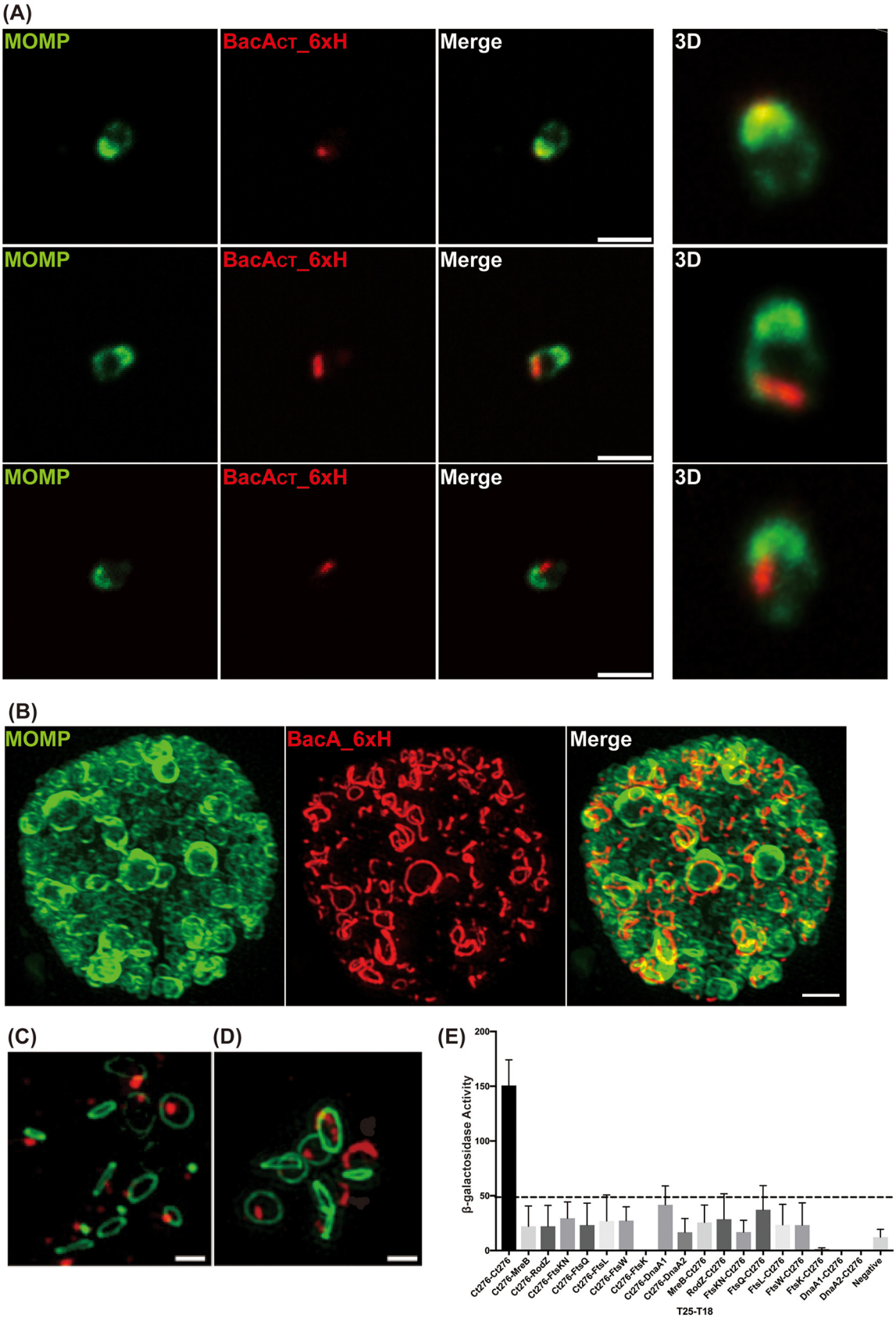

(A)
MOMP
BacAct_6xH
Merge
3D
MOMP
BacAct_6xH
Merge
3D
MOMP
BacAct_6xH
Merge
3D
(B)
MOMP
BacA_6xH
Merge
(C)
(D)
(E)
β-galactosidase Activity
200
150
100
50
0
Ct276-Ct276
Ct276-MreB
Ct276-RodZ
Ct276-FtsKN
Ct276-FtsQ
Ct276-FtsL
Ct276-FtsW
Ct276-FtsK
Ct276-DnaA1
Ct276-DnaA2
MreB-Ct276
RodZ-Ct276
FtsKN-Ct276
FtsQ-Ct276
FtsL-Ct276
FtsW-Ct276
FtsK-Ct276
DnaA1-Ct276
DnaA2-Ct276
Negative
T25-T18

Figure 9. $BacA_{CT}$ forms filaments that do not colocalize or interact with peptidoglycan or proteins associated with cell division in *Chlamydia* species.
(A) *C. trachomatis* strain L2 434/Bu 10.5 h postinfection expressing $BacA_{CT}$ with a six-histidine (6×H) tag at the C terminus (from pTLR2-*bacA*_6×H::L2). RBs, defined by the labeling of the outer surface membrane protein, MOMP, are shown undergoing the first step of their division process: polar expansion. The images were acquired on a Nikon Ti2 spinning disc confocal microscope using a 60× lens objective. Single imaging planes and 3D maximum intensity projections are shown. Images are representative of >50 imaging fields. Authors overlaid an equivalent scale bar over the burnt-in scale bar from the microscope image capture. Bar, 0.5 μm. (B) Maximum intensity 3D projection of a structured illumination superresolution image of *C. trachomatis* L2 expressing $BacA_{CT}$-6×H (from pTLR2-*bacA*_6×H::L2) at 24 h postinfection (hpi) after induction with 5 nM aTc at 8 hpi. Note the clear ring-shape forms as well as filaments and puncta. The width of the inclusion is approximately 12 μm. Bar, 1.5 μm. (C and D) Superresolution microscopy of *C. trachomatis* expressing $BacA_{CT}$-6×H (from pREF100-*bacA*$_{CT}$-His; red) at 18 hpi. Cells were coincubated with the PG-intercalating agent EDA-DA (1 mM) and labeled with azide-conjugated Alexa Fluor 488 (green). Images are 3D maximum intensity projections and representative of >100 imaged fields. Bars, 1 μm. For panels B to D, images were acquired on a Zeiss ELYRA PS.1 superresolution microscope with a 63× lens objective. (E) BACTH and β-galactosidase assays were performed for $BacA_{CT}$ interactions with proteins related to cell division and PG synthesis. The experiments were performed as described in Materials and Methods. The negative control was the lack of interaction between T25 and a mixture of T18-MreB and T18-FtsKN. The dashed line represents the cutoff for positive interactions as determined by five times the negative control levels. Data represent three independent biological replicates, and bars represent standard deviations from the means.

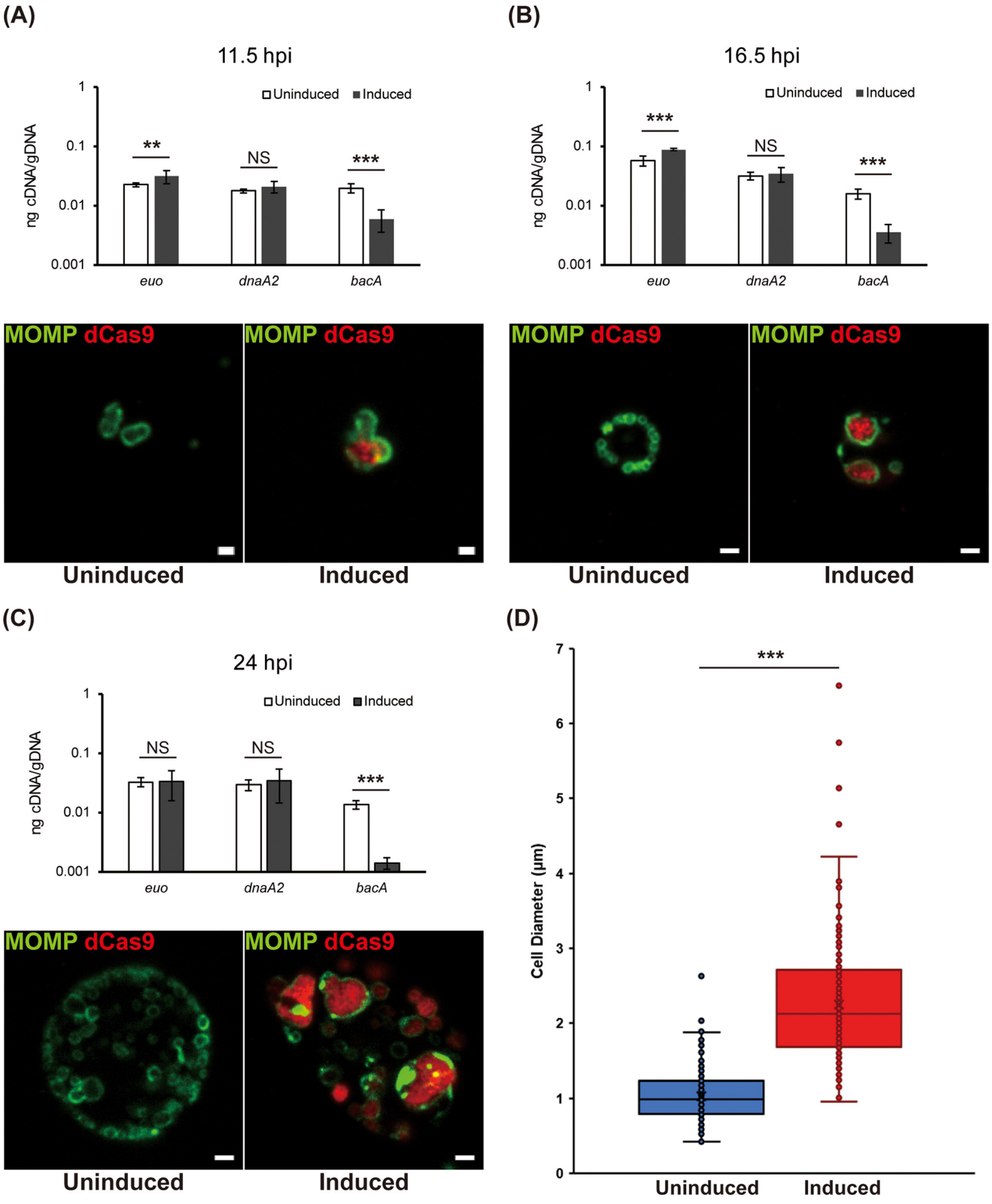

(A)
11.5 hpi
Uninduced
Induced
ng cDNA/gDNA
1
0.1
0.01
0.001
**
NS
***
euo
dnaA2
bacA
(B)
16.5 hpi
Uninduced
Induced
ng cDNA/gDNA
1
0.1
0.01
0.001
***
NS
***
euo
dnaA2
bacA
MOMP dCas9
MOMP dCas9
Uninduced
Induced
MOMP dCas9
MOMP dCas9
Uninduced
Induced
(C)
24 hpi
Uninduced
Induced
ng cDNA/gDNA
1
0.1
0.01
0.001
NS
NS
***
euo
dnaA2
bacA
MOMP dCas9
MOMP dCas9
Uninduced
Induced
(D)
***
Cell Diameter (µm)
7
6
5
4
3
2
1
0
Uninduced
Induced

Figure 10. Conditional knockdown of *bacA*$_{CT}$ expression alters the morphology of *C. trachomatis*.

C. trachomatis without plasmid (–pL2) was transformed with the aTc-inducible pBOMBLCRia::L2 (*bacA*) vector expressing a guide RNA targeting the 5′ region of *bacA*$_{CT}$ and the mutated *Staphylococcus aureus* Cas9, which cannot cleave DNA (dCas9). (A to C) After induction at 4 h postinfection (hpi), transcript levels of *bacA*, *dnaA2*, and *euo* were measured by reverse transcription quantitative-PCR (RT-qPCR) at 11.5, 16.5, and 24 hpi. RT-qPCR was performed as described in Materials and Methods. In addition, an immunofluorescence assay (IFA) was performed to check the induction of dCas9 and the morphology of the bacteria as assessed by labeling of the major outer membrane protein (MOMP). The merged channel is shown for each treatment. Images were acquired on a Zeiss AxioImager.Z2 equipped with an Apotome2 using a 100× lens objective. Bars, 0.5 μm (A) or 2 μm (B and C). (D) Bacterial cell diameter was measured from 216 individual bacteria from each condition as noted. **, $P < 0.05$; ***, $P < 0.001$; NS, not significant.

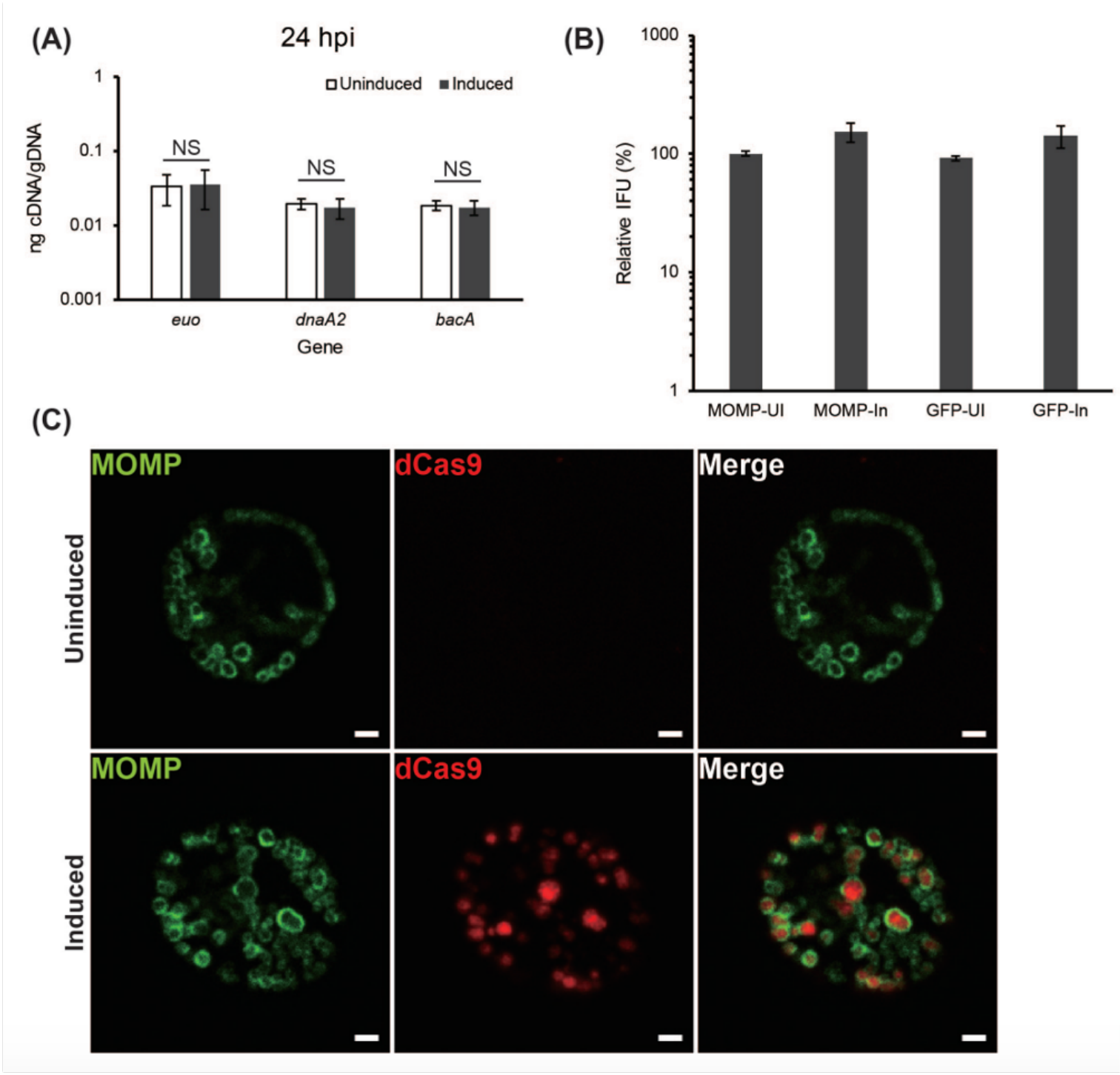

(A)
24 hpi
Uninduced
Induced
ng cDNA/gDNA
1
0.1
0.01
0.001
NS
NS
NS
euo
dnaA2
bacA
Gene
(B)
Relative IFU (%)
1000
100
10
1
MOMP-UI
MOMP-In
GFP-UI
GFP-In
(C)
Uninduced
Induced
MOMP
dCas9
Merge

Figure 11. The effect of dCas9 over-expression without gRNA in *C. trachomatis*.
(A) *C. trachomatis* serovar L2 transformed with a vector encoding dCas9 only (i.e. pBOMBLSa_dCas9vaa::L2) was used to infect HeLa cells. At 4 hpi, dCas9 was induced with 20 nM aTc, and the transcriptional levels of *euo, dnaA2*, and *bacA* were measured by qPCR at 24 hpi (A). Also, to check the expression of dCas9, an immunofluorescence assay was performed at 24 hpi (B). The staining was performed as described in Materials and Methods. Images were acquired on a Zeiss AxioImager.Z2 equipped with an Apotome2 using a 100X objective. Scale bar, 2 μm. NS, Not significant

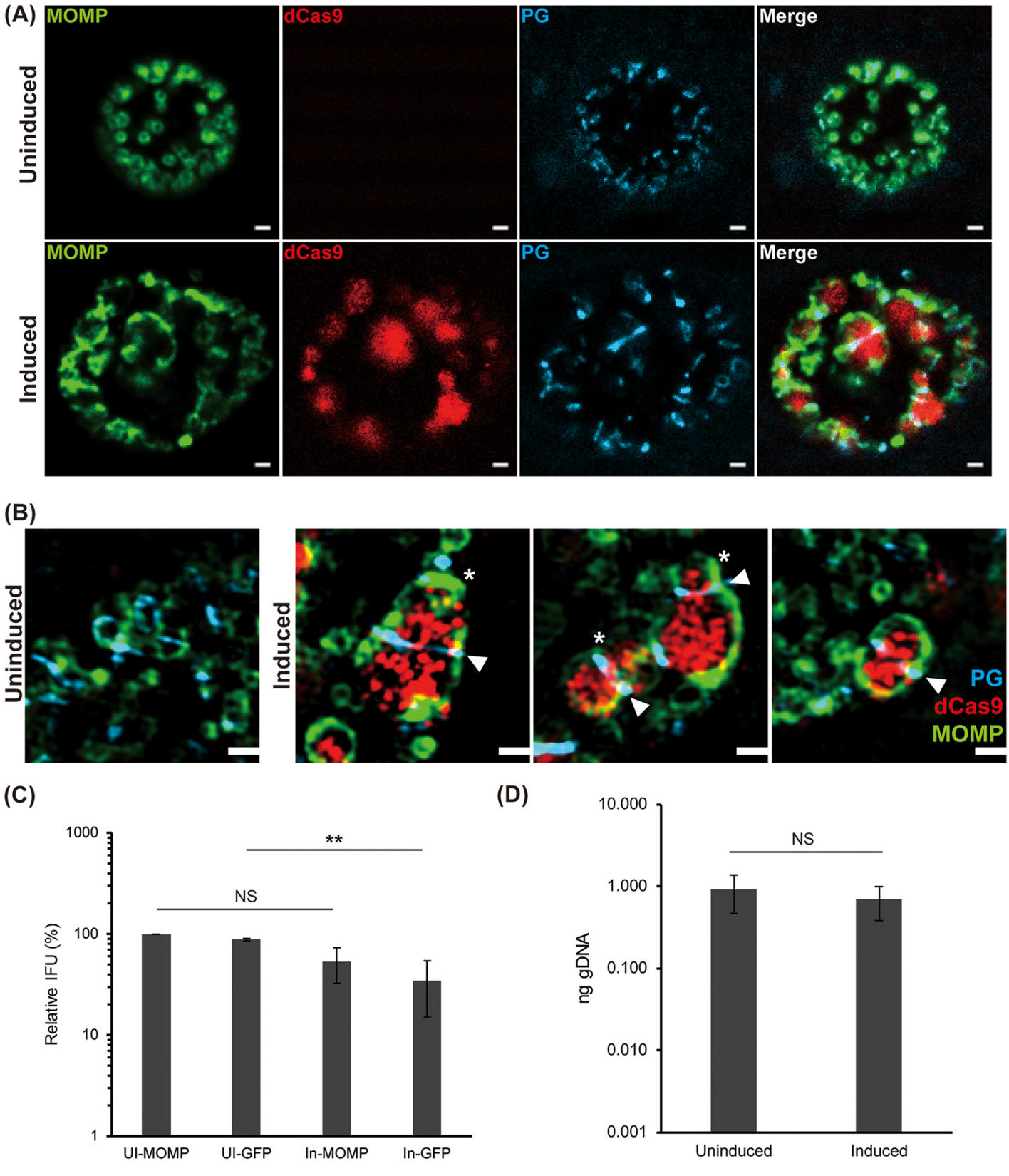

(A)
MOMP
dCas9
PG
Merge
Uninduced
Induced
(B)
Uninduced
Induced
PG
dCas9
MOMP
(C)
Relative IFU (%)
1000
100
10
1
**
NS
UI-MOMP
UI-GFP
In-MOMP
In-GFP
(D)
ng gDNA
10.000
1.000
0.100
0.010
0.001
NS
Uninduced
Induced

Figure 12. Conditional knockdown of *bacA*$_{CT}$ expression has minimal impact on chlamydial peptidoglycan (PG) synthesis or developmental cycle progression.
(A and B) The PG was labeled in live cells as described in Materials and Methods, and we performed fixation and labeling of the *C. trachomatis* pBOMBLCRia::L2 (*bacA*) transformants, induced or not, with anti-dCas9 antibodies for immunofluorescence analysis. (B) Arrowheads indicate the PG septum, whereas * indicates budding daughter cells. Images were acquired on a Zeiss AxioImager.Z2 equipped with an Apotome2 using a 100× lens objective. Bar, 1 μm (A) or 0.5 μm (B). (C) The effect of knocking down *bacA*$_{CT}$ on the production of infectious progeny was quantified by measuring the inclusion forming units (IFU) by assessing MOMP and GFP fluorescence. (D) The genomic DNA levels of uninduced and induced samples were also measured by qPCR to monitor the effect of *bacA*$_{CT}$ knockdown on chlamydial replication. **, $P < 0.05$; NS, not significant.

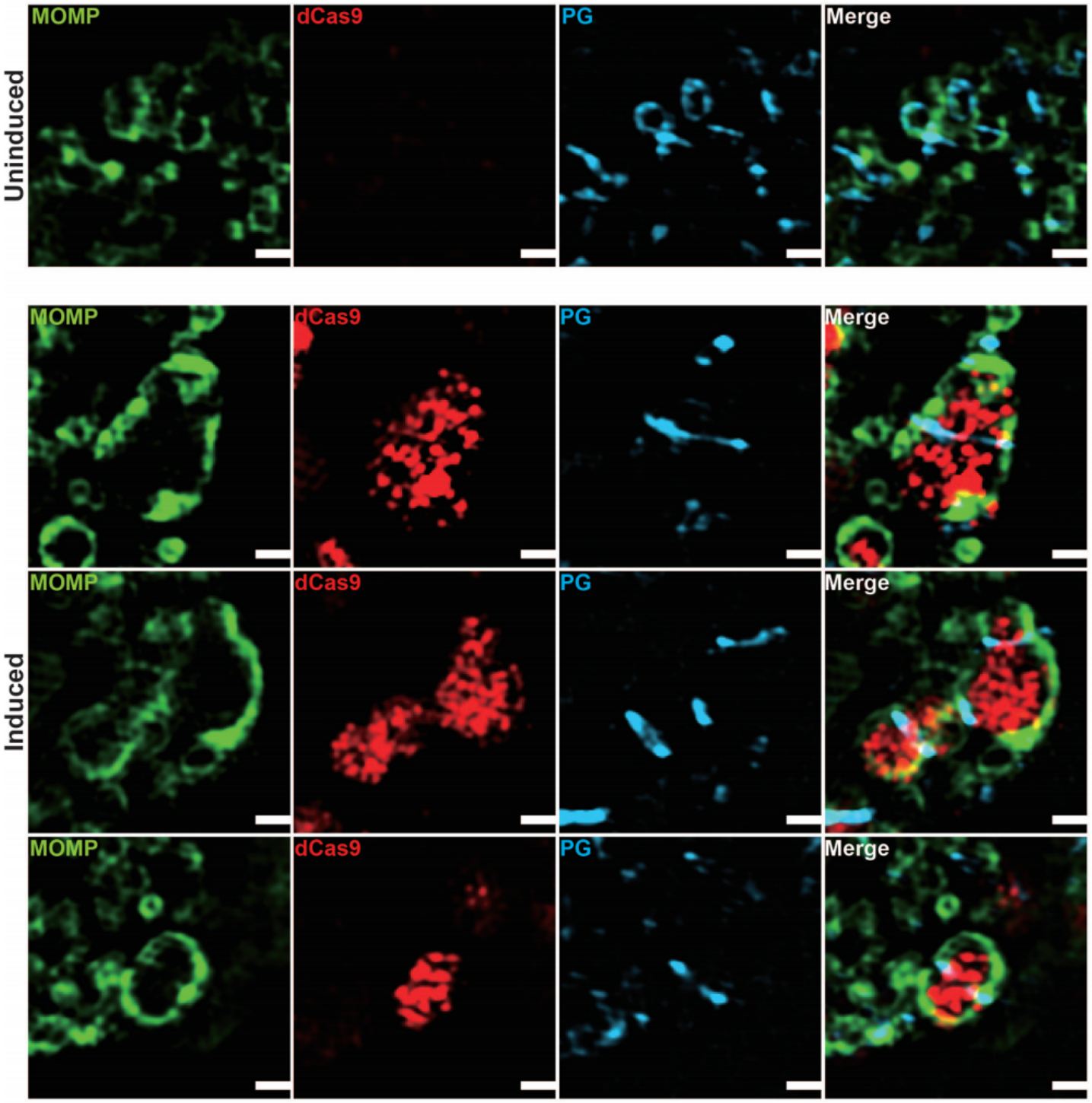


Figure 13. Knockdown of $BacA_{CT}$ does not alter peptidoglycan ring formation. Images are separated channels from data shown in Figure 12B.

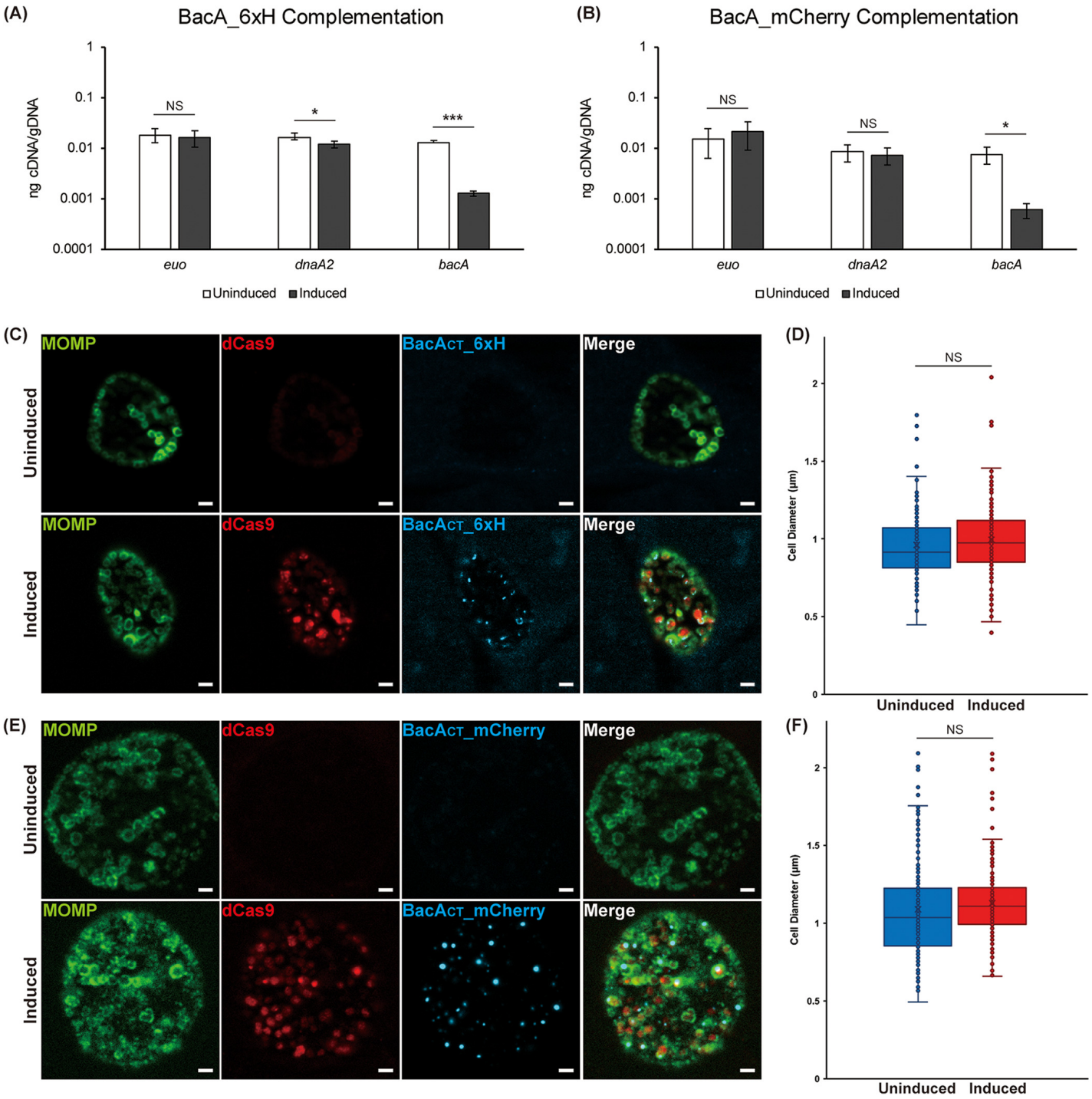


Figure 14. Ectopic expression of $BacA_{CT}$ complements the morphological defects during knockdown of *bacA*$_{CT}$ expression in *C. trachomatis*.
Constructs encoding an aTc-inducible dCas9 transcriptionally fused to $BacA_{CT}$_6×H (pBOMBLCRia-*bacAm_6×H*::L2 [*bacA*]) or $BacA_{CT}$_mCherry (pBOMBLCRia-

bacAm_mCherry::L2 [*bacA*]) and a constitutively expressed gRNA targeting *bacA* were made and transformed into *C. trachomatis* L2 (–pL2). Silent mutations were substituted into the qPCR primer binding and gRNA targeting sequences of $bacA_{CT}$ (*bacAm*) in the plasmid. Therefore, when RT-qPCR was performed, only endogenous $bacA_{CT}$ was detected and only the endogenous $bacA_{CT}$ was targeted for knockdown. The transformants were infected into HeLa cells. (A and B) The constructs were induced at 4 hpi, and the transcriptional level of endogenous $bacA_{CT}$ was measured by RT-qPCR at 24 hpi. The RT-qPCR was performed as described in Materials and Methods. (C and E) To confirm the expression of dCas9 and ectopic $BacA_{CT}$, an immunofluorescence assay was performed. (D and F) Bacterial cell diameters from induced and uninduced conditions were measured. At 24 hpi, the samples were fixed with 1× DPBS containing 3.2% formaldehyde and 0.022% glutaraldehyde for 2 min. Afterwards, the samples were permeabilized with 90% methanol (MeOH). The staining of the major outer membrane protein (MOMP), dCas9, and BacAm_6×H/BacAm_mCherry was performed as described in Materials and Methods. Images were acquired on a Zeiss AxioImager.Z2 equipped with an Apotome2 using a 100× lens objective. Bars, 2 μm. (D) The diameters of 190 individual bacteria were measured for each condition. (F) The diameters of 211 individual bacteria were measured for each condition. *, $P < 0.05$; ***, $P < 0.001$; NS, not significant.

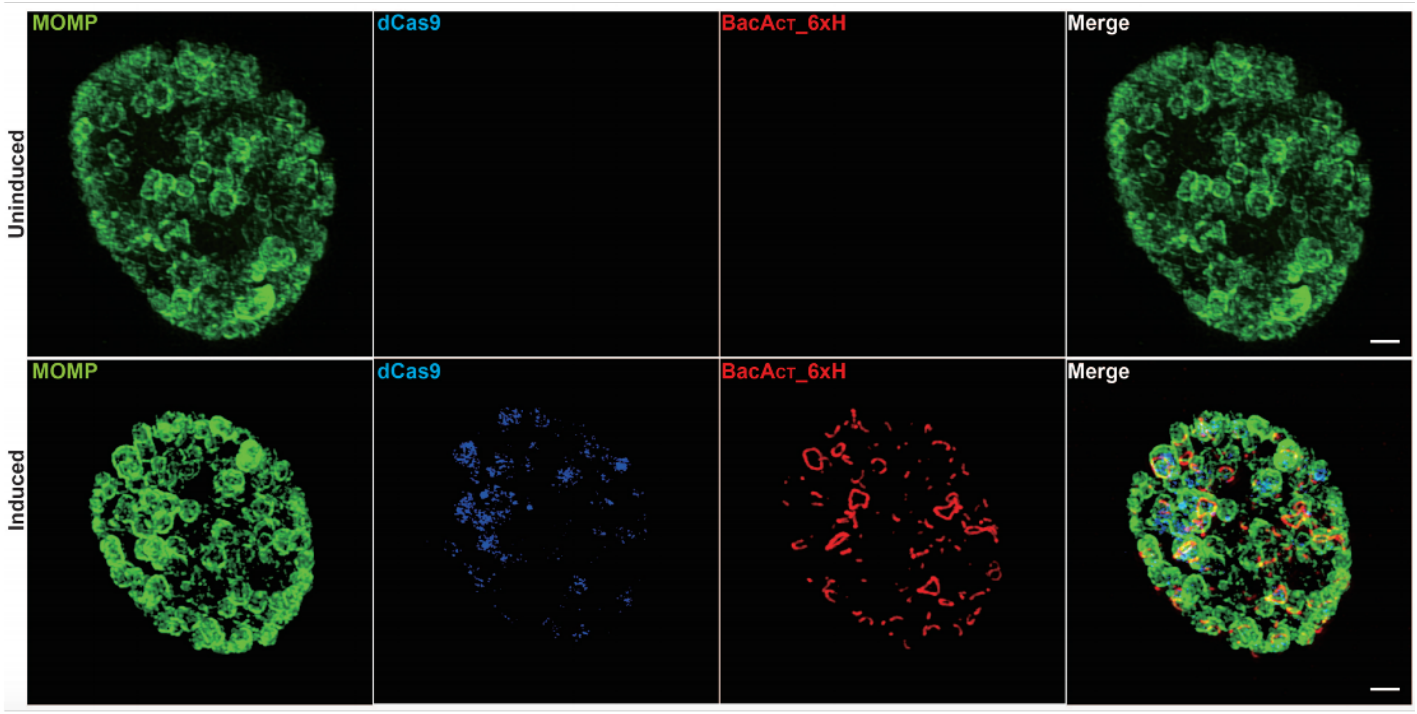


Figure 15. 3D super-resolution images of $BacA_{CT}$_6xH-complemented *$bacA_{CT}$* knockdown strain. Cells were infected and processed as described in the legend of Figure 6 in the main text. Images were acquired on a Zeiss ELYRA PS.1 Super Resolution Microscope with a 63x objective and are 3D max intensity projections. Note the clear ring-shape forms as well as filaments and puncta of the $BacA_{CT}$_6xH label. Note that cytoplasmic antigens, like dCas9, lacking defined structures do not image well by SIM super-resolution. See Figures 10 or 11 for representative imaging of dCas9. Scale bar = 1.5 μm.

Supplementary table 1. The list of strains, plasmids and primers used in this study.

Construct Plasmid	Relevant genotype	Ori	Source of Reference
pASK-GFP-mKate-L2 (pTLR2)	*bla* P_{tet}	ColE1	(267)
pTLR2-bacA_6xH::L2	*bla* P_{tet}::*ct276_6xH*	ColE1	This study
pBOMB4-Tet::L2	*bla* P_{tet}::mCherry	pUC19	(15)
pBOMBLCRia *(bacA)*	*bla* P_{tet}::Sa_dCas9 $P_{dnaKmut}$::Sa_gRNA(*ct276*)	pUC19	This study
pBOMBL-Sa_dCas9vaa::L2	*bla* P_{tet}::Sa_*dCas9*_VAA	pUC19	This study
pBOMBLCRia-bacAm_6xH::L2 (bacA)	*bla* P_{tet}::Sa_*dCas9*_VAA-*ct276m_6xH* $P_{dnaKmut}$::Sa_gRNA(*ct276*)	pUC19	This study
pBOMBLCRia-*bacAm*_mCherry: : L2 (*bacA*)	*Bla* Ptet::Sa_*dCas9*_VAA-*ct276m_mCherry* $P_{dnaKmut}$::Sa_gRNA(*ct276*)	pUC19	This study
pREF100	*aadA* P_{tet}	pUC19	(229)
pREF100-$bacA_{CT}$-mCherry	*aadA* P_{tet}::*Ctr_ct276_mCherry*	pUC19	This study
pREF100-$bacA_{CT}$-His	*aadA* P_{tet}::*Ctr_ct276_6XH*	pUC19	This study
pKT25	*aph* P_{lac}::*t25*	p15A	(117)
pUT18C	*bla* P_{lac}::*t18*	ColE1	(117)
pKT25-*bacA*	*aph* P_{lac}::*t25-Ctr_ct276*	p15A	This study
pUT18C- *bacA*	*bla* P_{lac}::*t18-Ctr_ct276*	ColE1	This study
pKT25-*mreB*	*aph* P_{lac}::*t25-Ctr_mreB*	p15A	de Boer
pUT18C-*mreB*	*bla* P_{lac}::*t18-Ctr_mreB*	ColE1	de Boer
pKT25-*rodZ*	*aph* P_{lac}::*t25-Ctr_rodZ*	p15A	(186)
pUT18C-*rodZ*	*bla* P_{lac}::*t18-Ctr_rodZ*	ColE1	(186)
pKT25-*ftsK*	*aph* P_{lac}::*t25-Ctr_ftsK*	p15A	(184)
pUT18C-*ftsK*	*bla* P_{lac}::*t18-Ctr_ftsK*	ColE1	(184)
pKT25-*ftsK*N	*aph* P_{lac}::*t25*-N-terminus of *Ctr_ftsK*	p15A	(184)
pUT18C-*ftsK*N	*bla* P_{lac}::*t18*-N-terminus of *Ctr_ftsK*	ColE1	(184)
pKT25-*ftsQ*	*aph* P_{lac}::*t25-Ctr_ftsQ*	p15A	(185)
pUT18C-*ftsQ*	*bla* P_{lac}::*t18-Ctr_ftsQ*	ColE1	(185)
pKT25-*ftsL*	*aph* P_{lac}::*t25-Ctr_ftsL*	p15A	(185)

pUT18C-*ftsL*	*bla* P_{lac}::*t18-Ctr_ftsL*	ColE1	(185)
pKT25-*ftsW*	*aph* P_{lac}::*t25-Ctr_ftsW*	p15A	Lab collection
pUT18C-*ftsW*	*bla* P_{lac}::*t18-Ctr_ftsW*	ColE1	Lab collection
pKT25-*dnaA1*	*aph* P_{lac}::*t25-Ctr_dnaA1*	p15A	Lab collection
pUT18C-*dnaA1*	*bla* P_{lac}::*t18-Ctr_dnaA1*	ColE1	Lab collection
pKT25-*dnaA2*	*aph* P_{lac}::*t25-Ctr_dnaA2*	p15A	Lab collection
pUT18C-*dnaA2*	*bla* P_{lac}::*t18-Ctr_dnaA2*	ColE1	Lab collection
pKT25-zip	*aph* $P_{lac}c$::*t25-zip*	p15A	(117)
pUT18C-zip	*bla* P_{lac}::*t18-zip*	ColE1	(117)

Strain	**Relevant genotype**	**Source of Reference**
MG1655	F^- , $lambda^-$, *rph-1*	Lab collection
DHT1	F^- *glnV44* (AS) *recA1 endA1 gyrA96* (Nal^R) *thi-1 hsdR17 spoT1 rfbD1 cya-854 ilv-691 ::Tn10 (TetR)*	(55)

Primer name	**Sequence**	**Features**	**Usage**
bacA-his/pTLR2/F	tttgtttaactttaagaaggagata ATGTTCAAAAGACCTGCAAAAAATTTC	lower case for plasmid overlap construction	for amplification of *ct276*
bacA -his/pTLR2/R	ccatttttcacttcacaggtcaacc ttaatggtgatggtgatggtg TGAGTCTATTTCCTCTTGCTCATTAG	lower case for plasmid overlap construction, adds six-histidines tag sequence	for amplification of *ct276*_6xH
bacA/pKT25/F	ctgcagggtcgactctagag TTCAAAAGACCTGCAAAAAATTTC	lower case for plasmid overlap construction	for amplification of *ct276*
bacA/pKT25/R	acgttgtaaaacgacggccg TTATGAGTCTATTTCCTCTTGCTC	lower case for plasmid overlap construction	for amplification of *ct276*
bacA /pUT18C/F	actgcaggtcgactctagag TTCAAAAGACCTGCAAAAAATTTC	lower case for plasmid overlap construction	for amplification of *ct276*
bacA /pUT18C/R	attacttagttatatcgatg TTATGAGTCTATTTCCTCTTGCTC	lower case for plasmid overlap	for amplification

		construction	of *ct276*
bacAct (NotI) F	CAGTGCGGCCGCATGTTCAAAAG ACCTGCAAAAAATTTC	Underline for the restriction site of NotI	for amplification of *ct276*
bacAct (HIS) R	TTAATGATGATGATGATGATGTG AG TCTATTTCCTCTTGC	Underline for hexa-histidine tag	for amplification of *ct276*
bacAct (HIS-KpnI) R	CAGTGGTACCTTAATGATGATGA TG ATGATG	Underline for the restriction site of Kpn1	for amplification of *ct276*
bacAct (link) R	AGAACCACCAGAACCACCTGAGT CTATTTCCTCTTGC	Underline for the overlap link	for amplification of *ct276*
mCherry (link) F	CAGGTGGTTCTGGTGGTTCTATG G TCTCTAAGGGCGAGGA	Underline for the overlap link	for amplification of *ct276*
mCherry (KpnI) R	CAGTGGTACCTTATTTGTACAGC TC ATCCATG	Underline for the restriction site of Kpn1	for amplification of *ct276*
ct446 euo FWD	CGAAGACTACTCGTTGGGAAATA	qPCR primer	for amplification of *euo* coding region
ct446/euo REV	AACAGAAGCTCTCCTTGATAAGT	qPCR primer	for amplification of *euo* coding region
bacA FWD	CCCGGAAGA ACCTGAAACTAC	qPCR primer	for amplification of *ct276* coding region
bacA REV	TTCGAACGTCCCGTCAATAC	qPCR primer	for amplification of *ct276* coding region
ct275/dnaA_2 FWD	AATCGGCAGCTCTAGGAATTG	qPCR primer	for amplification of *dnaA2* coding region
ct275/dnaA_2 REV	CATGAAGCAAATGCGTCTTACC	qPCR primer	for amplification of *dnaA2* coding region

gBlock name	Sequence	Features	Usage
bacA-w/o target sequences of qPCR or gRNA *(bacAm)*	aaagggcgtagcagcataaggaggagaatctgc**atgt tcaaaagacctgcaaaaaatttctttgatgaagtcc aaactctg tacgaagactccggtgctaattccacgagttacagt atatatccccaaagaacagaacgtttagaaaatca ttcaaatatttttgaaccagctaagcccgcggaaac acgattgctatctcaagaagaacattctcaatgga ctgatcaacaagaaggactcgcaactcaagaaag ctcctttccagaggagcccgagaccactttaggtg agggagtctctttcaaaggagaattaacttttgaga gactccttcgtattgacgggacgttcgaaggtattc ttgtctctaaaggaaagattattgttggccctcaag gatatgtcaaagccaatatagaacttgaagaagct gtgatagcaggagtcgttgaaggcaatattacagt aactggaagagtatctcttcaaggaagagctatgg ttacaggagatattcaagcaggaagtctatgtgtg gatgagggtgtacgcctgtgtggttatgtctctattc aaggagccccctctaatgagcaagaggaaataga ctcacaccatcaccatcaccattaa**cgtaccggtcg accattcaa	Underlined lower case for overlap plasmid construction, **bold** for the ct276 sequences, **bold** for changed sequences annealing region of qPCR primer	For the ectopic expression of bacAm from pBOMBL dCas9_VA A-bacAm (bacA) compleme ntation vectors
bacA- targeting gRNA gBlock cassette	tgaatataatttaattatatcacgcactagctcagattca gtagaccgctgttgATAAAACGAAAGGC CCAGTCTTTCGACTGAGCCTTTCG TTTTATTTGAAAAATCTCGCCAA CAAGTTGACGAGATAAACACGGC ATTTTGCCTTGTTTTAGTAGATTC TGTTTCCAGAGTACTAAAAC**TAT GAGGATAGTGGCGCCAAC**GGT GTCATTATAAGAAAACCGTCTCC ACCGGTGAAtgcatgatctacgtgcgtcacat gcagtaccgacgtcttaagacccactttcaca	Lower case for plasmid overlap and spacer, *italicized* for $P_{dnaKmut}$ promoter sequence, **bold** for bacA targeting sequence, underlined for gRNA scaffold, Upper case for rrnB1 terminator	For insertion into BamHI site of pBOMBL-Sa_dCas9v aa

DISCUSSION

Bactofilins, originally named due to their intermediate filament-like characteristics, have been identified in many bacterial species and have been described to function in various cellular processes including maintenance of cell shape and morphology, establishment of cell polarity, and orientation of cell division proteins (131; 226; 254; 282). Given the previously described functions of bactofilins in other bacteria, we initially hypothesized that $BacA_{CT}$ would serve to direct the polarized division process of *Chlamydia*. However, based on our findings, our initial hypothesis of $BacA_{CT}$ function is likely incorrect but does not preclude $BacA_{CT}$ from functioning in the division process indirectly.

Although we failed to reveal a direct link between $BacA_{CT}$ and cell division, we did observe that *Chlamydia* RBs exhibited distinct changes in their morphology when $bacA_{CT}$ expression was knocked down by CRISPR interference. Specifically, loss of $BacA_{CT}$ led to a roughly two-fold increase in bacterial cell diameter. Changes in morphology due to the loss of a bacterium's bactofilin has been reported previously. The *P. mirabilis* protein, CcmA (curved cell morphology), was identified following the loss of straight cell morphology in a transposon mutant (94). Subsequently, other bactofilins were identified and found to be important in maintenance of bacterial cell morphology. For instance, loss of BacM in *M. xanthus* causes a kinked morphology (126), while the absence of CcmA in *H. pylori* results in curved rod morphology instead of the microbe's distinct helical morphology (238), owing to the inability of PG remodeling proteins to properly localize. These bacteria are rod-shaped species and have PG sacculi regulated in part by the function of their respective bactofilin. In contrast, members of the

Chlamydiaceae do not have a PG sacculus, thus the exact mechanism by which $BacA_{CT}$ regulates morphology is likely to be unique to these organisms. Further support for this comes from the fact that no homolog for $BacA_{CT}$ is encoded in the genomes of '*Chlamydia*-related' bacteria. These bacteria may infect a large diversity of eukaryotes including amoebae, ticks, and mammals, and they share *Chlamydia*'s biphasic developmental cycle. However, they physiologically differ from pathogenic *Chlamydia* species in that they retain a peptidoglycan sacculus (200).

Because pathogenic *Chlamydia* species lack sacculi, they must utilize an alternative means of maintaining cell shape and membrane integrity. In the microbe's extracellular form, this is achieved via disulfide crosslinked, cysteine-rich outer membrane proteins. This structure is strong and rigid but does not provide for the membrane dynamics necessary for chlamydial cell growth and division. Peptidoglycan, and by extension its interacting partners in the divisome, and the Tol-Pal system (previously characterized in the *Chlamydia*-related organism *Waddlia chondrophila* (110)) have been shown to provide stability to the outer membrane in homologous systems, and $BacA_{CT}$ may function similarly by stabilizing membrane regions outside the division plane, in conjunction with an as yet uncharacterized interacting partner in the periplasmic space. While this is one possibility, $BacA_{CT}$'s function may prove inherently simpler. In addition to enabling bacterial cell division, peptidoglycan is essential for maintaining cell size and shape. Without a sacculus, the only way peptidoglycan can affect cell morphology in *Chlamydia* species is prior to division when its ring form places limitations on membrane expansion. However, upon septation, this structural scaffold is momentarily disassembled, leaving nothing to define the size and shape of a chlamydial RB in this intermediate state. $BacA_{CT}$ rings could potentially bridge this critical stage in the division cycle and provide a

degree of structural stability until a new peptidoglycan ring is formed. Although this study is the first to identify and characterize a bactofilin ortholog in *Chlamydia trachomatis*, there still remains much to uncover about the mechanism by which $BacA_{CT}$ maintains cell morphology. By understanding the function of $BacA_{CT}$ in *Chlamydia*, we will further understand the development of this unique obligate intracellular bacterium.

ACKNOWLEDGMENTS

We thank the following individuals for providing reagents used in this study: Harlan Caldwell (National Institutes of Health), Ian Clarke (University of Southampton), Ted Hackstadt (Rocky Mountain Labs/NIH), Anthony Maurelli (University of Florida), Michael VanNieuwenhze (University of Indiana), Scott Hefty (University of Kansas), and D. Scott Merrell (Uniformed Services University). We also thank Caske' Pappan for technical assistance with BACTH experiments.

This work was supported by grants from the National Institute for General Medical Science (R35GM124798-01 to S.P.O. and R35GM138202-01 to G.W.L.) within the National Institutes of Health as well as a faculty start-up package awarded by the Uniformed Services University to G.W.L. The University of Nebraska Medical Center Advanced Microscopy Core Facility receives partial support from the National Institute for General Medical Science INBRE (P20 GM103427) and COBRE (P30 GM106397) grants, as well as support from the National Cancer Institute (NCI) for The Fred & Pamela Buffett Cancer Center support grant (P30 CA036727) and the Nebraska Research Initiative.

The funders had no role in study design, data collection and interpretation, or the decision to submit the work for publication. The opinions and assertions expressed herein are those of the

author(s) and do not necessarily reflect the official policy or position of the Uniformed Services University or the Department of Defense.

Chapter 3: Persistence alters the interaction between *Chlamydia trachomatis* and its host cell

PUBLISHED AS: Brockett MR, Liechti GW. 2021. Persistence alters the interaction between *Chlamydia trachomatis* and its host cell. Infect Immun 89:e00685-20. https://doi.org/10.1128/IAI.00685-20.

AUTHOR CONTRIBUTIONS: MRB conducted all experiments except: the MOMP volume analysis, PG label, initial NOD1 assay, and the homotypic fusion assay (conducted by GWL). GWL assisted MRB with some of the imaging.

ABSTRACT

In response to stress, the obligate intracellular pathogen *Chlamydia trachomatis* stops dividing and halts its biphasic developmental cycle. The infectious, extracellular form of this bacterium is highly susceptible to killing by the host immune response, and by pausing development, *Chlamydia* can survive in an intracellular, 'aberrant' state for extended periods of time. The relevance of these aberrant forms has long been debated, and many questions remain concerning how they contribute to the persistence and pathogenesis of the organism. Using reporter cell lines, fluorescence microscopy, and a di-peptide labeling strategy, we measured the ability of *C. trachomatis* to synthesize, assemble, and degrade peptidoglycan under various aberrance-inducing conditions. We found that all aberrance-inducing conditions affect chlamydial peptidoglycan, and that some actually halt the biosynthesis pathway early enough to prevent the release of an immunostimulatory peptidoglycan component, muramyl tripeptide. In addition, utilizing immunofluorescence and electron microscopy, we determined that the induction of aberrance can detrimentally affect the development of the microbe's pathogenic vacuole (the inclusion). Taken together, our data indicate that aberrant forms of *Chlamydia* generated by different environmental stressors can be sorted into two broad categories based on their ability to continue releasing peptidoglycan-derived, immunostimulatory muropeptides and their ability to secrete effector proteins that are normally expressed at the mid- and late- stages of the microbe's developmental cycle. Our findings reveal a novel, immuno-evasive feature inherent to a subset of aberrant chlamydial forms and provide clarity and context to the numerous persistence mechanisms employed by these ancient, genetically-reduced microbes.

IMPORTANCE

The term ‘persistence’ has been used as a catch-all term to describe any condition resulting in the reversible inhibition of cell division in *Chlamydia* species. These phenotypes have been observed under laboratory conditions and there is an ongoing debate as to their relevance during active infections. Herein, we provide a classification system for defining persistent forms of *Chlamydia* based on measurable biomarkers that influence the degree to which the microbe interacts with its host cell. Our data indicate that, rather than simply allowing *Chlamydia* species to remain intracellular, persistence halts the production of a major signaling molecule recognized by the innate immune system for targeting intracellular bacterial pathogens for cell-mediated killing. Our findings also highlight the importance of the underlying molecular mechanisms driving these phenotypes *in vivo,* and the need for future studies to assess how these aberrant forms contribute to the pathogenesis of the organism during active infections**.**

INTRODUCTION

Chlamydia trachomatis is the leading cause of infectious blindness and bacterial sexually transmitted infectious disease with a hundred million individuals infected worldwide (265). Over 1.7 million new genital tract infections are reported to the CDC annually (43). Due to the large number of asymptomatic infections that go unreported each year, estimates place the true number of annual infections in the US at closer to 3 million (220). The disease burden falls disproportionately on young women between the ages of 15-24, and while infections are treatable, untreated infections can result in pelvic inflammatory disease, ectopic pregnancy, and infertility in women, and epididymitis or urethritis in men (37).

Chlamydia species utilize a distinctive, biphasic developmental cycle (Fig. 16a), alternating between a small ($\leq$0.5 μm) extracellular, infectious form (Elementary Body or EB) and a larger (~1 μm), intracellular, replicative form (Reticulate Body or RB). Because each

developmental form is highly specialized and can only carry out either the infection or replication process, preventing the development of either form effectively halts the infection cycle. EBs are rapidly internalized upon attachment to a host cell, and utilize a type III secretion system (T3SS) to inject over 150 different effector proteins into the cell's cytosol. These effectors have a number of diverse activities. They permit the *Chlamydia*-containing vacuole (inclusion) to escape the cell's endosomal maturation pathway and lysosomal fusion, inhibit the host cell from triggering apoptosis, alter the dynamics of the infected cell's cytoskeletal proteins, and redirect intracellular vesicle trafficking (68). The expression of these effectors is highly regulated, and the timing of their expression and secretion largely aligns with their function and role in the microbe's developmental process. Inclusion membrane proteins (Incs) are one class of effectors that are inserted into the outer leaflet of the inclusion membrane, and permit *Chlamydia* to control the vast majority of vesicle fusion events that occur within the infected cell as the inclusion enlarges. This allows the microbe to control the overall composition of the inclusion and direct its localization, as well as that of several organelles, within the host cell. Within ~8-12 hours of invading a cell, EBs begin differentiating into RBs, initiate replication, and begin to divide by a process that is dependent on the synthesis and turnover of septal peptidoglycan (141; 143). At roughly 24 hours post infection (hpi), RBs begin asynchronously converting back into EBs. *Chlamydia* EBs eventually exit their host cell by one of two pathways: the inclusion expands enough to either i) lyse the host cell, expelling the newly-formed EBs or ii) portions of the inclusion begin to bleb off into the extracellular environment in a process termed extrusion (104).

Researchers have long known of the existence of an additional, non-replicative form of *Chlamydia* that is capable of remaining viable within the inclusion vacuole for extended periods

of time. These forms are referred to as 'aberrant bodies' (ABs) and have been classically distinguished by their enlarged size (~2-10 μm). *Chlamydia* AB formation is the result of cell division inhibition while cell growth continues unabated (Fig. 16a). Because cell division is required for the bacterium to eventually return to its infectious form, halting the process also inhibits the production of infectious EBs. This pause in development is reversible, and in most cases upon removal of the stressor, cell division resumes, and eventually infectious progeny are once again observed. This unusual morphology was noted in early studies investigating the effects of the antibiotic penicillin on intracellular *Chlamydia* species (154). It was originally proposed that this unique morphology resulted from the inhibition of the *Chlamydia* penicillin-binding proteins (PBPs; the target of all β-lactam-based antibiotics) that are essential for bacterial cell division (88). Subsequent studies identified additional stressors that induce *Chlamydia* AB formation in tissue culture cells. Examples include the addition of the cytokine interferon gamma (IFNγ) (18), tryptophan (17) and iron starvation (212), heat shock (116), amino acid starvation (50; 194), infection of monocytes (127) and macrophages (83; 172), co-infection with viruses (27; 58), and a number of other pressures (16). Aberrant forms have also been observed *in vivo* (30; 205; 211) indicating that they can develop during the course of infection. This phenotype is not unique to members of the Chlamydiaceae, as prominent members of the Chlamydiales have recently been shown to exhibit the aberrance phenotype under a number of experimental conditions *in vitro* (221).

Given their appearance under a wide array of culture conditions, it has been proposed that AB formation results from an underlying stress response pathway that provides *Chlamydia* species a level of protection during the course of infection (71). In the context of pathogenic *Chlamydia* species, 'persistence' has generally been defined as i) the reversible inhibition of cell

division that results in an interruption of the pathogen's developmental cycle and ii) a corresponding increase in bacterial cell size. While the mechanisms of cell division arrest have been previously investigated in great detail for a number of aberrance-inducing conditions (189), considerably less effort has been spent investigating the degree to which these persistent forms differ in their basic physiology and their interactions with host cells. While a few studies have characterized the structural (166), transcriptional (20; 169; 187) and translational (26; 34) regulatory mechanisms underlying AB formation, there continues to be much speculation and debate concerning the relevance of *Chlamydia* ABs *in vivo* and their contribution to the pathogenesis and persistence of these organisms in human and animal infections (16; 29; 275; 278).

Currently the defining features of *Chlamydia's* 'persistent state' are 1) inhibition of cell division, 2) cell size enlargement, 3) the inhibition of EB production, and 4) the reversibility of the process. In this study, we set out to explore the physiological underpinnings that define these aberrant forms of *Chlamydia*, and delineate how their structural and functional differences impact the microbe's interaction with its host cell. We found that two prominent factors differ between *Chlamydia's* aberrant forms: i) the synthesis and turnover of immunostimulatory peptidoglycan and ii) the presentation of effector proteins on the inclusion surface that are associated with the mid- and late- stages of the pathogen's developmental cycle.

MATERIALS AND METHODS

Bacterial strains and cell lines

C. trachomatis serovar L2 strain 434/Bu was provided by Dr. Anthony Maurelli (University of Florida). Chlamydial infections were carried out in HeLa cells (also provided by Dr. Anthony Maurelli) unless otherwise noted. HEK-Blue-hNOD1 and -Null1 cells were

purchased from Invigogen and propagated according to the manufacturer's instructions. Cell lines were passaged in high glucose *Dulbecco's* Modified Eagle Medium (DMEM, Gibco) and 10% Fetal Bovine Serum (FBS, HyClone).

Chlamydial infections

HeLa cells were plated on a glass coverslip in 24 well tissue culture treated plate wells (Costar) at confluency of ~70-80%. Cells were infected with *C. trachomatis* L2 434/Bu in cold *Dulbecco's* Modified Eagle Medium (DMEM) (Gibco) (250 μl per well) and placed on a rocker in the 37°C tissue culture incubator for 2 hours. Subsequently, the DMEM was removed and replaced with DMEM supplemented with 10% FBS (HyClone), and 1x MEM Non-Essential Amino Acids Solution (Sigma) (250 μl per well). The following aberrance inducing conditions were tested in this study: 50 U IFN-γ, 100 μM DPP (iron chelator), 10 μM ampicillin, 6-8% sucrose, 50 μM C1 (T3SS inhibitor), and 125 μM MP265 (polymerization inhibitor of the bacterial cytoskeletal protein MreB). The concentration of azithromycin used with 3 μg/ml. IFN-Y and DPP was added at the time of infection. Ampicillin and sucrose were added at 2 hpi, while C1, azithromycin, or MP265 were added 8 hpi, following the EB to RB conversion.

Analysis of the total bacterial volume within individual inclusion

Volumetric measurements were taken utilizing an immune-labeling/ fluorescence approach. Infected cells were left either untreated or subjected to aberrance-inducing conditions for 24 hours. Cells were fixed and permeabilized with methanol for 5 minutes, gently washed three times with 1X PBS, further permeabilized with 0.5% Triton™ X-100 for an additional 5 minutes and subsequently washed three times with 1X PBS. To prevent non-specific binding, cells were blocked for 1 hour with 3% Bovine Serum Albumin (BSA) (Sigma), and subsequently labeled with goat anti-MOMP (1:500 dilution in 3% BSA) for 1 hour, washed with 3% BSA, and

incubated with donkey anti-goat AlexaFluor™ 594 (1: 2000 in 3% BSA). Cells were washed with 3% BSA, 1X PBS, and coverslips were subsequently mounted on slides with ProLong Gold Antifade Mounting Media and stored in the dark at 4°C until imaged via confocal microscopy. All confocal imaging was conducted with a Zeiss 710 laser scanning microscope, confocal Z-stacks were taken using the 40x objective, and all processing was conducted on Zen 2012 (Carl Zeiss) software. Settings were fixed at the beginning of image acquisition and the same parameters were applied for collecting and post processing all images taken. ImageJ was used for all subsequent image analysis utilizing the FIJI addon '3D Objects Counter' to identify the 3-dimensional spatial constraints of individual *Chlamydia* inclusions based on positive MOMP-labeling and to calculate their corresponding volumes in μm^3. Statistical significance values were calculated utilizing a one-way ANOVA coupled with a multiple comparisons test with each condition compared with the azithromycin treatment group. RB diameters were calculated using radius values derived from the RB volumes, with the assumption that *C. trachomatis* RBs and ABs are spherical; d = 2r = 2 [3(V / 4π)^(1/3)].

Quantification of inclusion forming units (IFU)

Chlamydia EBs were mechanically harvested at 44 hpi with glass beads at the indicated time points, suspended in 200 µL of 1X sucrose-phosphate-glutamate (SPG) and stored at -80°C. For recovery assays, at 44 hpi cells were washed with cold DMEM and replaced with DMEM supplemented with 10% FBS (HyClone), and 1x MEM Non-Essential Amino Acids Solution (Sigma) for 24 or 48 additional hours prior to EB harvests. To ascertain infectious titers, EBs were serially diluted and used to infect HeLa cells that had been plated 24 hours prior (200 µl of 200,000 cells/ml per well seeded in a 96 well plate) (in technical duplicates). Plates were centrifuged for 1 hour at 2,000 g at 35°C to enhance synchronous infection. At 24 hpi, cells were

fixed and permeabilized with methanol for 10 min., incubated with a Pathfinder direct fluorescent antigen (DFA) kit (BIORAD) for 30 min., and washed twice with 1X PBS. Ninety-five-percent glycerol was placed in each well and inclusions were subsequently counted via epifluorescence microscopy. Twenty fields of view were counted in duplicate for each treatment condition.

Fluorescent labeling of PG, cell nuclei, actin filaments, and inclusion membrane proteins

PG labeling was carried out as previously described (141; 143). Briefly, HeLa cells were infected with *C. trachomatis* L2 434/Bu as described previously, with 1 mM EDA-DA probe added to the infection media at 2 hpi. At 24 hpi, infection media was removed and cells were washed three times with 1X PBS. Cells were fixed and permeabilized with methanol for 5 minutes and gently washed three times with 1X PBS. Cells were then further permeabilized and blocked as described previously. A click chemistry reaction was then performed utilizing the Click-iT Cell Reaction Buffer Kit (Invitrogen) and Alexa Fluor 488-azide (10 μM). Subsequent MOMP labeling was then conducted, as previously described. For labeling inclusion membrane proteins, fixed / permeabilized cells were incubated for 1 hour with polyclonal mouse or rabbit serum raised against the inclusion membrane proteins IncA, CT229, CT813, or IncG. Cells were then washed with 3% BSA and incubated with donkey anti-mouse or donkey anti- rabbit AlexaFluor™ 488 (1:1000 in 3% BSA). For visualizing cell nuclei, methanol-fixed and permeabilized cells were incubated with Hoechst stain for 3 mins and then washed with 3% BSA and 1X PBS. For labeling host cell actin, at 46 hpi cells were fixed with 3.7% paraformaldehyde for 15 mins at room temperature and subsequently washed with 1X PBS. Cells were then permeabilized with 0.01% Triton™ X-100 for 25 mins and subsequently washed twice with 1X PBS. Cells were then blocked for 1 hour with 1% BSA and incubated with AlexaFluor™ 488

phalloidon (ThermoFischer Scientific A12379) that was prepared in methanol as described by the manufacturer to a final concentration of 1X for 1 hour, before washing labeled cells with 1% BSA and PBS. All coverslips were mounted on slides with ProLong Gold Antifade Mounting Media and stored in the dark at 4°C prior to imaging via confocal (Zeiss 710) or structured illumination (ELYRA PS.1) microscopy.

Homotypic Fusion Assay

HeLa cells were infected with *C. trachomatis* L2 434/Bu at a MOI of 10 and infections were allowed to proceed normally, or in the presence of either AMP or DPP. At 24 hpi, infection media was removed and cells were washed fixed, and labeled, as previously described. Cells were incubated with goat anti-MOMP and polyclonal rabbit anti-CT229 for 1 hour, washed with 3% BSA, and co-incubated with chicken anti-goat AlexaFluor™ 594 and donkey anti-rabbit AlexaFluor™ 488, before being washed and coverslips mounted on slides with ProLong Gold Antifade Mounting Media. An analysis was conducted of inclusions present per cell by counting cell and inclusion numbers across 10 random imaging planes for each condition examined (untreated, AMP, and DPP). Data points represent average values of the number of inclusions per cell per imaging plane examined (10 for each condition). Lines represent mean values of all data points per condition and error bars represent standard deviations. Statistical significance values were calculated utilizing a one-way ANOVA coupled with a multiple comparisons test. **, $p < 0.005$; ns, not significant.

Infection of HEK-Blue-hNOD1 and -Null1 cells with *C. trachomatis* and NF-ϰB reporter assay

HEK-Blue cells expressing the hNOD1 receptor and carrying the NF-ϰB SEAP (secreted embryonic alkaline phosphatase) reporter gene (InvivoGen) were used according to the

manufacturer's instructions and adapted to assess NOD1-specific NF-κB activity during infection with *C. trachomatis*. Briefly, 3 X 10^5 cells/ml of HEK-Blue-hNOD1 or -Null1 cells were plated in 96-well plates (total reaction volume of 200 ml per well [~6.0 X 10^4 cells per well]) and allowed to settle/adhere for 6 h at 37°C. These cells were infected with *C. trachomatis* L2 434/Bu at an MOI of 1. To enhance the synchronization of the infections, plates were centrifuged for 1 h at 2,000 X g. Plates were then incubated in a CO_2 incubator at 37°C, and supernatants were collected for subsequent analysis of SEAP activity at the indicated time points. A colorimetric reporter assay was then utilized in order to quantify the abundance of SEAP in cell supernatants, providing an estimate of the relative abundance of residual stimulatory ligand (MurNAc-L-Ala-D-Glu-mDAP) in experimental and control cells. Twenty microliters of the supernatants collected from infected cells was added to 180 μl of the SEAP detection solution (InvivoGen), followed by incubation at 37°C for ~8 h. SEAP enzymatic activity was then quantified using a plate reader set to 650 nm. Infected cells were compared to uninfected controls as well as infected cells that had been treated with either the iron chelator DPP or IFN-γ. Uninfected cells treated with the known NOD1 signaling ligand TriDAP (1mg/ml) were used as a positive control. Additionally, to ensure that changes in alkaline phosphatase activity were NOD1 dependent under each of the experimental conditions tested, all experiments were carried out in parallel in the HEK-Blue-Null1 cell line, which contains the empty expression vector but lacks hNOD1. HEK-Blue NOD1 SEAP reporter assays were carried out in three separate experiments, statistical analysis was conducted by 2-way ANOVA, and significance values were analyzed by utilizing Sidak's multiple-comparison test. Values plotted are means of the raw optical density at 650 nm (OD_{650}) measurements.

Azithromycin study

HeLa cells were plated at confluency of ~70-80% in 24 well tissue culture treated plate wells (Costar). Cells were infected with *C. trachomatis* L2 434/Bu in cold DMEM and placed on a rocker in the 37°C tissue culture for 2 hours. Subsequently, the DMEM was removed and replaced with DMEM supplemented with 10% FBS (HyClone), and 1x MEM Non-Essential Amino Acids Solution (Sigma). DPP was added at the time of infection, while AMP was added at 2 hpi. At 18 hpi, 3 μg/ml azithromycin was added to infected cells. Infections were allowed to proceed for an additional 24 hours, and then the monolayers were gently washed with 1X PBS. Half of the wells were then mechanically harvested with glass beads and 200 µl of 1X sucrose-phosphate-glutamate buffer and stored at -80°C. In the other half of the wells, the media was replaced with DMEM supplemented with 10% FBS (HyClone), and 1x MEM Non-Essential Amino Acids Solution (Sigma) for 48 additional hours, at which point they were also lysed and EBs harvested. IFU were then quantified for both treatment and recovery conditions, as previously described. The assay was conducted three separate times. Statistical significance values were calculated utilizing student T-tests comparing the groups indicated.

Investigation of compound C1 effects under high iron conditions

HeLa cells were plated at confluency of ~70-80% in 24 well tissue culture treated plate wells (Costar). Cells were infected with *C. trachomatis* L2 434/Bu in cold DMEM and placed on a rocker in the 37°C tissue culture for 2 hours. Subsequently, the DMEM was removed and replaced with DMEM supplemented with 10% FBS (HyClone), and 1x MEM Non-Essential Amino Acids Solution (Sigma). DPP was added at the time of infection, while C1 was added at 8 hpi. 0 or 250 μM $FeSO_4$ was added at the time of infection. At the 44 hpi, monolayers were washed with 1X PBS and *Chlamydia* EBs were mechanically harvested with glass beads at the indicated time points, suspended in 200 µL of 1X sucrose-phosphate-glutamate (SPG) and stored

at -80°C. Inclusion forming units were quantified as previously described. The assay was conducted three separate times. Statistical significance values were calculated utilizing a one-way ANOVA coupled with a multiple comparisons test.

RESULTS

C. trachomatis aberrant body formation results in cell division arrest and temporarily pauses the developmental cycle

We began by testing a panel of aberrance-inducing conditions to determine if the ABs produced met the classical criteria for chlamydial persistence. Seven aberrance-inducing conditions were compared: β-lactam antibiotics (ampicillin; AMP), non-ionic osmotic stress (induced by sucrose supplementation), MreB inhibition (induced by the polymerization inhibitor MP265), T3SS inhibition (induced by the T3S inhibitor compound C1), iron depletion (induced by 2,2‘-Bipyridyl; DPP), and tryptophan starvation (induced by interferon gamma; IFNγ). At 24 hpi, we fixed and labeled the outer surface of *Chlamydia trachomatis* L2 strain 434/Bu under different treatment conditions and conducted an imaging analysis to assess the average volume of microbial material present within individual inclusions. By 24 hours, *C. trachomatis* inclusions are filled with hundreds of RBs and EBs, and therefore do not provide sufficient resolution for delineating individual RB cell boundaries by fluorescence microscopy (Fig. 16b, control). Azithromycin inhibits protein synthesis in *Chlamydia spp*. preventing RB growth and division. RB volume and diameter measurements in infected cells treated with azithromycin at 8 hpi were ~0.9 μm^3 and ~1.2 μm, respectively. These measurements align well with what has been published previously regarding average RB size early in chlamydial development (138), and we used this condition to serve as a positive control representing normal RB size in our subsequent analysis. All aberrance-inducing conditions tested halted or severely limited cell division in *C. trachomatis* within 24 hours; however, we found that the resultant ABs differed dramatically in

size (Fig. 16b-e). AMP-induction resulted in the largest AB volumes and average diameters (~ 50 μm^3, and ~ 5 μm, respectively), with the rest of the conditions resulting in ABs with much smaller volumes and average diameters (~5-10 μm^3 and ~ 1.5-3 μm, respectively). Examination of inclusions from different aberrance-inducing conditions by electron microscopy revealed that smaller ABs were generally found within smaller inclusions when compared to both untreated and AMP-treated controls (Fig. 16c-e).

Because cell division and differentiation are linked in *Chlamydia* species, the inhibition of cell division results in the halting of the developmental cycle and prevents the formation of *Chlamydia's* infectious form. In order to validate that our AB-induction conditions successfully halted EB formation, we lysed infected cells at 44 hpi, and infected new cell monolayers with these lysates. After 24 hours we counted the resultant inclusions and used them as a readout for the number of infectious EBs resulting from the previous infection. The majority of aberrance-inducing conditions tested effectively halted EB production, and few, if any, infectious forms were recoverable after 44 hours (Fig. 16f).

While 'aberrance' is defined by the absence of cell division and a corresponding increase in chlamydial cell size, for this morphotype to be defined as 'persistence' the phenotype must also be reversible. To assess this, we removed the aberrance-inducing media from each treatment group and allowed the cells to recover (as described in the methods). Under most conditions we observed a partial recovery in infectious progeny production after 24 hours (Fig. 16g) and close to full recovery after 48 hours (Fig. 16h). Only *C. trachomatis* treated with compound C1 failed to recover to within one log of the untreated control group within 48 h. Previous studies have found that compounds similar to C1 used as T3SS inhibitors may also function as iron chelators (95; 232), and we hypothesized that this dual functionality might explain why *C. trachomatis*

was unable to recover as efficiently from this treatment condition. When exogenous iron sulfate was added to the infection media containing compound C1, we observed a partial recovery in infectious progeny, indicating that C1 may also act as an iron chelator (Fig. 17). Overall, our observations were largely consistent with previous studies (20; 141; 154; 212; 271), and we concluded that our testing conditions were suitable for inducing persistence in *C. trachomatis* L2 strain 434/Bu.

Persistent forms of *Chlamydia* differ in their capacity to assemble septal peptidoglycan

Peptidoglycan (PG) is a principal component of the bacterial cell wall and is essential for maintaining cell shape, regulating osmotic pressure, and constriction of the septum during the last stage of the bacterial division process (270). Recent technical advances have allowed us to label PG in *Chlamydia spp*. utilizing a novel dipeptide incorporation strategy (102; 143). This labeling is specific for newly synthesized PG (Fig. 18a) as incorporation of the probes occurs in living microbes during the initial synthesis of muramyl-pentapeptide in the bacterial cell cytoplasm (134). Previously, we determined that members of the Chlamydiaceae (pathogenic *Chlamydiae*) possess PG (143) (Fig. 18b, row 1, column 1). Whereas other bacterial species, including other members of the Chlamydiales (200), synthesize PG as a major component of their cell wall, pathogenic *Chlamydia* species limit PG to their septum (141), representing a significant reduction in PG abundance in these microbes and highlighting its importance for chlamydial cell division. As aberrant forms of *Chlamydia* no longer divide, we hypothesized that this deficiency was likely due to the inhibition of either PG synthesis or assembly.

Our labeling studies revealed that *C. trachomatis* is still capable of synthesizing PG glycan chains when subjected to β-lactam antibiotics that induce AB formation, however PG localization is no longer restricted to a single division septum (Fig. 118b, row 1, column 2) (141;

143). In contrast, when PG assembly is completely prevented by inhibiting MreB, the major organizer of the microbe's division complex (184), no PG labeling is discernable (Fig. 18c, row 1, column 1) (141). We hypothesized that different inducers of persistence may similarly differ in whether they cause cell division arrest as a result of deficiencies in either PG assembly or PG synthesis. To distinguish between these two possibilities, we tested our panel of aberrance-inducing conditions in conjunction with our PG labeling assay. We found that sucrose-induced aberrance produced ABs that contained labeled PG in an irregular arrangement (Fig. 18b, row 1, column 3) similar to that observed in β-lactam-induced aberrance. Conversely, inhibition of the microbe's T3SS, iron-depletion, and tryptophan-depletion all resulted in ABs that lacked detectable PG (Fig. 18c, row 1, column 2-4). As the mechanism of action by which this second category of stressors induces aberrance involves the downregulation of transcription or post-transcriptional regulation (20; 26; 34; 169; 187), we also examined the effect of azithromycin on the chlamydial PG ring when added at 8 hpi, a time point immediately following to the EB-RB transition (21; 143). This treatment resulted in normal-sized RBs (~ 1-1.5 μm) that completely lacked discernable PG (Fig. 18b, row 1, column 4). Taken together, these results indicate that all chlamydial ABs examined exhibited alterations in their PG, but that they diverged in terms of whether those changes were in PG localization or abundance.

Aberrant *Chlamydia* forms differ in their ability to release PG-derived, immunostimulatory muropeptides

While PG is continuously synthesized during bacterial cell growth and division, changes in cell size, shape, and the constriction of the division plane also require localized PG degradation. This process results in replicating microbes shedding PG-derived muropeptides into the environment. In the case of invading pathogens these muropeptides are recognizable by a

host's innate immune system, specifically the nucleotide oligomerization domain (NOD) receptors (270). NOD1 recognizes peptides containing a *meso*-diaminopimelic acid (*m*DAP), which is normally present at the third position of the PG stem peptide in Gram-negative bacteria. NOD1 signaling triggers the production of a number of host cell cytokines via an NFκB-dependent pathway, and both NOD1 and NOD2 recognize intracellular *C. pneumoniae* and play an essential role in bacterial clearance *in vivo* (227).

As a number of chlamydial ABs appeared to lack detectable PG labeling, we wanted to eliminate the possibility that PG biosynthesis was still occurring, but was simply being degraded too rapidly to be visualized. We utilized a human NOD1 reporter cell line to determine the abundance of PG-derived muropeptide released by *C. trachomatis* during three aberrance-inducing conditions thought to be most physiologically relevant to human infections: β-lactam antibiotics, iron restriction, and IFNγ. As we failed to detect PG labeling in our iron restriction and IFNγ -induced conditions, we hypothesized that the block on PG biosynthesis must be earlier in the synthesis pathway than the addition of the di-peptide probes to the PG stem peptide by the UDP-N-acetylmuramoyl-tripeptide-D-alanyl-D-alanine ligase; MurF (Fig. 18a). We found that under AMP-induced aberrance, significant amounts of NOD1 ligand continued to be released by *C. trachomatis* 24 hpi (Fig. 19a), whereas under iron-depleted conditions (Fig. 19b) and in the presence of IFNγ (Fig. 19c), NOD1 signaling was significantly reduced. This reduction was specific for *Chlamydia* infected cells, as interferon and iron-depletion had no discernable effect on NOD1 signaling induced by the NOD-stimulatory ligand L-Ala-γ-D-Glu-*m*DAP (TriDAP). No significant signal was observed in the Null1 cell line (contains empty expression vector) under any of the conditions tested (Fig. 19a- c), indicating that the NFκB expression was NOD1-specific. When combined with PG-targeting antibiotics (AMP) iron

depletion continued to exhibit a complete loss of NOD1 signaling (Fig. 19a), indicating that the PG-synthesis inhibition phenotype is dominant under the conditions tested. This result indicates that the block on PG biosynthesis under iron/ tryptophan depletion conditions occurs prior to the synthesis of muramyl tri-peptide. When taken together, these results indicate that chlamydial ABs induced by penicillin-derived antibiotics and iron-/ tryptophan- starvation differ in their capacity to synthesize, assemble, and subsequently shed immunostimulatory, PG-derived muropeptides. The inability to detect muramyl tri-peptide in infected cells under iron/ tryptophan depletion conditions also indicates that PG biosynthesis is inhibited prior to the addition of mDAP to the PG stem peptide by the chlamydial UDP-N-acetylmuramoyl-L-alanyl-D-glutamate-diaminopimelate ligase, MurE (191).

The timing of persistence induction directly affects *Chlamydia* morphology and PG-derived muropeptide release

During active infections *C. trachomatis* develops asynchronously, with infected cells in close proximity often containing bacteria in completely different stages of the pathogen's developmental cycle. The ability of *C. trachomatis* to form enlarged, aberrant bodies is largely dependent on when induction conditions are introduced during the chlamydial developmental cycle. Previous studies have used fast-acting, aberrance-inducing compounds to investigate how persistence induction affects *C. trachomatis* at different stages of its development. For example, when MreB is inhibited prior to the EB-RB transition, development completely halts and very few EBs successfully transition to RBs (141). Similar results have been reported when protein synthesis is inhibited prior to the EB-RB transition, and protein synthesis is known to be globally affected by aberrance induction under iron restriction (34). To determine whether this is the case for other aberrance-inducing conditions, we examined the effect that individual aberrance

inducers had on chlamydial morphology when added at different time points in the developmental cycle. We added the fast-acting T3SS inhibitor C1 at key points throughout the developmental cycle of *C. trachomatis*: 2 hpi (immediately post invasion), 8hpi (EB-RB transition), and 22 hpi (RBs undergoing active cell division). We found that compound C1 exhibited a similar phenotype to MreB-inhibiting compounds A22 and MP265: when it was added prior to the EB-RB transition (at 2 hpi), only PG-negative, EB-sized particles were observable in infected cell monolayers 24 hpi (Fig. 20b), and when it was added just after the EB-RB transition (8 hpi), enlarged ABs were observed that lacked discernable PG (Fig. 20c).

Unlike a PG sacculus that largely retains its form when PG synthesis is inhibited, septal PG in *Chlamydia* species is more transient, and begins to degrade within minutes of inhibiting PG synthesis (141). Given the absence of PG in the majority of ABs examined (Fig. 18) and lack of immunostimulatory muropeptides released into host cells (Fig. 19), we postulated that induction of aberrance in *Chlamydia* likely affects PG biosynthesis. We sought to test this by inducing aberrance with compound C1 for a short, two-hour duration later in the developmental cycle (at 22 hpi), and subsequently examined the effects on PG localization. We found that two hour-treated RBs appeared larger and exhibited a swollen morphology compared to untreated controls (Fig. 20d). PG was discernable, but labeling intensity appeared significantly reduced. A closer examination of individual ABs revealed the presence of incomplete PG rings that appeared to be undergoing degradation (Fig. 20e-g), matching previous observations with the MreB inhibitors (141). This data largely supports our previous conclusion that PG synthesis and degradation pathways are decoupled in *C. trachomatis*, and also indicates that during persistence induced by T3S inhibition, PG degradation continues despite a halt in PG biosynthesis.

We hypothesized that if chlamydial persistence halts new PG biosynthesis but does not stop PG degradation, then RBs that transition to aberrant forms later in development will actively degrade and shed their PG in a time-dependent manner. Inhibition of protein synthesis has been previously shown to prevent PG biosynthesis in *C. trachomatis* (188) and iron sequestration has previously been linked to a general reduction of translation in *C. trachomatis* (34). Therefore, we hypothesized that iron restriction likely prevents PG biosynthesis in *C. trachomatis*. To examine the temporal kinetics of PG muropeptide release under aberrance-inducing conditions, we compared NOD1 signaling in *Chlamydia*-infected cells in which persistence via iron depletion was induced at different time points throughout the developmental cycle. We found that the earlier in the developmental cycle that DPP was added to the infected cells, the greater the decrease in *Chlamydia*-specific, NOD1 signaling (Fig. 21). No discernable difference was observed between untreated cells and those treated at 12- and 16- hpi, indicating that the abundance of immunostimulatory peptides present at 12 hpi was sufficient to effectively saturate the assay's upper detection limit. By comparison, the timing of exposure with the immunostimulatory ligand for cells treated with exogenous TriDAP appeared to have no effect on NOD1 signaling (Fig. 21). Taken together, these results indicate that some persistence induction conditions inhibit the synthesis of chlamydial PG in a time dependent manner, but do not inhibit PG degradation.

Persistent forms of *Chlamydia* differ in the presentation of mid- and late-stage effector proteins

Chlamydia maturation is temporally regulated, and Inc proteins are secreted and integrate into the inclusion membrane at different time points during the pathogen's development. Secreted effectors are categorized into three general groups that fit into different phases of the

developmental cycle; early, mid, and late (8; 20). As an inclusion 'matures' it gradually accumulates newly secreted Inc proteins, which results in changing the overall composition of the inclusion membrane. Many of these early and mid-stage Inc proteins are involved in redirecting exocytic vesicles to the inclusion, enabling it to steadily enlarge over time (68). We reasoned that an interruption in the inclusion maturation pathway could explain the reduction in inclusion size we previously observed under various persistence-inducing conditions (Fig. 16b-e). To test this hypothesis, we selected four Inc proteins that are expressed and secreted at different times during inclusion development (8). *ct229* and *incG* are expressed early in development, with peak expression at 2 and 12 hpi, respectively. *incA* is expressed closer to the mid-way point in the inclusion maturation pathway with peak expression at ~20 hpi, and *ct813* is a late-stage effector whose expression peaks at ~30 hpi. Using polyclonal antibodies to each of these four Inc proteins, we examined whether they were present or absent on the inclusion membranes in *Chlamydia*-infected cells under different aberrance-inducing conditions. We found that CT229 was present under all conditions tested (Fig. 22a), whereas IncG was present on AMP- and sucrose-treated cells, and to a lesser degree on cells treated with the iron chelator *DPP* (Fig. 22b). IncA and CT813 were only present on inclusions in the control, AMP- and sucrose-treated groups and all other conditions resulted in no discernable labeling (Fig. 23. a, b). When combined with our inclusion size (Fig. 16b) and PG labeling data (Fig. 18b, c), imaging analysis suggests that a strong correlation exists between inclusion maturation and size and PG biosynthesis in persistent forms of *C. trachomatis*.

Persistent forms of *Chlamydia* exhibit differences in their ability to undergo homotypic fusion and induce actin cage formation

Given the differences in Inc presentation we observed on the inclusion membranes of different persistent forms of *C. trachomatis*, we hypothesized that persistent forms also differ in their interaction with host cells, particularly interactions that occur at later stages of development. A *Chlamydia* inclusion will traffic to the microtubule-organizing center (MOTC) of a host cell relatively early in development (within 4-5 hpi) in a process dependent on dynein and chlamydial protein synthesis (85). As this process occurs early in development, we predicted that it would not be adversely affected by the induction of aberrance, because the relevant effector proteins will have already been generated and secreted. Supporting this premise, we found that, under all of the aberrance-inducing conditions tested, all inclusions were capable of successfully trafficking to the cell nucleus (Fig. 24a).

In contrast to trafficking to the MOTC, homotypic vesicle fusion of *C. trachomatis* inclusions within a single cell occurs later in the developmental cycle and is mediated by the secreted effector protein IncA (86). Therefore, we hypothesized that in cells infected at a heightened multiplicity of infection (MOI) inclusions exposed to aberrance-inducing conditions with discernable labeling of IncA (Fig. 25a) should successfully undergo homotypic fusion resulting in fewer inclusions per cell, while those lacking discernable labeling of IncA should exhibit higher numbers of inclusions per cell. We found that in cells infected at a MOI of 10:1, DPP-treated cells contained higher numbers of inclusions per cell when compared to untreated and AMP treated cells (Fig. 25b). We also noted that despite containing more inclusions per cell, these inclusions still appeared to congregate in the same area of the cell (Fig. 25c), further supporting the premise that early developmental processes such as inclusion trafficking to the MOTC are retained by these persistent forms. Despite being in close proximity, inclusions in

DPP-treated cells appeared to be incapable of fusion, in line with the observed absence of IncA (Fig. 25a).

Actin rearrangement is important for maintaining the integrity of the chlamydial inclusion (132), as well as enabling *Chlamydia* to eventually exit the host cell (48). During normal chlamydial development, actin recruitment around the chlamydial inclusion is directly mediated by the late-stage effector protein CT813 (128). Recruitment of actin to the inclusion begins around 20 hpi and continues to increase as the chlamydial inclusion matures (48). As we observed an absence in CT813 labeling in a number of chlamydial ABs, we hypothesized that these inclusions should be defective in their ability to recruit actin. We found that actin cage formation roughly corresponded to our CT813 imaging study (Fig. 24b, 26a) in that actin cages were only observed in untreated and AMP-treated cells (Fig. 24b, 26b). Taken together, this result indicates that while all *Chlamydia* ABs are effectively paused in the developmental cycle, only a subset of ABs also paused the maturation of the chlamydial inclusion.

Iron depletion-induced persistence enhances the susceptibility of *C. trachomatis* to azithromycin treatment

'Persistence' is often used to describe a general survival mechanism by which pathogens avoid clearance by a host, but it is also frequently used to describe a mechanism to avoid killing by antibiotic treatment. We sought to determine whether *C. trachomatis* ABs are protected against treatment with azithromycin, a frontline antibiotic commonly used to treat human chlamydial infections (136). We found that viable EBs were recoverable from the sub-inhibitory azithromycin treatment group, while treatment with AMP or DPP induced aberrance and prevented EB formation (Fig. 27). Interestingly, we successfully recovered EBs in the AMP/ azithromycin-treated group post-recovery but were unable to detect viable EBs in the DPP/

azithromycin-treated group post-recovery (Fig. 27). These results indicate that iron depletion-induced persistence enhances the susceptibility of *C. trachomatis* to killing by azithromycin while AMP-induced persistence does not.

FIGURES

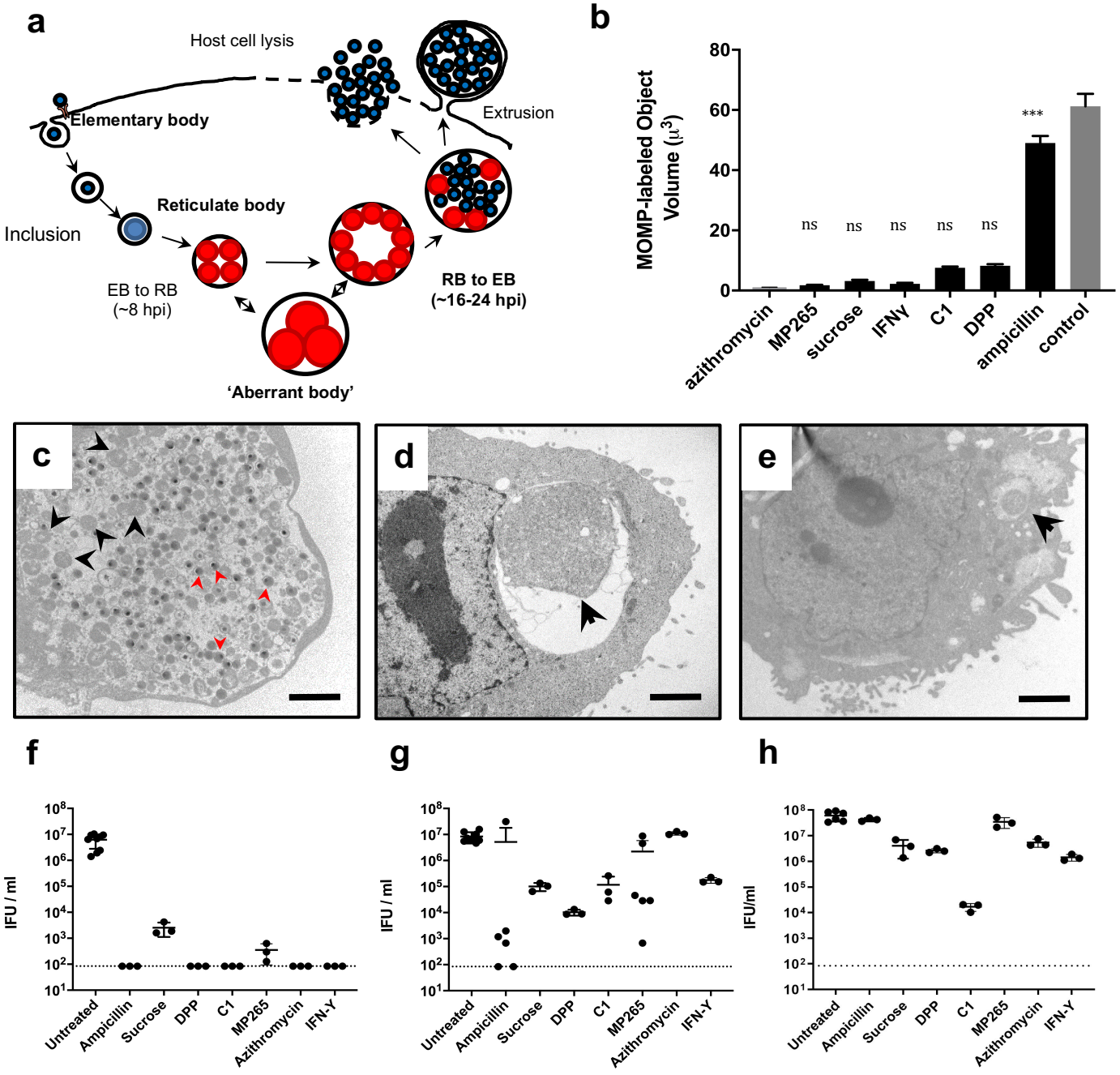

a
Host cell lysis
Elementary body
Extrusion
Reticulate body
Inclusion
EB to RB
(~8 hpi)
RB to EB
(~16-24 hpi)
'Aberrant body'
b
MOMP-labeled Object Volume (μ3)
80
60
40
20
0
ns
ns
ns
ns
ns
***
azithromycin
MP265
sucrose
IFNγ
C1
DPP
ampicillin
control
c
d
e
f
IFU / ml
Untreated
Ampicillin
Sucrose
DPP
C1
MP265
Azithromycin
IFN-Y
g
IFU / ml
Untreated
Ampicillin
Sucrose
DPP
C1
MP265
Azithromycin
IFN-Y
h
IFU/ml
Untreated
Ampicillin
Sucrose
DPP
C1
MP265
Azithromycin
IFN-Y

Figure 16. *C. trachomatis* aberrant body formation results in cell division arrest and pausing of the developmental cycle.
(a) Diagram of the *Chlamydia* developmental cycle. (b) Volume measurements of *C. trachomatis* present within inclusions at 24 hpi under untreated and aberrance-inducing conditions. Data were collected by fluorescence microscopy over three independent experiments. Each data point represents the collective total of contiguous, MOMP labeled material (~100 inclusion measurements taken per group). (c to e) Electron micrographs of HeLa cells infected with *C. trachomatis* at 24 hpi that were either untreated (c) or treated with AMP (d) or the iron chelator DPP (e). Black arrowheads indicate RBs and ABs, and red arrowheads indicate the much smaller, electron-dense EBs. Bars, ~2μm. (f to h) Inclusion-forming unit (IFU) counts were conducted at 44 h postinfection/posttreatment (f) and after recovery in the absence of treatment for an additional 24 h (g) and 48 h (h). The dotted lines represent the assay's limit of detection. C1, T3SS inhibitor compound C1; MP265, MreB polymerization inhibitor. Each data point plotted represents data from an independent experiment, and error bars represent the standard deviations from the means.

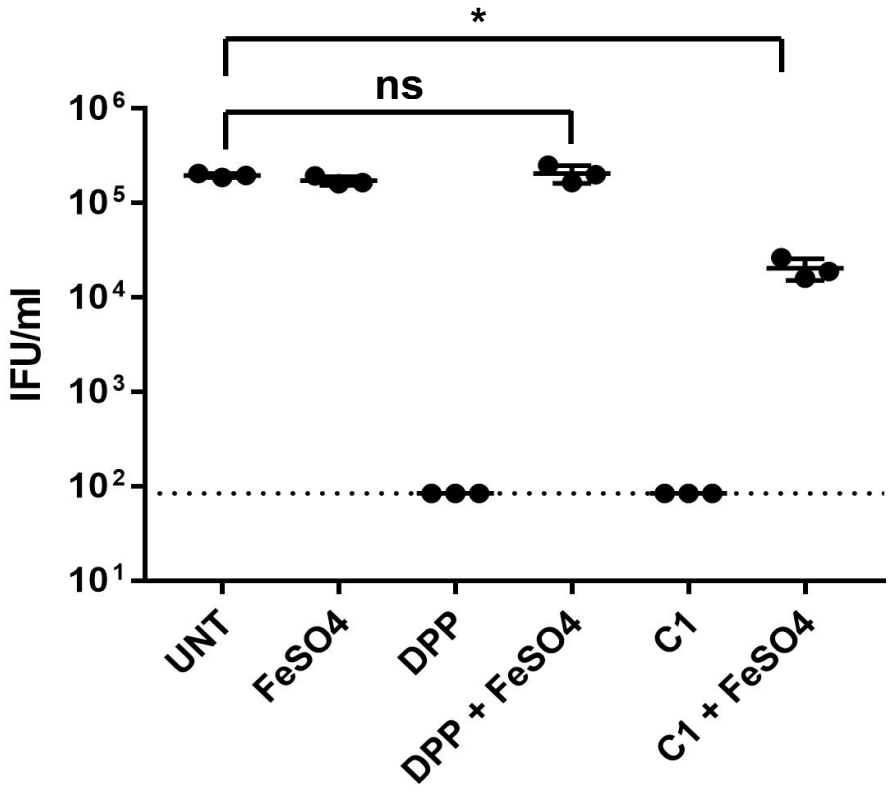


Figure 17. The effects of T3SS inhibitor on the development of *C. trachomatis* are significantly reduced in cells supplemented with exogenous iron.
0 or 250 μM FeSO4 was added to HeLa cells at the time of infection with *Chlamydia trachomatis*. At 2 hpi or 8 hpi, DPP or C1 (respectively) was added. EBs were harvested at 44 hpi. Inclusion forming units (IFU) were then calculated by conducting serial dilutions, infecting fresh monolayers, and counting new inclusions at 24 hpi. The dotted line represents the limit of detection for the assay. Data plotted represent three independent biological replicates and error bars represent the standard deviations from the mean. **, $p < 0.01$.

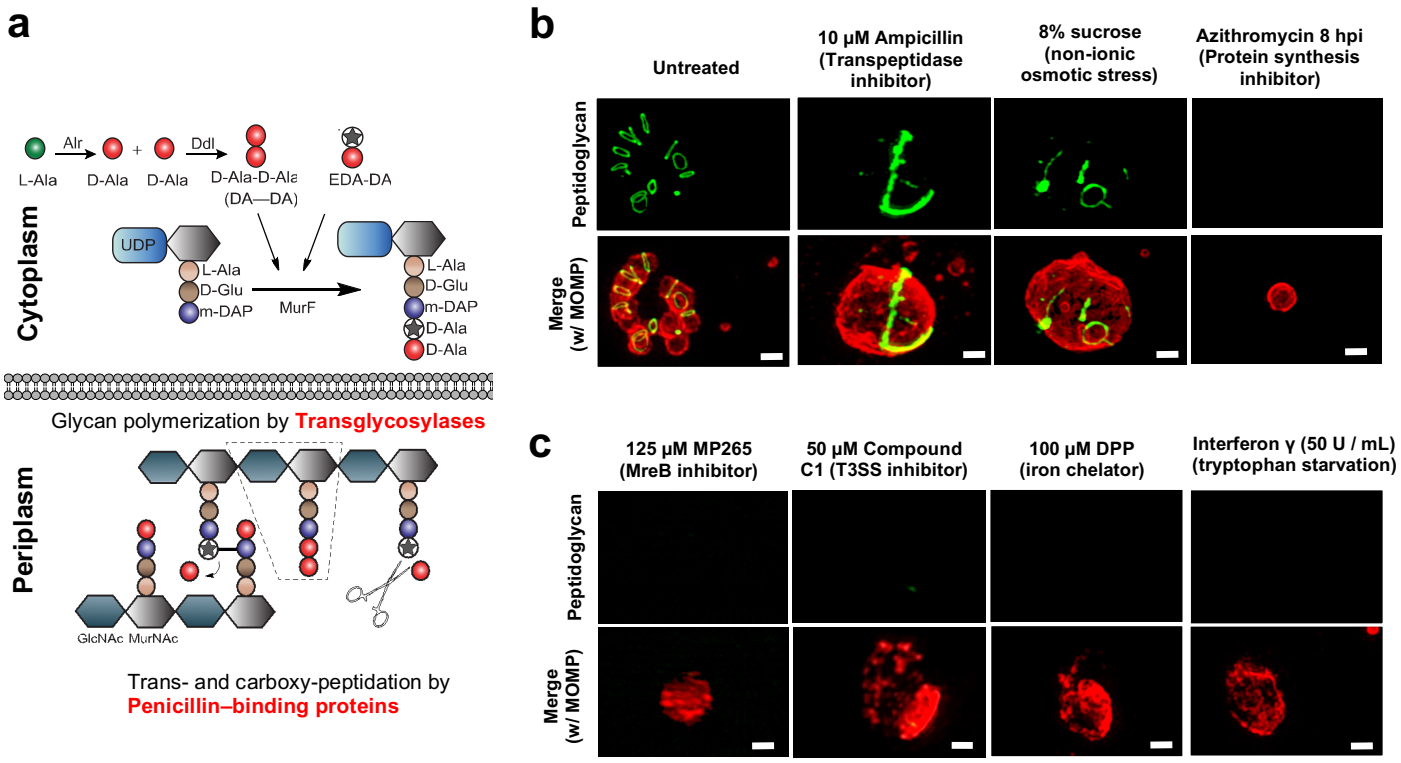
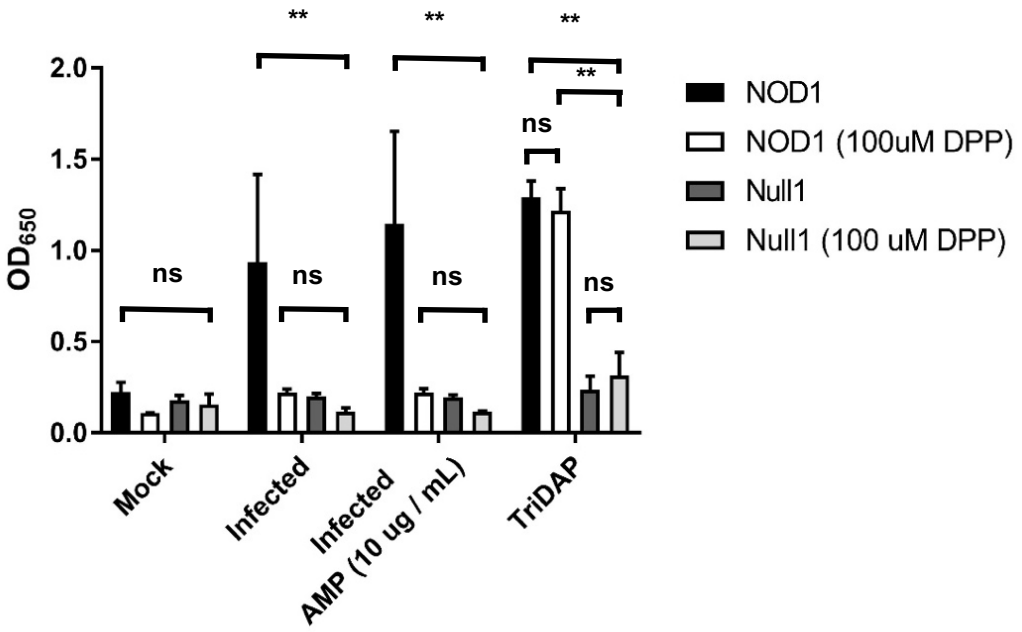
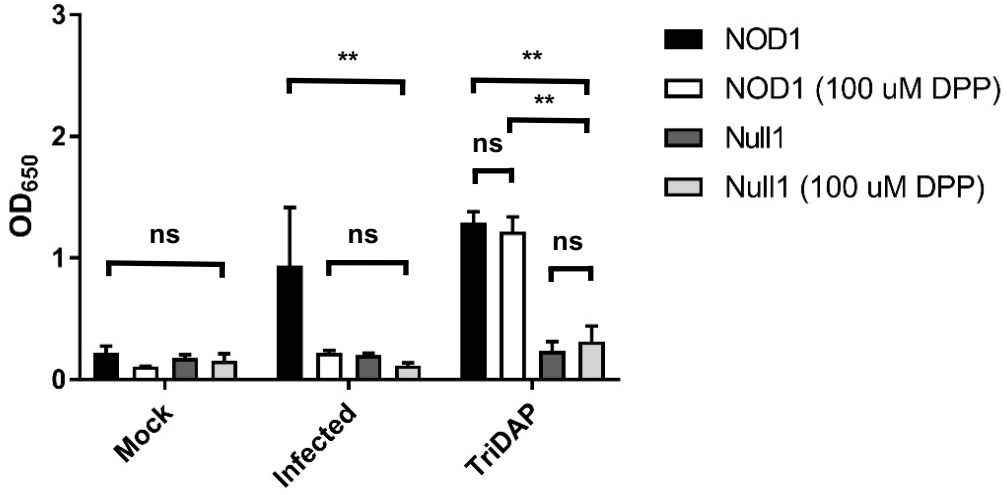


Figure 18. Aberrant Chlamydia forms differ in their ability to synthesize peptidoglycan. (a) The Park nucleotide biosynthesis pathway in Gram-negative bacteria. Peptidoglycan can be labeled utilizing a modified D-Ala-D-Ala (EDA-DA, green), which is subsequently incorporated into newly synthesized stem peptides (143). Alr; alanine racemase, Ddl, D-Alanine-D-alanine ligase, MurE; UDP-N-acetylmuramoyl-L-alanyl-D-glutamate-diaminopimelate ligase, MurF; UDP-N-acetylmuramoyl-tripeptide-D-alanyl-D-alanine ligase. (b, c) *Chlamydia*–infected cells were grown in the presence of a variety of aberrance-inducing conditions. Peptidoglycan was labeled via click-chemistry and *Chlamydia* RBs and ABs were visualized utilizing a monoclonal antibody to the major outer membrane protein (MOMP; red). Images are representative of 20-30 viewing planes carried out over three independent experiments. *** , $p < 0.001$; ns, not significant. Scale bars; ~ 1 µm.

a


**
**
**
**
ns
ns
ns
ns
2.0
1.5
1.0
0.5
0.0
OD650
Mock
Infected
Infected
AMP (10 ug / mL)
TriDAP
NOD1
NOD1 (100uM DPP)
Null1
Null1 (100 uM DPP)

b


**
**
**
ns
ns
ns
ns
3
2
1
0
OD650
Mock
Infected
TriDAP
NOD1
NOD1 (100 uM DPP)
Null1
Null1 (100 uM DPP)

c

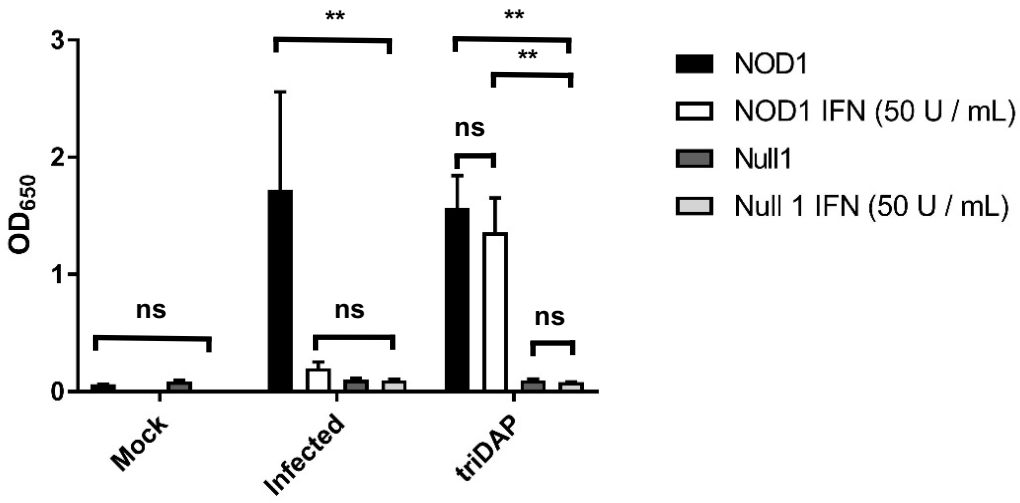

**
**
**
ns
ns
ns
ns
3
2
1
0
OD650
Mock
Infected
triDAP
NOD1
NOD1 IFN (50 U / mL)
Null1
Null 1 IFN (50 U / mL)

Figure 19. Aberrant *Chlamydia* forms differ in their ability to synthesize immunostimulatory peptidoglycan.

A HEK hNOD1 SEAP reporter cell line was utilized to quantify the relative abundance of PG shed when cells were infected with *C. trachomatis* in the presence of ampicillin (AMP) (a), the iron chelator DPP (a and b), and interferon gamma (IFN) (c). TriDAP was used in each experiment as a positive control for NOD1 signaling and Null1 cell line as a negative control. Data presented are the means from three independent biological replicates, and the error bars represent standard deviations from the mean. **, $p < 0.005$; ns, not significant.

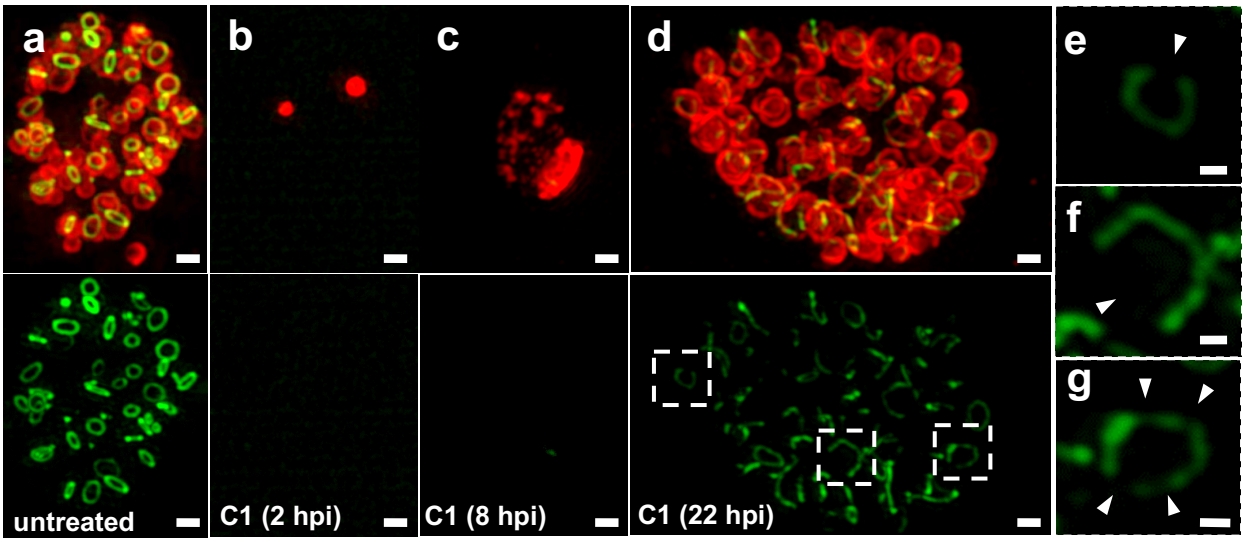


Figure 20. The presence of PG and differences in cell / inclusion size are dependent on the timing of persistence induction.
(a-d) *Chlamydia*–infected HeLa cells were grown in the presence of PG-labeling reagent EDA-DA for 24 hours (a). Persistence was induced with T3SS inhibitor compound C1 at 2 (b), 8 (c), and 22 (d) hpi. Regions of interest from panel d were enhanced / magnified and provided in panels e-g. Arrowheads indicate discernable breaks in the RB PG rings. Images are representative of 20-30 viewing planes carried out over three separate and independent experiments. Scale bars; ~ 1 μm.

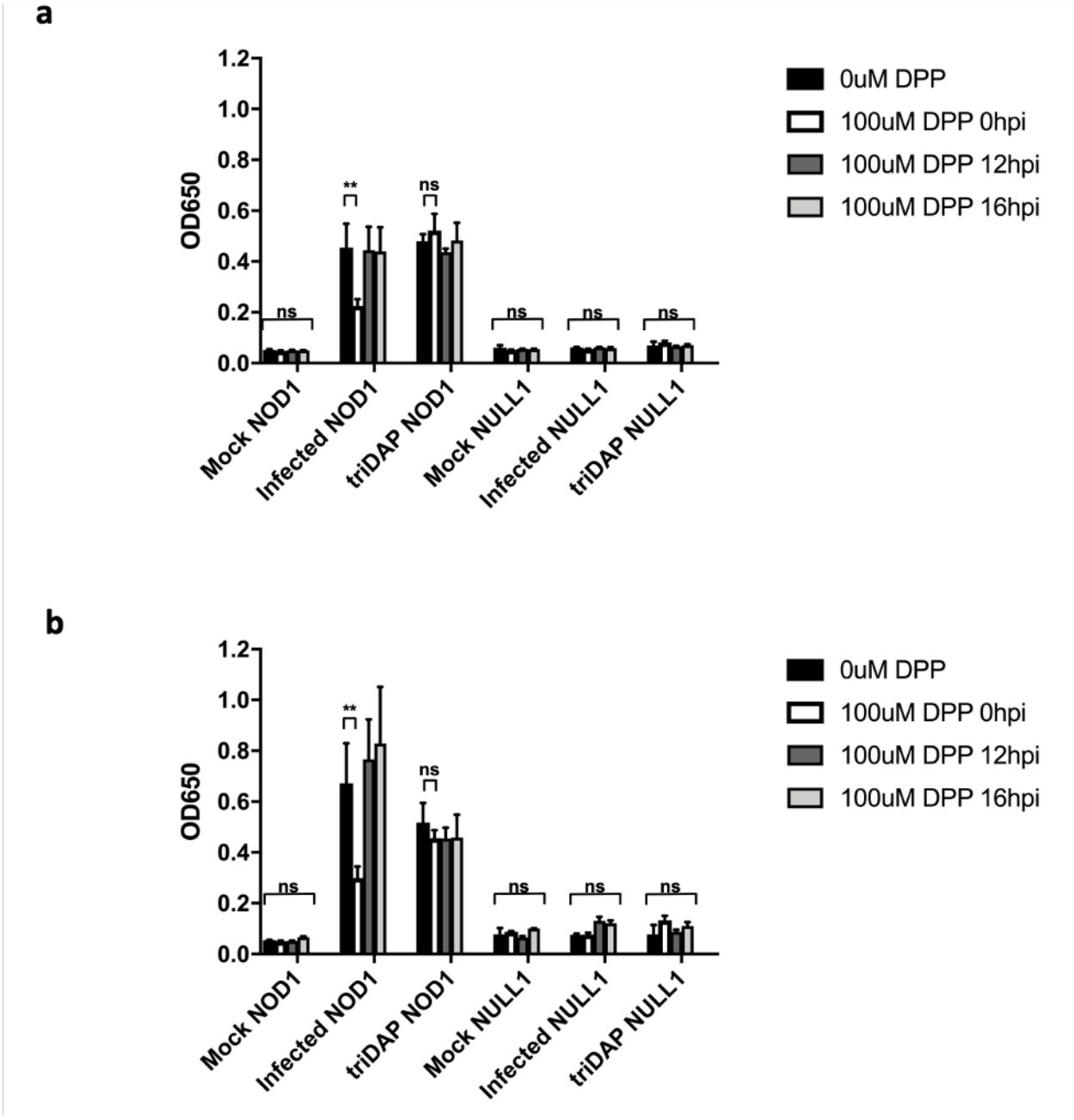


Figure 21. The presence of immunostimulatory peptidoglycan is dependent on the timing of persistence induction.
HEK hNOD1 SEAP-reporter assay comparing the abundance of shed, immunostimulatory peptidoglycan when iron sequestration is initiated at different time points throughout the *Chlamydia* developmental cycle. NOD activity was tested from cell supernatants at 24 hpi (a) and 36 hpi (b). Data presented are the mean of three biological replicates and error bars represent standard deviation from the mean. **, $p < 0.05$; ns, not significant.

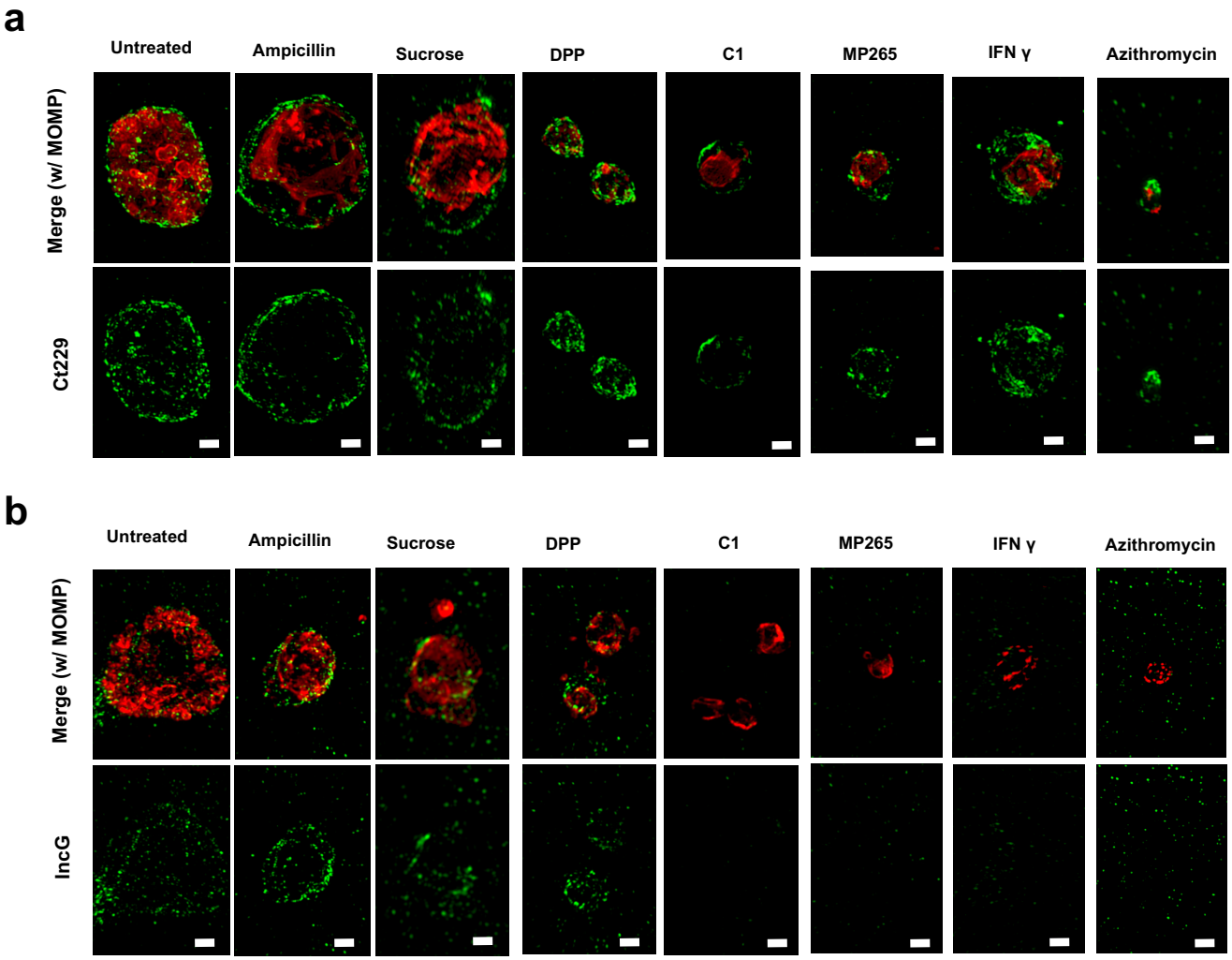


Figure 22. *Chlamydia* ABs differ in their presentation of early-stage inclusion membrane proteins.
Immunolabeling of inclusion membrane proteins CT229 (a) and IncG (b) in *Chlamydia*-infected cells at 24 hpi. Inc presentation was compared for six different aberrance-inducing conditions. Cells treated with the protein synthesis inhibitor azithromycin at 8 hpi were used as a control. Scale bars; ~ 2 μm.

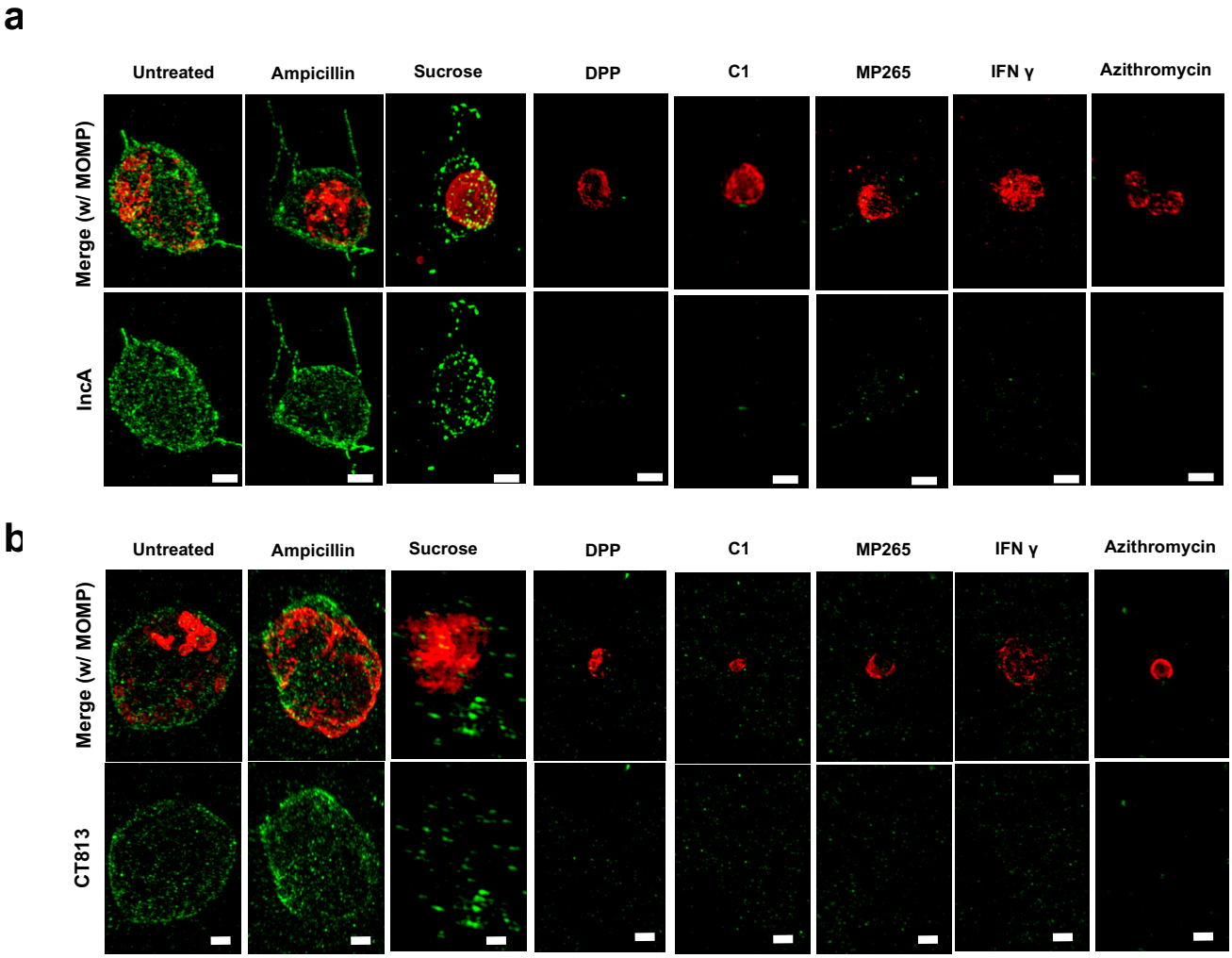


Figure 23. *Chlamydia* ABs differ in presentation of mid- and late- stage inclusion membrane proteins.
Immunolabeling of inclusion membrane proteins IncA (a), and CT813 (b) in *Chlamydia*-infected cells at 24 hpi. Inc presentation was compared for six different aberrance-inducing conditions with the protein synthesis inhibitor azithromycin used as a control. Scale bars; ~ 2 μm.

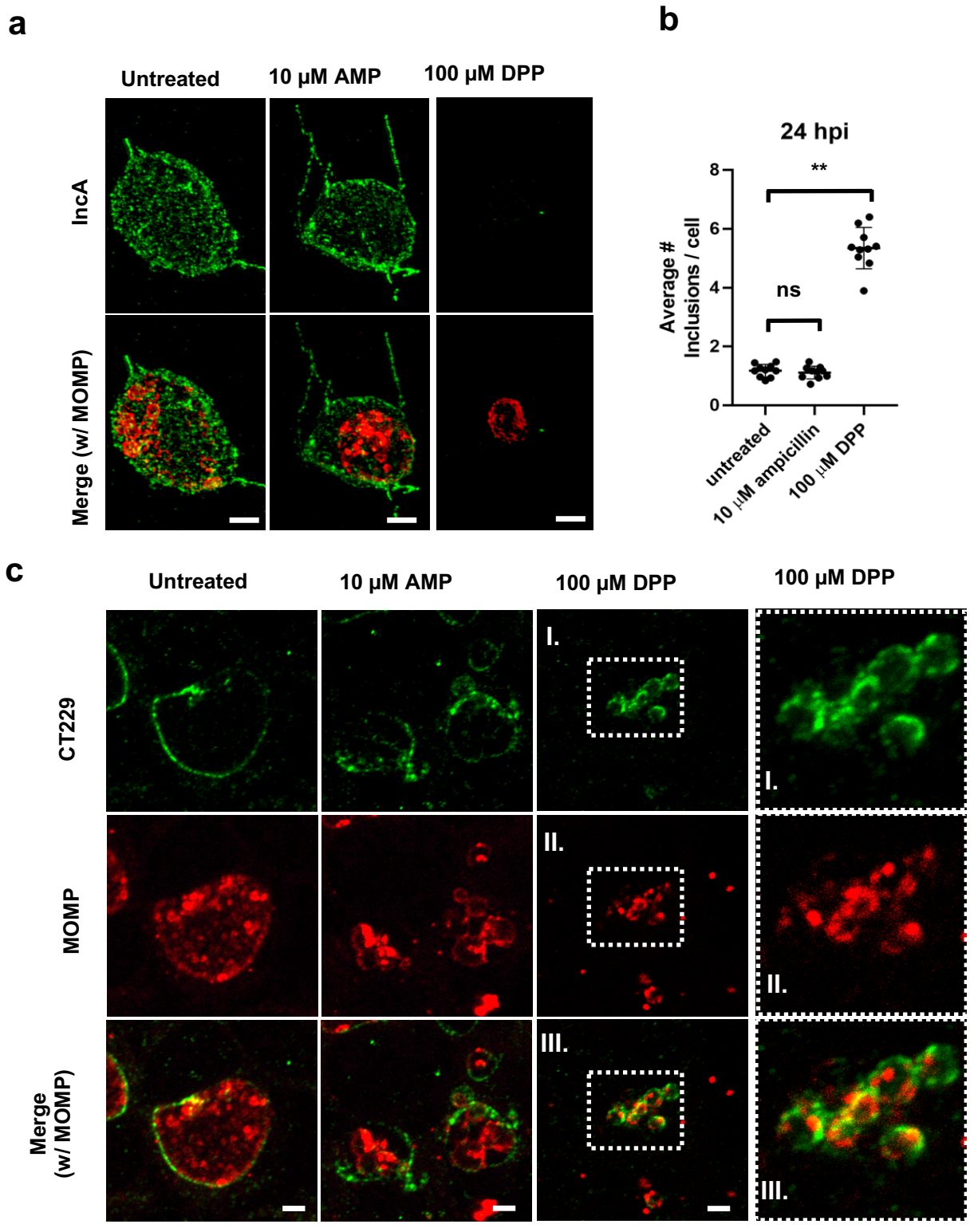

a
Untreated
10 μM AMP
100 μM DPP
IncA
Merge (w/ MOMP)
b
24 hpi
**
ns
Average # Inclusions / cell
0
2
4
6
8
untreated
10 μM ampicillin
100 μM DPP
c
Untreated
10 μM AMP
100 μM DPP
100 μM DPP
CT229
MOMP
Merge (w/ MOMP)
I.
II.
III.

Figure 24. *Chlamydia* ABs differ in their presentation of the mid-stage inclusion membrane protein IncA.

Chlamydia ABs differ in their presentation of the mid-stage inclusion membrane protein IncA. HeLa cells were infected at an MOI of 1. Cells were either left untreated or treated with various aberrance inducers, and cells under all conditions were fixed at 24 hpi. Immunolabeling was conducted for IncA as well as MOMP. (a) Ampicillin (AMP) and DPP treatments. See Fig. 23 for the rest of the conditions. Images are representative of between 10 and 20 inclusions observed under each condition, and the experiment was carried out three times. (b) To assess the fusogenic potential of inclusions under aberrance induction, HeLa cells were infected at an MOI of 10, fixed at 24 hpi, and labeled for CT229. Inclusions present per cell were measured by counting cell and inclusion numbers across 10 random imaging planes under each condition (untreated, AMP treatment, and DPP treatment). Data points represent average values of the numbers of inclusions per cell per imaging plane examined with 10 imaging planes under each condition. The assay was carried out at least twice under each condition tested. Lines represent mean values for all data points under each condition, and error bars represent standard deviations. **, $p < 0.005$; ns, not significant. (c) Representative images from the analysis of fusogenic and nonfusogenic inclusions. The rightmost panels are magnifications of the boxed areas. Bars, ~2μm.

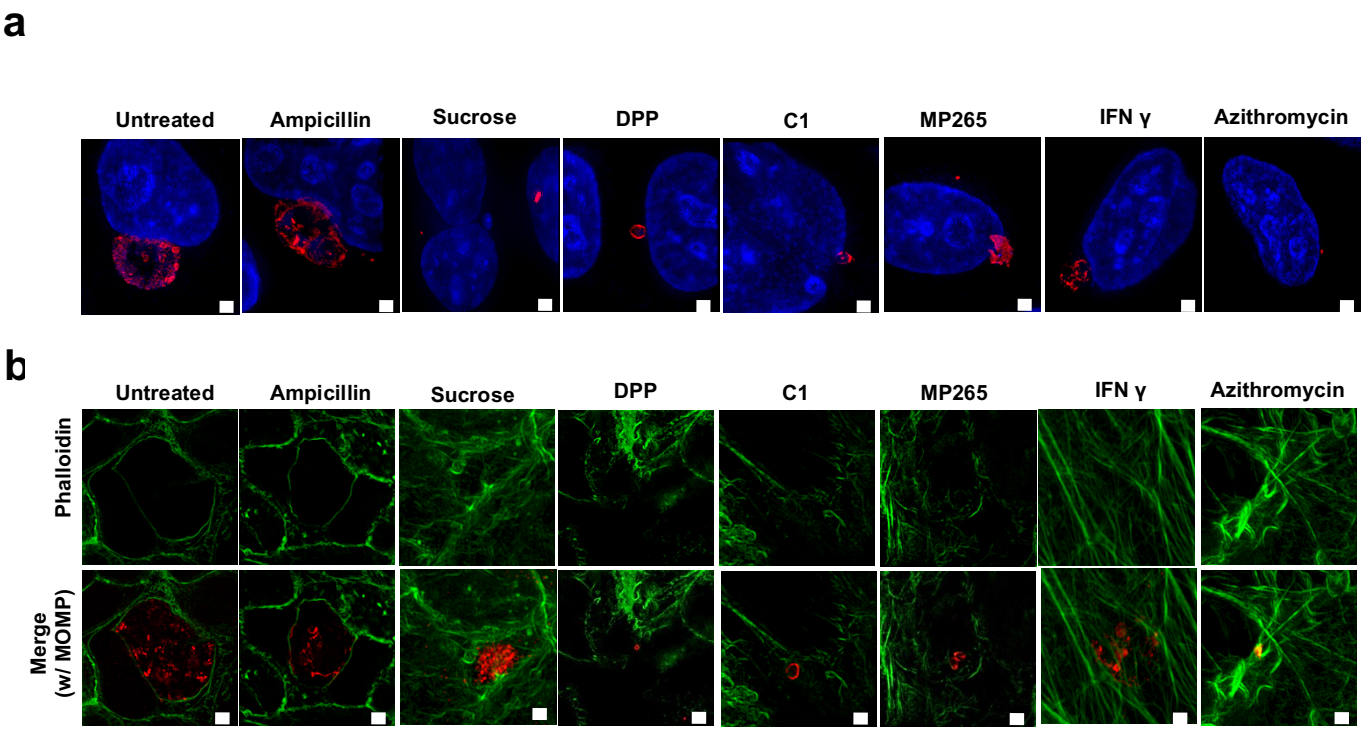


Figure 25. Assessment of inclusion trafficking to the nucleus and actin cage formation. (a) The proximity of normal and aberrant *Chlamydia* inclusions to host cell nuclei was assessed by immunolabeling of normal and aberrant forms of *Chlamydia*. Nuclei were stained with Hoechst solution (blue) at 24 hpi. (b) The presence of actin cages about the inclusion periphery of normal and ABs of *Chlamydia* was assessed by staining cells with conjugated phalloidin at 46 hpi. *Chlamydia* was visualized utilizing MOMP monoclonal antibodies. Images are representative of 10-20 viewing planes carried out over three biological replicates. Scale bars; ~ 5 μm.

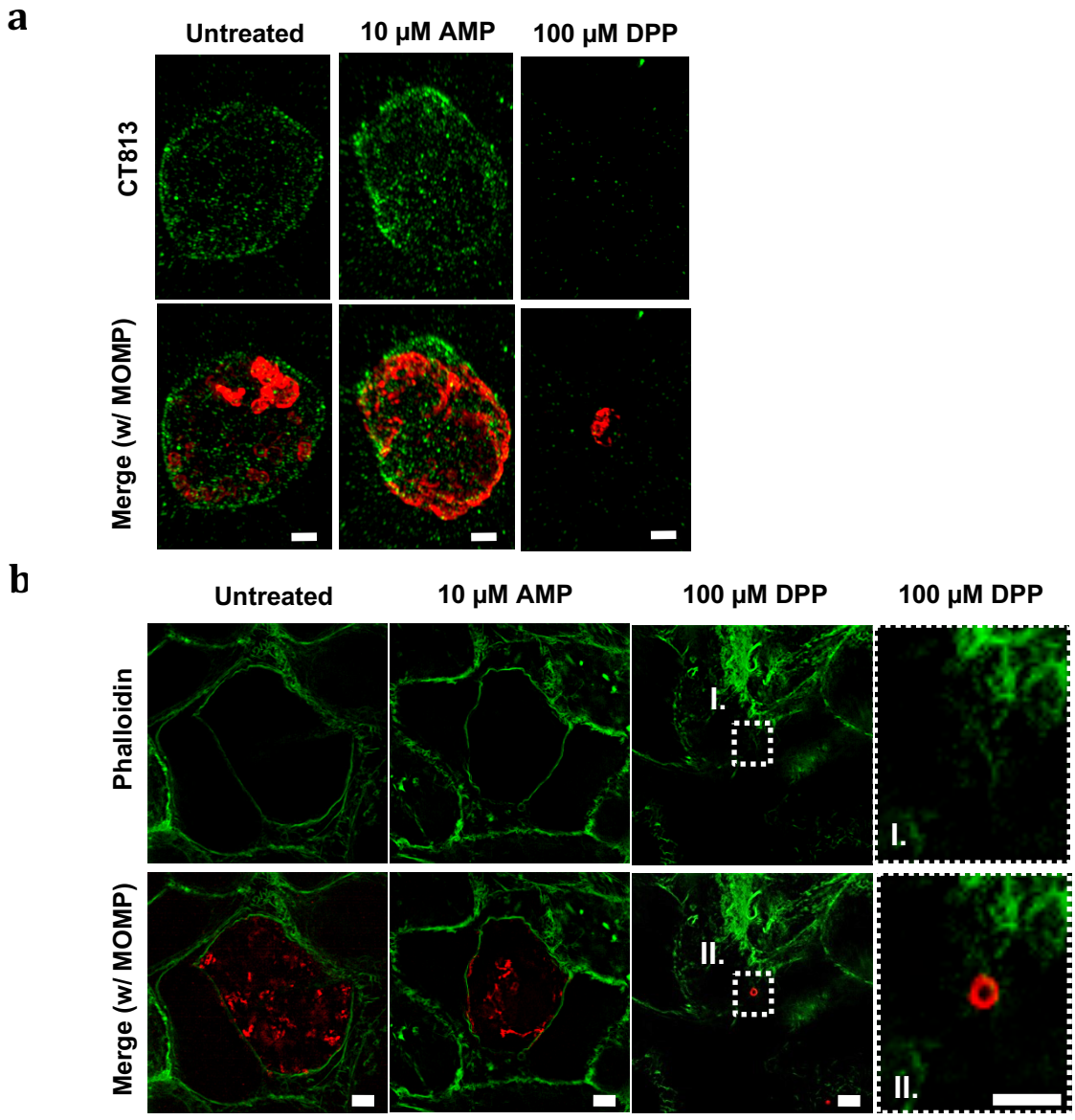

a
Untreated
10 μM AMP
100 μM DPP
CT813
Merge (w/ MOMP)
b
Untreated
10 μM AMP
100 μM DPP
100 μM DPP
Phalloidin
Merge (w/ MOMP)
I.
II.

Figure 26. *Chlamydia* ABs differ in their presentation of the late-stage inclusion membrane protein CT813.

Chlamydia ABs differ in their presentations of the late-stage inclusion membrane protein CT813. HeLa cells were infected at an MOI of 1. At 2 hpi, cells were either left untreated or treated with various aberrance inducers, and cells under all conditions were fixed at 24 hpi. Immunolabeling was conducted for the inclusion membrane protein CT813 as well as MOMP. (a) Ampicillin (AMP) and DPP treatments. See Fig. 25 the rest of the conditions. Bars, ~2μm. Images are representative of between 10 and 20 inclusions observed under each condition over the course of three separate experiments. To assess actin cage formation, HeLa cells were infected at an MOI of 1, fixed at 46 hpi, and labeled for MOMP and phalloidin. (b) AMP and DPP treatments. The right most panels are magnifications of the boxed areas. The remaining aberrance-inducing conditions are presented in Fig. 25 in the supplemental material. Images are representative of 20 fields of view under each condition examined over three separate experiments. Bars, ~5 μm.

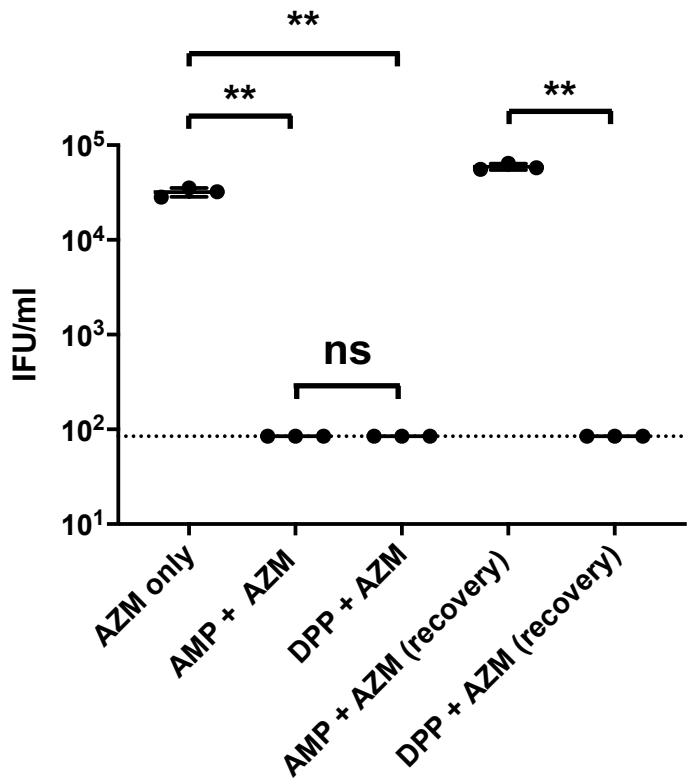


Figure 27. Iron-depletion-induced persistence enhances the susceptibility of *C. trachomatis* to azithromycin treatment.

Subinhibitory doses of azithromycin (AZM) were added to *Chlamydia*-infected cells (18 hpi) either alone or following the addition of 10mg/ml ampicillin (AMP) or 100 mM the iron chelator DPP at the time of infection. EBs were harvested at 44 hpi from treated cells, or cells were washed and *Chlamydia* cells were allowed to recover for an additional 48 h. Inclusion-forming units (IFU) were then calculated by conducting serial dilutions, infecting fresh monolayers, and counting new inclusions at 24 hpi. The dotted line represents the limit of detection for the assay. Data were gathered over three separate experiments, the data plotted represent the results of three independent biological replicates, and error bars represent the standard deviations from the means. **, $p < 0.01$.

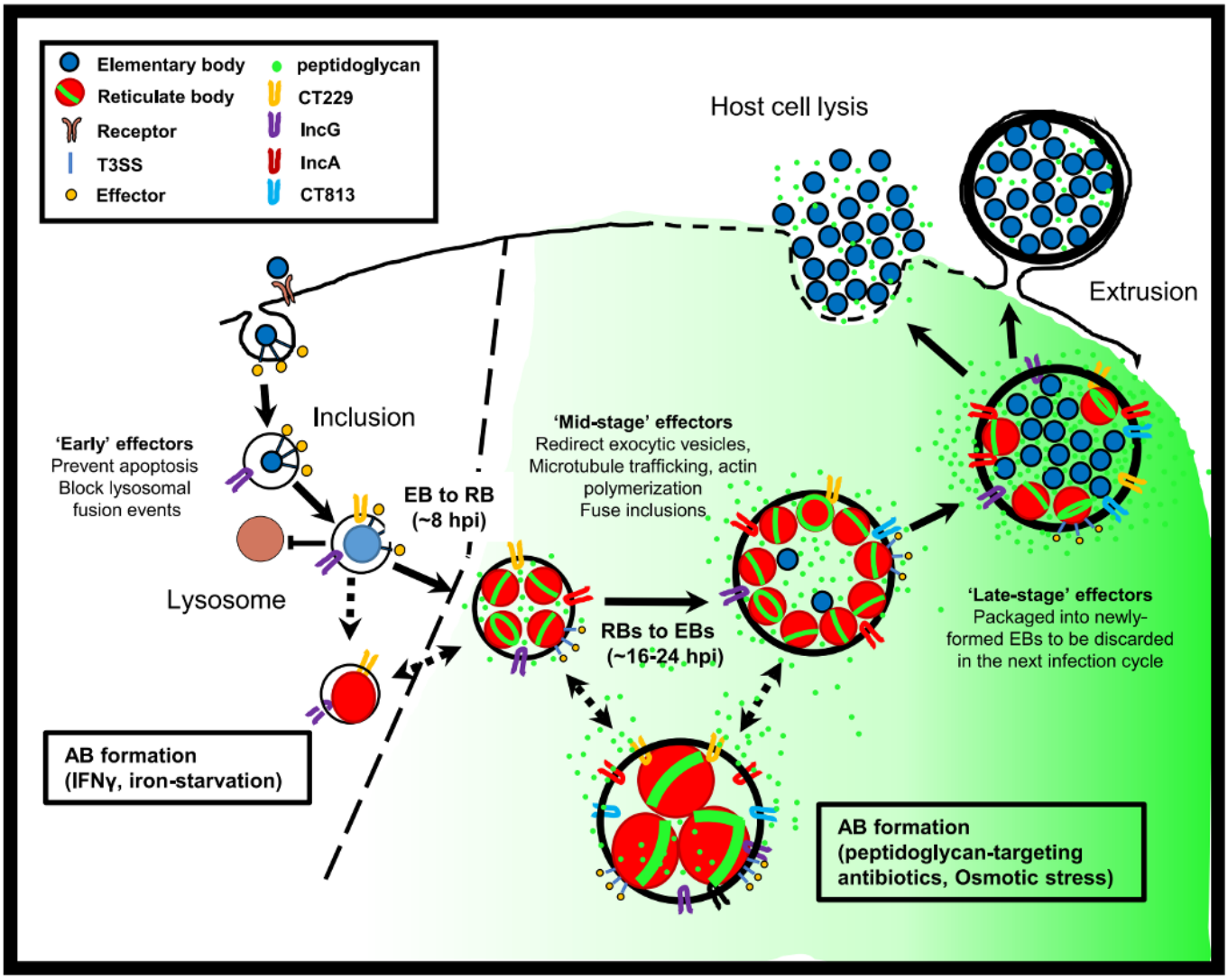


Figure 28. Persistence halts the *Chlamydia* developmental cycle while simultaneously altering bacteria-host cell interactions.

The induction of persistence in response to a cell's innate response to infection results in *C. trachomatis* significantly reducing the synthesis and shedding of immunostimulatory peptidoglycan (green) while concurrently minimizing the deleterious reorganization of host cell processes. This is not the case when *C. trachomatis*-infected cells are treated with peptidoglycan- targeting antibiotics or exposed to osmotic shock. We propose that inducing persistence prior to mid-stage development (dotted line) allows *C. trachomatis* to remain intracellular and escape clearance by the cell-mediated immune response for extended periods of time.

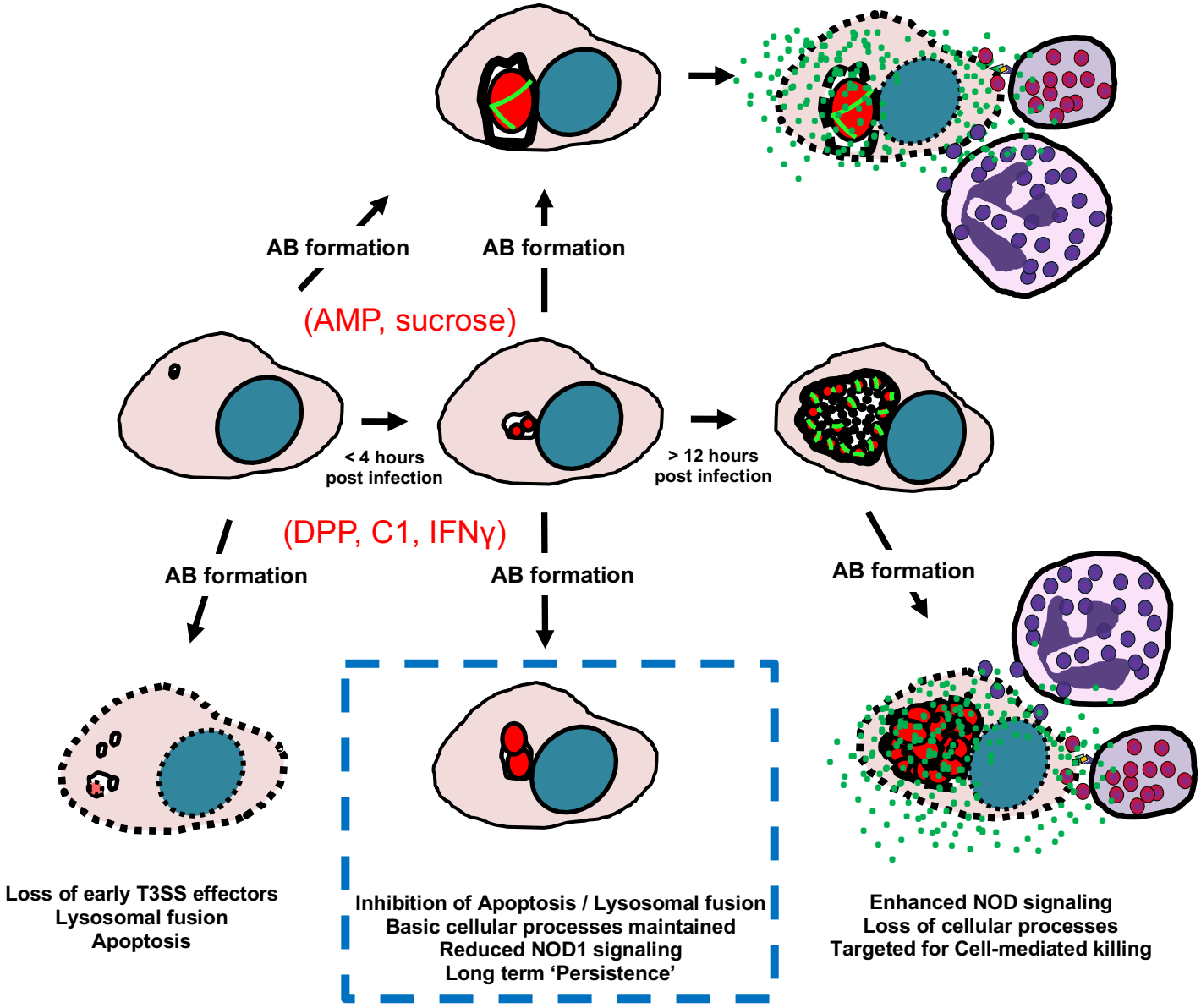


Figure 29. Modeling chlamydial persistence in the context of infection.
For stress conditions that do not affect PG synthesis and inclusion maturation (AMP and sucrose), *C. trachomatis* benefits from remaining intracellular but eventually will be targeted by cell-mediated killing mechanisms. Under stress conditions that halt PG synthesis and inclusion maturation (DPP, C1, and IFNγ), the timing of induction directly affects the pathogen's survival. If aberrance is induced early, prior to the establishment of the inclusion and the secretion of antiapoptotic factors, the microbe will be eradicated by either lysosomal fusion or host cell apoptosis. If aberrance is induced late in development, host cell processes such as chromosomal segregation and actin remodeling will be irreversibly affected, and immunostimulatory PG release will result in cytokine production, leading to cell-mediated killing. In this persistence model, *Chlamydia* survival is maximized when aberrance is induced subsequent to the host cell's intracellular defenses being overcome but prior to the initiation of a cytokine-induced, innate immune response.

DISCUSSION

For decades researchers have debated whether aberrant forms of *Chlamydia* play any role during active infections. Because these forms have been defined solely by their enlarged size and inability to divide and produce infectious progeny, discussion concerning how they could potentially benefit the pathogen *in vivo* has been largely restricted to these phenotypes. Recent studies have demonstrated that aberrant *Chlamydia* differ in their transcriptional (20; 169) and translational (26) profiles. The investigation of aberrance in *Chlamydia*-related bacteria has also provided evidence that this phenotype transcends the human and zoonotic pathogens (the Chlamydiales) and likely is important for many other members of the *Chlamydiae* phylum (221). However, very little is known about the underlying physiology of chlamydial ABs, and the degree to which they differ in their interactions with the microbe's intracellular niche. Our results indicate that persistent forms of *C. trachomatis* differ significantly in their interaction with host cells as a result of disparities in PG biosynthesis and the secretion of mid- and late-stage effector proteins (Fig. 28). In addition, our data also challenge the notion that bacterial cell enlargement is a pre-requisite for persistence in *C. trachomatis*, as many of our treatment conditions did not result in a statistically significant increase in the average size of intracellular *C. trachomatis*.

In the presence of β-lactam antibiotics, actively growing bacterial cells are highly susceptible to cell lysis as a result of the weakening of their cell walls and the inherent osmotic pressure differential across their cell membranes (250). *Chlamydia* species reside within an osmotically-stable, intracellular environment that protects them from the bactericidal effects of PG-targeting antibiotics. Inhibitors of MreB, a cytoskeletal protein that is the major organizer of the chlamydial division complex and directs septal PG synthesis, also induces aberrance in *C.*

trachomatis (184). Iron depletion via chelators, such as DPP induced aberrance in *Chlamydia* species through the downregulation of translation and T3SS function (34). In primate-derived cell lines, IFNγ induction in response to intracellular pathogens results in the expression of the enzyme indoleamine deoxygenase (IDO) which effectively depletes cellular pools of tryptophan (241). Numerous studies have demonstrated the importance of IFNγ in fighting/ clearing *Chlamydia* infections (52; 114; 196; 215). Tryptophan depletion significantly alters protein expression in a number of *Chlamydia spp*., and also results in the induction of aberrant bodies (20). It has also been suggested that these aberrant forms may also lower *Chlamydia's* sensitivity to frontline antibiotics. There are numerous reports of *Chlamydia*-infected patients exhibiting antibiotic-treatment failures despite the demonstrated absence of any known resistance genes being encoded by the pathogen (28; 219).

When *Chlamydia* species are exposed to PG targeting antibiotics, such as β-lactams, D-cycloserine, and fosmidomycin, the synthesis of PG precursors continues, but the completion of PG assembly is inhibited (141; 143; 188; 231). This counter-intuitive result was clarified when researchers determined that bacteria respond to PG-induced stress by continuing to degrade and re-synthesize peptidoglycan (49). We now report that non-ionic osmotic stress also appears to inhibit chlamydial cell division in a similar fashion. However, the greater novelty inherent to this work is that for all of the other aberrance-inducing conditions we examined, both PG assembly and synthesis appeared to be inhibited while PG degradation continued unabated. PG degradation is largely carried out by two major enzymatic activities; amidase activity and lytic transglycosylase activity, and both have been successfully characterized in *Chlamydia* species (112; 124). Changes in the transcription of PG processing enzymes, such as the chlamydial amidase (encoded by *amiA*) and the PG synthase (encoded by *ftsW*) have been shown to occur

during IFNγ-induced persistence (20), hinting at one potential regulatory pathway underlying this phenotype. However, given previous studies linking persistence to a global down-regulation in genes essential for protein synthesis (34) and our data indicating that 1) persistence enhances susceptibility to protein synthesis inhibitors and 2) protein synthesis inhibition directly results in the disappearance of the PG ring, PG degradation in aberrant *C. trachomatis* may occur as a result of a reduction in protein synthesis. Future studies comparing the relative half-lives and activities of PG biosynthesis and degradation enzymes in *Chlamydia* species will bring some clarity on this point. Another possibility is that differences in the ability to replicate DNA between aberrance-inducing conditions could account for the observed differences in PG synthesis and release. A recent study has established that a breakdown in genome replication in *C. trachomatis* results in the disruption of PG biosynthesis (35). While genome replication has been shown to proceed under some persistence-inducing conditions (79; 135), it is frequently delayed when compared to untreated controls (169; 202). PG-dependent septum formation is regulated by nucleoid occlusion in a number of bacterial species (3; 11; 22; 277), and the inability of *C. trachomatis* to properly complete replication or the segregation of its chromosomes during persistence could potentially explain the absence of a PG septum during persistence.

We previously hypothesized that reduced utilization of PG in *Chlamydia spp.* also reduces the generation of immunostimulatory, PG-derived muropeptides, conferring a pathoadaptive advantage (143). In support of this theory, a rudimentary PG recycling pathway has recently been characterized in *C. trachomatis*, which the microbe utilizes to limit the shedding of PG-derived immunostimulatory peptides (229). Our finding that persistence induction results in the inhibition of PG synthesis also supports this basic premise, as limiting the

production and release of immunostimulatory muropeptides during an active infection would likely be beneficial to these organisms. PG signaling through NOD1 is a large contributor to the overall interleukin-8 (IL-8) response to *C. trachomatis* (39). IL-8 is the most highly induced inflammatory cytokine and a major driver of inflammation during *C. trachomatis*, *C. muridarum,* and *C. pneumoniae* infections (178; 262). IL-8 transcript levels are significantly up-regulated ~15 hpi and this upregulation is dependent on chlamydial protein synthesis (38). Interestingly, this timing roughly correlates with the time points at which we see PG-induced NOD1 signaling peak in our *in vitro* experiments, suggesting that PG production by *C. trachomatis* is likely driving this signaling cascade. Although DPP induced-iron starvation can affect host cell processes (34), it does not appear to significantly alter NOD1 signaling activity (as indicated by our positive control in Fig. 19b). It is also possible that additional alterations in cell-microbe interaction are affected, which may indirectly affect *Chlamydia* growth, and thereby peptidoglycan biosynthesis.

We found that a number of aberrance-inducing conditions resulted in inclusions lacking mid- and late-stage Inc proteins on their membranes, and that this appeared to correlate with the previously described PG synthesis phenotype. PG-positive ABs were present in larger, mature inclusions containing all four Inc proteins and PG-negative ABs were housed in smaller, immature inclusions that lacked mid- and late-stage Incs in their inclusion membranes. These data strongly suggest that these mid- and late-stage T3S effectors are either not being produced or are not being secreted, under these aberrance-inducing conditions. Previous studies have reported that inhibitors of the chlamydial T3SS prevent the presentation of various inclusion membrane proteins (such as IncA and CT813) on the inclusion surface and result in *Chlamydia* exhibiting a swollen, aberrant-like morphology (170; 271). These inclusions were also

significantly smaller than untreated controls, indicating that they fail to undergo the normal maturation process associated with chlamydial development (141).

Our observations take on additional significance when the functions of the Inc proteins examined in this study are fully considered. CT229 is expressed early in chlamydial development and aids in the formation and maintenance of the inclusion by recruiting and binding several Rab GTPases that alter host vesicular trafficking, thus enabling *C. trachomatis* to avoid the host cell surveillance and suicide programs (70; 163; 218; 230). *Chlamydia* inclusions that lack CT229 lyse prematurely during development, resulting in host cell death (259). IncG functions by binding with the 14-3-3β protein (225) and is thought to interact directly with lipid droplets and recruits them to the growing chlamydial inclusion (68). IncA enables homotypic vesicle fusion of adjoining *Chlamydia* inclusions, an event that significantly enhances chlamydial development (86). Actin recruitment to the inclusion is mediated directly by CT813; CT813 recruits ARF1 and ARF4 to the inclusion membrane, which are essential for repositioning Golgi complex fragments around the inclusion (263; 264). As CT813 is not present on inclusions whose maturation processes have been paused early in development, it is likely that host cell actin and Golgi complexes remain in their original, unaltered states. It is currently unclear whether the absence of CT813 on inclusions is beneficial to infected host cells or provides additional immunoevasive benefit to persistent chlamydial forms. While only four inclusion membrane proteins were examined in this study, we suspect that our results are representative of T3S effectors as a whole and that aberrance induction halts inclusion maturation.

Assuming *Chlamydia's* aberrant forms enhance persistence *in vivo* by lowering its immunogenic profile, it follows that the timing of persistence induction is likely critical. *Chlamydia* begins synthesizing PG upon transitioning to the replicative form. The longer the

microbe's developmental cycle proceeds, the greater the number of RBs produced and the higher concentration of muropeptides that will accumulate in infected cells. As chlamydial development is not synchronized between cells during active infections, aberrance induction likely occurs at various stages of the developmental cycle (Fig. 29). We postulate that the time at which *C. trachomatis* pauses its developmental cycle is likely what determines an individual bacterium's fate. Because persistence-induction pauses T3S (either directly or indirectly), halting the developmental cycle too early would prevent the secretion of early effector proteins essential for host cell invasion, resulting in either apoptosis or targeting of immature inclusions to lysosomes where they are subsequently destroyed. Conversely, if persistence is induced late in infection, RB replication and shedding of PG prior to AB formation will have already resulted in NOD1 signaling, IL-8 secretion, and targeting of infected cells by the cell-mediated immune response. Under this principle, if development is instead halted at a midway point in development, between 8-12 hpi, theoretically the inclusion would be relatively stable within a host cell and sufficiently removed from the endocytic pathway, while also limiting the release of immunostimulatory PG muropeptides and subsequent targeting of the host cell for cell-mediated killing.

There has been much debate as to whether *Chlamydia*'s aberrant state provides a level of protection against antibiotic treatment. Treatment failures have continued to increase over the last two decades (101), and a genetic analysis of the genomes from clinical samples indicate that the acquisition of canonical antibiotic resistance mechanisms is not occurring (237). We found that susceptibility of *C. trachomatis* to azithromycin was enhanced by iron-depletion, indicating that this aberrance mechanism does not appear to confer protection. A major mechanism for persistence induction is thought to be the downregulation of protein synthesis (34), and it logically follows that the effect of a sub-inhibitory dose of a protein synthesis inhibitor

(azithromycin) under these conditions would be additive, resulting in a lethal phenotype. Our findings are consistent with a previous study that examined the effects of sub-inhibitory concentrations of azithromycin on chlamydial development. Researchers found that *C. trachomatis* is more resistant to killing by low doses of azithromycin if it is allowed to first enter the mid-stage of its developmental cycle (279). These data largely fit our time-dependent model, which illustrates how mid-stage persistence may be selectively advantageous *in vivo* with *C. trachomatis* exhibiting the highest tolerance to aberrance-inducing conditions at a midway point in its development.

As only a few observational studies have reported the presence of ABs *in vivo*, these reports have been viewed with a healthy degree of skepticism. The general consensus within the field has been that chlamydial ABs represent rare, dead-end morphotypes that are likely cleared rapidly by the cell's natural defenses or by the host's innate immune response. However, our results offer an alternative proposition: 1) that ABs exist in much smaller inclusions, making them more difficult to identify by conventional screening approaches *in vivo*, 2) that ABs resist killing by host cell apoptosis and the endosomal maturation pathway because they retain early Inc proteins in their inclusion membrane, and 3) that ABs inhibit PG biosynthesis prior to incorporating mDAP into the PG stem peptide and subsequently fail to release NOD1-stimulating muropeptides into the host cell, thus limiting the recruitment of innate and cellular defenses. As NOD1-/ NFkB-mediated IL-8 signaling is a hallmark of the immune response to chlamydial infections, the prevention of this signaling pathway by persistent forms of *Chlamydia* inhibiting PG synthesis likely enables the pathogen to mask itself from the host's response to infection. We propose that these findings offer a significant, biologically relevant purpose for ABs during *Chlamydia* infections, and link the persistent state with enhanced evasion of both

extracellular and intracellular host defenses. The future examination of PG and Inc protein abundance and localization in tissue specimen samples will be needed to definitively demonstrate the importance of persistent forms in the pathogenesis of *Chlamydia* species.

ACKNOWLEDGMENTS

We would like to thank Dr. Anthony Maurelli (University of Florida) for providing us *Chlamydia* strains. We would like to thank our long-time collaborator Dr. Michael VanNieuwenhze (Indiana University) and his laboratory for providing us with the 'clickable' D-alanine dipeptides (EDA-DA) used in our peptidoglycan-labeling experiments. We also thank Drs. Ted Hackstadt (NIAID), Daniel Rockey (Oregon State University), Ken Fields (University of Kentucky), and Raphael Valdivia (Duke University) for graciously sharing their Inclusion membrane protein and T3SS-specific polyclonal antibodies for use in these studies. We would like to thank Dr. D. Scott Merrell (Uniformed Services University) for providing us with DPP, and Dr. Dennis McDaniel (Uniformed Services University) for preparing samples for transmission electron microscopic analysis and conducting the electron microscopy. We would like to thank Kieran Broder for his assistance with conducting inclusion forming unit counts. Finally, we would like to thank both Drs. Anthony Maurelli and Ann Jerse (Uniformed Services University) for their helpful comments in preparing this manuscript.

This work was supported by a MIRA ESI award (R35 GM138202) and a USU faculty start up award (HP73LIEC18) to GL. The funders had no role in study design, data collection and interpretation, or the decision to submit the work for publication. The opinions and assertions expressed herein are those of the author(s) and do not necessarily reflect the official policy or position of the Uniformed Services University or the Department of Defense.

DECLARATIONS OF INTEREST

The authors declare that no competing interests exist.

Chapter 4: Discussion

OVERALL SUMMARY

The primary goal of this work was to explore the mechanism of cell division in *C. trachomatis*. Thus, we aimed to identify factors that allow *C. trachomatis* to establish polarity in order to initiate the first stage in the microbe's polarized cell division process, test conditions that lead to cell division arrest in the microbe, and establish how this affects the bacterium's physiology and the interaction with its host. As we determined that the chlamydial cytoskeletal protein $BacA_{CT}$ does not have a direct role in the cell division process, we shifted our study to examine how the filament-forming protein affects the microbe's basic physiology. In doing so, we were able to draw parallels between these two otherwise disparate aims by focusing on a common phenotypic feature inherent to both studies: the expansion of the microbe's cell membrane and the enlargement of the chlamydial cell, otherwise referred to as the 'aberrance phenotype.'

RESULT SUMMARY FROM CHAPTER TWO

In Chapter 2, we described our characterization of a novel bactofilin protein in *C. trachomatis*. Following the description of *Chlamydia*'s unique polarized cell division process (as described in Chapter 1) (2; 54), we set out to determine how polarity is established by this genetically reduced organism. Polymer-forming landmark proteins, also known as bactofilins, have been shown to establish cell polarity in a number of bacterial species (131; 252). We initially hypothesized that $BacA_{CT}$ would play a similar role in *C. trachomatis*. Specifically, we hypothesized that $BacA_{CT}$ would aid in establishing polarity in the initial stages of chlamydial cell division. To address this question, we constructed fluorescent fusion constructs to examine

the configuration and localization of $BacA_{CT}$ in both fixed and living cells. We initially wanted to determine whether $BacA_{CT}$ localized to key cellular components of the bacterium's cell division complex. We found that $BacA_{CT}$ did not localize to PG septum or MreB (the protein responsible for organizing the chlamydial division complex (137; 141; 184; 186; 210)) at any time points during cell division. In order to understand whether $BacA_{CT}$ contributes to establishing cell polarity, we quantified the frequency at which $BacA_{CT}$ localizes to the membrane of a budding daughter cell, the mother cell, or to the division plane. We found that there was a similar percentage of $BacA_{CT}$ present at all three locations within dividing RBs. Given these observations, we were unable to directly associate $BacA_{CT}$ with establishing cell polarity or the cell division process.

As we were forced to reject our initial hypothesis, we next set out to determine the function of this protein in *C. trachomatis*. Our imaging studies revealed that $BacA_{CT}$ forms ring-like and filamentous structures and that there is a transition state between these forms. In an attempt to understand how $BacA_{CT}$ affects the pathogen's physiology, we knocked down expression of $bacA_{CT}$ using an inducible CRISPRi system (180). We found that knockdown of $bacA_{CT}$ produced enlarged intracellular forms of the bacteria compared to controls. The native morphology (cell diameter) was restored upon complementation *in trans* with either our $BacA_{CT}$-mCherry or $BacA_{CT}$-His fusion constructs.

We propose two putative hypotheses to address why the knockdown of $bacA_{CT}$ may result in this cell expansion. The first hypothesis is $BacA_{CT}$ may stabilize the bacterial membrane during cell division. In most bacteria, the cell membrane is surrounded by a sacculus composed of PG, which provides membrane stability and support. Conversely, *Chlamydia spp*. lack a canonical sacculus, and only the replicative form maintains PG only at the septum (the site of

cell division). *Chlamydia spp*. rely on highly crosslinked outer membrane proteins (OmpB, OmpC) to maintain membrane integrity in their extracellular forms (EBs); however, this structure is rigid and does not allow for the membrane expansion and fluidity required during cell growth and division. Thus, the disulfide bonds of the crosslinked outer membrane complexes are relaxed in replicative forms (RBs) (87; 93; 141; 143; 173). It is currently unknown which proteins or cellular components are mediating the stabilization of the chlamydial membrane. We hypothesize that $BacA_{CT}$, likely in conjunction with other periplasmic elements, functions to stabilize the inner membrane at sites other than the septum, effectively stabilizing specific areas of the periplasmic space and allowing transmembrane complexes to function in the absence of a sacculus (Fig. 30). The role of a bactofilin in membrane stabilization is not implausible. The vast majority of bactofilins are cytosolic proteins, and given its membrane localization, it likely has effects on membrane dynamics and influences cell shape. To investigate this hypothetical role in membrane stability, one potential approach would be to study $BacA_{CT}$ under non-ionic osmotic stress conditions by increasing sucrose levels in the cell. As we demonstrated in Chapter 3, sucrose supplementation causes *C. trachomatis* to transition into an aberrant state, halting cell division and preventing infectious progeny production. Sucrose-induced membrane stress results in phenotypes very similar to when $BacA_{CT}$ is depleted, namely the enhancement in cell size characteristic of *Chlamydia*'s aberrant state. Therefore, it would be interesting to see whether sucrose supplementation exacerbates morphology defects when $bacA_{CT}$ expression is reduced utilizing the CRISPRi knockdown approach.

Another potential hypothesis is that $BacA_{CT}$ acts as a molecular ruler for maintaining cell size in dividing RBs, similar to how the PG ring aids in regulating the size of the septal division plain during polar budding and septation (54). Given the observation that $bacA_{CT}$ knockdown

results in an enlargement in chlamydial RBs, we proposed that this bactofilin may influence cell size. The protein could theoretically affect the size of the whole cell or, given the microbe's asymmetric division process, individual hemispheres of the cell. In order to establish whether $BacA_{CT}$ plays an important role in the maintaining cell size in dividing RBs, there needs to be further exploration into the dynamics of $BacA_{CT}$ during early cell division events. Our initial study was limited in that we only examined the effects of *bacA*$_{CT}$ knockdown late in development via confocal microscopy. Future studies utilizing high resolution, live cell imaging will allow us to examine the size of dividing RBs early in cell division and observe the early cell division events when expression of *bacA*$_{CT}$ is reduced.

RING-FORMING BACTOFILINS: IMPLICATIONS, LIMITATIONS AND FUTURE DIRECTIONS

In our characterization of $BacA_{CT}$, we found that this chlamydial bactofilin possesses characteristics that have not been described in other bactofilin proteins to date. Our work is the first to describe a bactofilin protein that forms ring-like structures within bacteria, and rather than existing as static structures, $BacA_{CT}$ filaments appear to oscillate between puncta and ring forms. We found that these forms differed in volume and fluorescence intensity, indicating that they likely exhibit differences in the density of their filaments or the compactness of individual bactofilin monomers. We were initially struck by how similar $BacA_{CT}$ localization appeared when compared to chlamydial PG. Chlamydial PG has been observed in puncta, disks, and rings and has been associated with key steps in the chlamydial cell division process (54; 141). Although we did not observe any co-localization of PG with $BacA_{CT,}$ these observations lead us to speculate that these structures may work together in tandem to direct changes in cell size and shape, thus directly and indirectly regulating chlamydial division and development.

To understand the role of $BacA_{CT}$, we employed CRISPRi to knockdown expression of the gene product. Although we did achieve a greater than 80% reduction in expression of $bacA_{CT}$, it is likely that enough of the native protein was produced to dampen any observable phenotypes considerably. A superior technique often used in model bacterial systems involves generating a targeted deletion mutant for the gene under investigation followed by replacement with a genetic copy (complementation) that enables the restoration of a particular phenotype, preferably utilizing an inducible promoter. Unfortunately, we were unable to utilize this particular technique in our bacterial system. Studying the function of genes in *C. trachomatis* has historically been difficult for several reasons, including the lack of genetic tools. As *C. trachomatis* utilizes a severely reduced genome, the vast majority of the genes encoding structural proteins are thought to be essential under most conditions. A group of researchers has developed a pair of techniques, Fluorescence-Reported Allelic Exchange Mutagenesis (FRAEM) and Floxed-Cassette Allelic Exchange Mutagenesis (FLAEM), which enable allelic exchange in *C. trachomatis* (62; 119; 120; 168); however, no other researchers have been able to successfully demonstrate the use of their methods to date. FRAEM can be used to replace chromosomal genes with an antibiotic resistance cassette, but this technique is limited by the fact that this can lead to downstream polar effects on other genes (62; 168). FLAEM was developed to significantly reduce the occurrence of polar effects; it utilizes the Cre-lox system to remove the antibiotic resistance marker (119; 120).

Heterologous systems have been employed in the past to demonstrate that chlamydial proteins function similarly to homologs encoded in other bacterial species. Several PG biosynthesis genes encoded by *C. trachomatis* have been studied in this manner utilizing *E. coli* as a surrogate system. The chlamydial gene is usually expressed on a plasmid and used to

demonstrate that the encoded protein is capable of rescuing a given phenotype in an *E. coli* deletion mutant (97; 142; 156; 158). We ultimately chose not to utilize this method for two reasons: i) *E. coli* does not possess a bactofilin homolog and ii) given the wide array of bactofilins with divergent functions present throughout all Gram negative bacteria, we had concerns about finding a suitable microbe for carrying out the characterization studies. We did initially attempt to visualize the localization of $BacA_{CT}$ in *E. coli* using our mCherry fusion construct; however, we found that the mCherry signal was diffuse throughout the cytosol (data not shown). The few bright foci that were visible appeared to represent the accumulation of the $BacA_{CT}$ in inclusion bodies (aggregations of insoluble protein), rather than physiologically relevant structures. Many bacterial species contain at least one bactofilin; however, there have been several phenotypes associated with these proteins, some of which rely on unique interaction partners within a bacterial cell (25; 40; 59; 118; 126; 131; 144; 226; 245; 254; 282). Thus, we reasoned that successfully using $BacA_{CT}$ to complement a deletion mutant in another bacterial species was unlikely to be successful.

In evaluating the limitations inherent to the methods utilized in this work, it is important to point out that the technology utilized in this study is still new to the field of chlamydiology. We utilized fluorescent gene fusions constructs to demonstrate $BacA_{CT}$ localization using four independent constructs in fixed and living cells. An inherent limitation of this approach is that the parental copy of the $bacA_{CT}$ still remains in the chromosome in each of these transformant strains and thus, may influence the assembly of $BacA_{CT}$ rings, filaments, and puncta. The fact that we were able to observe all three forms of $BacA_{CT}$ in all four of our expression strains as well as observe the transition between the filamentous/ punctate forms of $BacA_{CT}$ to the ring-like form increases our confidence that these forms are genuine and not artificial in nature. Given the

similarity in the dimensions of the bactofilin's ring-like structures to chlamydial septa, we hypothesize that this bactofilin acts similarly to chlamydial PG in that it transitions its configuration as the cell division processes proceeds (141).

Future experiments to investigate the structural features of $BacA_{CT}$ are currently ongoing. The protein contains a large, disordered N-terminal domain, and experiments are planned that will attempt to overcome the knockdown of *bacA*$_{CT}$ with N-terminal truncation mutants to determine if they are capable of complementing the previously described cell size enlargement phenotype. These studies will also investigate whether the resulting 'chimeric filaments,' composed of both truncated and native proteins, can successfully localize to cell membranes and form filaments/ structures similar to the native fusion $BacA_{CT}$ constructs. The expression and purification of wildtype $BacA_{CT}$ and truncated versions of $BacA_{CT}$ will allow additional characterization studies to be conducted: examine the conditions under which filamentation occurs and determine which protein domains essential for that process. An examination of purified $BacA_{CT}$ via TEM will allow us to i) demonstrate whether the protein can form filaments *in vitro* and ii) determine the importance of each protein domain to filament formation.

RESULT SUMMARY FROM CHAPTER THREE

In Chapter 3, we characterized six different persistence-inducing conditions in *C. trachomatis* and examined how they altered the pathogen's interaction with the host cell. Chlamydial 'persistence' is currently defined by the following characteristics: enlarged bacterial cell size, the inhibition of cell division, an inability to produce infectious progeny. Importantly, each of these phenotypes is reversible upon removal of the stress condition. All known persistence-inducing conditions are commonly grouped together, despite observed differences in transcription (20; 169; 187), translation (26; 34), and structure (166), leading many to question

the significance and ultimately the relevance of this odd collection of 'abnormal' chlamydia forms. In our investigation of chlamydial persistence, we first confirmed that the induction conditions resulted in persistence. We succeeded in demonstrating that EB production was halted when exposed to persistence-inducers and that this phenotype was largely reversible when removed. In examining infected cell monolayers via SIM and EM under persistence-inducing conditions, we noted that individual chlamydial RBs appeared enlarged. Thus, we hypothesized that persistence leads to a halt in chlamydial division. Division has been previously linked to EB development (242); thus our phenotypic observations appeared to complement each other.

We next conducted a series of experiments examining different aspects of chlamydial biology under these different persistence-inducing conditions. We examined PG synthesis and degradation, indirectly measured the secretion of T3SS effector proteins, and scrutinized inclusion maturation/ localization over time within infected cells. Based on our observations, we categorized *Chlamydia*'s aberrant forms into two general types based on the microbe's interactions with the host cell through i) the ability to synthesize immunostimulatory PG and ii) the ability to present mid/ late-stage effector proteins on the inclusion surface. As we found these two phenotypes to be correlative, we propose that the halted developmental cycle under stress conditions may provide a mechanism of immune evasion to mediate the survival of *Chlamydia* until the conditions within the host cell are more favorable to chlamydial development.

CHLAMDYIAL ABERRANCE VS. PERSISTENCE: IMPLICATIONS, LIMITATIONS AND FUTURE DIRECTIONS

In this study, we originally set out to determine the relationship between ABs and persistence. Bacterial persister cells are classically defined as cells that are not dividing, have reduced metabolic processes, and are less sensitive to host immune response and antibiotic

treatment (71). These persisters can subsist for long periods of time within unfavorable environments (71). Our data indicate that ABs that can downregulate PG synthesis and mid/ late T3SS may be able to survive in the host while evading the immune response.

From this body of work, we established a panel of temporally expressed secreted factors for use as biomarkers to identify the stage of development that an individual inclusion is in. Using this panel, we were the first to identify and differentiate subsets of ABs that are not enlarged (as they have been historically described). The enlarged-cell phenotype (aberrance) long associated with these forms has largely become the sole criteria researchers use for identifying 'persistent' forms of *Chlamydia spp*. The fact that cell division can be halted without a corresponding increase in cell size seemingly breaks a long-held tenant of chlamydial biology. However, considering the reduced size of these smaller ABs have likely been overlooked in the past. Perhaps small ABs were missed due to their similar size to RBs and that they reside within small, immature inclusions. We found these smaller ABs have a reduced immunogenic profile, which would likely make them much harder targets for the immune system to target and clear. Thus, we hypothesize that these smaller, less immunogenic ABs may be the dominant and more biologically relevant subset of ABs in natural infections as they may provide a selective advantage to avoid the host's immune response. This finding changes our understanding of what is currently understood to be an AB and the field needs to expand the definition of ABs to include ABs of smaller size.

Furthermore, we propose that as a result of this work, we now have the tools to address the unresolved controversy concerning the relevance of ABs in natural infections. The ability to detect ABs in tissue samples will allow us to characterize the frequency of ABs *in vivo,* which persistence 'subset' they resemble, and the response of the immune system. Future experiments

will focus on this area by harvesting the reproductive tracts of mice that have been infected with *Chlamydia spp*. in order to identify and characterize aberrant bodies *ex vivo*. Previous literature has raised potential difficulties that may be faced when trying to detect aberrant bodies in infections (human or animal) (222). This is largely due to the lack of biomarkers that can be utilized for their discrimination and detection. Given our observations, we believe such a study could be undertaken to characterize (*ex vivo*) aberrant bodies present in murine tissue and/ or resected human genital tissue. Immediately following resection, tissue can be exposed to the PG-labeling reagent EDA-DA, fixed, sectioned, and stained with other bacterial and/ or cellular markers, such as inclusion membrane proteins, Hsp60, and MOMP. This method will allow us to categorize which subset of aberrant bodies may be biologically relevant; we can effectively determine the presence of bacteria, bacterial cell size, PG status, inclusion maturation, and (indirectly) T3SS function. Furthermore, it is pertinent to understand the impact that a localized immune response has on AB formation *in vivo*. Thus, we would also stain for immune cells, such as polymorphonuclear neutrophils, in order to understand the degree to which aberrant *Chlamydia spp*. elicit an immune response and whether this significantly affects immune cell tracking to chlamydial infected cells. It is important to note that there are inherent differences between mouse and human physiology and how *C. muridarum* and *C. trachomatis* interact with the hosts. Researchers will need to take into consideration differences in the duration of colonization, human and murine IFNγ production and function, and the absence of IDO in murine cells (37).

Additionally, there is currently an active debate concerning whether persistent forms of *C. trachomatis* exhibit enhanced tolerance to killing by antibiotics. This has major implications regarding clinical infections, with the major question being whether persistence observed in the

laboratory can be linked to antibiotic treatment failure in the clinic. Although *C. trachomatis* infections are generally treatable with antibiotics, such as azithromycin or doxycycline, there are numerous examples of treatment failure and the trend suggests that these events are increasing (101; 123; 201). This debate has been historically difficult to address due to the lack of tools to identify ABs in samples. As previously discussed, the tools developed in this work will also help us to determine whether these ABs may contribute to treatment failure and the associated long-term sequalae.

However, in our pursuit to understand the contribution of ABs in treatment failure, we compared the ability of a subclinical dose of azithromycin added at mid-development to kill iron depletion-induced aberrant bodies and ampicillin-induced aberrant bodies. We found iron depletion-induced persistence enhances the susceptibility of *C. trachomatis* to killing by azithromycin while ampicillin-induced persistence does not. Shortly prior to the publication of our work, it was reported that clinical isolates are more susceptible to killing by azithromycin when exposed to iron depletion conditions, and the researchers found that even when exogenous iron is added to the system, infectious progeny production did not recover to that of the negative control condition (248). The same group found that penicillin-induced persistence also results in the same phenotype (248), which differs from our findings. These differences are likely a result of the two studies attempting to address slightly different questions. A key characteristic of chlamydial persistence is reversibility, which our study examined but the comparable study did not address. Rather than removing azithromycin after exposure for a specific period of time as a means to determine whether the bacteria could recover, researchers carrying out the clinical isolate study left azithromycin on the *C. trachomatis* infected cells for the entirety of the experiment. The loss in viable progeny could be due to a subset of the population remaining

aberrant, as they did not remove the penicillin from the media completely. Additionally, azithromycin is a protein synthesis inhibitor and is bacteriostatic, rather than bactericidal, particularly over short time intervals. Given that iron-induced persistence downregulates protein synthesis in *C. trachomatis* (34; 249), it is likely that iron chelation enhances the effectiveness of azithromycin resulting in an additive effect. The clinical isolate study also used the minimum inhibitory concentration of azithromycin, while our study used a sub-inhibitory dose.

The current hypothesis is that ABs are a significant contributor to antibiotic treatment failure. Although ABs have been proposed to have an increased tolerance to frontline antibiotics, there is not a lot of studies that demonstrates this. One study showed in an amoxicillin-induced persistence mouse model, azithromycin treatment did not as effectively clear *C. muridarum* compared to untreated mouse model (199). These data suggest that ABs may be more tolerant to azithromycin treatment. However, there has not been further exploration on the tolerance of ABs induced by other mechanisms to azithromycin. We propose that the smaller, less immunogenic ABs (induced by iron deprivation, IFNγ) may be more biologically relevant in natural infection as iron restriction and IFNγ production are two mechanisms that are used by the immune system to fight bacterial infections. Therefore, we hypothesize that these smaller ABs may not be a significant contributor to antibiotic treatment failure as we were unable to observe recoverable EBs when treated with a subclinical doses of azithromycin.

While our study focused on several of the commonly described aberrance-inducing conditions, there are additional, biologically relevant aberrance-inducing conditions that need to be examined in the future. These include co-infection with viruses (Herpes Simplex Virus) (27; 58), and chlamydial infection of M1 macrophages (83; 172) or monocytes (127). As macrophages and monocytes can produce IFNγ (130), we hypothesize that these conditions will

lack the ability to produce immunostimulatory PG and mid/ late-stage effectors. Other potential aberrance-inducing conditions likely also exist that have yet to be discovered. For instance, it would be imperative to understand whether co-infections with other sexually transmitted pathogens, such as *N. gonorrhoeae*, result in the aberrant state.

Furthermore, there are likely additional changes in chlamydial physiology resulting from persistence induction that impact the immune response. Our work demonstrated that differences in the ability of ABs to produce PG altered the ability of NOD1 receptors to detect aberrant bacteria. Other chlamydial components, such as DNA, lipoproteins, lipooligoaccharides (LOS), and Hsp60 have been demonstrated to activate Toll-like receptors (TLR) and stimulate the innate immune system (115; 240). Using HEK hTLR SEAP reporter cell lines, future studies can examine differences in the ability of ABs to signal through these other innate receptors. We predict that there will be differences in the ability of ABs to signaling through innate receptors, as differences in LOS and Hsp60 production have been shown in ABs (278).

Our studies were conducted entirely in *in vitro* cell culture assays, which is an important starting point in basic research. However, it is important to also recognize the limitations of this work. Our study relies primarily on a cell culture-based infection model of a lab adapted *C. trachomatis* strain. We chose to use an LGV serovar (L2) of *C. trachomatis* because these serovars are easier to work with and replicate more quickly in cell culture lines than non-LGV serovars (224). Thus, it is pertinent to conduct similar experiments with recent clinical isolates of *C. trachomatis* as a means to determine if recent isolates of *C. trachomatis* are as sensitive to the aberrance-inducing conditions and whether the bacteria retain the physiological differences we described in this work. The challenge with recent clinical isolates of *C. trachomatis* is that they need to be serially passaged in culture in order to adapt and grow in the laboratory; this may alter

their phenotypes. There is evidence of the accumulation of minor single nucleotide polymorphisms (SNPs) after one year of serial passaging *C. trachomatis* strains in cell culture, which could potentially confer a selective advantage; however, that study found no changes in rate of growth, cell adherence, or plasmid copy number compared to original isolates (31). The induction of persistence (mediated by penicillin or iron depletion) in recent clinical *C. trachomatis* isolates confirmed that there are differences in sensitivity to the induction conditions compared to a laboratory passaged strain (248). Furthermore, a previous study found that there are inter-strain differences in sensitivities to IFNγ-induced persistence (165).

Our study also utilizes an immortalized cell line, which is another potential limitation of this work, as certain cellular functions have been compromised in order for the cells to continuously proliferate under tissue culture conditions (42). Therefore, it is essential that subsequent work utilize primary cervical epithelial cells to confirm if aberrance-inducing conditions affect the bacteria's interaction with the host cell in the same manner as in our HeLa cell infection model. A major challenge with this approach is that primary cells are often less susceptible to chlamydial infections (244). However, it is important to note that primary cells show a stronger pro-inflammatory cytokine profile than HeLa cells in response to chlamydial infections (244), which might reveal subtle differences in cellular responses that may be missed by using immortalized cells lines.

OVERARCHING THEMES AND CONCLUSIONS

Investigating dynamic processes in the obligate intracellular bacteria *C. trachomatis* necessitated the development and adaptation of molecular and high-resolution imaging techniques for use in both fixed and living cells. These methods, both of which are new to the field and were only recently introduced in this work, allowed us to observe and quantify subtle

differences in cell size and development. Our work represents the first successful use of a fluorescent gene fusion in *C. trachomatis* and is the first to use high resolution microscopy. The advent of these technologies in the field of chlamydiology allowed us to examine dynamic processes in real-time and in relation to key proteins and complexes, such as MreB, PG, and MOMP. These techniques can be utilized broadly to better understand chlamydial cell division and differentiation.

In Aim 2, we examined the aberrance phenotype in great detail across a wide range of assay conditions. We found unique, phenotypic differences in ampicillin and sucrose-induced aberrant bodies that closely resemble the phenotype in the $bacA_{CT}$ knockdown experiment conducted in Aim 1. All three aberrance inducers led to an increase in cell size, despite the bacteria being capable of synthesizing un-crosslinked peptidoglycan. The regulation of cell size is important in chlamydial development (138). *C. trachomatis* must first reduce its size prior to transitioning to its infectious form (138). However, the mechanism by which the microbe accomplishes this cell size reduction is unknown. Unlike the ampicillin and sucrose-induced phenotype; however, we did not see a measurable difference in the production of infectious EBs during the $bacA_{CT}$ knockdown experiment. Given that the change in cell size is modest when $BacA_{CT}$ is depleted (Fig. 10), and since we only examined infectious progeny at late time points in the developmental cycle, it is possible that we may have missed subtle effects on EB production.

Although tightly crosslinked outer membrane complexes provide membrane stability to extracellular EBs, these complexes must be relaxed in RBs during cell division. It is unknown how changes in cell size affect presentation and enrichment of cell surface antigens in *Chlamydia spp*. Thus, alterations in outer membrane protein content and abundance may influence cell size.

One example of alterations in surface protein content was demonstrated in response to IFNγ-induced persistence (18). Protein levels of MOMP, LOS, and a 60 kDa outer membrane protein were decreased in response to IFNγ, while Hsp60 levels remained steady (18). However, it is unclear whether changes in cell size alter surface protein quantity or if the quantity of these surface molecules leads to changes in cell size. Alterations in surface protein quantity can affect interaction with the immune system and clinical outcomes. Hsp60 is associated with inflammation in genital tract infections and can lead to infertility (269). Thus, clinically it is important to understand how changes in cell size affects cell surface antigens.

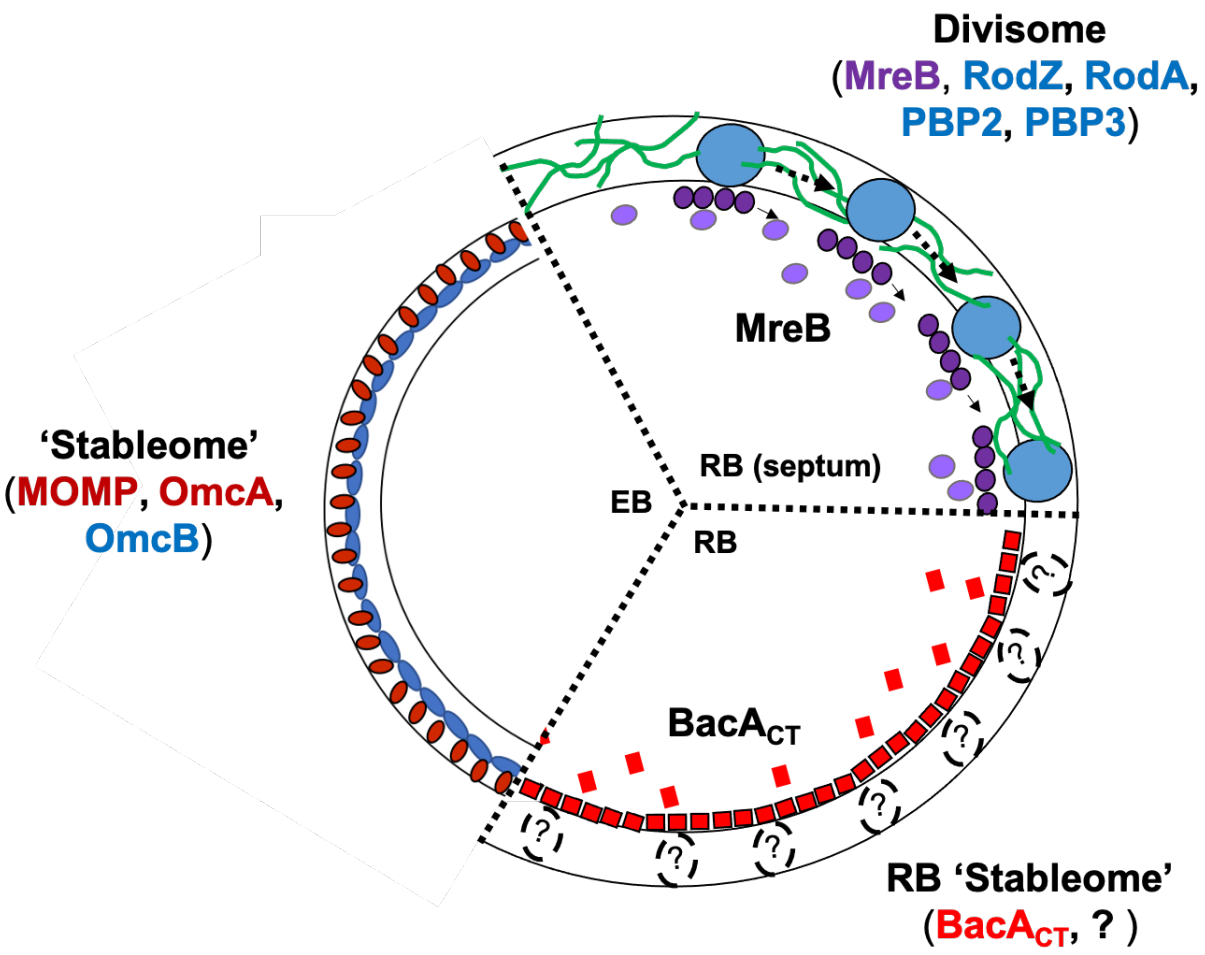


Figure 30. Membrane stabilization mechanisms are spatially restricted and differ between *Chlamydia*'s developmental forms.
Chlamydia species rely on highly crosslinked outer membrane proteins (OmpB, OmpC) to maintain membrane integrity in their extracellular forms; however, this structure is rigid and does not allow for the membrane expansion and fluidity required during bacterial growth and division. Conversely, the microbe's replicative form maintains peptidoglycan only at the septum, as this is the only place where the pathogen's peptidoglycan synthases (divisome) localize. We hypothesize that BacA$_{CT}$, likely in conjunction with other periplasmic elements, may function to stabilize the inner membranes at areas other than the septum, effectively stabilizing specific areas of the periplasmic space and allowing transmembrane complexes to function in the absence of a sacculus.

Appendix A: Additional unpublished data from chapter 2

INTRODUCTION

This appendix contains unpublished data that was not included Chapter 2.

$BacA_{CT}$ expression has no effect on chlamydial viability

As described in Chapter 2, our goal was to ensure that the overexpression of the $BacA_{CT}$ fusion constructs did not adversely affect the development of *C. trachomatis*. Thus, as a control experiment, we quantified the ability of *C. trachomatis* to complete its developmental cycle and produce infectious progeny (EBs) while producing tagged and fusion variants of $BacA_{CT}$. We found that the induction of the $BacA_{CT}$ constructs with between 1-10 ng/ ml of anhydrous tetracycline (aTc) resulted in no measurable differences in the number of IFU recovered at 44 hpi (Fig. 31). This demonstrates that under both induction conditions, EB development is unaffected, and indicates that the induction of HIS-tagged $BacA_{CT}$ and the $BacA_{CT}$-mCherry fusion protein does not significantly affect the developmental cycle of *C. trachomatis*.

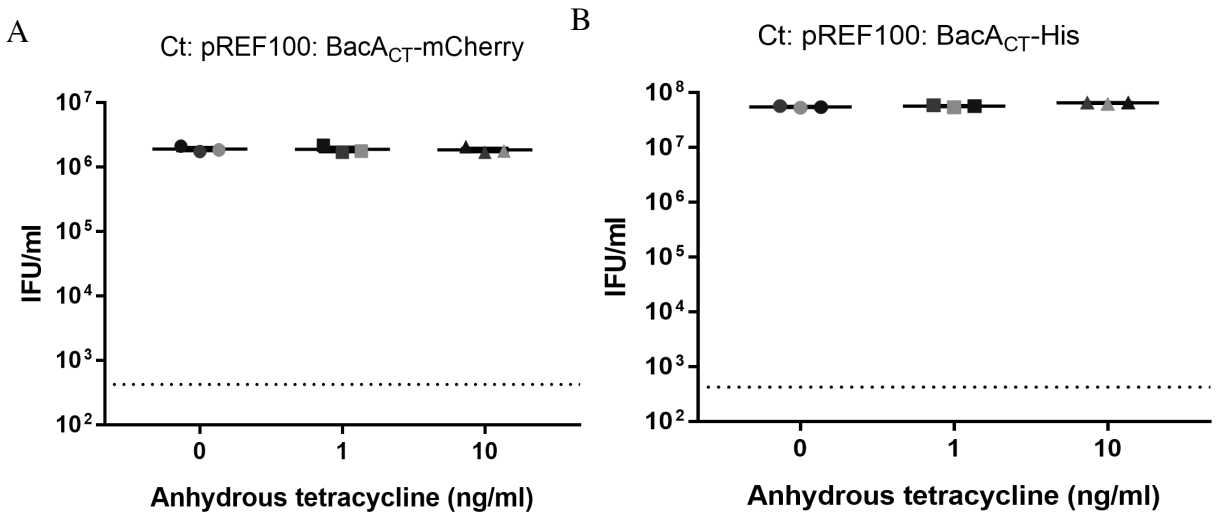


Figure 31. Induction of BacA$_{CT}$ fusion constructs does not affect chlamydial development. L2 mouse fibroblast cells were infected with (A) *C. trachomatis* L2 434/Bu: pREF100: BacA$_{CT}$-mCherry or (B) BacA$_{CT}$-His at an MOI of 1 in a 24 well plate with 0, 1, or 10 ng/ml of aTc for 44 hours. EBs were then mechanically harvested, serially diluted, and used to infect new L2 cell monolayers in a 96 well plate. At 24 hpi, 20 fields of view of GFP$^+$ inclusion forming units (IFU) were counted in duplicate for each treatment condition. The solid line represents the mean of three biological replicates, and the dotted line represents the assay's limit of detection.

$BacA_{CT}$ filament characterization

Given our observation (described in Chapter 2) that defects in $BacA_{CT}$ expression appeared to coincide with an enlargement of chlamydial RBs, we tested the stability of chlamydial $BacA_{CT}$ filaments by treating transformants that express $BacA_{CT}$ fusion proteins with cell division inhibitors. As described previously, in response to various stress conditions, *Chlamydia* species become enlarged and halt cell division and differentiation (189). Once the stressor is removed, cell division can resume, and the bacteria proceed through their normal developmental cycle. Disruption of chlamydial MreB filaments by cell division inhibitors has been previously shown (137; 141), and we wanted to determine if $BacA_{CT}$ acts similarly. To determine the degree to which halting chlamydial cell division affects $BacA_{CT}$ ring formation, we exposed *C. trachomatis* expressing a $BacA_{CT}$-mCherry fusion construct to the following compounds: ampicillin, D-cycloserine (PG-targeting antibiotic), compound C1 (T3SS inhibitor), DPP (iron chelator), or MP265 (MreB inhibitor).

MATERIALS AND METHODS

HeLa cells were plated on a glass coverslip in 24 well tissue culture treated plate wells (Costar) at confluency of ~70-80%. Cells were infected with *C. trachomatis* L2 434/Bu in cold Dulbecco's Modified Eagle Medium (DMEM) (Gibco) (250 µl per well) and placed on a rocker in the 37°C tissue culture incubator for 2 hours. Subsequently, the DMEM was removed and replaced with DMEM supplemented with 10% FBS (HyClone), and 1x MEM Non-Essential Amino Acids Solution (Sigma) (250 µl per well). The following aberrance-inducing conditions were tested in this study: 100 µM DPP (iron chelator), 10 µM ampicillin, 30 µg/ml D-cycloserine, 50 µM C1 (T3SS inhibitor), and 125 µM MP265 (polymerization inhibitor of the bacterial cytoskeletal protein MreB). DPP was added at the time of infection. Ampicillin or D-cycloserine were added at 2 hpi, while C1 or MP265 were added 10 hpi, following the EB to RB conversion. At 24 hpi, cells were fixed with 4% paraformaldehyde, and Z-stacks were generated utilizing a Zeiss PS.1 ELYRA in structural illumination mode (SIM). For live cell imaging studies, Z-stacks were generated utilizing a Zeiss LSM 710 confocal microscope either after adding the inhibitors or after washing out the inhibitors at various timepoints (as described in the corresponding figure legends). Images are representative of at least 20 fields of view and two biological replicates.

RESULTS AND DISCUSSION

Cell division inhibitors prevent $BacA_{CT}$ ring formation

To determine the effect of inhibiting chlamydial cell division on $BacA_{CT}$ ring formation, we exposed *C. trachomatis* expressing a $BacA_{CT}$-mCherry fusion construct to the following

compounds: ampicillin, D- cycloserine (PG-targeting antibiotics), C1 (T3SS inhibitor), DPP (iron chelator), or MP265 (MreB inhibitor). We found that following treatment with each inhibitor, the ring-like form of $BacA_{CT}$ was no longer observed in any imaging plane (Fig. 32). To investigate the stability of the BacA ring-like structures, we allowed *C. trachomatis* expressing $BacA_{CT}$-mCherry to grow and replicate for 18h prior to adding the cell division inhibitors MP265, DPP, or ampicillin. We found that upon treatment with MP265 the $BacA_{CT}$ rings dissociated within 3h (Fig. 33), while complete ring dissociation as a result of DPP or ampicillin occurred between 3 and 24h (data not shown). This dissociation of $BacA_{CT}$ filaments is comparable to previous observations of chlamydial MreB filaments, which dissociate from the membrane after treatment with MreB polymerization inhibitors (137; 141). As the arrest in cell division inherent to *Chlamydia*'s aberrant forms is known to be reversible upon the removal of aberrance-inducers (189), we hypothesized that the inhibition of $BacA_{CT}$ ring formation was likely reversible. When infected cells were washed with PBS and the medium was replaced with ampicillin-free infection medium, the $BacA_{CT}$ rings were observable within 24 hours post-wash (Fig. 34).

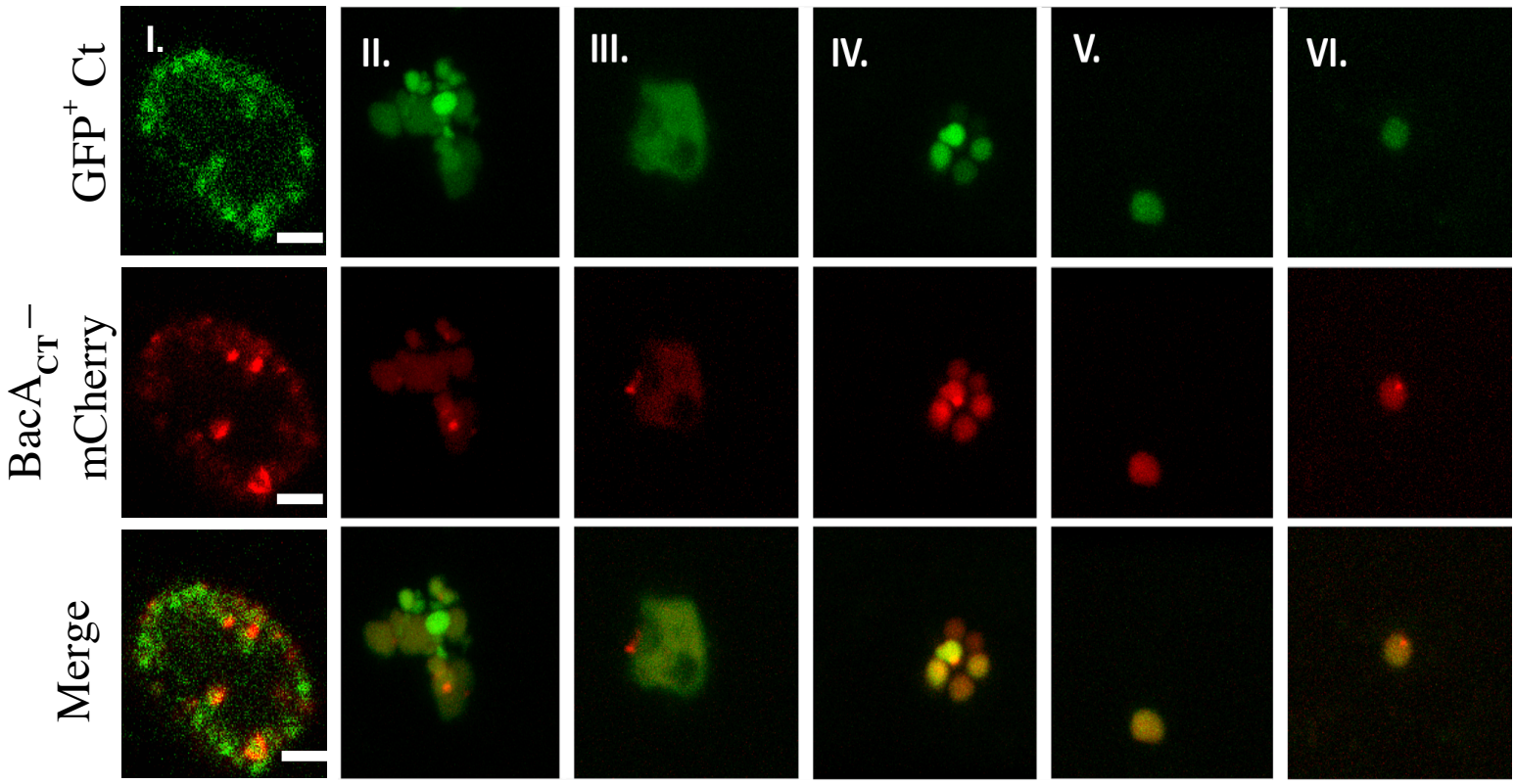


Figure 32. Treatment with cell division inhibitors prevents $BacA_{CT}$ filament formation. HeLa cells were infected with *C. trachomatis* L2 434/Bu: pREF100: $BacA_{CT}$-mCherry with aTc induction (10 ng/ml). At 2 hpi or 10 hpi, cells were (from left to right): (i) untreated or exposed to (ii) D-cycloserine (30 μg/ml), (iii) Ampicillin (5 μg/ml), (iv) 2,2′-Bipyridyl (DPP) (100 μM), (v) C1 (T3SS inhibitor) (50 μM), or (vi) MP265 (150 μM). At 24 hpi, cells were fixed with 4% paraformaldehyde. The panel represents the following (from top to bottom): GFP+ *Chlamydia* (green), $BacA_{CT}$-mCherry (red) and merged Z-stack images. Scale bar ~2 μm. Images are representative of at least 20 fields of view. Experiments were conducted in two biological replicates.

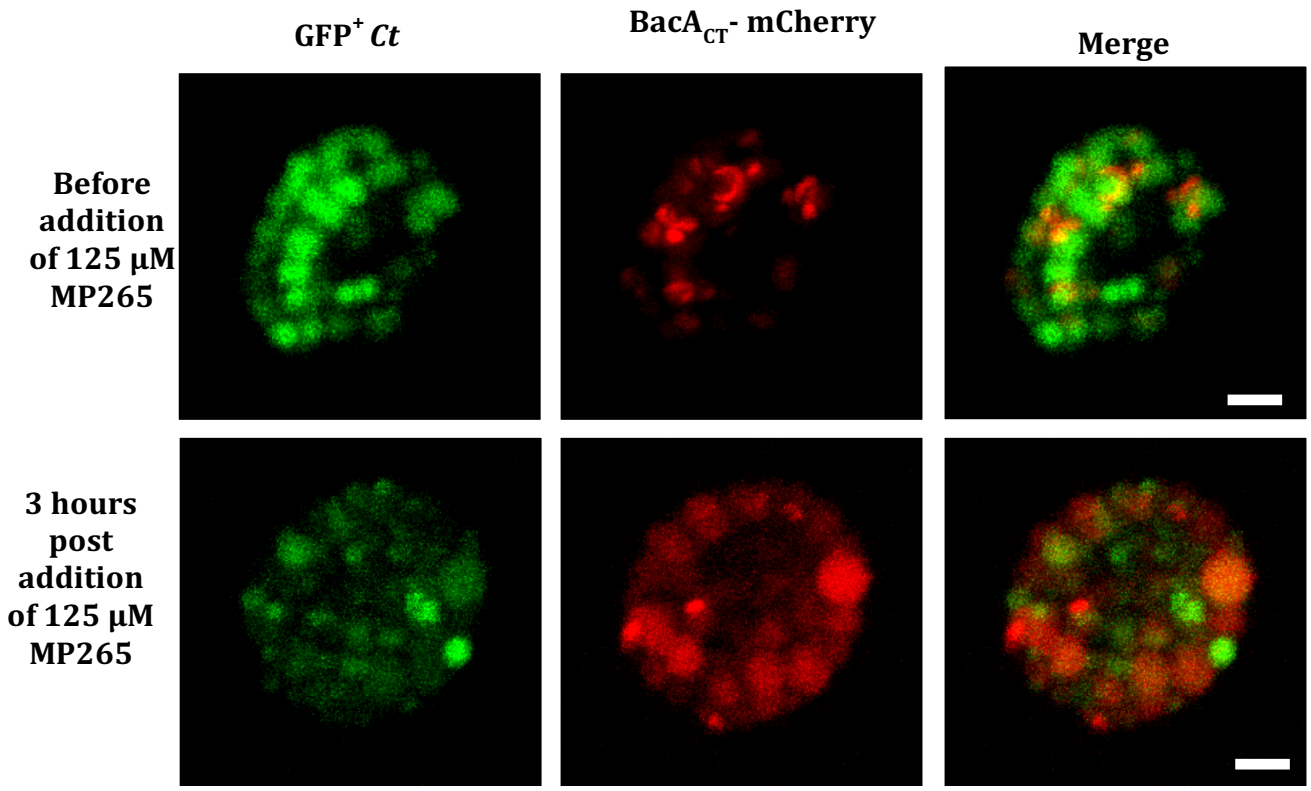


Figure 33. $BacA_{CT}$-mCherry rings exhibit reversible dissociation following inhibition of MreB. HeLa cells were infected with *C. trachomatis* L2 434/Bu: pREF100: $BacA_{CT}$-mCherry with aTc induction (10 ng/ml). Cells were exposed to either 125 uM MP265 for 3 hours. Each panel represents the following (from left to right): GFP^+ *C. trachomatis* (green), $BacA_{CT}$-mCherry (red) and merged Z-stack confocal images. Scale bar ~2 μm. Images are representative of at least 20 fields of view.

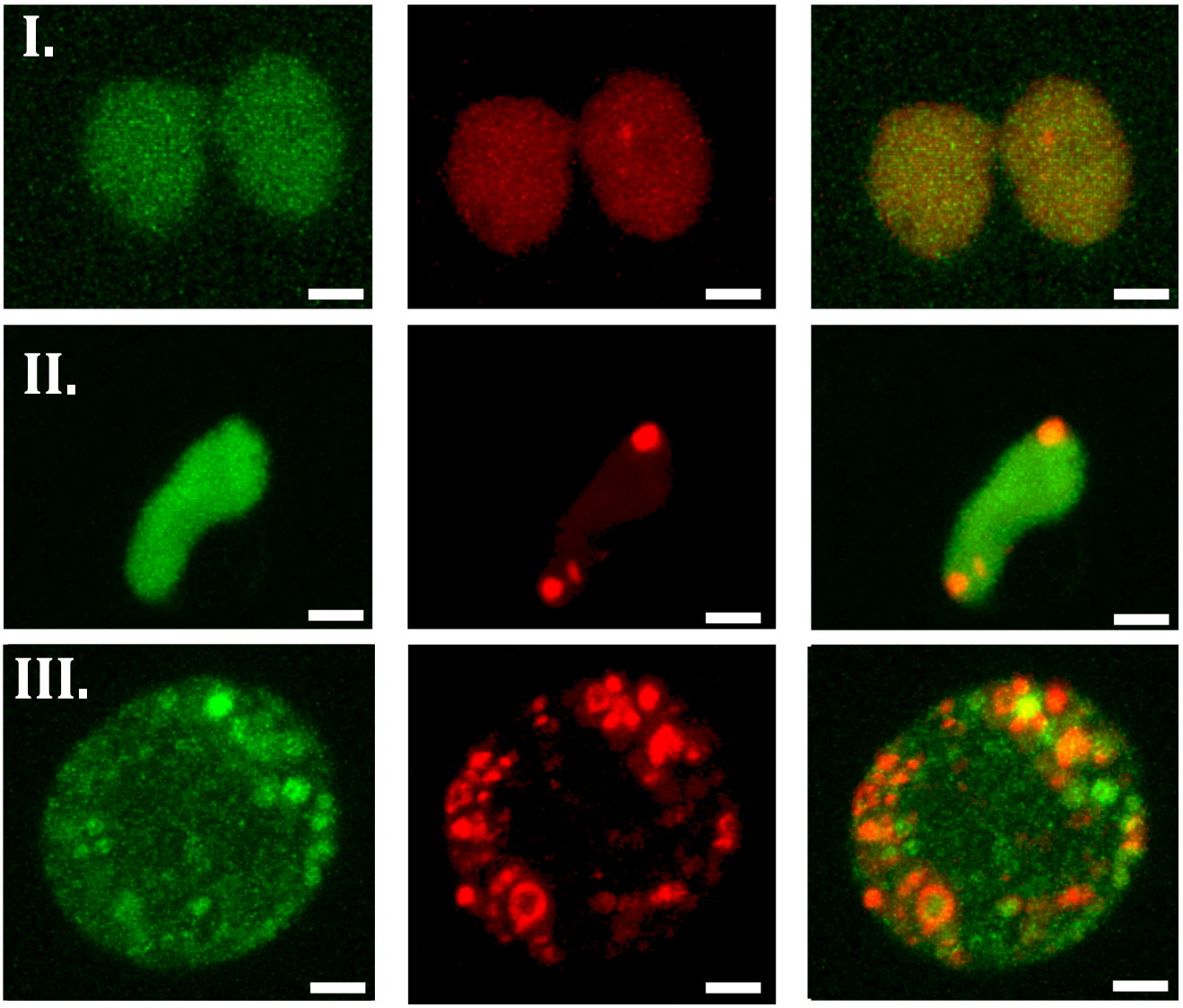


Figure 34. $BacA_{CT}$ polymerization resumes upon the removal of ampicillin.
HeLa cells were infected with *C. trachomatis* L2 434/Bu: pREF100: $BacA_{CT}$- mCherry with aTc induction (10 ng/ml). At 2 hpi., cells were exposed to ampicillin (0.5 µg/ml). At 17.5 hpi, ampicillin was removed and cell monolayers were washed with PBS. At (I. top panel) 18, (II. Middle panel) 22, and (III. Bottom panel) 42 hpi, live cells were imaged via confocal microscopy. Each panel represents the following (from left to right): GFP^+ *C. trachomatis* (green), $BacA_{CT}$- mCherry (red) and merged Z-stack confocal images. Scale bar ~2 μm. Images are representative of at least 20 fields of view.

Appendix B: Additional unpublished data from chapter 3

INTRODUCTION

This appendix includes unpublished data that was not included in Chapter 3. The experiments herein describe an intermediate aberrance phenotype that we identified in our original characterization studies.

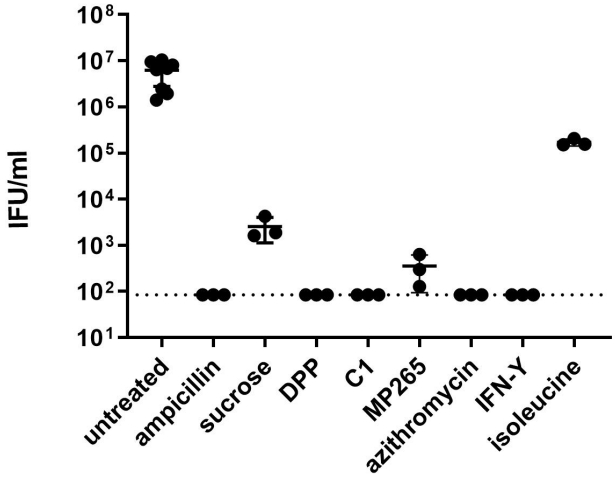
RESULTS AND DISCUSSION: ESSENTIAL AMINO ACID STARVATION (INDUCED BY ISOLEUCINE SUPPLEMENTATION)

As a result of genetic reduction, *Chlamydia* species encode only a few, multipurpose amino acid transporters (235). Previous studies have shown that some of these transporters that are susceptible to competitive substrate inhibition; the addition of exogenous amino acids can lead to deficiencies in the uptake of essential amino acids and result in aberrance induction (4; 33; 92). Thus, we set out to examine the effects of essential amino acid starvation (induced by isoleucine supplementation) on the ability of *C. trachomatis* to i) synthesize PG and ii) successfully secrete effector proteins utilizing its T3SS. Using the techniques we used to characterize other aberrance-inducing conditions (Chapter 3), we found that isoleucine supplementation produced an 'intermediate' aberrance phenotype. Unlike other aberrance-inducing conditions, the addition of exogenous isoleucine did not result in a comparable reduction in EBs recovered after 44 hours of treatment (Fig. 35). We suspect that this result is likely due to the high levels of valine present in the tissue culture media, which has previously been shown to allow *C. trachomatis* to overcome isoleucine-induced aberrance (33). Furthermore, we found that amino acid starvation-induced aberrance produced ABs that contained labeled PG in an irregular arrangement, similar to sucrose-induced aberrance and β-

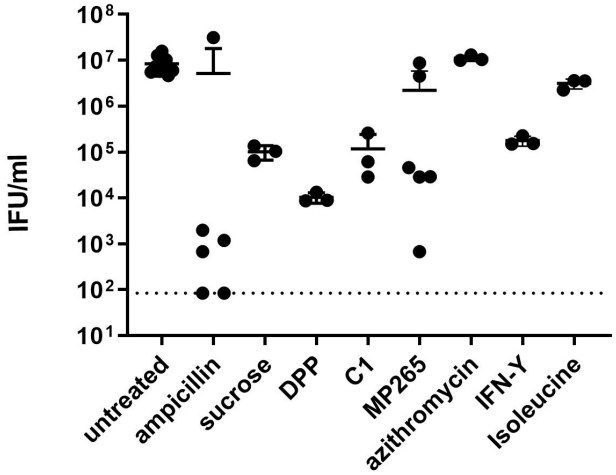
lactam-induced aberrance (Fig. 36). To determine whether Inc proteins are capable of being expressed, secreted, and presented on the inclusion membranes in *C. trachomatis*-infected cells under isoleucine-induced aberrance conditions, we used antibodies to fluorescently label early-, mid-, and late-stage Inc proteins. In *C. trachomatis*-infected cells that had been treated with exogenous isoleucine, the early-stage effectors, CT229 (Fig. 37a) and IncG (Fig. 37b), and the mid-stage effector IncA were present on all inclusions (Fig. 37c). However, there was no discernable labeling of the late-stage effector CT813 (Fig. 37d). There was also no difference in the proximity of normal and isoleucine-induced aberrant *C. trachomatis* to host cell nuclei (Fig. 38). The trafficking of the inclusion to the cell nucleus occurs within the first 12 hours of infection (41), and our observations indicate that the T3SS is functional in isoleucine-treated cells at this time. Nevertheless, we infer by the lack of labeling of the late-stage effector CT813 that the inclusion is either unable to fully mature or that the maturation process is delayed significantly. These experiments should be repeated in the future using a valine deplete media, enhancing the effects of isoleucine supplementation. We hypothesize that under these conditions, ABs would more closely resemble those observed when using other induction conditions that inhibit protein synthesis (IFN-γ, iron depletion, and C1).

FIGURES

A


IFU/ml
10^8
10^7
10^6
10^5
10^4
10^3
10^2
10^1
untreated
ampicillin
sucrose
DPP
C1
MP265
azithromycin
IFN-Y
isoleucine

B


IFU/ml
10^8
10^7
10^6
10^5
10^4
10^3
10^2
10^1
untreated
ampicillin
sucrose
DPP
C1
MP265
azithromycin
IFN-Y
Isoleucine

C

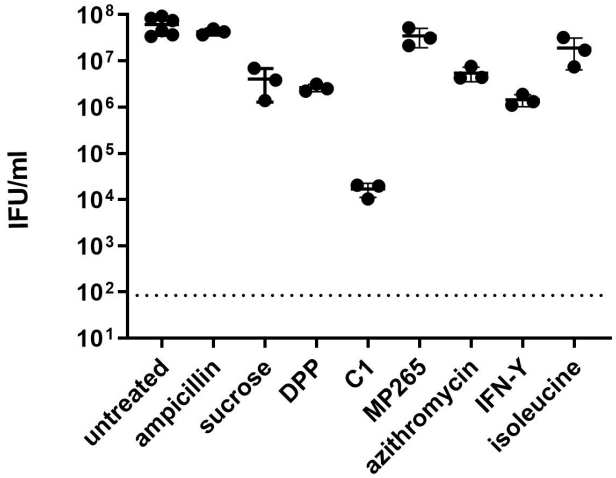

IFU/ml
10^8
10^7
10^6
10^5
10^4
10^3
10^2
10^1
untreated
ampicillin
sucrose
DPP
C1
MP265
azithromycin
IFN-Y
isoleucine

Figure 35. Aberrant body formation inhibited by amino acid limitation (via the addition of exogenous isoleucine) partially results in cell division arrest and pausing of the *Chlamydia* developmental cycle.
Inclusion forming unit (IFU) counts were conducted 44 hours post-infection/treatment (a) and subsequent to recovery in the absence of treatment for an additional 24 (b) and 48 (c) hours. Dotted line represents the assay's limit of detection. Each data point plotted represents an independent biological replicate, and error bars represent the standard deviations from the mean. The dotted line represents the limit of detection for the assay. Note: This is a modification of Figure 16 to include the isoleucine data, as the experimental conditions were conducted in tandem.

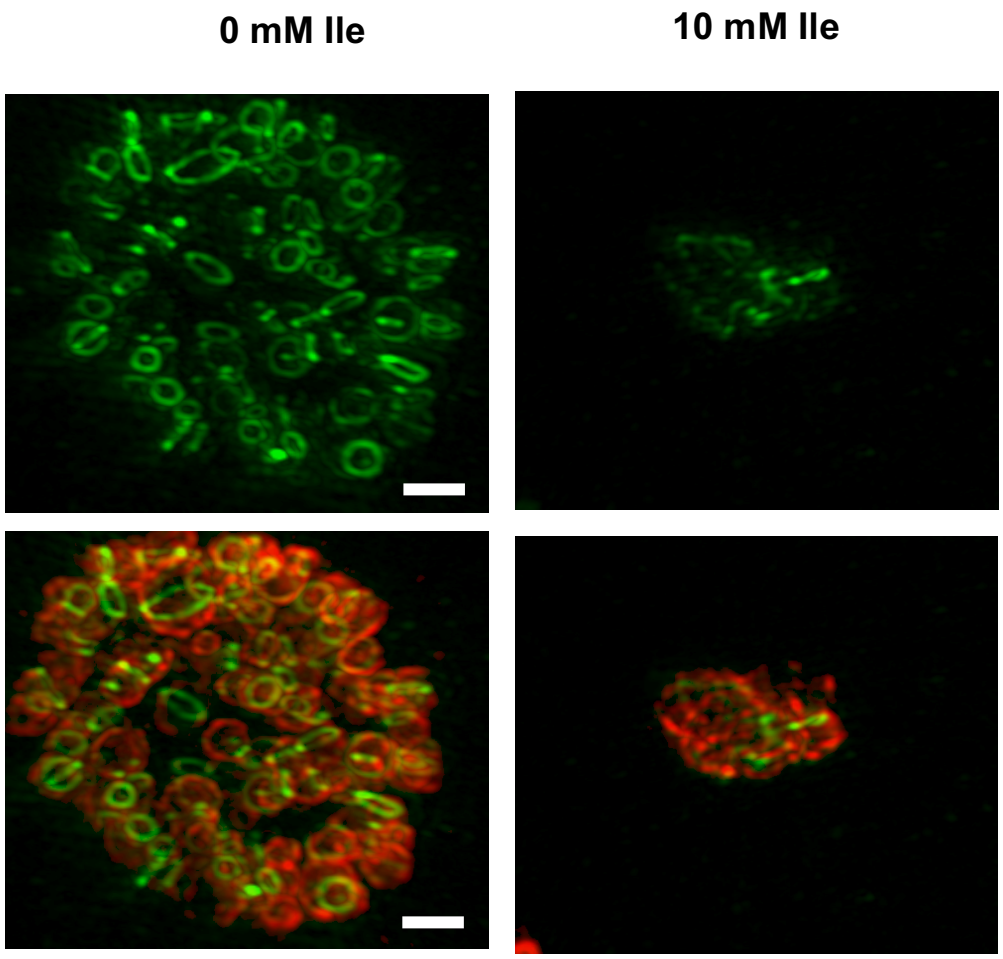


Figure 36. Cell division is only partially inhibited by amino acid limitation (via the addition of exogenous isoleucine).
Chlamydia–infected HeLa cells were grown in the presence of PG-labeling reagent EDA-DA (143) with 10 mM exogenous isoleucine. Cells were fixed at 24 hpi. PG (green) was labeled via click-chemistry whereas chlamydial RBs and ABs were visualized utilizing a monoclonal antibody to the major outer membrane protein (MOMP) (red). Scale bar ~2 μm. Images are representative of at least 20 fields of view. Experiments were conducted in two biological replicates.

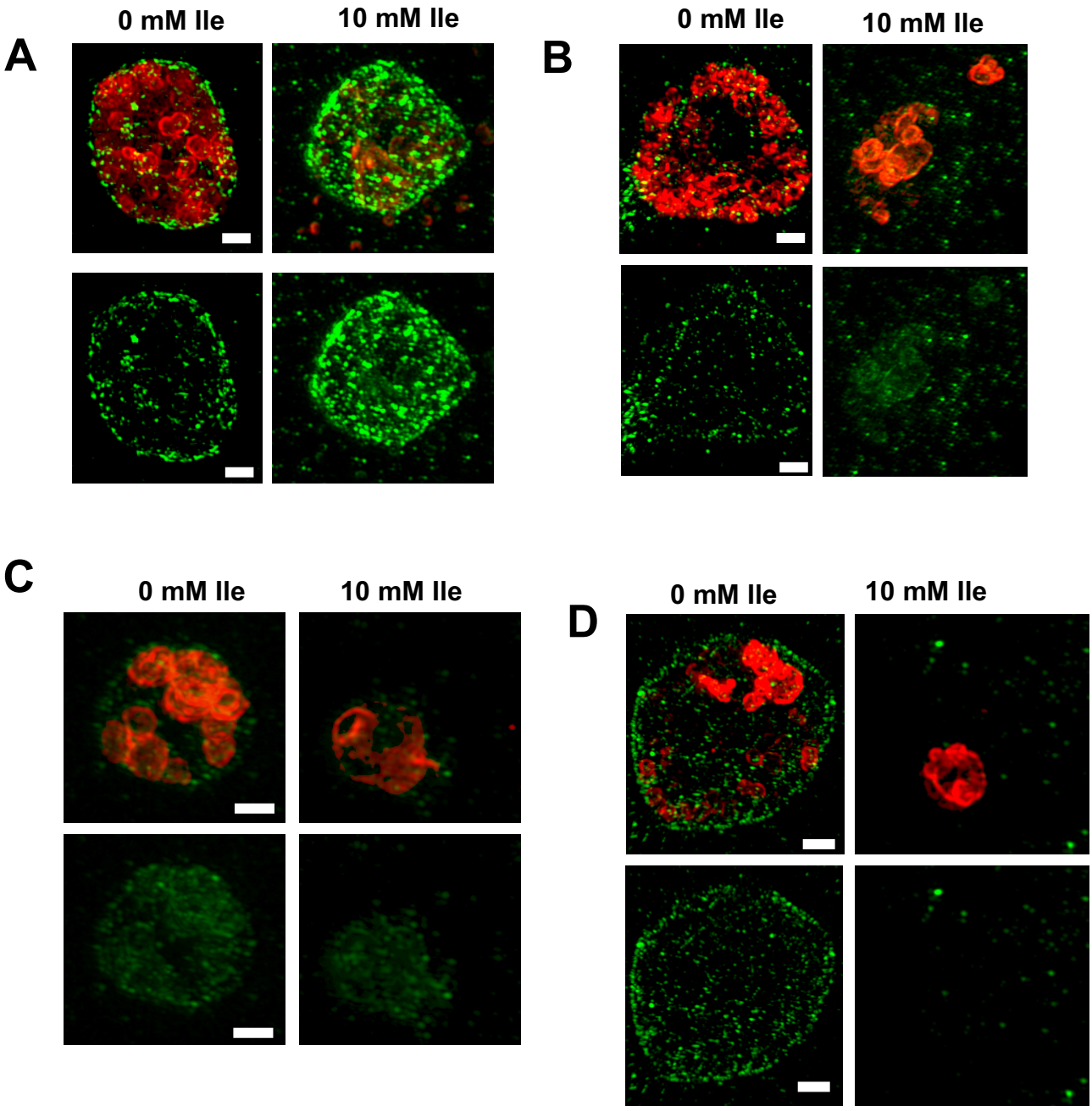


Figure 37. Inclusion maturation was partially inhibited by amino acid limitation (via the addition of exogenous isoleucine).
Immunolabeling of inclusion membrane proteins CT229 (a), IncG (b), IncA (c), and CT813 (d) (green) in *Chlamydia*-infected cells +/- 10 mM exogenous isoleucine at 24 hpi. Chlamydial RBs and ABs were visualized utilizing a monoclonal antibody to the major outer membrane protein (MOMP) (red) at 24 hpi. Scale bar ~2 μm. Images are representative of at least 20 fields of view. Experiments were conducted in two biological replicates

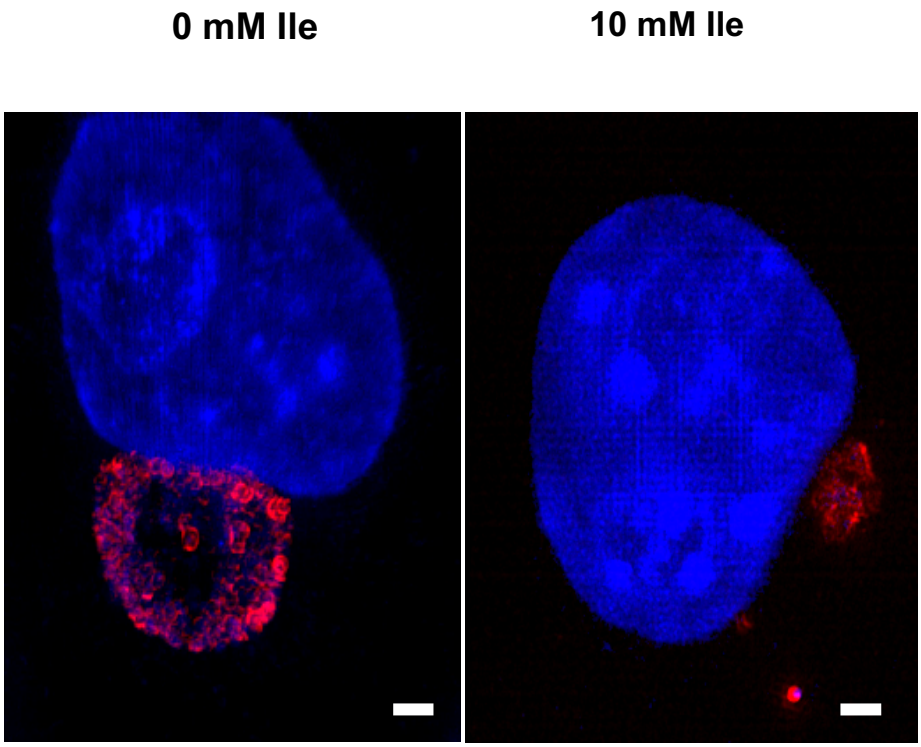


Figure 38. Assessment of inclusion trafficking to the nucleus upon exposure to amino acid limitation (via the addition of exogenous isoleucine).
The proximity of normal and aberrant *Chlamydia* inclusions to host cell nuclei was assessed by immunolabeling of normal and aberrant forms of *Chlamydia*. Chlamydial RBs and ABs were visualized utilizing a monoclonal antibody to the major outer membrane protein (MOMP) (red). Nuclei were stained with Hoechst solution (blue) at 24 hpi. Scale bar~ 5μm.

References

1. 2020. *CHLAMYDIA BIOLOGY : from genome to disease*. [S.l.]: CAISTER ACADEMIC PRESS
2. Abdelrahman Y, Ouellette SP, Belland RJ, Cox JV. 2016. Polarized cell division of *Chlamydia trachomatis*. *PLoS Pathogens* 12:e1005822
3. Adams DW, Wu LJ, Errington J. 2015. Nucleoid occlusion protein Noc recruits DNA to the bacterial cell membrane. *EMBO J* 34:491-501
4. Al-Younes HM, Gussmann J, Braun PR, Brinkmann V, Meyer TF. 2006. Naturally occurring amino acids differentially influence the development of *Chlamydia trachomatis* and *Chlamydia (Chlamydophila) pneumoniae*. *J. of Med Microbiol* 55:879-86
5. Al-Younes HM, Rudel T, Brinkmann V, Szczepek AJ, Meyer TF. 2001. Low iron availability modulates the course of *Chlamydia pneumoniae* infection. *Cell Microbiol* 3:427-37
6. Albrecht M, Sharma CM, Dittrich MT, Muller T, Reinhardt R, et al. 2011. The transcriptional landscape of *Chlamydia pneumoniae*. *Genome Biol* 12:R98
7. Albrecht M, Sharma CM, Reinhardt R, Vogel J, Rudel T. 2010. Deep sequencing-based discovery of the *Chlamydia trachomatis* transcriptome. *Nucleic Acids Res* 38:868-77
8. Almeida F, Borges V, Ferreira R, Borrego MJ, Gomes JP, Mota LJ. 2012. Polymorphisms in inc proteins and differential expression of inc genes among C*hlamydia trachomatis* strains correlate with invasiveness and tropism of lymphogranuloma venereum isolates. *J Bacteriol* 194:6574-85
9. Ausmees N, Kuhn JR, Jacobs-Wagner C. 2003. The bacterial cytoskeleton: an intermediate filament-like function in cell shape. *Cell* 115:705-13
10. Bachmann NL, Polkinghorne A, Timms P. 2014. *Chlamydia* genomics: providing novel insights into chlamydial biology. *Trends Microbiol* 22:464-72
11. Bailey MW, Bisicchia P, Warren BT, Sherratt DJ, Mannik J. 2014. Evidence for divisome localization mechanisms independent of the Min system and SlmA in Escherichia coli. *PLoS Genet* 10:e1004504
12. Barbour AG, Amano K, Hackstadt T, Perry L, Caldwell HD. 1982. *Chlamydia trachomatis* has penicillin-binding proteins but not detectable muramic acid. *J Bacteriol* 151:420-8
13. Barry WC, Teare EL, Uttley AH, Wilson SA, McManus TJ, et al. 1986. *Chlamydia trachomatis* as a cause of neonatal conjunctivitis. *Arch Dis Child* 61:797-9
14. Batteiger BE, Tu W, Ofner S, Van Der Pol B, Stothard DR, et al. 2010. Repeated *Chlamydia trachomatis* genital infections in adolescent women. *J Infect Dis* 201:42-51
15. Bauler LD, Hackstadt T. 2014. Expression and targeting of secreted proteins from *Chlamydia trachomatis*. *J Bacteriol* 196:1325-34
16. Bavoil PM. 2014. What's in a word: the use, misuse, and abuse of the word "persistence" in *Chlamydia* biology. *F Cell Infect Microbiol* 4:27
17. Beatty WL, Belanger TA, Desai AA, Morrison RP, Byrne GI. 1994. Tryptophan depletion as a mechanism of gamma interferon-mediated chlamydial persistence. *Infect Immun* 62:3705-11

18. Beatty WL, Byrne GI, Morrison RP. 1993. Morphologic and antigenic characterization of interferon gamma-mediated persistent *Chlamydia trachomatis* infection *in vitro. Proc Natl Acad Sci U S A* 90:3998-4002
19. Bedson SPaM, H.B. 1945. Penicillin in experimental psittacosis of mice. *Lancet* 2:394-7
20. Belland RJ, Nelson DE, Virok D, Crane DD, Hogan D, et al. 2003. Transcriptome analysis of chlamydial growth during IFN-gamma-mediated persistence and reactivation. *Proc Natl Acad Sci U S A* 100:15971-6
21. Belland RJ, Zhong G, Crane DD, Hogan D, Sturdevant D, et al. 2003. Genomic transcriptional profiling of the developmental cycle of Chlamydia trachomatis. *Proc Natl Acad Sci U S A* 100:8478-83
22. Bernhardt TG, de Boer PA. 2005. SlmA, a nucleoid-associated, FtsZ binding protein required for blocking septal ring assembly over Chromosomes in E. coli. *Mol Cell* 18:555-64
23. Bi E, Lutkenhaus J. 1992. Isolation and characterization of *ftsZ* alleles that affect septal morphology. *J Bacteriol* 174:5414
24. Black CM. Introduction.
25. Blair KM, Mears KS, Taylor JA, Fero J, Jones LA, et al. 2018. The *Helicobacter pylori* cell shape promoting protein Csd5 interacts with the cell wall, MurF, and the bacterial cytoskeleton. *Mol Microbiol* 110:114-27
26. Bonner CA, Byrne GI, Jensen RA. 2014. *Chlamydia* exploit the mammalian tryptophan-depletion defense strategy as a counter-defensive cue to trigger a survival state of persistence. *Front Cell Infect Microbiol* 4:17
27. Borel N, Dumrese C, Ziegler U, Schifferli A, Kaiser C, Pospischil A. 2010. Mixed infections with *Chlamydia* and porcine epidemic diarrhea virus - a new in vitro model of chlamydial persistence. *BMC microbiology* 10:201
28. Borel N, Leonard C, Slade J, Schoborg RV. 2016. Chlamydial Antibiotic Resistance and Treatment Failure in Veterinary and Human Medicine. *Current clinical microbiology reports* 3:10-8
29. Borel N, Pospischil A, Hudson AP, Rupp J, Schoborg RV. 2014. The role of viable but non-infectious developmental forms in chlamydial biology. *Front Cell Infect Microbiol* 4:97
30. Borel N, Summersgill JT, Mukhopadhyay S, Miller RD, Ramirez JA, Pospischil A. 2008. Evidence for persistent *Chlamydia pneumoniae* infection of human coronary atheromas. *Atherosclerosis* 199:154-61
31. Borges V, Ferreira R, Nunes A, Sousa-Uva M, Abreu M, et al. 2013. Effect of long-term laboratory propagation on *Chlamydia trachomatis* genome dynamics. *Infect Genet Evol* 17:23-32
32. Bragina EY, Gomberg MA, Dmitriev GA. 2001. Electron microscopic evidence of persistent chlamydial infection following treatment. *J Eur Acad Dermatol Venereol* 15:405-9
33. Braun PR, Al-Younes H, Gussmann J, Klein J, Schneider E, Meyer TF. 2008. Competitive inhibition of amino acid uptake suppresses chlamydial growth: involvement of the chlamydial amino acid transporter BrnQ. *J Bacteriol* 190:1822-30
34. Brinkworth AJ, Wildung MR, Carabeo RA. 2018. Genomewide Transcriptional Responses of Iron-Starved *Chlamydia trachomatis* Reveal Prioritization of Metabolic Precursor Synthesis over Protein Translation. *mSystems* 3: e00184-17

35. Brothwell JA, Brockett M, Banerjee A, Stein BD, Nelson DE, Liechti GW. 2021. Genome copy number regulates inclusion expansion, septation, and infectious developmental form conversion in *Chlamydia trachomatis*. *J Bacteriol* 203: e00630-20
36. Brown WJ, Rockey DD. 2000. Identification of an antigen localized to an apparent septum within dividing chlamydiae. *Infect Immun* 68:708-15
37. Brunham RC, Rey-Ladino J. 2005. Immunology of *Chlamydia* infection: implications for a *Chlamydia trachomatis* vaccine. *Nat Rev Immunol* 5:149-61
38. Buchholz KR, Stephens RS. 2006. Activation of the host cell proinflammatory interleukin-8 response by *Chlamydia trachomatis*. *Cell microbiol* 8:1768-79
39. Buchholz KR, Stephens RS. 2008. The cytosolic pattern recognition receptor NOD1 induces inflammatory interleukin-8 during *Chlamydia trachomatis* infection. *Infect Immun* 76:3150-5
40. Bulyha I, Lindow S, Lin L, Bolte K, Wuichet K, et al. 2013. Two small GTPases act in concert with the bactofilin cytoskeleton to regulate dynamic bacterial cell polarity. *Dev Cell* 25:119-31
41. Campbell S, Richmond SJ, Yates PS. 1989. The Effect of *Chlamydia trachomatis* Infection on the Host Cell Cytoskeleton and Membrane Compartments. *Microbiol* 135:2379-86
42. Carter M, Jennifer S, Farra N, Harris G. 2015. *Guide to research techniques in neuroscience*. Amsterdam, [Netherlands: Academic Press]
43. CDC. 2019. Sexually Transmitted Disease Surveillance 2018, U.S. Department of Health and Human Services
44. Cecil JA, Howell MR, Tawes JJ, Gaydos JC, McKee KT, Jr., et al. 2001. Features of Chlamydia trachomatis and Neisseria gonorrhoeae infection in male Army recruits. *J Infect Dis* 184:1216-9
45. Chen Y, Wang C, Mi J, Zhou Z, Wang J, et al. 2021. Characterization and comparison of differentially expressed genes involved in *Chlamydia psittaci* persistent infection *in vitro* and in vivo. *Vet Microbiol* 255:108960
46. Chen YS, Bastidas RJ, Saka HA, Carpenter VK, Richards KL, et al. 2014. The *Chlamydia trachomatis* type III secretion chaperone Slc1 engages multiple early effectors, including TepP, a tyrosine-phosphorylated protein required for the recruitment of CrkI-II to nascent inclusions and innate immune signaling. *PLoS Pathog* 10:e1003954
47. Cheong HC, Lee CYQ, Cheok YY, Tan GMY, Looi CY, Wong WF. 2019. Chlamydiaceae: Diseases in Primary Hosts and Zoonosis. *Microorganisms* 7:146
48. Chin E, Kirker K, Zuck M, James G, Hybiske K. 2012. Actin recruitment to the *Chlamydia* inclusion is spatiotemporally regulated by a mechanism that requires host and bacterial factors. *PloS One* 7:e46949
49. Cho H, Uehara T, Bernhardt TG. 2014. Beta-lactam antibiotics induce a lethal malfunctioning of the bacterial cell wall synthesis machinery. *Cell* 159:1300-11
50. Coles AM, Reynolds DJ, Harper A, Devitt A, Pearce JH. 1993. Low-nutrient induction of abnormal chlamydial development: a novel component of chlamydial pathogenesis? *FEMS Microbiol Letters* 106:193-200
51. Control CfD. 2014. Recommendations for the laboratory-based detection of *Chlamydia trachomatis* and *Neisseria gonorrhoeae*. *MMWR Recomm Rep* 63:1-19

52. Cotter TW, Ramsey KH, Miranpuri GS, Poulsen CE, Byrne GI. 1997. Dissemination of *Chlamydia trachomatis* chronic genital tract infection in gamma interferon gene knockout mice. *Infect Immun* 65:2145-52
53. Courtright P, West SK. 2004. Contribution of sex-linked biology and gender roles to disparities with trachoma. *Emerg Infect Dis* 10:2012-6
54. Cox JV, Abdelrahman YM, Ouellette SP. 2020. Penicillin-binding proteins regulate multiple steps in the polarized cell division process of *Chlamydia*. *Sci Rep* 10:12588
55. Dautin N, Karimova G, Ullmann A, Ladant D. 2000. Sensitive genetic screen for protease activity based on a cyclic AMP signaling cascade in *Escherichia coli*. *J Bacteriol* 182:7060-6
56. De Benedetti S, Buhl H, Gaballah A, Klockner A, Otten C, et al. 2014. Characterization of serine hydroxymethyltransferase GlyA as a potential source of D-alanine in *Chlamydia pneumoniae*. *Front Cell Infect Microbiol* 4:19
57. De Clercq E, Kalmar I, Vanrompay D. 2013. Animal models for studying female genital tract infection with *Chlamydia trachomatis*. *Infect Immun* 81:3060-7
58. Deka S, Vanover J, Dessus-Babus S, Whittimore J, Howett MK, et al. 2006. *Chlamydia trachomatis* enters a viable but non-cultivable (persistent) state within herpes simplex virus type 2 (HSV-2) co-infected host cells. *Cell Microbiol* 8:149-62
59. Deng X, Gonzalez Llamazares A, Wagstaff JM, Hale VL, Cannone G, et al. 2019. The structure of bactofilin filaments reveals their mode of membrane binding and lack of polarity. *Nat Microbiol* 4:2357-68
60. Diseases WHO. 2021. WHO Alliance for the Global Elimination of Trachoma by 2020: progress report on elimination of trachoma, 2020
61. Divakaruni AV, Baida C, White CL, Gober JW. 2007. The cell shape proteins MreB and MreC control cell morphogenesis by positioning cell wall synthetic complexes. *Mol Microbiol* 66:174-88
62. E. MK, Katerina W, A. FK. 2017. Chlamydia trachomatis Transformation and Allelic Exchange Mutagenesis. *Curr Protoc in Microbiol* 45:11A.3.1-A.3.5
63. Early RL, Morgan HR. 1946. Studies on the chemotherapy of viruses in the psittacosis-lymphogranuloma venereum group; effect of certain chemotherapeutic agents on psittacosis virus (6BC strain) infections in mice. *J Immunol* 53:251-7
64. Egan AJ, Biboy J, van't Veer I, Breukink E, Vollmer W. 2015. Activities and regulation of peptidoglycan synthases. *Philos Trans R Soc Lond B Biol Sci* 370
65. Egan AJ, Vollmer W. 2013. The physiology of bacterial cell division. *Ann N Y Acad Sci* 1277:8-28
66. Egan AJF, Errington J, Vollmer W. 2020. Regulation of peptidoglycan synthesis and remodelling. *Nat Rev Microbiol* 18:446-60
67. El Andari J, Altegoer F, Bange G, Graumann PL. 2015. *Bacillus subtilis* bactofilins are essential for flagellar hook- and filament assembly and dynamically localize into structures of less than 100 nm diameter underneath the cell membrane. *PLoS One* 10:e0141546
68. Elwell C, Mirrashidi K, Engel J. 2016. *Chlamydia* cell biology and pathogenesis. *Nat Rev Microbiol* 14:385-400
69. Eswara PJ, Ramamurthi KS. 2017. Bacterial cell division: nonmodels poised to take the spotlight. *Annu Rev Microbiol* 71:393-411

70. Faris R, Merling M, Andersen SE, Dooley CA, Hackstadt T, Weber MM. 2019. *Chlamydia trachomatis* CT229 subverts Rab GTPase-Dependent CCV trafficking pathways to promote chlamydial infection. *Cell Rep* 26:3380-90 e5
71. Fisher RA, Gollan B, Helaine S. 2017. Persistent bacterial infections and persister cells. *Nat Rev Microbiol* 15:453-64
72. Fox A, Rogers JC, Gilbart J, Morgan S, Davis CH, et al. 1990. Muramic acid is not detectable in *Chlamydia psittaci* or *Chlamydia trachomatis* by gas chromatography-mass spectrometry. *Infect Immun* 58:835-7
73. Frandi A, Jacquier N, Theraulaz L, Greub G, Viollier PH. 2014. FtsZ-independent septal recruitment and function of cell wall remodelling enzymes in chlamydial pathogens. *Nat Commun* 5:4200
74. Freidank HM, Billing H, Wiedmann-Al-Ahmad M. 2001. Influence of iron restriction on *Chlamydia pneumoniae* and *C. trachomatis*. *J Med Microbiol* 50:223-7
75. Gaballah A, Kloeckner A, Otten C, Sahl HG, Henrichfreise B. 2011. Functional analysis of the cytoskeleton protein MreB from *Chlamydophila pneumoniae*. *PloS One* 6:e25129
76. Galasso GJ, Manire GP. 1961. Effect of antiserum and antibiotics on persistent infection of HeLa cells with meningopneumonitis virus. *J Immunol* 86:382
77. Garrett AJ, Harrison MJ, Manire GP. 1974. A search for the bacterial mucopeptide component, muramic acid, in *Chlamydia*. *J Gen Microbiol* 80:315-8
78. Gaylord WH, Jr. 1954. Intracellular forms of meningopneumonitis virus. *J Exp Med* 100:575-80
79. Gerard HC, Krausse-Opatz B, Wang Z, Rudy D, Rao JP, et al. 2001. Expression of *Chlamydia trachomatis* genes encoding products required for DNA synthesis and cell division during active versus persistent infection. *Mol Microbiol* 41:731-41
80. Gitai Z. 2005. The new bacterial cell biology: moving parts and subcellular architecture. *Cell* 120:577-86
81. Gogolak FM, Weiss E. 1950. The effect of antibiotics on agents of the psittacosis-lymphogranuloma group. *J Infect Dis* 87:264-74
82. Golden MR, Whittington WL, Handsfield HH, Hughes JP, Stamm WE, et al. 2005. Effect of expedited treatment of sex partners on recurrent or persistent gonorrhea or chlamydial infection. *N Engl J Med* 352:676-85
83. Gracey E, Lin A, Akram A, Chiu B, Inman RD. 2013. Intracellular survival and persistence of *Chlamydia muridarum* is determined by macrophage polarization. *PloS One* 8:e69421
84. Greub G, Raoult D. 2003. History of the ADP/ATP-translocase-encoding gene, a parasitism gene transferred from a Chlamydiales ancestor to plants 1 billion years ago. *Appl Environ Microbiol* 69:5530-5
85. Grieshaber SS, Grieshaber NA, Hackstadt T. 2003. *Chlamydia trachomatis* uses host cell dynein to traffic to the microtubule-organizing center in a p50 dynamitin-independent process. *J Cell Sci* 116:3793-802
86. Hackstadt T, Scidmore-Carlson MA, Shaw EI, Fischer ER. 1999. The *Chlamydia trachomatis* IncA protein is required for homotypic vesicle fusion. *Cell Microbiol* 1:119-30
87. Hackstadt T, Todd WJ, Caldwell HD. 1985. Disulfide-mediated interactions of the chlamydial major outer membrane protein: role in the differentiation of chlamydiae? *J Bacteriol* 161:25-31

88. Haeusser DP, Margolin W. 2016. Splitsville: structural and functional insights into the dynamic bacterial Z ring. *Nat Rev Microbiol* 14:305-19
89. Hammerschlag MR, Kohlhoff SA, Gaydos CA. 2015. *Chlamydia pneumoniae*. *Mandell, Douglas, and Bennett's Principles and Practice of Infectious Diseases*:2174-82.e2
90. Handsfield HH. 2018. Lymphogranuloma venereum treatment and terminology. *Sex Trans Dis* 45: 409-411
91. Handsfield HH, White JA. 2020. *Chlamydia trachomatis* biovar genotyping and treatment of lymphogranuloma venereum. *Sex Trans Dis* 47: 253
92. Harper A, Pogson CI, Jones ML, Pearce JH. 2000. Chlamydial development is adversely affected by minor changes in amino acid supply, blood plasma amino acid levels, and glucose deprivation. *Infect Immun* 68:1457-64
93. Hatch TP. 1996. Disulfide cross-linked envelope proteins: the functional equivalent of peptidoglycan in chlamydiae? *J Bacteriol* 178:1-5
94. Hay NA, Tipper DJ, Gygi D, Hughes C. 1999. A novel membrane protein influencing cell shape and multicellular swarming of *Proteus mirabilis*. *J Bacteriol* 181:2008-16
95. He Q-z, Zeng H-c, Huang Y, Hu Y-q, Wu Y-m. 2015. The Type III Secretion System (T3SS) of *Chlamydophila psittaci* is involved in the host inflammatory response by activating the JNK/ERK signaling pathway. *BioMed Res Int* 2015:652416
96. Heilman FRaH, W. E. 1944. Penicillin in the treatment of experimental psittacosis. *Proe. Staff Meetings Mayo Clinic* 19:204-7
97. Hesse L, Bostock J, Dementin S, Blanot D, Mengin-Lecreulx D, Chopra I. 2003. Functional and biochemical analysis of *Chlamydia trachomatis* MurC, an enzyme displaying UDP-N-acetylmuramate:amino acid ligase activity. *J Bacteriol* 185:6507-12
98. Higashi N. 1965. Electron Microscopic studies on the mode of reproduction of trachoma virus and psittacosis virus in cell cultures. *Exp Mol Pathol* 4:24-39
99. Hill AV, Perez-Patron M, Tekwe CD, Menon R, Hairrell D, Taylor BD. 2020. *Chlamydia trachomatis* is associated with medically indicated preterm birth and preeclampsia in young pregnant women. *Sex Trans Dis* 47: 246-252
100. Horn M, Collingro A, Schmitz-Esser S, Beier CL, Purkhold U, et al. 2004. Illuminating the evolutionary history of chlamydiae. *Science* 304:728-30
101. Horner PJ. 2012. Azithromycin antimicrobial resistance and genital Chlamydia trachomatis infection: duration of therapy may be the key to improving efficacy. *Sex Transm Infect* 88:154-6
102. Hsu YP, Booher G, Egan A, Vollmer W, VanNieuwenhze MS. 2019. d-amino acid derivatives as in situ probes for visualizing bacterial peptidoglycan biosynthesis. *Acc Chem Res* 52:2713-2722
103. Hurst EW, Landquist JK, Melvin P, Peters JM, Senior N, et al. 1953. The therapy of experimental psittacosis and lymphogranuloma venereum (inguinale) II. The activity of quinoxaline-1:4-dioxide and substituted and related compounds, with a note on the morphological changes induced in lymphogranuloma virus by these compounds and by antibiotics. *Br J Pharmacol Chemother* 8:297-305
104. Hybiske K, Stephens RS. 2007. Mechanisms of host cell exit by the intracellular bacterium *Chlamydia*. P*roc Natl Acad Sci U S A* 104:11430-5
105. Hyman CL, Roblin PM, Gaydos CA, Quinn TC, Schachter J, Hammerschlag MR. 1995. Prevalence of asymptomatic nasopharyngeal carriage of *Chlamydia pneumoniae* in

subjectively healthy adults: assessment by polymerase chain reaction-enzyme immunoassay and culture. *Clin Infect Dis* 20:1174-8
106. Ibana JA, Belland RJ, Zea AH, Schust DJ, Nagamatsu T, et al. 2011. Inhibition of indoleamine 2,3-dioxygenase activity by levo-1-methyl tryptophan blocks gamma interferon-induced *Chlamydia trachomatis* persistence in human epithelial cells. *Infect Immun* 79:4425-37
107. Iwai N, Nagai K, Wachi M. 2002. Novel S-benzylisothiourea compound that induces spherical cells in *Escherichia coli* probably by acting on a rod-shape-determining protein(s) other than penicillin-binding protein 2. *Biosci Biotechnol Biochem* 66:2658-62
108. Jackson KM, Schwartz C, Wachter J, Rosa PA, Stewart PE. 2018. A widely conserved bacterial cytoskeletal component influences unique helical shape and motility of the spirochete *Leptospira biflexa*. *Mol Microbiol* 108:77-89
109. Jacquier N, Frandi A, Pillonel T, Viollier P, Greub G. 2014. Cell wall precursors are required to organize the chlamydial division septum. *Nat Commun* 5:3578
110. Jacquier N, Frandi A, Viollier PH, Greub G. 2015. Disassembly of a medial transenvelope structure by antibiotics during intracellular division. *Chem Biol* 22:1217-27
111. Jacquier N, Viollier PH, Greub G. 2015. The role of peptidoglycan in chlamydial cell division: towards resolving the chlamydial anomaly. *FEMS Microbiol Rev* 39:262-75
112. Jacquier N, Yadav AK, Pillonel T, Viollier PH, Cava F, Greub G. 2019. A SpoIID homolog cleaves glycan strands at the chlamydial division septum. *mBio* 10: e01128-19
113. Jenkin HM. 1960. Preparation and properties of cell walls of the agent of meningopneumonitis. *J Bacteriol* 80:639-47
114. Johansson M, Schon K, Ward M, Lycke N. 1997. Genital tract infection with *Chlamydia trachomatis* fails to induce protective immunity in gamma interferon receptor-deficient mice despite a strong local immunoglobulin A response. *Infect Immun* 65:1032-44
115. Joyee AG, Yang X. 2008. Role of toll-like receptors in immune responses to chlamydial infections. *Curr Pharm Des* 14:593-600
116. Kahane S, Friedman MG. 1992. Reversibility of heat shock in *Chlamydia trachomatis*. *FEMS Microbiol Letters* 76:25-30
117. Karimova G, Ullmann A, Ladant D. 2001. Protein-protein interaction between *Bacillus stearothermophilus* tyrosyl-tRNA synthetase subdomains revealed by a bacterial two-hybrid system. *J Mol Microbiol Biotechnol* 3:73-82
118. Kassem Maher M, Wang Y, Boomsma W, Lindorff-Larsen K. 2016. Structure of the bacterial cytoskeleton protein bactofilin by NMR chemical shifts and sequence variation. *Biophys J* 110:2342-8
119. Keb G, Fields KA. 2020. Markerless gene deletion by floxed cassette allelic exchange mutagenesis in *Chlamydia trachomatis*. *JoVE*
120. Keb G, Hayman R, Fields KA. 2018. Floxed-cassette allelic exchange mutagenesis enables markerless gene deletion in chlamydia trachomatis and can reverse cassette-induced polar effects. *J Bacteriol* 200:e00479-18
121. Kemege KE, Hickey JM, Barta ML, Wickstrum J, Balwalli N, et al. 2015. *Chlamydia trachomatis* protein CT009 is a structural and functional homolog to the key morphogenesis component RodZ and interacts with division septal plane localized MreB. *Mol Microbiol* 95:365-82

122. Keseler IM, Mackie A, Santos-Zavaleta A, Billington R, Bonavides-Martinez C, et al. 2017. The EcoCyc database: reflecting new knowledge about *Escherichia coli* K-12. *Nucleic Acids Res* 45:D543-D50
123. Khosropour CM, Dombrowski JC, Barbee LA, Manhart LE, Golden MR. 2014. Comparing azithromycin and doxycycline for the treatment of rectal chlamydial infection: a retrospective cohort study. *Sex Trans Dis* 41: 79-85
124. Klockner A, Otten C, Derouaux A, Vollmer W, Buhl H, et al. 2014. AmiA is a penicillin target enzyme with dual activity in the intracellular pathogen *Chlamydia pneumoniae*. *Nat Commun* 5:4201
125. Kocaoglu O, Carlson EE. 2015. Profiling of β-Lactam selectivity for penicillin-binding proteins in *Escherichia coli* Strain DC2. *Antimicrob Agents Chemother* 59:2785
126. Koch MK, McHugh CA, Hoiczyk E. 2011. BacM, an N-terminally processed bactofilin of *Myxococcus xanthus*, is crucial for proper cell shape. *Mol Microbiol* 80:1031-51
127. Koehler L, Nettelnbreker E, Hudson AP, Ott N, Gerard HC, et al. 1997. Ultrastructural and molecular analyses of the persistence of *Chlamydia trachomati*s (serovar K) in human monocytes. *Microb Pathog* 22:133-42
128. Kokes M, Dunn JD, Granek JA, Nguyen BD, Barker JR, et al. 2015. Integrating chemical mutagenesis and whole-genome sequencing as a platform for forward and reverse genetic analysis of *Chlamydia*. *Cell Host Microbe* 17:716-25
129. Kong FY, Tabrizi SN, Law M, Vodstrcil LA, Chen M, et al. 2014. Azithromycin versus doxycycline for the treatment of genital chlamydia infection: a meta-analysis of randomized controlled trials. *Clin Infect Dis* 59:193-205
130. Kraaij MD, Vereyken EJ, Leenen PJ, van den Bosch TP, Rezaee F, et al. 2014. Human monocytes produce interferon-gamma upon stimulation with LPS. *Cytokine* 67:7-12
131. Kuhn J, Briegel A, Morschel E, Kahnt J, Leser K, et al. 2010. Bactofilins, a ubiquitous class of cytoskeletal proteins mediating polar localization of a cell wall synthase in *Caulobacter crescentus*. *EMBO J* 29:327-39
132. Kumar Y, Valdivia RH. 2008. Actin and intermediate filaments stabilize the *Chlamydia trachomatis* vacuole by forming dynamic structural scaffolds. *Cell Host Microbe* 4:159-69
133. Kuo CC, Jackson LA, Campbell LA, Grayston JT. 1995. *Chlamydia pneumoniae* (TWAR). *Clin Microbiol Rev* 8:451-61
134. Kuru E, Radkov A, Meng X, Egan A, Alvarez L, et al. 2019. Mechanisms of incorporation for D-Amino acid probes that target peptidoglycan biosynthesis. *ACS chem Biol* 12:2745-2756
135. Lambden PR, Pickett MA, Clarke IN. 2006. The effect of penicillin on *Chlamydia trachomatis* DNA replication. *Microbiol*152:2573-8
136. Lau CY, Qureshi AK. 2002. Azithromycin versus doxycycline for genital chlamydial infections: a meta-analysis of randomized clinical trials. *Sex Transm Dis* 29:497-502
137. Lee J, Cox JV, Ouellette SP. 2020. Critical Role for the Extended N Terminus of Chlamydial MreB in Directing Its Membrane Association and Potential Interaction with Divisome Proteins. *J Bacteriol* 202
138. Lee JK, Enciso GA, Boassa D, Chander CN, Lou TH, et al. 2018. Replication-dependent size reduction precedes differentiation in Chlamydia trachomatis. *Nat Commun* 9:45

139. Lesiak-Markowicz I, Schötta A-M, Stockinger H, Stanek G, Markowicz M. 2019. Chlamydia trachomatis serovars in urogenital and ocular samples collected 2014–2017 from Austrian patients. *Scientific Reports* 9:18327
140. Lewis ME, Belland RJ, AbdelRahman YM, Beatty WL, Aiyar AA, et al. 2014. Morphologic and molecular evaluation of Chlamydia trachomatis growth in human endocervix reveals distinct growth patterns. *Front Cell Infect Microbiol* 4:71
141. Liechti G, Kuru E, Packiam M, Hsu YP, Tekkam S, et al. 2016. Pathogenic Chlamydia Lack a Classical Sacculus but Synthesize a Narrow, Mid-cell Peptidoglycan Ring, Regulated by MreB, for Cell Division. *PLoS pathogens* 12:e1005590
142. Liechti G, Singh R, Rossi PL, Gray MD, Adams NE, Maurelli AT. 2018. Chlamydia trachomatis dapF Encodes a Bifunctional Enzyme Capable of Both d-Glutamate Racemase and Diaminopimelate Epimerase Activities. *MBio* 9
143. Liechti GW, Kuru E, Hall E, Kalinda A, Brun YV, et al. 2014. A new metabolic cell-wall labelling method reveals peptidoglycan in Chlamydia trachomatis. *Nature* 506:507-10
144. Lin L, Osorio Valeriano M, Harms A, Søgaard-Andersen L, Thanbichler M. 2017. Bactofilin-mediated organization of the ParABS chromosome segregation system in Myxococcus xanthus. *Nature Communications* 8:1817
145. Lutkenhaus JF, Wolf-Watz H, Donachie WD. 1980. Organization of genes in the ftsA-envA region of the Escherichia coli genetic map and identification of a new fts locus (ftsZ). *Journal of bacteriology* 142:615-20
146. Löwe J, Amos LA. 1998. Crystal structure of the bacterial cell-division protein FtsZ. *Nature* 391:203-6
147. Madeira F, Park YM, Lee J, Buso N, Gur T, et al. 2019. The EMBL-EBI search and sequence analysis tools APIs in 2019. *Nucleic Acids Res*
148. Mallika P, Asok T, Faisal H, Aziz S, Tan A, Intan G. 2008. Neonatal conjunctivitis - a review. In *Malaysian family physician : the official journal of the Academy of Family Physicians of Malaysia*, pp. 77-81
149. Manire GP, Tamura A. 1967. Preparation and chemical composition of the cell walls of mature infectious dense forms of meningopneumonitis organisms. *J Bacteriol* 94:1178-83
150. Marchler-Bauer A, Bo Y, Han L, He J, Lanczycki CJ, et al. 2017. CDD/SPARCLE: functional classification of proteins via subfamily domain architectures. *Nucleic Acids Res* 45:D200-d3
151. Martin DH, Koutsky L, Eschenbach DA, Daling JR, Alexander ER, et al. 1982. Prematurity and Perinatal Mortality in Pregnancies Complicated by Maternal Chlamydia trachomatis Infections. *JAMA* 247:1585-8
152. Matsumoto A. 1981. Electron microscopic observations of surface projections and related intracellular structures of Chlamydia organisms. *J Electron Microsc (Tokyo)* 30:315-20
153. Matsumoto A. 1981. Isolation and electron microscopic observations of intracytoplasmic inclusions containing Chlamydia psittaci. *J Bacteriol* 145:605-12
154. Matsumoto A, Manire GP. 1970. Electron microscopic observations on the effects of penicillin on the morphology of Chlamydia psittaci. *J Bacteriol* 101:278-85
155. McCoy AJ, Adams NE, Hudson AO, Gilvarg C, Leustek T, Maurelli AT. 2006. L,L-diaminopimelate aminotransferase, a trans-kingdom enzyme shared by Chlamydia and plants for synthesis of diaminopimelate/lysine. *Proceedings of the National Academy of Sciences of the United States of America* 103:17909-14

156. McCoy AJ, Maurelli AT. 2005. Characterization of Chlamydia MurC-Ddl, a fusion protein exhibiting D-alanyl-D-alanine ligase activity involved in peptidoglycan synthesis and D-cycloserine sensitivity. *Molecular microbiology* 57:41-52
157. McCoy AJ, Maurelli AT. 2006. Building the invisible wall: updating the chlamydial peptidoglycan anomaly. *Trends in Microbiology* 14:70-7
158. McCoy AJ, Sandlin RC, Maurelli AT. 2003. In vitro and in vivo functional activity of Chlamydia MurA, a UDP-N-acetylglucosamine enolpyruvyl transferase involved in peptidoglycan synthesis and fosfomycin resistance. *Journal of bacteriology* 185:1218-28
159. Meiklejohn G, Wagner JC, Beveridge GW. 1946. Studies on the chemotherapy of viruses in the psittacosis-lymphogranuloma group; effect of penicillin and sulfadiazine on ten strains in chick embryos. *J Immunol* 54:1-8
160. Meyer KF, Eddie B. 1947. The knowledge of human virus infections of animal origin.*JAMA* 133:822-8
161. Miller K, Pakpour N, Yi E, Melese M, Alemayehu W, et al. 2004. Pesky trachoma suspect finally caught. *Br J Ophthalmol* 88:750-1
162. Miller WC, Ford CA, Morris M, Handcock MS, Schmitz JL, et al. 2004. Prevalence of chlamydial and gonococcal infections among young adults in the United States. *JAMA* 291:2229-36
163. Mirrashidi KM, Elwell CA, Verschueren E, Johnson JR, Frando A, et al. 2015. Global mapping of the inc-human interactome reveals that retromer restricts chlamydia infection. *Cell Host Microbe* 18:109-21
164. Moore DL, MacDonald NE, Canadian Paediatric Society ID, Immunization C. 2015. Preventing ophthalmia neonatorum. *Paediatrics child health* 20:93-6
165. Morrison RP. 2000. Differential sensitivities of *Chlamydia trachomatis* strains to inhibitory effects of gamma interferon. *Infect Immun* 68:6038-40
166. Moulder JW. 1993. Why is *Chlamydia* sensitive to penicillin in the absence of peptidoglycan? *Infect Agen Dis* 2:87-99
167. Moulder JW, Novosel DL, Officer JE. 1963. Inhibition of the growth of agents of the psittacosis group by D-Cycloserine and its specific reversal by D-Alanine. *J Bacteriol* 85:707-11
168. Mueller KE, Wolf K, Fields KA. 2016. Gene Deletion by fluorescence-reported allelic exchange mutagenesis in *Chlamydia trachomatis. mBio* 7:e01817-15
169. Muramatsu MK, Brothwell JA, Stein BD, Putman TE, Rockey DD, Nelson DE. 2016. Beyond tryptophan synthase: identification of genes that contribute to *Chlamydia trachomatis* survival during gamma interferon-induced persistence and reactivation. *Infect Immun* 84:2791-801
170. Muschiol S, Bailey L, Gylfe A, Sundin C, Hultenby K, et al. 2006. A small-molecule inhibitor of type III secretion inhibits different stages of the infectious cycle of *Chlamydia trachomatis*. *Proc Nat Acad Sci USA* 103:14566-71
171. Myers GS, Mathews SA, Eppinger M, Mitchell C, O'Brien KK, et al. 2009. Evidence that human *Chlamydia pneumoniae* was zoonotically acquired. *J Bacteriol* 191:7225-33
172. Nettelnbreker E, Zeidler H, Bartels H, Dreses-Werringloer U, Daubener W, et al. 1998. Studies of persistent infection by *Chlamydia trachomatis* serovar K in TPA-differentiated U937 cells and the role of IFN-gamma. *J Med Microbiol* 47:141-9
173. Newhall WJ, Jones RB. 1983. Disulfide-linked oligomers of the major outer membrane protein of chlamydiae. *J Bacteriol* 154:998-1001

174. Newman L, Rowley J, Vander Hoorn S, Wijesooriya NS, Unemo M, et al. 2015. Global estimates of the prevalence and incidence of four curable sexually transmitted infections in 2012 based on systematic review and global reporting. *PLoS One* 10:e0143304
175. Nsuami M, Cammarata CL, Brooks BN, Taylor SN, Martin DH. 2004. Chlamydia and Gonorrhea co-occurrence in a high school population. *Sex Trans Dis* 31: 424-7
176. O'Meara CP, Andrew DW, Beagley KW. 2014. The mouse model of *Chlamydia* genital tract infection: a review of infection, disease, immunity and vaccine development. *Curr Mol Med* 14:396-421
177. Olson-Chen C, Balaram K, Hackney DN. 2018. *Chlamydia trachomatis a*nd adverse pregnancy outcomes: meta-analysis of patients with and without infection. *Maternal Child Health J* 22:812-21
178. Opitz B, Forster S, Hocke AC, Maass M, Schmeck B, et al. 2005. Nod1-mediated endothelial cell activation by *Chlamydophila pneumoniae*. *Circ Res* 96:319-26
179. Otten C, De Benedetti S, Gaballah A, Bühl H, Klöckner A, et al. 2015. Co-Solvents as Stabilizing agents during heterologous overexpression in *Escherichia coli* – Application to chlamydial penicillin-binding protein 6. *PLoS One* 10:e0122110
180. Ouellette Scot P, Blay Emmanuel A, Hatch Nathan D, Fisher-Marvin Laura A, Roy Craig R. 2021. CRISPR interference to inducibly repress gene expression in *Chlamydia trachomatis*. *Infect Immun* 89:e00108-21
181. Ouellette SP. 2018. Feasibility of a conditional knockout system for *Chlamydia* based on CRISPR interference. *Front Cell Infect Microbiol* 8:59
182. Ouellette SP, Abdelrahman YM, Belland RJ, Byrne GI. 2005. The *Chlamydia pneumoniae t*ype III secretion-related lcrH gene clusters are developmentally expressed operons. *J Bacteriol* 187:7853-6
183. Ouellette SP, Hatch TP, AbdelRahman YM, Rose LA, Belland RJ, Byrne GI. 2006. Global transcriptional upregulation in the absence of increased translation in *Chlamydia* during IFN gamma-mediated host cell tryptophan starvation. *Mol Microbiol* 62:1387-401
184. Ouellette SP, Karimova G, Subtil A, Ladant D. 2012. *Chlamydia* co-opts the rod shape-determining proteins MreB and Pbp2 for cell division. *Mol Microbiol* 85:164-78
185. Ouellette SP, Rueden KJ, AbdelRahman YM, Cox JV, Belland RJ. 2015. identification and partial characterization of potential FtsL and FtsQ homologs of *Chlamydia*. *Front Microbiol* 6:1264
186. Ouellette SP, Rueden KJ, Gauliard E, Persons L, de Boer PA, Ladant D. 2014. Analysis of MreB interactors in *Chlamydia* reveals a RodZ homolog but fails to detect an interaction with MraY. *Front Microbiol* 5:279
187. Ouellette SP, Rueden KJ, Rucks EA. 2016. Tryptophan codon-dependent transcription in *Chlamydia pneumoniae* during gamma interferon-mediated tryptophan limitation. *Infect Immun* 84:2703-13
188. Packiam M, Weinrick B, Jacobs WR, Jr., Maurelli AT. 2015. Structural characterization of muropeptides from *Chlamydia trachomatis* peptidoglycan by mass spectrometry resolves "chlamydial anomaly". *Proc Natl Acad Sci U S A* 112:11660-5
189. Panzetta ME, Valdivia RH, Saka HA. 2018. *Chlamydia* Persistence: A survival strategy to evade antimicrobial effects *in-vitro* and *in-vivo*. *Front Microbiol* 9:3101
190. Park JT, Strominger JL. 1957. Mode of action of penicillin. *Science* 125:99-101
191. Patin D, Bostock J, Blanot D, Mengin-Lecreulx D, Chopra I. 2009. Functional and biochemical analysis of the *Chlamydia trachomatis* ligase MurE. *J Bacteriol* 191:7430-5

192. Patin D, Bostock J, Chopra I, Mengin-Lecreulx D, Blanot D. 2012. Biochemical characterisation of the chlamydial MurF ligase, and possible sequence of the chlamydial peptidoglycan pentapeptide stem. *Arch Microbiol* 194:505-12
193. Patton DL, Askienazy-Elbhar M, Henry-Suchet J, Campbell LA, Cappuccio A, et al. 1994. Detection of *Chlamydia trachomatis* in fallopian tube tissue in women with postinfectious tubal infertility. *Amer J Obstetrics Gynecol* 171:95-101
194. Pearce J, Gaston H, Deane K, Devitt A, Harper A, Jecock R. 1994. 'Persistent' forms and persistence of *Chlamydia*. *Trends in Microbiol* 2:257-9
195. Perkins HR, Allison AC. 1963. Cell-wall constituents of rickettsiae and psittacosis-lymphogranuloma organisms. *J Gen Microbiol* 30:469-80
196. Perry LL, Feilzer K, Caldwell HD. 1997. Immunity to *Chlamydia trachomatis* is mediated by T helper 1 cells through IFN-gamma-dependent and -independent pathways. *J Immunol* 158:3344-52
197. Pettersen EF, Goddard TD, Huang CC, Couch GS, Greenblatt DM, et al. 2004. UCSF Chimera--a visualization system for exploratory research and analysis. *J Comput Chem* 25:1605-12
198. Phillips Campbell R, Kintner J, Whittimore J, Schoborg RV. 2012. *Chlamydia muridarum e*nters a viable but non-infectious state in amoxicillin-treated BALB/c mice. *Microbes Infect* 14:1177-85
199. Phillips-Campbell R, Kintner J, Schoborg RV. 2014. Induction of the *Chlamydia muridarum* stress/persistence response increases azithromycin treatment failure in a murine model of infection. *Antimicro Agen Chemother* 58:1782-4
200. Pilhofer M, Aistleitner K, Biboy J, Gray J, Kuru E, et al. 2013. Discovery of chlamydial peptidoglycan reveals bacteria with murein sacculi but without FtsZ. *Nat Comm* 4:2856
201. Pitt RA, Alexander S, Horner PJ, Ison CA. 2013. Presentation of clinically suspected persistent chlamydial infection: a case series. *Int J STD & AIDS* 24:469-75
202. Pokorzynski ND, Brinkworth AJ, Carabeo R. 2019. A bipartite iron-dependent transcriptional regulation of the tryptophan salvage pathway in *Chlamydia trachomatis. Elife* 8:e42295
203. Pokorzynski ND, Thompson CC, Carabeo RA. 2017. Ironing Out the unconventional mechanisms of iron acquisition and gene regulation in *Chlamydia*. *Front Cell Infect Microbiol* 7:394
204. Pospischil A. 2009. From disease to etiology: historical aspects of *Chlamydia*-related diseases in animals and humans. *Drugs Today* 45:141-6
205. Pospischil A, Borel N, Chowdhury EH, Guscetti F. 2009. Aberrant chlamydial developmental forms in the gastrointestinal tract of pigs spontaneously and experimentally infected with *Chlamydia suis*. *Vet Microbiol* 135:147-56
206. Pospischil A, Thoma R, Hilbe M, Grest P, Gebbers JO. 2002. Abortion in woman caused by caprine *Chlamydophila abortus (Chlamydia psittaci* serovar 1). *Swiss Med Wkly* 132:64-6
207. Prevention CfDCa. 2017. Sexually Transmitted Disease Surveillance 2016 U.S. Department of Health and Human Services
208. Páez-Canro C, Alzate JP, González LM, Rubio-Romero JA, Lethaby A, Gaitán HG. 2019. Antibiotics for treating urogenital *Chlamydia trachomatis* infection in men and non-pregnant women. *Cochrane Database Syst Rev* 1:Cd010871

209. Ran FA, Cong L, Yan WX, Scott DA, Gootenberg JS, et al. 2015. *In vivo* genome editing using *Staphylococcus aureus* Cas9. *Nature* 520:186-91
210. Ranjit DK, Liechti GW, Maurelli AT. 2020. Chlamydial MreB directs cell division and peptidoglycan synthesis in *Escherichia coli* in the absence of ftsz activity. *mBio* 11
211. Rank RG, Whittimore J, Bowlin AK, Wyrick PB. 2011. *In vivo* ultrastructural analysis of the intimate relationship between polymorphonuclear leukocytes and the chlamydial developmental cycle. *Infect Immun* 79:3291-301
212. Raulston JE. 1997. Response of *Chlamydia trachomatis* serovar E to iron restriction in vitro and evidence for iron-regulated chlamydial proteins. *Infect Immun* 65:4539-47
213. Robert X, Gouet P. 2014. Deciphering key features in protein structures with the new ENDscript server. *Nucleic Acids Res* 42:W320-4
214. Rosenvinge M, Lau R. 2009. Screening for asymptomatic chlamydia in women–how often would gonorrhoea be missed? *Int J STD & AIDS* 20:571-2
215. Rottenberg ME, Gigliotti Rothfuchs AC, Gigliotti D, Svanholm C, Bandholtz L, Wigzell H. 1999. Role of innate and adaptive immunity in the outcome of primary infection with *Chlamydia pneumoniae*, as analyzed in genetically modified mice. *J Immunol* 162:2829-36
216. Rotz LD, Khan AS, Lillibridge SR, Ostroff SM, Hughes JM. 2002. Public health assessment of potential biological terrorism agents. *Emerg Infect Dis* 8:225-30
217. Rucks EA, Olson MG, Jorgenson LM, Srinivasan RR, Ouellette SP. 2017. Development of a proximity labeling system to map the *Chlamydia trachomatis* Inclusion membrane. *Front Cell Infect Microbiol* 7:40
218. Rzomp KA, Moorhead AR, Scidmore MA. 2006. The GTPase Rab4 interacts with *Chlamydia trachomatis* inclusion membrane protein CT229. *Infect Immun* 74:5362-73
219. Sandoz KM, Rockey DD. 2010. Antibiotic resistance in Chlamydiae. *Future microbiol* 5:1427-42
220. Satterwhite CL, Torrone E, Meites E, Dunne EF, Mahajan R, et al. 2013. Sexually transmitted infections among US women and men: prevalence and incidence estimates, 2008. *Sex transm dis* 40:187-93
221. Scherler A, Jacquier N, Kebbi-Beghdadi C, Greub G. 2020. Diverse Stress-inducing treatments cause distinct aberrant body morphologies in the *Chlamydia*-related bacterium, *Waddlia chondrophila*. *Microorganisms* 8:1
222. Schoborg RV. 2011. *Chlamydia* persistence -- a tool to dissect chlamydia--host interactions. *Microbes Infect* 13:649-62
223. Schwebke JR, Rompalo A, Taylor S, Seña AC, Martin DH, et al. 2011. Re-Evaluating the Treatment of nongonococcal urethritis: emphasizing emerging pathogens–a randomized clinical trial. *Clin Infect Dis* 52:163-70
224. Scidmore MA. 2006. Cultivation and laboratory maintenance of *Chlamydia trachomatis*. *Curr Prot Microbiol* 00:11A.1.1-A.1.25
225. Scidmore MA, Hackstadt T. 2001. Mammalian 14-3-3 beta associates with the *Chlamydia trachomatis* inclusion membrane via its interaction with IncG. *Mol Microbiol* 39:1638-50
226. Shi C, Fricke P, Lin L, Chevelkov V, Wegstroth M, et al. 2015. Atomic-resolution structure of cytoskeletal bactofilin by solid-state NMR. *Sci Adv* 1

227. Shimada K, Chen S, Dempsey PW, Sorrentino R, Alsabeh R, et al. 2009. The NOD/RIP2 pathway is essential for host defenses against *Chlamydophila pneumoniae* lung infection. *PLoS Path* 5:e1000379
228. Sigalova OM, Chaplin AV, Bochkareva OO, Shelyakin PV, Filaretov VA, et al. 2019. *Chlamydia* pan-genomic analysis reveals balance between host adaptation and selective pressure to genome reduction. *BMC Genomics* 20:710
229. Singh R, Liechti G, Slade JA, Maurelli AT. 2020. *Chlamydia trachomatis* oligopeptide transporter performs dual functions of oligopeptide transport and peptidoglycan recycling. *Infect Immun* 88:e00086-20
230. Sixt BS, Bastidas RJ, Finethy R, Baxter RM, Carpenter VK, et al. 2017. The *Chlamydia trachomatis* inclusion membrane protein CpoS counteracts STING-mediated cellular surveillance and suicide programs. *Cell Host Microbe* 21:113-21
231. Slade JA, Brockett M, Singh R, Liechti GW, Maurelli AT. 2019. Fosmidomycin, an inhibitor of isoprenoid synthesis, induces persistence in *Chlamydia* by inhibiting peptidoglycan assembly. *PLoS Path* 15:e1008078
232. Slepenkin A, Enquist PA, Hägglund U, de la Maza LM, Elofsson M, Peterson EM. 2007. Reversal of the antichlamydial activity of putative type III secretion inhibitors by iron. *Infect Immun* 75:3478-89
233. Spaeth KE, Chen Y-S, Valdivia RH. 2009. The *Chlamydia* Type III Secretion System C-ring engages a chaperone-effector protein complex. *PLoS Path* 5:e1000579
234. Steinmetz JD, Bourne RR, Briant PS, Flaxman SR, Taylor HR, et al. 2021. Causes of blindness and vision impairment in 2020 and trends over 30 years, and prevalence of avoidable blindness in relation to VISION 2020: the Right to Sight: an analysis for the Global Burden of Disease Study. *The Lancet Global Health* 9:e144-e60
235. Stephens RS, Kalman S, Lammel C, Fan J, Marathe R, et al. 1998. Genome sequence of an obligate intracellular pathogen of humans: *Chlamydia trachomatis*. *Science* 282:754-9
236. Su H, Zhang, Y. X., and Li, R. 1985. Presence of muramic acid in *Chlamydia trachomatis* proved by liquid chromatography-mass spectrometry. *Kexue Tongbao* 30:695-9.
237. Suchland RJ, Dimond ZE, Putman TE, Rockey DD. 2017. Demonstration of persistent infections and genome stability by whole-genome sequencing of repeat-positive, same-serovar *Chlamydia trachomatis* collected from the female genital tract. *J Infect Dis* 215:1657-65
238. Sycuro LK, Pincus Z, Gutierrez KD, Biboy J, Stern CA, et al. 2010. Peptidoglycan crosslinking relaxation promotes *Helicobacter pylori*'s helical shape and stomach colonization. *Cell* 141:822-33
239. Tajima M, Samejima T, Nomura Y. 1959. Morphology of meningopneumonitis virus exposed to penicillin as observed with the electron microscope. *J Bacteriol* 77:23-34
240. Takeda K, Akira S. 2005. Toll-like receptors in innate immunity. *Int Immuol* 17:1-14
241. Takikawa O, Kuroiwa T, Yamazaki F, Kido R. 1988. Mechanism of interferon-gamma action. Characterization of indoleamine 2,3-dioxygenase in cultured human cells induced by interferon-gamma and evaluation of the enzyme-mediated tryptophan degradation in its anticellular activity. *J Biol Chem* 263:2041-8
242. Tamura A, Manire GP. 1967. Preparation and chemical composition of the cell membranes of developmental reticulate forms of meningopneumonitis organisms. *J bacteriol* 94:1184-8

243. Tamura A, Manire GP. 1968. Effect of penicillin on the multiplication of meningopneumonitis organisms (*Chlamydia psittaci*). *J bacteriol* 96:875-80
244. Tang C, Liu C, Maffei B, Niragire B, Cohen H, et al. 2021. Primary ectocervical epithelial cells display lower permissivity to *Chlamydia trachomatis* than HeLa cells and a globally higher pro-inflammatory profile. *Sci Rep* 11:5848
245. Taylor JA, Bratton BP, Sichel SR, Blair KM, Jacobs HM, et al. 2020. Distinct cytoskeletal proteins define zones of enhanced cell wall synthesis in *Helicobacter pylori*. *eLife* 9:e52482
246. Taylor-Robinson D. 2017. The discovery of *Chlamydia trachomatis*. *Sex Trans Infect* 93:10
247. Templeton DJ, Manokaran N, O'Connor CC. 2012. Prevalence and predictors of chlamydia co-infection among patients infected with gonorrhoea at a sexual health clinic in Sydney. *Sex Health* 9:392-4
248. Thomas M, Lawrence A, Kroon S, Vodstrcil LA, Phillips S, et al. 2021. Chlamydial clinical isolates show subtle differences in persistence phenotypes and growth in vitro. *Access Microbiol* 3:000204
249. Timms P, Good D, Wan C, Theodoropoulos C, Mukhopadhyay S, et al. 2009. Differential transcriptional responses between the interferon-gamma-induction and iron-limitation models of persistence for *Chlamydia pneumoniae*. *J Microbiol Immunol Infect* 42:27-37
250. Tomasz A. 1979. The mechanism of the irreversible antimicrobial effects of penicillins: how the beta-lactam antibiotics kill and lyse bacteria. *Ann Rev Microbiol* 33:113-37
251. Trembizki E, Costa A-MG, Tabrizi SN, Whiley DM, Twin J. 2015. Opportunities and pitfalls of molecular testing for detecting sexually transmitted pathogens. *Patholog* 47:219-26
252. Treuner-Lange A, Søgaard-Andersen L. 2014. Regulation of cell polarity in bacteria. *The J Cell B* 206:7-17
253. Unemo M, Shafer WM. 2011. Antibiotic resistance in *Neisseria gonorrhoeae*: origin, evolution, and lessons learned for the future. *Ann N Y Acad Sci* 1230:E19-28
254. Vasa S, Lin L, Shi C, Habenstein B, Riedel D, et al. 2015. β-Helical architecture of cytoskeletal bactofilin filaments revealed by solid-state NMR. *Proc Nat Acad Sci* 112:E127-E36
255. Vedyaykin AD, Ponomareva EV, Khodorkovskii MA, Borchsenius SN, Vishnyakov IE. 2019. Mechanisms of bacterial cell division. *Microbiol* 88:245-60
256. Vollmer W, Blanot D, De Pedro MA. 2008. Peptidoglycan structure and architecture. *FEMS Microbiol Rev* 32:149-67
257. Wagenlehner FME, Weidner W, Naber KG. 2006. Chlamydial infections in urology. *World J Urolog* 24:4-12
258. Waterhouse A, Bertoni M, Bienert S, Studer G, Tauriello G, et al. 2018. SWISS-MODEL: homology modelling of protein structures and complexes. *Nucleic Acids Res* 46:W296-W303
259. Weber MM, Lam JL, Dooley CA, Noriea NF, Hansen BT, et al. 2017. Absence of specific *Chlamydia trachomatis* inclusion membrane proteins triggers premature inclusion membrane lysis and host cell death. *Cell Rep* 19:1406-17
260. Weiss DS. 2004. Bacterial cell division and the septal ring. *Mol Microbiol* 54:588-97

261. Weiss E. 1950. The effect of antibiotics on agents of the psittacosis-lymphogranuloma group. I. The effect of penicillin. *J Infect Dis* 87:249-63
262. Welter-Stahl L, Ojcius DM, Viala J, Girardin S, Liu W, et al. 2006. Stimulation of the cytosolic receptor for peptidoglycan, Nod1, by infection with *Chlamydia trachomatis* or *Chlamydia muridarum*. *Cell Microbiol* 8:1047-57
263. Wesolowski J, Paumet F. 2017. Taking control: reorganization of the host cytoskeleton by *Chlamydia*. *F1000Res* 6:2058
264. Wesolowski J, Weber MM, Nawrotek A, Dooley CA, Calderon M, et al. 2017. *Chlamydia* hijacks ARF GTPases to coordinate microtubule posttranslational modifications and golgi complex positioning. *mBio* 8:e02280-16
265. WHO. 2007. Global strategy for prevention and control of sexually transmitted infections: 2006-2015. *World Health Organization, Geneva, Switzerland*.
266. Wichlan DG, Hatch TP. 1993. Identification of an early-stage gene of *Chlamydia psittaci* 6BC. *J Bacteriol* 175:2936-42
267. Wickstrum J, Sammons LR, Restivo KN, Hefty PS. 2013. Conditional Gene Expression in Chlamydia trachomatis Using the Tet System. *PLoS One* 8:e76743
268. Wiseman RW, Meiklejohn G, et al. 1946. Studies on the chemotherapy of viruses in the psittacosis-lymphogranuloma group; effect of penicillin and sulfadiazine on seven strains in mice. *J Immunol* 54:9-16
269. Witkin SS, Minis E, Athanasiou A, Leizer J, Linhares IM, Papasian CJ. 2017. *Chlamydia trachomatis*: the Persistent Pathogen. *Clin Vacc Immunol* 24:e00203-17
270. Wolf AJ, Underhill DM. 2018. Peptidoglycan recognition by the innate immune system. *Nat Rev Immunol* 18:243-54
271. Wolf K, Betts HJ, Chellas-Gery B, Hower S, Linton CN, Fields KA. 2006. Treatment of *Chlamydia trachomatis* with a small molecule inhibitor of the *Yersinia* type III secretion system disrupts progression of the chlamydial developmental cycle. *Mol Microbiol* 61:1543-55
272. Wood NA, Blocker AM, Seleem MA, Conda-Sheridan M, Fisher DJ, et al. 2020. The ClpX and ClpP2 orthologs of *Chlamydia trachomatis* perform discrete and essential functions in organism growth and development. *mBio* 11:e02016-20
273. Work E. 1961. The mucopeptides of bacterial cell walls. A review. *J Gen Microbiol* 25:169-89
274. Workowski KA, Bolan GA. 2015. Sexually transmitted diseases treatment guidelines, 2015. *MMWR Recomm Rep* 64:1-137
275. Workowski KA, Lampe MF, Wong KG, Watts MB, Stamm WE. 1993. Long-term eradication of *Chlamydia trachomatis* genital infection after antimicrobial therapy. Evidence against persistent infection. *JAMA* 270:2071-5
276. Wright HR, Turner A, Taylor HR. 2008. Trachoma. *The Lancet* 371:1945-54
277. Wu LJ, Errington J. 2004. Coordination of cell division and chromosome segregation by a nucleoid occlusion protein in *Bacillus subtilis*. *Cell* 117:915-25
278. Wyrick PB. 2010. *Chlamydia trachomatis* persistence *in vitro*: an overview. *J Infect Dis* 201 Suppl 2:S88-95
279. Xue Y, Zheng H, Mai Z, Qin X, Chen W, et al. 2017. An in vitro model of azithromycin-induced persistent *Chlamydia trachomatis* infection. *FEMS Microbiol letters* 364

280. Yin Y-P, Han Y, Dai X-Q, Zheng H-P, Chen S-C, et al. 2018. Susceptibility of *Neisseria gonorrhoeae* to azithromycin and ceftriaxone in China: A retrospective study of national surveillance data from 2013 to 2016. *PLoS Med* 15:e1002499
281. Zikic A, Schünemann H, Wi T, Lincetto O, Broutet N, Santesso N. 2018. Treatment of neonatal chlamydial conjunctivitis: a systematic review and meta-analysis. *J Ped Infect Dis Society* 7:e107-e15
282. Zuckerman DM, Boucher LE, Xie K, Engelhardt H, Bosch J, Hoiczyk E. 2015. The bactofilin cytoskeleton protein BacM of *Myxococcus xanthus* forms an extended beta-sheet structure likely mediated by hydrophobic interactions. *PLoS One* 10:e0121074